The University of Nottingham

# Modelling and Controlling Variation Propagation in Mechanical Assembly of High Speed Rotating Machines

By


## Tanweer Hussain

P.G.D. (Manufacturing Eng)
B.Eng. (Mechanical)
**Mehran University of Engineering and Technology Jamshoro, Sindh, Pakistan**


**Thesis Submitted to The University of Nottingham for the Degree of Doctor of Philosophy**

**2012**

I dedicate My work

**To Him Who will fill the Earth with justice and harmony as it is filled with oppression and tyranny**

&

**To My Parents**

(Whom I see everywhere I look, Who meant everything to me in the World)

# Acknowledgement

I thank to Almighty ALLAH for giving me the courage, determination, and the guidance in conducting this research study.

I wish to extend my utmost gratitude to my respected supervisors, Prof. Atanas Popov, and Prof. Stewart McWilliam, You were so wonderful to me. Your invaluable comments and suggestions enhanced the quality of this thesis. You showed me light in a tunnel where everything was dark. You were very tolerant and determined to see me through. Your patience and support helped me overcome many crisis situations and finish this dissertation. It has been honour for me to be Your Ph.D. student.

My sincere thanks are also due to Prof. Dariusz Ceglarek and Dr. Niels Lohse, the assessors of my PhD thesis for their detailed review, and advice in order to improve the quality of this thesis.

I wish to thank Dr. Zhufang Yang, for her continuous support as a team member. I also gratefully acknowledge help and advice from Matthew Yates, Steve Slack, and Stuart Bone at Rolls-Royce plc.

During this work I have collaborated with many friends and colleagues for whom I have great regards, and I wish to extend my warmest thanks to all those who have helped me with my work, especially Rupesh Patel, Sharad Jain, Nawazish Ali Zaidi and Shakir Jiffri who helped me in Matlab programming during initial stages of my PhD. Rupesh, you have always been very kind, you never said 'No' to me whenever I need you for help with Matlab. My warm thanks are also due to Mr. Javed Hussain

Brohi, Lecturer Department of Mathematics and Statistics, IBA Sukkur, Sindh, Pakistan for his help during initial stages of probabilistic modelling.

I am also indebted to all the members of Al-Zahra Foundation Nottingham, for their care and moral support during my stay at Nottingham, especially Mirza Muhammad Abbas for keeping alive the spiritual and moral values in my life.

I am grateful for the fun group of friends in University of Nottingham, who has been a source of good time and happiness during my stay in Nottingham, especially Zeeshan Ali, Shakir Jiffri, Rupesh Patel, Saad Alkhafaji, Situ Kyaw, Stefan Sieberer, Kuok Mak, Andrew Pimm, Otto Bakker (mooo!), Simon Woolhead, Kang Ji Jun (John), Ali Balhassn, Mutaz Bashir, Mohammad Saber, Joe Griffin, Shakil Shaikh and Christian Spiteri. I greatly value your friendship.

I gratefully acknowledge the funding sources that made my Ph.D. work possible. I was honoured with fully funded Scholarship by the Mehran University of Engineering and Technology, Jamshoro, Sindh, Pakistan.

Most importantly, none of this work would have been possible without the love and patience of my loving Wife and Sons. Without the encouragement of my wife and our understanding it would have been impossible for me to finish this work. My special gratitude is due to my brothers, sisters and their families for their loving support. They have been a constant source of love, concern, support and strength all these years.

# Abstract

Assembly plays a vital role in the quality of a final product and has a great impact on the manufacturing cost. The mechanical assemblies consist of parts that inevitably have variations from their ideal dimensions. These variations propagate and accumulate as parts are assembled together. Excessive amount of variations in an assembly may cause improper functionality of the product being assembled.

Improving assembly quality and reducing the assembly time and cost are the main objectives of this thesis. The quality of an assembly is determined in terms of variations in critical assembly dimensions, also known as Key Characteristics (KCs). Key Characteristics are designated to indicate where excess variation will affect product quality and what product features and tolerances require special attention. In order to improve assembly quality and reduce assembly time and cost, it is necessary to: (1) model non-ideal parts based on tolerances defined in design standards or current industrial practice of component inspection, (2) model assemblies and their associated assembly processes to analyse tolerance stack-up in the assembly, (3) develop probabilistic model to predict assembly variation after product assembly, and (4) implement control strategies for minimising assembly variation propagations to find optimum configuration of the assembly.

Two assembly models have been developed, a linear model and a fully non-linear model for calculating assembly variation propagations. The assembly models presented in this thesis also allows for inclusion of geometric feature variation of each assembly component. Methods of incorporating geometric feature variations into an assembly variation model are described and analysis techniques are explained. The assembly variation model and the geometric variation models have been developed for 2D and 3D assemblies. Modelling techniques for incorporating

process and measurement noise are also developed and described for the non-linear assembly model and results are given to demonstrate the calculation of assembly variations while considering part, process and measurement errors.

Two assembly case studies originating in sub-assemblies of aero-engines have been studied: Case Study 1, representing the rotating part (rotor) of an aero-engine, and Case Study 2, representing non-rotating part (stator) of an aero-engine. A probabilistic method based on the linear model is presented as a general analytical method for analysis of 3D mechanical assemblies. Probability density functions are derived for assembly position errors to analyse a general mechanical assembly, and separate probability functions are derived for the Key Characteristics (KCs) for assembly in Case Studies 1 and 2. The derived probability functions are validated by using the Monte Carlo simulation method based on the exact (fully non-linear) model. Results showed that the proposed probabilistic method of estimating tolerance accumulation in mechanical assemblies is very efficient and accurate when compared to the Monte Carlo simulation method, particularly if large variations at the tails of the distributions are considered.

Separate control strategies have been implemented for each case study. Four methods are proposed to minimise assembly variations for Case Study 1, and one error minimisation method is suggested for assemblies of Case Study 2. Based on the developed methods to optimise assembly quality, the two case studies were investigated, and it was found that the proposed optimisation methods can significantly improve assembly quality. The developed optimisation methods do not require any special tooling (such as fixtures) and can easily be implemented in practice.

## Research Publications

### Journal Papers

1. Hussain T, Yang Z, Popov AA and McWilliam S. Straight-Build Assembly Optimization: A Method to Minimize Stage-by-Stage Eccentricity Error in the Assembly of Axisymmetric Rigid Components (Two-Dimensional Case Study). *ASME Journal of Manufacturing Science and Engineering*. 2011; 133(3): 031014.
2. Yang Z, Hussain T, Popov AA and McWilliam S. Novel Optimization Technique for Variation Propagation Control in an Aero-Engine Assembly. *Proceedings of the Institution of Mechanical Engineers, Part B: Journal of Engineering Manufacture*. 2011; 225(1): 100-11.
3. Yang Z, Hussain T, Popov AA and McWilliam S. A Comparison of Different Optimization Techniques for Variation Propagation Control in Mechanical Assembly. *IOP Conference Series: Materials Science and Engineering*. 2011; 26(1): 1-11.
4. Hussain T, McWilliam S, Popov AA and Yang Z. Geometric Error Reduction in the Assembly of Axi-symmetric Rigid Components - a 2D Case Study. *Proceedings of the Institution of Mechanical Engineers, Part B, Journal of Engineering Manufacture*. (In Press).
5. Yang Z, McWilliam S, Popov AA and Hussain T. A Probabilistic Approach to Variation Propagation Control for Straight Build in Mechanical Assembly International Journal of Advanced Manufacturing Technology. (In Press).
6. Yang Z, McWilliam S, Popov AA and Hussain T. Variation Propagation in Straight-Build Mechanical Assemblies Using a Probabilistic Approach – 2D Assembly. *(under review)*.

**Conference Paper**

7. Hussain T, Yang Z, Popov AA and McWilliam S. Controlling Variation Propagations in Straight Build of an Assembly by Process Optimization Methods (2D Case Study). *21st International Computer –Aided Production Engineering Conference* (CAPE 2010), *Edinburgh, UK*, 2010.

# Contents

# Nomenclature

| | |
|---|---|
| $\oplus$ | Minkowski sum. |
| $\Theta$ | Minkowski subtraction. |
| $t_M$ | Maximum limit of tolerance. |
| $t_L$ | Least limit of tolerance. |
| $S$ | Nominal geometry of solid part. |
| $\mathrm{M}_1$ | Model variable representing size deviations. |
| $\mathrm{M}_2$ | Model variable representing orientation deviations. |
| $ST$ | Size tolerance. |
| $FT$ | Form tolerance. |
| $dX, dY, dZ$ | Position error in $x$, $y$, and $z$ directions, respectively. |
| $d\theta$ | Orientation error due to geometric tolerance measured in local coordinates. |
| $d\theta_{max}$ | Maximum orientation error due to geometric tolerance. |
| $d\theta_x, d\theta_y, d\theta_z$ | Orientation error of a feature about $x$, $y$, and $z$ axes due to geometric tolerance. |
| $\mathbf{dp}_k$ | A vector representing position error of $k^{th}$ feature frame in assembly measured in global coordinates. |
| $\mathbf{d\theta}_k$ | A vector representing orientation error of $k^{th}$ feature frame in assembly measured in global coordinates. |
| $\mathbf{V_p}$ | Covariance matrix of translation error vector $\mathbf{dp}$. |
| $\mathbf{V_\theta}$ | Covariance matrix of rotational error vector $\mathbf{d\theta}$. |
| $T_i$ | Tolerance of $i^{th}$component. |
| $T_{ASM}$ | Assembly tolerance. |
| $\mu$ | Mean. |
| $\sigma$ | Standard deviation. |

| | |
|---|---|
| $\sigma^2$ | Variance. |
| $\partial f/\partial x_i$ | Sensitivity of the assembly tolerance to variations in individual component dimensions. |
| $C_f$ | Correction factor. |
| $H$ | Nominal height of as component. |
| $z$ | Actual height of as component after considering manufacturing error. |
| $R$ | Nominal radius of the circle. |
| $r$ | Actual radius of a point on circular element after considering run-out variation. |
| $a_{run-out}$ | Actual value of axial run-out at a point on circular element. |
| $r_{run-out}$ | Actual value of radial run-out at a point on circular element. |
| $a_{run-out}^{random}$ | Randomly simulated value of axial run-out at a point on circular element. |
| $r_{run-out}^{random}$ | Randomly simulated value of radial run-out at a point on circular element. |
| $\mathbf{Trans}$ | A transform matrix representing purely translation. |
| $\mathbf{Rot}_x$, $\mathbf{Rot}_y$, $\mathbf{Rot}_z$ | Matrices representing individual rotations about the $x$, $y$ and $z$ axes, respectively. |
| $\mathbf{T}$ | Transformation matrix representing relationship of a Coordinate frame with the reference frame. |
| $\mathbf{R}$ | Rotation matrix representing the rotational component of a transform matrix $\mathbf{T}$. |
| $\mathbf{p}$ | Translation vector representing the translational components of a transformation matrix $\mathbf{T}$. |
| $\mathbf{R}_{Ai}$ | Rotation matrix representing the rotational component of a transform $\mathbf{A}_i$ representing assembly of nominal components. |

| | |
|---|---|
| $\mathbf{p}_{Ai}$ | Translation vector representing the translational component of a transform $\mathbf{A}_i$ representing assembly of nominal components. |
| $\mathbf{DT}$ | Variation transformation matrix. |
| $\boldsymbol{\delta}\mathbf{R}$ | Differential matrix representing the rotational error component of variation transform matrix $\mathbf{DT}$. |
| $\mathbf{dp}$ | Translation vector representing the translational error component of variation transform matrix $\mathbf{DT}$. |
| $\mathbf{dTrans}$ | Differential transform for translation error. |
| $\mathbf{dRot}_x$, $\mathbf{dRot}_y$, $\mathbf{dRot}_z$ | Differential transforms representing the angular orientation error about the $x$, $y$ and $z$ axes, respectively. |
| $\mathbf{R}'_{Ai}$ | Rotation matrix representing the rotational component of a transform $\mathbf{A}'_i$ representing assembly of manufactured (non-nominal) components. |
| $\mathbf{p}'_{Ai}$ | Translation vector representing the translational component of a transform $\mathbf{A}'_i$ representing assembly of manufactured (non-nominal) components. |
| $dp_i^X, dp_i^Y, dp_i^Z$ | Position error of $i^{th}$ feature frame in assembly along $x$, $y$, and $z$ directions, respectively measured in global coordinates. |
| $\lvert dp_i^X \rvert$ | Eccentricity error in assembly of 2D axi-symmetric components. |
| $e_i^{Ecc}$ | Eccentricity error in assembly of 3D axi-symmetric components. |
| $e_i^R$ | Mis-position error in the radial direction in the assembly of uniformly segmented circular component |
| $f\left(e^{Ecc}\right)$ | Probability density function of eccentricity error |
| $P\left(e^{Ecc}\right)$ | Cumulative distribution function of eccentricity error |
| $\varepsilon_{ta}^{RMS}$ | RMS assembly variation from the table axis |

| | |
|---|---|
| $\varepsilon_i^{ota}$ | Optimised table axis error for the $i^{th}$ component of the assembly |
| $\varepsilon^{otaa}$ | Optimised table axis error for the whole assembly |
| $T_{rr}$ | Radial run-out tolerance. |
| $T_{ar}$ | Axial run-out tolerance. |
| $T_s$ | Size tolerance. |
| $T_f$ | Flatness tolerance. |
| $R_o$ | Outer radius. |
| $R_i$ | Inner radius. |
| $t$ | Thickness. |

# List of Abbreviations

| | |
|---|---|
| DFA | Design for Assembly |
| DFC | Datum Flow Chain |
| DOF | Degrees of Freedom |
| FEA | Finite Element Analysis |
| GD&T | Geometric Dimensioning and Tolerancing |
| HTM | Homogeneous Transform Matrix |
| KC | Key Characteristic |
| KCC | Key Control Characteristics |
| KPC | Key Product Characteristics |
| LMC | Least Material Condition |
| LMP | Least Material Part |
| MCS | Monte Carlo Simulation |
| MMC | Maximum Material Condition |
| MMP | Maximum Material Part |
| RSS | Root Sum Square |
| SOVA | Stream of Variation Analysis |
| TTRS | Topologically and Technologically Related Surfaces |
| VBR | Virtual Boundary Requirement |
| VDOF | Variations along Degrees of Freedom |
| WC | Worst-case |
| pdf | Probability Density Function |

# List of Figures

# List of Tables

# Chapter 1 INTRODUCTION

## 1.1 Introduction

Mechanical assembly is the process of putting together parts to get a required final product. Assembly is different from other manufacturing processes because it is inherently integrative and requires coordination of many parts, tools, fixtures, packages, people, and companies. An assembly enables parts to perform functions by working together as a system, which otherwise were nothing but a collection of parts. The design and analysis of an assembly is very important for the manufacture of a product. Design is the first step in manufacturing, and it is where most of the important decisions are made that affect the quality and cost of the final product. The design practice not only focuses on the design aspect of a part but also on the producibility, including ease to manufacture a product or assembly. On the other hand, the analysis of assembly is carried out to check the achievability of assembly

requirements. During product assembly, a number of design requirements need to be satisfied to meet the requirements of the final assembly.

For a mechanical assembly, accuracy is the key factor because it affects product quality and production yield. Manufacturing fluctuations result in small deviations in parts from their nominal geometry. These deviations propagate and accumulate as parts are assembled and the final assembly quality depends upon the magnitudes of these deviations and the choice of assembly procedures. Effectively controlling the propagation of variations in the assembly process is one way to help achieve the desired assembly quality [1]. This research focuses on modelling and controlling variation propagations in mechanical assemblies, in particular of high-value low-volume products.

## 1.2 Motivation and Goals

Most engineering products from pencil sharpeners to aircraft engines are assembled units. In all these assembled products, mechanical assembly plays an important role in the quality of final product. In manufacturing industry, assembly is one of the most important stages for product development that consumes about 45% of production workload, and nearly 54% of cost [2, 3]. Product quality in mechanical assemblies is determined by the propagation of manufacturing variations as the structure is built. By looking closely at the problems affecting assembly quality and taking effective measures to avoid these problems, one can improve final product quality with a huge impact in reducing the cost and product development time.

In high-value low-volume complex assemblies, it is desired to perform assembly analysis to calculate assembly variation propagations before putting parts together

in a real assembly. This will save assembly and dis-assembly time and cost, and will also enable the assembly engineer to take effective measures to control assembly variation propagations. Therefore, it is essential to have a quantitative design tool for specifying tolerances and estimation of tolerance stack-up in assembly. The tolerance analysis tools can also be used to evaluate the design of an existing assembly. The goal here is to present a robust method for calculating assembly variation propagations and to provide a statistical tool for performing tolerance analysis in order to estimate accumulations of variations in assembly parameters during each assembly stage. The assembly model should be capable enough to incorporate geometric variations in assembly components and assembly process and measurement errors.

Rotating machines are commonly used in industries, including machining tools, industrial turbo-machinery, and aircraft engines. In high-precision complex products, such as aero-engines, there is a need to satisfy precisely the design variables that are critical to product quality and performance. These measurable design variables are termed as product Key Characteristics (KCs) [4, 5]. The focus of this thesis is on the assembly issue of rotating machines such as aero-engine assembly. Vibration is the main factor that affects the reliability of high-speed rotating machines [6]. In aircrafts, the vibration of the engine directly affects the flight stability and safety of an airplane. The aero-engine assembly can be divided into two separate sub-assemblies, a sub-assembly of the rotating part called engine rotor and a sub-assembly of the non-rotating structure called engine casing (as shown in Figure 1-1).

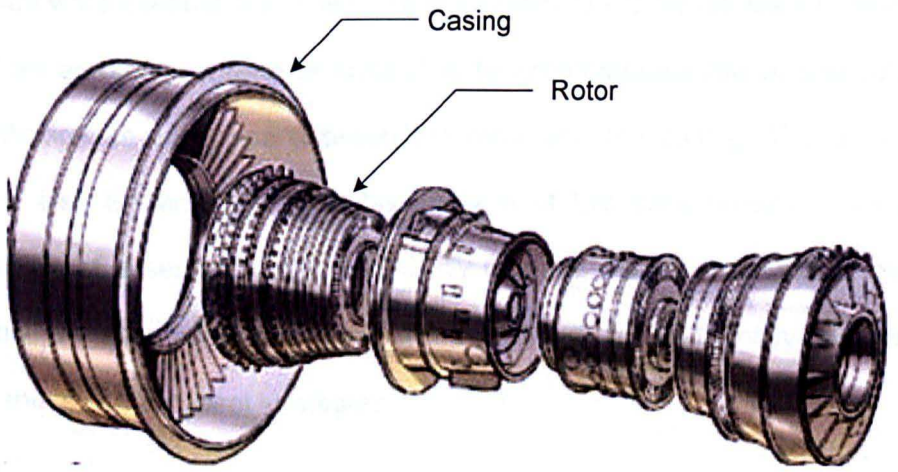


**Figure 1-1: Schenetic diagram of an aero-engine assembly.**

This thesis discusses the assembly issues of the two sub-assemblies (a rotating part and a non-rotating part of rotating machines).

There are various factors causing rotor vibration such as; (1) mass imbalance, (2) geometric eccentricities caused during the assembly of rotor components (that results in internal bending of the rotor), (3) clearance in the bearings carrying the engine rotor. This research is only concerned with the assembly issues, therefore factors such as mass imbalance and the bearing clearance are out of the scope of this thesis. If during the assembly of a rotor, the geometric axis of the rotor constituted by assembling rotor stages is not built straight, this may result in the excessive vibration in the rotor. In such a case, the goal is to build the assembly in a manner such that the geometric axis of the rotor is maintained as straight as possible. Therefore, the assembly KC for an engine rotor can be extracted as to build the assembly as straight as possible between the two ends of the rotor.

The casings of the aero-engines are large heavy circular structure made by casting. Recently, the replacement of these large heavy castings with fabricated structures consisting of small castings and sheet components [7] is introduced to provide

significant weight reductions. Therefore the assembly KC for fabricated non-rotating part of an aero-engine (engine casing) is to accommodate the engine rotor with uniformly precise clearance between the rotor and the casing. The goal of this thesis is also to carry out assembly analysis of two case studies to check the achievability of assembly KCs. This initially requires control strategies to minimise assembly variation propagations and a method to statistically analyse the effectiveness of the control strategies.

## 1.3 Thesis Outline

This thesis presents an integrated framework of modelling non-ideal parts, assemblies, assembly processes, and control strategies to minimise assembly variation propagation. The proposed framework can be employed for designing assemblies and assembly processes, and also can be used for analysis of assemblies and processes to ensure that the assembly of existing components meets the design requirements.

Chapter 2 reviews past research work relevant to this thesis. Past work is presented for current practices in modelling non-ideal parts, modelling variation propagation in assemblies, statistical assembly variation analysis, and minimising and controlling variations in mechanical assemblies.

Chapter 3 presents an overview of the research methodology adopted to undertake this research.

Chapter 4 gives details of the proposed assembly variation propagation models along with background knowledge. Two variation propagation model are proposed: "Linear Model" and "Exact Model". Their detailed mathematical derivation is given

for both 2D and 3D assemblies. Based on the assembly models, two assembly case studies are presented to describe the process of error accumulation in 2D and 3D assemblies.

Chapter 5 describes modelling for non-ideal manufactured components. This chapter is concerned with geometric variations in the parts used in the two assembly case studies considered, based on their tolerance specifications. Geometric modelling for component variations based on inspection data for assembly components used for Case Study 1 is also presented in this chapter.

Chapter 6 gives details for probabilistic analysis for linear propagation of errors based on a linear model for calculating assembly variation propagation, as proposed in Chapter 4 of this thesis. The comparison of results for a probabilistic model for linear propagation of errors is presented together with a non-linear analysis using Monte Carlo simulation method.

Chapter 7 presents control strategies for minimising assembly variation propagations. For Case Study 1 of an engine rotor, four optimisation techniques are proposed to minimise assembly variation propagations, whereas, for Case Study 2 of an engine casing, one method is proposed to minimise assembly variation propagations. For both assembly case studies, the error minimisation methods are presented in both 2D and 3D assemblies. In this chapter, the results for Case Study 1 are presented in 2D only, whereas, the results for Case Study 2 are presented in both 2D as well as 3D context.

Chapter 8 deals with detailed results for straight-build assemblies in Case Study 1 for 3D assemblies. This chapter also presents suggestions for incorporating

assembly process and measurement errors in the modelling of assembly variation propagations.

Chapter 9 concludes with a discussion on the modelling and results presented together with the advantages and limitations of the work presented in the thesis. The chapter also provides suggestions for future work and further research.

# Chapter 2 LITERATURE REVIEW

## 2.1 Introduction

Assembly modelling and variation propagation control are the constituent part of the assembly design and both are very important for quality manufacture of mechanical products. This chapter thus provide a review of the literature in the area of assembly modelling; mainly focusing on the literature related modelling assembly variation propagation and assembly variation control. Initially, in Section 2.2, this chapter gives definition along with detailed description of a commonly used term in assembly design and modelling called "assembly feature". To familiarise the reader with assembly modelling, the requirement for assembly modelling and design are explained in Section 2.3. To model assembly variation, it is necessary to know the sources of assembly variations. Thus, sources of assembly variation in the light of literature reviewed are described in Section 2.4.

The initial requirement for modelling assembly variation is to model component variations and the current practices in modelling component variations are described in Section 2.5. Various approaches of assembly modelling are described in Section 2.6. Statistical methods for analysing assembly variation are referred in Section 2.7. A review of the current practices in minimising and controlling assembly variation is given in Section 2.8. A summary of the whole survey and the identification of the knowledge gaps can be found in Section 2.9. Finally, the aims and objectives of this research are explained in Section 2.10.

## 2.2 Assembly Feature

What "*feature*" means is quite different from different points of view. With respect to geometric modelling, in [8], "features are generic shapes with which the engineers associate certain properties or attributes and knowledge useful in reasoning about the product". Another definition of features in the context of object-oriented programming from [9] is: features are "objects that may contain method for manufacturing, analysis geometry creation, assembly; or pointers to geometry, geometric constraints, or inherited properties". Several other authors also differentiate between design or functional features, manufacturing features, and geometric features [10].

From assembly point of view, a feature is the elementary connection containing mating relations between the components [11]. Assembly features are divided into connection features and handling features [12]. Connection features represent connections between components and handling features represent handling information. Since connections between features play significant role in the assembly, therefore, the assembly features of connection type are considered in this thesis. The connection features are also known as mating features.

Mating features in assembly form the links that establish the desired state of constraint among adjacent parts, leading to the achievement of the assembly-level geometric relationships [13]. DeFazio *et al.* [14] defined an assembly feature as "any geometry or non-geometric (mating relations) attribute of a discrete part whose presence or dimensions are relevant to the product's or part's function, manufacture, engineering analysis and use". They presented a feature-based design environment aimed at the design of assemblies of parts.

## 2.3 Assembly Requirements

Assembly is the activity in which all the upstream processes of design, engineering, manufacturing, and logistics are brought together to create an object that performs a function [15]. It has been found in the literature that design for assembly (DFA) at the early conceptual stage of design was implemented to make the assembly process easier, to reduce manufacturing costs, to reduce overheads, and to improve product quality [16-18]. During product development and the design stage, the main task is to develop a product that meets the requirements [9, 19]. These requirements come from many sources, which include [20]:

- Customer and market demand (e.g. functions, appearance, price, etc.)
- Government regulations demand (environmental friendliness, absence of toxicity, specific safety rules, etc.)
- Company standards demand (use of particular design methods, materials, off-the-shelf parts, etc.)
- Performance and quality requirements (reliability, durability, safety, fitness for use, etc.)

In this thesis, the research is concerned with performance and quality requirements that are delivered by mechanical assemblies. The measurable design variables that

are critical to product quality and performance are termed as Key Characteristics (KCs) [4, 5]. KCs are designated to identify where excess variation will most significantly affect product quality, what product features and tolerances require special attention from manufacturing, and what assembly process/stages need special attention to control variation [21, 22]. A definition of a KC as given by [4]:

> "Key characteristics are the product, subassembly, part, and process features whose variation from nominal significantly impacts the final cost, performance (including the customer's perception of quality), or safety of a product. Special control should be applied to those KCs if the cost of variation justifies the cost of control."

Key characteristic is called by different names, as Significant Characteristics, Key Product Characteristics, Functionally Important Topics, Engineering Characteristics, Critical-to-Function, and Critical-to-Quality [23-26]. The hierarchy of KCs is described at different levels of the product design and development stage by a tree diagram shown in Figure 2-1.

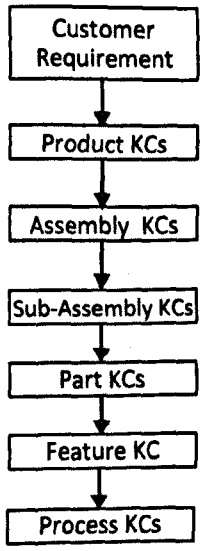


**Figure 2-1: KC flow-down [4, 23]**

The tree structure given in Figure 2-1 is referred as KC flow-down. The KC flow-down links customer requirements of the product to its component features. KC flow-downs allow for a decomposition of the product into essential features and processes, enabling traceability of cause and effect [5]. Product level KCs are identified at the highest level of the flow-down and are the product requirements that must be maintained to meet performance requirements and customer satisfaction [5]. Any number of levels can exist between the system level KCs and feature level KCs depending on the product complexity.

Assembly level KCs refers to the requirements imposed on features and functions of the product [23]. Assembly level KCs depend upon chain of manufactured parts that act together to form an assembly [27]. Each manufactured part has associated KCs with them that are certain dimensions that part must meet in order to deliver assembly level KCs when put together [28, 29]. The feature level KCs (key features) and the associated components and subassembly KCs can be identified by performing a tolerance analysis of a product assembly [30] . A feature-based tolerance analysis focus on key-feature tolerances, their relations during assembly, and the tolerance stack-up during assembly [31]. In order to perform assembly tolerance analysis, the part tolerances for all assembly components need to be described mathematically in order to be incorporated into the assembly model.

Lee and Thronton [29] distinguished KCs of two types: Key Product Characteristics (KPC) and Key Control Characteristics (KCC), associated with product and manufacturing process respectively. Their definitions as given in [29] are as follows:

A Key Product Characteristic is "a product characteristic for which reasonably anticipated variation could significantly affect the product's safety or compliance with

governmental standards or regulations, or is likely to significantly affect customer satisfaction with a product."

A Key Control Characteristic is "a process parameter (such as temperature, line speed, pressure, and viscosity) for which variation must be controlled around some target value to ensure that variation in a Key Product Characteristic is maintained around its target value."

Various methods are used to identify Key Characteristics. The two most common methods are the 'top-down' approach and the 'bottom-up' approach. The top-down design approach firstly formulates an overview of the system being designed, the system is then broken down to subsystem levels. Each subsystem is sometimes refined in many additional subsystem levels, until the entire specification is reduced to base elements [32]. The bottom-up approach is traditionally performed during existing production to identify and reduce variation in individual parts and processes. The bottom-up approach identifies individual processes and features that affect the quality of a part. This approach attempts to resolve variation problems at the feature level, as a result, the end quality of the product is expected to be improved [5]. Many organisations that are in production use this as a means to troubleshoot and address variation problems [33].

## 2.4 Sources of Assembly Variations

There are four main sources of variation in a mechanical assembly:

- individual component variations,
- variations due to small kinematic adjustments,
- fixture and assembly process variation,
- variations due to measurement errors.

The first is the result of the natural variations in manufacturing processes, the second is a function of the first source of assembly variation (that is it depends on the input from the dimensional variation and geometric feature variation) and the last two may be encountered during the assembly of parts at each station.

Individual component variations can be categorised as dimensional variation and geometric feature variation. The dimensional variation according to [34], are the variation of the individual part from its nominal dimensions, whereas, geometric feature variation are the variations in shape of the component features. Geometric feature variation refers to orientation, and location of the features of produced components. Such variations are inevitable due to fluctuations of machining conditions, such as tool wear, fixture errors, set-up errors, material property variations, temperature, and worker skills.

Variations due to small kinematic adjustments refer to in-process adjustment of the assembly components due to fit-up problems. The two-component assembly shown in Figure 2-2 demonstrates the relationship between dimensional variations in an assembly and the small kinematic adjustments which occur at assembly time. In part 'a' of the figure, the assembly has three component dimensions that vary, two on the tapered groove and one on the cylinder, as shown. The variations in the dimensions $A, R$, and $\theta$ from their nominal dimensions have an effect on the placement of cylinder from $U_1$ (nominal position of the cylinder) to $U_2$ (position of the cylinder when the variations are present). The difference between $U_1$ and $U_2$ is the kinematic adjustment of the assembly to variation in the components. In part 'b' of the figure, it can be seen that $U$ is also dependant upon form variation of the groove's surface.

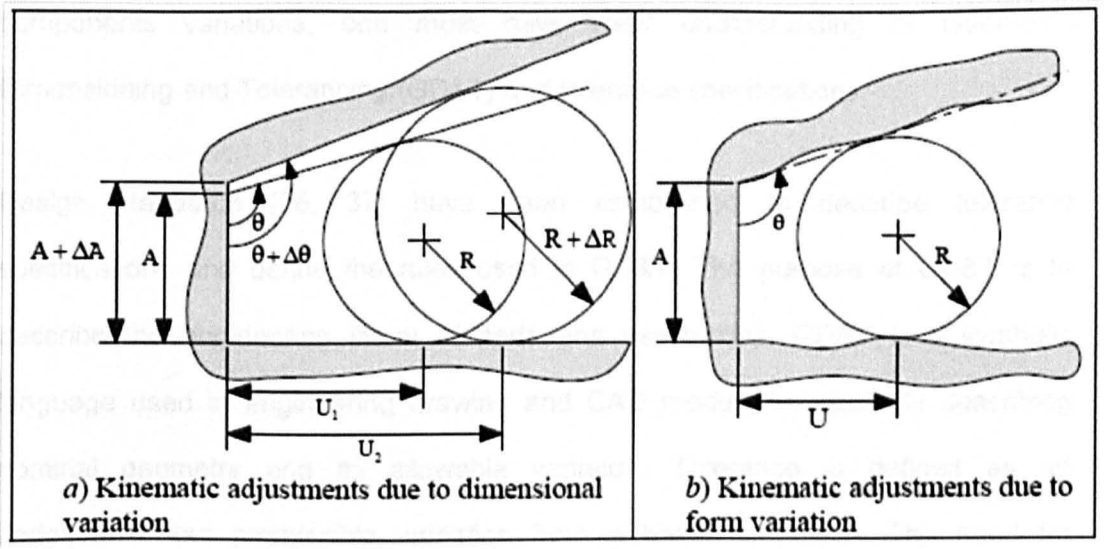


**Figure 2-2: Kinematic assembly variation [35]**

Fixture and assembly process variations are the variations caused by either error in location of a part by a fixture or error due to assembly process variation like variation due to heat effects during interference/shrink fits, welding etc.

Variations due to measurement errors are the variation caused by inaccurate in-process assembly measurement. During assembly, various in process measurements are carried to monitor the critical parameters of the product. The measurement data of one stage of the assembly is used to predict the error and make some in-process adjustments in the next stage. The amount of these measurement errors depends on the level of the accuracy of the individual measuring instrument.

## 2.5 Modelling Component Variations

Variations in parts and assemblies are unavoidable. These variations are the physical result of manufacturing processes. The parts and assemblies that are supposed to be identical, differ from each other in reality. In order to model

components variations, one must have clear understanding of Geometric Dimensioning and Tolerancing (GD&T) and tolerance specifications.

Design standards [36, 37] have been established to describe tolerance specifications and define the rules used in GD&T. The purpose of GD&T is to describe the engineering intent of parts and assemblies. GD&T is a symbolic language used in engineering drawing and CAD models for explicitly describing nominal geometry and its allowable variation. Tolerance is defined as an undesirable, but permissible, variation from a basic dimension. The need for tolerances comes from the fact that it is neither practically possible nor economically advantageous to produce parts to exact dimensions. The dimensioning and tolerancing standards describe two types of tolerances: traditional plus/minus tolerances (also known as dimensional tolerances) that control the size of the part, and geometric tolerances that control form, orientation, location and run-out of a feature [38]. Each type of dimensional and geometric variation has different significance in engineering [39]. The tolerance standards contain a classification of these variations. The classification of component variations based on different types of tolerances is given in Chapter 5 of this thesis.

Modern geometric tolerances provide the foundation for creating mathematical models that are essential for the development of computational tools. The technique of representing component variations mathematically is also known as tolerance modelling, modelling component variations, or modelling variation along degrees of freedom of error [40-42]. Work in this area of describing part variations mathematically was initially done by Sutherland [43]. Sutherland used constraints between the coordinates of a part to constrain the error introduced into the system. He made use of constraints not to define complete geometry of part but as a design aid in the creation of a part.

The work in the area of describing part variations mathematically can be classified into the following categories: (1) offset method; (2) parametric space method; (3) algebraic methods; (4) vectorial tolerancing method; and, (5) homogeneous transformation matrix method.

### 2.5.1 Offset Method

The offset model proposed by Requicha and Voelcker [44, 45] is one of the earliest methods. Requicha introduced a mathematical technique for representation of part variations based on the tolerance zone approach. In his work [44], the issue of tolerance zone formation was discussed, and a method that uses an offset operation to generate tolerance zones was implemented. Requicha defined tolerance zone as a region that must lie within the maximal and minimal object boundaries obtained by offsetting the object by equal amount on each side of the nominal. An example of tolerance zone for geometric tolerance specification is illustrated in Figure 2-3 taken from [46]. Figure 2-3(a) illustrates a part with geometric tolerance specification. The shaded area in Figure 2-3(b) indicates the corresponding tolerance zone, as per specifications, within which the manufactured part should lie. In Figure 2-3(b) MMC refers to Maximum Material Condition, that limits the boundary of maximum variability of the part outside the nominal condition. Similarly, LMC refers to Least Material Condition that limits the boundary of maximum variability of the part inside the nominal condition. The parts with such boundaries are called maximum material part (MMP) or least material part (LMP) respectively.

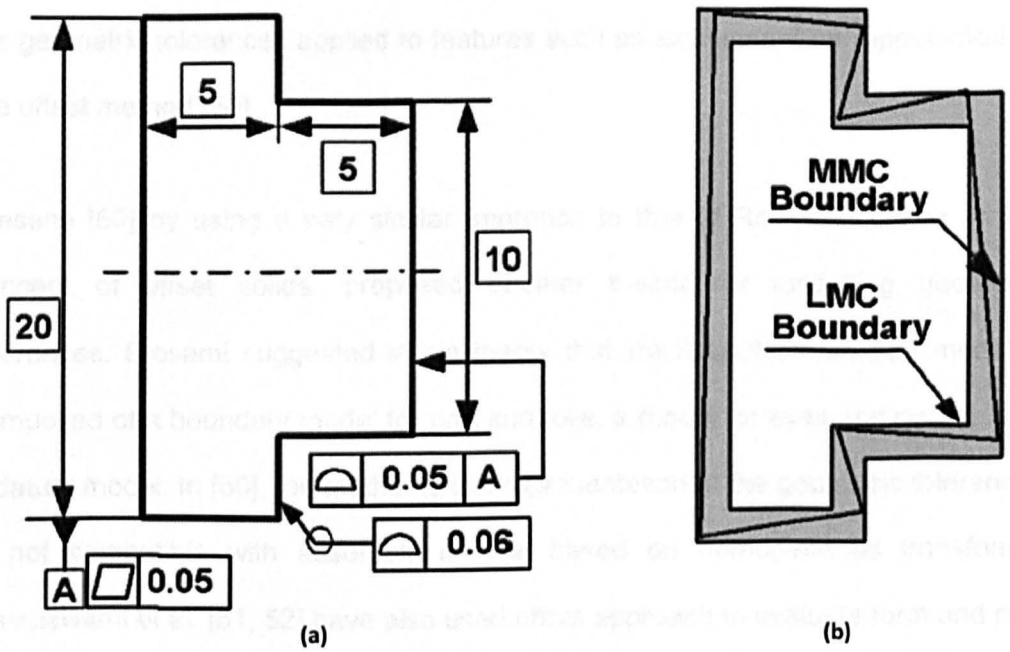


**Figure 2-3: (a) A part with geometric tolerance callouts, (b) An instance of the actual part that is acceptable as per specification provided in (a) [46].**

Requicha [47] put forward a theory and proposed that with Minkowski sums the tolerance zones can be constructed to contain all the features of a variational part. Here the feature means geometric entities such as point, line of face and the variational part refers to a part with the allowable ranges of variations [48]. The Minkowski sum of two sets $P$ and $Q$ is defined as a set of pair-wise sums of points from $P$ and $Q$ [49], such that $P \oplus Q = \{p + q | p \in P, q \in Q\}$. Therefore, the MMC and LMC of a solid part can be described by Minkowski sum as:

$$MMC\ solid = S \oplus t_M, \tag{2.1}$$

$$LMC\ solid = S \Theta t_L \quad \text{respectively,} \tag{2.2}$$

where, $S$ represents the nominal geometry of solid part, $\oplus$ represents Minkowski sum, $t_M$ is the maximum limit of tolerance, $t_L$ is the least limit of tolerance and $\Theta$ represents Minkowski subtraction. The main deficiency of this theory is that the tolerance specification can only be applied onto surface features. For this reason,

the geometric tolerances applied to features such as axis cannot be represented by the offset method [50].

Etesami [50] by using a very similar approach to that of Requicha based on the concept of offset solids, proposed another theory for modelling geometric tolerances. Etesami suggested in his theory that the manufactured part model is composed of a boundary model for part surfaces, a model for axes and curves, and a datum model. In [50], the mathematical representation of the geometric tolerances is not compatible with assembly models based on homogeneous transforms. Ramaswami et al. [51, 52] have also used offset approach to evaluate form and run-out tolerances, but their work does not express form and run-out variations in terms of translation and rotation error of the component.

Jayaraman and Srinivasan [53, 54] state that Requicha theory is not adequate for describing allowable variations from the nominal, when the functional constrains are considered. They refined Requicha theory and proposed a tolerancing framework based on the virtual boundary requirement (VBR). Virtual boundary is a boundary of perfect form, established at a theoretically exact position that models the fit between two part surfaces in assembly. For a non-interference fit, one surface must lie entirely inside the virtual boundary, while the other surface must lie entirely outside. The virtual boundary also serves as the maximum material envelope for both surfaces. In virtual boundary, the individual tolerances of each component are derived from these virtual boundary requirements. Due to this reason the virtual boundary requirement is not an adequate representation of the part functional requirement, which require separate and individual tolerance specifications.

## 2.5.2 Parametric Space Model

The theory of parameter spaces was one of the first concepts proposed to evaluate tolerances on geometric models. Hillyard and Braid [55, 56] discussed the possibility of using variable dimensions or parameters in a solid modeller to represent dimensional variation. They proposed a general theory which uses geometric constraints between coordinates of a part to constrain variations in the dimensions as specified by the tolerances. Lin et al. [57] extended and refined the above constraint-based variational-geometry approach from the standpoint of the user interface and computational efficiency.

An example taken from [46] is presented in Figure 2-4 to describe the concept of parametric approach of tolerance modelling. Figure 2-4(a) shows a 2D part with variance feature A that is free to orient within the tolerance zone, and Figure 2-4(b) shows the extent of feature variation.

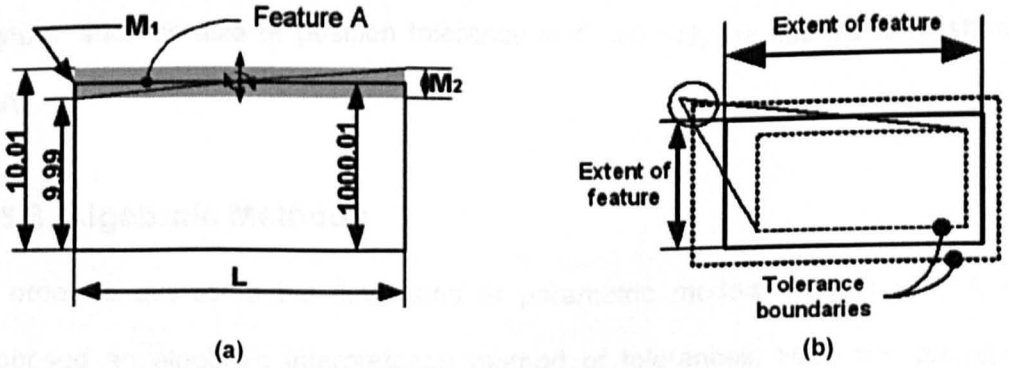


**Figure 2-4: (a) Variability of feature A, (b) Errors in worst cases in parametric space models[46].**

In Figure 2-4(a), model variables are introduced to parameterise the possible variations of the vertices of the edges in terms of position or orientation. In the example, model variables $M_1$ and $M_2$ represent size and orientation deviations, respectively. The model variations are defined as:

$$-0.1 \leq M_1 \leq 0.1, \tag{2.3}$$

and,

$$-0.2 \leq M_2 \leq 0.2, \quad \text{respectively.} \tag{2.4}$$

In the parametric approach, the part tolerances are expressed as variations to the parameters defining nominal geometry such as vertices in case of a rectangular component (as shown in Figure 2-4). Turner [58] suggests the introduction of additional vertices to break the edge of part into segments.

Turner et al. [59, 60] improve the earlier model to a surface-based variational model in which the model variables are associated with the coefficients of the equations of each surface, and the vertex coordinates are computed from the intersection of surface equations. According to Pasupathy et al. [46], research in the domain of parametric modelling was not much suitable for form tolerance, because the parametric approach for form tolerances was limited to single tolerance control of a feature, such as size or position tolerance and can only be applied to polyhedral parts.

### 2.5.3 Algebraic Methods

In order to overcome the limitations of parametric models, Inui et al. [61, 62] proposed an algebraic interpretation method of tolerances. Here the variational model for tolerances is developed using algebraic constraints. Mullins and Anderson [63] also proposed a method that translates the semantics of geometric tolerances into an algebraic form. Another major development in algebraic method was the research by Roy and Li [64, 65]. They proposed a similar approach and considered the resultant zones from multiple controls, such as size and form tolerances, on a

To demonstrate the concept of tolerance representation based on algebraic method, an example of 2D part (taken from [46]) is shown in Figure 2-5. The 2D part shown in Figure 2-5 is similar to one given in Figure 2-4. The feature $F$ of the 2D part in Figure 2-5(a) has a simultaneous size and form tolerance ($ST$ and $FT$) specification. The tolerance zone is obtained by offsetting the nominal feature $F$ corresponding to $ST$ specification as shown in Figure 2-5(b). An extreme instance of the resultant variation due to simultaneous effect of size and form tolerance is shown in Figure 2-5(b). Here, $dY$ is the position error in $y$ direction and $d\theta$ is the orientation error due to form tolerance.

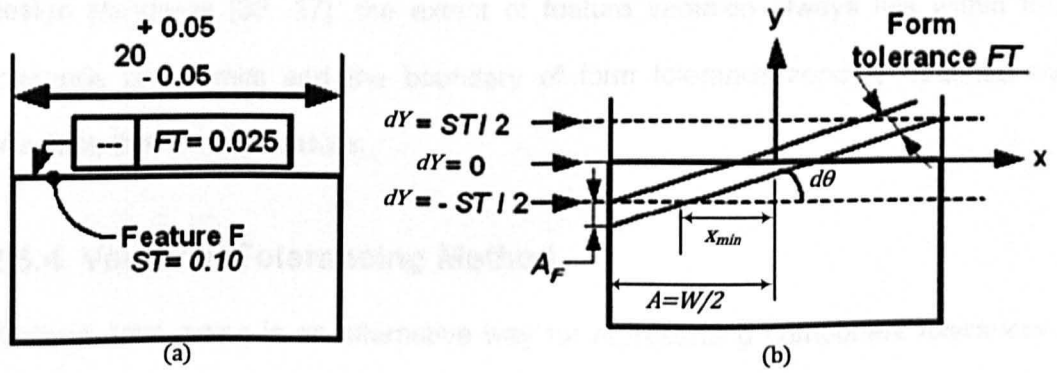


**Figure 2-5: (a) Feature with simultaneous tolerances, (b) An extreme instance of the resultant zones specified for feature F in (a) [46].**

Here, the variational model for tolerances is developed using algebraic constraints. The algebraic constraints for variables $dY$ and $d\theta$ are defined by the inequalities:

$$-d\theta_{\max} \le d\theta \le d\theta_{\max}, \tag{2.5}$$

$$-(ST/2) - A_F \le dY \le ST/2, \tag{2.6}$$

where, $d\theta_{max} = sin^{-1}\left(FT \div (A - X_{min})\right)$ and $A$ is half the extent of feature $F$.

The algebraic model given by Roy and Li [64, 65] is applied to extract the size, position and orientation error from given tolerance zones, but they consider the

The algebraic model given by Roy and Li [64, 65] is applied to extract the size, position and orientation error from given tolerance zones, but they consider the extent of feature variation to be the same as that considered in the parametric zone model (see Figure 2-4(b)). The calculated extreme variations about the extent of a feature are neither accurate nor conservative, because the intersections extend beyond the boundary specified by the design intent.

A form tolerance zone boundary and the extent of feature variation defined as above, for the studies conducted in the domain of parametric and algebraic models, contradict with the definition given in current design standards [36, 37]. According to design standards [36, 37], the extent of feature variation always lies within the tolerance zone limits and the boundary of form tolerance zone is obtained by offsetting the nominal feature.

### 2.5.4 Vectorial Tolerancing Method

Vectorial tolerancing is an alternative way for representing component tolerances. Vectorial tolerancing represents a chain of dimensions and tolerances as a link of vectors. Fortini [67] first introduced the concept of vector tolerancing. A comprehensive study of vector tolerancing applied to 2D assemblies was advanced by Bjorke [68]. The major development in vectorial method was done by Wirtz [69]. An overall perspective of the application of vectorial tolerancing is described in Wirtz [69]. In [69], deviations between the nominal part and the actual part are represented by using the vectors characterising their relative orientation and location. Thus, the deviation vector between these vectors represents the tolerance.

Vector models have been utilised extensively for both 2D and 3D assemblies by a group of researchers in Brigham Young University [34, 35, 70-73]. Their work showed that vector tolerancing methods can be applied to define individual parts

composed of different surfaces. Based on vectorial representation of part variations, they developed a vector loop method to calculate assembly variation propagations.

### 2.5.5 Homogenous Transformation Matrix Method

A mathematical representation of part variations using homogeneous transforms is a combination of the parameter space and offset solid modelling approach [74, 75]. The work of representing part tolerances using homogeneous transforms was initially seen in the thesis of Bernstein [76]. The inspiration of representing part variations using transform matrices came from the field of robot manipulators [21, 77]. Jastrzebski [78] and Whitney et al. [74] present a tolerance representation approach using matrix transforms to obtain part variation information that is suitable for tolerance analysis of assembly. In [74], the first order partial derivative of analysed variations with respect to its component's nominal dimensions in terms of a transformation matrix was employed for tolerance analysis.

Clement et al. [79] and Desrochers and Riviere [80] also used homogenous transformation matrix to develop tolerance zones. In [80] elementary surfaces were introduced and they were divided into seven types, called topologically and technologically related surfaces (TTRS). A homogeneous matrix transform represents six degrees of freedom (three translational degrees of freedom and three rotational degrees of freedom of error) of variation of a toleranced feature as:

$$\mathbf{DT} = \begin{bmatrix} 1 & -d\theta_z & d\theta_y & dX \\ d\theta_z & 1 & -d\theta_x & dY \\ -d\theta_y & d\theta_x & 1 & dZ \\ 0 & 0 & 0 & 1 \end{bmatrix}. \tag{2.7}$$

The method of representing part variation using homogeneous transform is also called as degrees of freedom (DOF) representation method. In this method, a small

variation torsor is defined as a 6D vector which contains three translational and three rotational values as under:

$$\tau = \left[ dX, dY, dZ, d\theta_X, d\theta_Y, d\theta_Z \right]^T . \quad (2.8)$$

Another method called "T-Map" was proposed by [39, 81, 82] which was similar to the set of model variables used in the DOF-based model. Recently a research group from Zhejiang University [83, 84] has conducted a detailed study on representing part geometric variation of complex surfaces using matrix transforms. They described the way of determining tolerance zone boundaries based on ISO standards, and interpreted tolerance semantics using a set of algebraic equations. This method was called Variations along DOF (VDOF) direction.

All homogeneous transforms methods are actually based on a tolerance zone defined in parametric space. These methods can be completed by a set of inequalities defining the bounds of the tolerance zone for each DOF of error such as:

$$-dX_{\min} \le dX \le dX_{\max} , \quad (2.9)$$

$$-dY_{\min} \le dY \le dY_{\max} , \quad (2.10)$$

$$-dZ_{\min} \le dZ \le dZ_{\max} , \quad (2.11)$$

$$-(d\theta_X)_{\min} \le d\theta_X \le (d\theta_X)_{\max} , \quad (2.12)$$

$$-(d\theta_Y)_{\min} \le d\theta_Y \le (d\theta_Y)_{\max} , \quad (2.13)$$

$$-(d\theta_Z)_{\min} \le d\theta_Z \le (d\theta_Z)_{\max} , \quad (2.14)$$

In all above cited literature, very little attention is given towards modelling variation (such as run-out variations) for axi-symmetric components, and no work has been

found that describes a variational model for axi-symmetric components capable of expressing component variation along degrees of freedom of component variation.

## 2.6 Assembly Modelling

Assembly quality mainly depend upon the variation of the component parts that are fastened together to form assembly. Assembly models are based on predicting the effect of size shape and location on overall assembly variation [33]. Modelling variation in mechanical assemblies has been a subject of intense research and has received attention by a wide spectrum of researchers. The work can be summarised into three main categories: assembly variation modelling, tolerance design and tolerance analysis.

### 2.6.1 Assembly Variation Propagation Modelling

Variation propagation modelling is a method of calculating the accumulation of tolerances in a mechanical assembly during individual assembly stages. It is the basic tool for statistical tolerance analysis. Several models have been proposed to represent the variation propagation in assembly processes. The models developed in broad spectrum can be grouped into two categories, depending on whether the model considers the assembly of rigid parts or flexible/compliant parts. Compliant refers to non-rigid parts like sheet metals used in the assembly of automotive body parts.

In the early stage of variation analysis research Veitschegger and Wu [85] performed calculations for the prediction of robot uncertainty. In their work they used the common method of $4 \times 4$ matrix transform [86] for the representation of relative locations of robot joints.

In later research [78], Jastrzebski generalised the derivations of Veitschegger and Wu and applied those calculations to the case of assembly modelling. In the work [85], position and orientation are described by five degrees of freedom, whereas, Jastrzebski considered six degrees of freedom to fully define the transformation in space. Jastrzebski provided the basic calculation for variation propagation in assemblies without looking into any type of tolerance. Gilbert [87] and Whitney et al. [74] extended the work of [78] and included geometric feature variation using matrix transform for assemblies compatible with tolerance analysis based on a closed form algorithm. These authors used $4 \times 4$ homogeneous matrix transform for representation of tolerance and developed individual homogeneous matrix transform to represent part and process associated errors.

Chase et al. [34] developed a vector loop-based assembly model for the analysis of tolerance stack-up in an assembly. They used vector assembly models based on 2D and 3D vector loops which represented the dimensional chains. This method allowed an assembly to be described in terms of vector chains added tip-to-tail, with kinematic joints inserted to represent the degrees of freedom between mating parts. Small dimensional variations were applied to the vectors, to calculate error accumulation [35].

Mantripragada and Whitney [88, 89] used state transition models to predict variation propagations in mechanical assemblies. In state transition model, the propagation of variations is treated as the propagation of errors during transformations of Cartesian frames. Cartesian frames are attached to mating features on every part. There exist six degrees of freedom for dimensional transformations of frames or their small errors. The model assumes that parts are assembled by joining mating features to each other and the state of an assembly at any assembly station is described by a $6 \times 1$ vector $\bar{\mathbf{X}}(k)$. The vector $\bar{\mathbf{X}}(k)$ describes the total deviation in the position

$(dp_k^X, dp_k^Y, dp_k^Z)$ and orientation $(d\theta_k^X, d\theta_k^Y, d\theta_k^Z)$ of a coordinate frame on a mating feature on the $k^{th}$ part along a KC chain, measured from its nominal or zero mean location, expressed in the coordinate frame of the part at the base of the chain. Mathematically, $\tilde{\mathbf{X}}(k)$ can be written as follows:

$$\tilde{\mathbf{X}}(k) = \begin{bmatrix} \mathbf{dp}_k \\ \mathbf{dR}_k \end{bmatrix} = \begin{bmatrix} dp_k^X \\ dp_k^Y \\ dp_k^Z \\ d\theta_k^X \\ d\theta_k^Y \\ d\theta_k^Z \end{bmatrix}. \tag{2.15}$$

The state transition form given by [88, 89] for rigid assemblies is as follows:

$$\tilde{\mathbf{X}}(k+1) = \mathbf{A}(k)\tilde{\mathbf{X}}(k) + \mathbf{F}(k)\tilde{\mathbf{w}}(k), \tag{2.16}$$

where,

$\tilde{\mathbf{X}}(k+1)$: $6 \times 1$ vector describing the total variation accumulated after the $k^{th}$ assembly station, defined with respect to the base coordinate frame for the KC chain.

$\mathbf{A}(k)$: Identity matrix.

$\mathbf{F}(k)$: $6 \times 6$ matrix that transforms the variation associated with the incoming part at the $k^{th}$ assembly station from part $k$'s coordinate frame to the base coordinate frame of the KC chain.

$\tilde{\mathbf{w}}(k)$: $6 \times 1$ vector describing the variation associated with the part being assembled at the $k^{th}$ assembly station, expressed in local part coordinates.

Mantripragada and Whitney [88, 89] also employed a state transition model to describe the propagation of variation in assembly of flexible parts and they refer to the flexible assemblies as Type-2 assemblies. In their work, the fixture is assumed to be perfect, implying they actually modelled the variation accumulation in assembly caused by part-fabrication imperfection. The work of Mantripragada and Whitney determines the in-process adjustments in Type-2 assemblies by the type of interface features between parts being assembled which are modelled as control inputs to the dynamic system. They also formulated a control problem to design these interfaces.

Zha et al. [90] proposed a knowledge-based expert system to support top-down design for assembled products. Their research involves the integration of artificial intelligence with the designer intelligence with the aim to increase productivity with improved quality. However, artificial intelligence in the manufacturing process industries requires advanced equipment for the assembly process which may result in considerably increased capital cost of the industry. The aim here is to propose cost effective methods to improve the quality of aero-engine assembly that does not require any additional tooling or equipment. Therefore artificial intelligence is not preferred.

Zhou et al. [91] refined the state transition model equation given by [89] and introduced a new term of un-modelled system noise $\mathbf{U}(k)$. The state-transition model equation given by Zhou et al. is given as:

$$\tilde{\mathbf{X}}(k+1)=\mathbf{A}(k)\tilde{\mathbf{X}}(k)+\mathbf{F}(k)\tilde{\mathbf{w}}(k)+\mathbf{U}(k). \tag{2.17}$$

Most of the above mentioned research work is focused on rigid assembly modelling at the conceptual stage of design, and are not fully compatible with all types of geometric tolerances (such as run-out tolerances).

Numerous studies have also been conducted in the area of variation analysis of flexible assembly. Flexible part models consider the possible deformation of the parts during the assembly process. Liu and Hu [92] proposed a model to analyse the effect of deformation and spring back on assembly variation by applying linear mechanics and statistics. Using finite element methods, they constructed a sensitivity matrix for compliant parts of complex shapes. The sensitivity matrix establishes the linear relationship between the incoming part deviation and the output assembly deviation.

Ding et al. [93] used state-space models to calculate variation propagation in a multi-station assembly system of compliant (flexible) parts while considering part, process and tooling variations. The study focuses on controlling variation propagation stage-by-stage in assembly using fixture adjustment only applicable to compliant assemblies. Ding et al. [24, 94] extended their model to diagnose process variations in order to identify the root cause of an occurred fault. They developed a diagnostic algorithm based on the system model which receives the input data from a series of sensors installed to monitor in-process variation in the assembly. They also developed an optimal sensor distribution algorithm known as "saturated sensing" to measure all degrees of freedom of each part and monitor the process functionality.

Hu et al. [95] proposed a numerical simulation method for the assembly process incorporating compliant non-ideal parts to consider the interaction and interference between compliant parts due to part variation, assembly tooling variation, welding distortion, and spring-back effects. Their method combines elastic and contact analyses by using FEM code in a commercial software ANSYS. Hu et al. [95] only considered four steps for the assembly process to analyse their effect on assembly variation, positioning, clamping, welding and releasing,

Camelio et al. [96-99] developed a methodology to evaluate the dimensional variation propagation in a multi-station compliant assembly system based on linear mechanics and a state-space representation. They analysed three sources of variation: part variation, fixture variation and welding-gun variation. They presented a methodology for modelling the impact of part and tooling variation on the dimensional quality on a multi-station assembly system with compliant sheet metal parts. This methodology states how variations propagate from different subassemblies to the final product. Camelio et al. [96] used a modified form of state transition method given by [91] for multistage machining process.

Kong et al. [100] proposed a method to model both fixture and part variation in multi-station assembly model. In this method instead of using Monte Carlo simulation or another statistical method, they directly calculated the dimensional variation by using as inputs tolerance assigned to fixture locator and part fabrication. The work is actually an expansion of 2D Stream of Variation Analysis (SOVA) model to 3D by including "3-2-1" fixture locating scheme.

Lee et al. [101] proposed a method to integrate Finite Element Analysis (FEA) with three dimensional variation analysis of assembly to determine the effect of part variation and flexibility on the assembly's variation. The research presents a procedure for variation analysis of a complex assembly that integrates Datum Flow Chain analysis, a commercial three-dimensional variation analysis, and FEA.

Huang and Kong [102] very recently proposed a rigid-compliant hybrid assembly model for stream of variation analysis. Rigid-compliant hybrid assembly modelling is an effort for providing an interface to rigid and compliant assembly models for variation analysis in compliant assembly.

Most of above mentioned literature use only linear model to calculate assembly variation propagation and also require mathematically intensive calculations. There is a need to develop a model that is more accurate and requires less mathematically intensive calculations.

### 2.6.2 Tolerance Design

Tolerance design is the assignment of tolerances based on process capabilities, cost, or performance requirements. This process is also known as tolerance synthesis or tolerance allocation [103]. In this, there is only one assembly tolerance condition and many unknown component tolerances that must be determined. It is performed early in the product development cycle, before any parts have been produced or tooling ordered. Tolerance allocation involves three tasks. First, deciding what tolerance limits to place on the critical clearances and fits for an assembly, based on performance requirements. Second, creating an assembly model to identify which dimensions contribute to the final assembly dimensions. Third, deciding how much of the assembly tolerance to assign to each of the contributing components in the assembly [71].

Most of the approaches that have been published in the field of tolerance design are based on the optimisation of the cost-tolerance function [104, 105]. These methods usually try to get optimal tolerance values while the tolerance types are assumed to be fixed [106]. Haugland [107] and Loosli [108] also performed research in this area. They applied the method of Lagrange multipliers and cost versus tolerance functions to allocate the specified assembly tolerance among the component dimensions to achieve the least cost. Chase et al. [109] extended the work of Loosli to find the least-cost set of tolerances and the least-cost process from a set of alternative processes for each dimension in the assembly.

The usage of these models in industry is very limited. One of the major reasons for this is that these methods usually try to take advantage of the superficial knowledge of processes, which is usually obtained from the machinist handbook or the company manual. As this research is focused on tolerance analysis, less attention is given to tolerance design for review in this thesis. The reader is referred to [110] for a more detailed review on tolerance design.

### 2.6.3 Tolerance Analysis

In an assembly there are critical dimensions (called assembly KCs) which must be controlled within a specified range. Controlling the critical dimensions ensures that the assembly will function as intended by the designer [35]. The need to control the quality of production and to manufacture parts interchangeably led to the development of tolerance specifications. Tolerance specifications are the critical link between the designer and the manufacturer. Designers prefer tight tolerances to ensure that the part will fit in the assembly and perform its function. Manufacturers, on the other hand, prefer loose tolerances to lower the production cost and decrease the need for quality machine tools, and precision measurement machines [106, 111]. Tolerance analysis methods play a key role in bridging between the two.

Tolerance analysis is carried out when the tolerances of individual parts are known and the designer intends to find out or allocate the dimensions for assembly. This involves: first, gathering data on the individual component variations; second, creating an assembly model to identify which dimensions contribute to the final assembly dimensions; third, applying the manufactured component variations to the model to predict the variations in assembly dimension [71]. Tolerance analysis is a method of predicting and analysing assembly variation due to tolerance of individual components and assembly operations [112]. Tolerance analysis verifies the proper functionality of a design while considering variations associated with the individual

parts in an assembly process. Tolerance analysis can be based on either deterministic method or statistical method for the analysis of one-, two-, or three-dimensional design models [106]. Deterministic tolerance analysis can also be termed as variation propagation modelling, which is carried out for existing assemblies. However, statistical tolerance analysis uses suitable statistical methods for predicting assembly variability or tolerance. This section (Section 2.6) discusses the review of literature related variation propagation modelling, whereas, the review of literature related to statistical tolerance analysis is given in Section 2.7.

## 2.7 Statistical Tolerance Analysis for Assemblies

Statistical tolerance analysis provides a quantitative design tool for predicting the effects of manufacturing variation on performance and cost. For tolerance analysis the stack-up effects on the functional requirements are computed analytically by means of approximation methods (e.g., worst-case, statistical or Monte-Carlo simulation, etc.). Here, three common types of statistical tolerance analysis methods for mechanical assemblies are described, whereas the reader is referred to [113] for more detailed review in the field of statistical tolerance analysis. Three common types of statistical tolerance analysis methods are:

- Worst Case;
- Statistical Method;
- Monte Carlo Simulation Method (MCS).

### 2.7.1 Worst Case

In worst case tolerance analysis, the analysis examines the assemblability of parts while considering the worst possible combination of individual tolerances. This results in un-necessarily tight part tolerances and hence high production cost. In the

early stages of tolerance analysis [114, 115] the most common worst case tolerance accumulation model was used, which are defined by equations given in [106]:

$$T_{ASM} = \sum_{i=1}^{N} T_i \text{ (one-dimensional assemblies)} \quad (2.18)$$

$$T_{ASM} = \sum_{i=1}^{N} \left( \left| \partial f / \partial x_i \right| T_i \right) \text{( multi -dimensional assemblies)} \quad (2.19)$$

where, $T_{ASM}$ is assembly tolerance, $T_i$ tolerance of individual component, $N$ = number of assembly components, and $\partial f / \partial x_i$ is the sensitivity of the assembly tolerance to variations in individual component dimensions.

The worst case model is no more used for tolerance analysis because the worst case model results in component tolerances which are tight and costly to produce.

### 2.7.2 Statistical Methods

Statistical tolerance analysis methods can be applied to geometric models of assemblies to predict the magnitude of variation in critical assembly features. The resulting statistical distributions may be used to estimate the percentage of rejects and to see if the assembly quality specifications will be met. In statistical tolerance analysis, each dimension of the assembly components is viewed as a random variable, which is distributed according to a specific probabilistic model. Specific probabilistic models are obtained from measured data if available, or empirical models [116].

Statistical tolerance analysis is more practical and economical way of looking at assembly and part tolerances. One objective of a statistical tolerance analysis is to determine the probability distribution of assembly response functions $Y$. Assembly response function is the measurable design characteristics of an assembly such as

assembly KC, which is the function of its constituent design variables $(X_1, X_2, \ldots X_n)$ of individual parts or subassemblies making up the assembly (such as dimensions and tolerances). In statistical tolerance analysis, each dimension of the assembly components $X_i$ is viewed as a random variable, which is described by an specific distribution. Specific distributions are obtained from measured data available for large number of manufactured components. The relationship between the value of $n$ variables of constituent parts and the assembly response may be expressed as:

$$Y = f(X_1, X_2, \ldots, X_N). \tag{2.20}$$

Any relation in any form can exist between assembly response and variables of constituent part (dimension or tolerance). Various statistical methods have been used for the estimation of magnitude of variation in critical assembly features and for predicting the effects of manufacturing variation on final assembly. The most common statistical method of tolerance accumulation used in early stage of tolerance analysis was the Root Sum Square (RSS) [67, 117]. RSS method takes into account statistically the low probability occurring in the worst case combination, assuming mean $\mu$ and standard deviation $\sigma$ of each component dimension are known and are normally distribution random variable $N(\mu, \sigma^2)$. Tolerances are commonly assumed to correspond to six standard deviations $(\pm 3\sigma)$ [72]. RSS can be defined by the following equations:

$$T_{ASM} = \sqrt{\sum_{i=1}^{n} T_i^2} \text{ (one-dimensional assemblies)} \tag{2.21}$$

$$T_{ASM} = \sqrt{\sum_{i=1}^{n} (\partial f / \partial x)^2 T_i^2} \text{ ( multi -dimensional assemblies)} \tag{2.22}$$

In a more general case, RSS for other than $\pm 3\sigma$ tolerance distributions can be calculated as [70]:

$$T_{ASM} = C_f z \sqrt{\sum_{i=1}^{n} (\partial f / \partial x)^2 (T_i / z_i)^2} \quad (2.23)$$

where, $z$ is the number of standard deviations desired for the specified assembly tolerance, $z_i$ is the expected standard deviations for each component tolerance, $C_f$ is a correction factor frequently added to account for any non-ideal conditions.

A statistical tolerance accumulation model given by [34, 35] is given by the equation:

$$\delta U_i = \sqrt{\sum_{j=1}^{n} (S_{ij} tol_j)^2} \cong T_{ASM_i} \ (i=1,2,.....,m) \quad (2.24)$$

where, $m$ is number of assembly variables which are critical to the design, $n$ is number of contributing manufactured dimensions, $tol_j$ is the tolerance of the $j^{th}$ manufactured dimension, $T_{ASM_i}$is design specification for the $i^{th}$ assembly variable, and $U_i$ and $S_{ij}$ are elements of the sensitivity matrix of the assembly constraint.Later Greenwood and Chase [70, 118] pointed out that, in the application of the simple RSS analysis, the mean is shifted due to set-up error or drifts caused by tool wear. They proposed an estimated mean shift model to improve the approximation by simple RSS method, but still these RSS methods does not produce accurate results. The tolerance accumulated by estimated mean shift model is given by:

$$T_{ASM} = m_i \frac{\partial f}{\partial x} T_i + \sqrt{\sum_{i=1}^{n} (1-m_i)^2 (\partial f / \partial x)^2 T_i^2} \quad (2.25)$$

where, $m_i$ is the estimated mean shift factor, whose value range from 0 to 1.

The above conventional statistical methods of tolerance analysis are inadequate, because these methods give results that are more optimistic.

Another statistical method known as tri-variate normal probability distribution method, introduced in [85] and used for variation analysis, is based on closed-form matrix transform solution. The tri-variate normal probability distribution method describes the variability of a system by a 3D differential vector of order $3 \times 1$. Veitschegger and Wu [85] worked in the domain of robot uncertainty prediction. Later this concept of a closed-form algorithm was applied to the case of mechanical assemblies in the work of Jastrzebski [78]. Jastrzebski's method deals with continuous statistical variables in three dimensions. Jastrzebski described assembly variation by tri-variate normal probability distribution functions while assuming all kinematic errors of the system are statistically independent normally-distributed random variables. The propagation of tolerances is statistically performed from part to part using a closed form error propagation algorithm. This method was used for the approximation of rotation and translation vectors of a system. Thus the tri-variate normal density functions for differential translation vector and the differential rotation vector are given as:

$$f(\mathbf{dp}) = \frac{1}{(2\pi)^{3/2}\left|\mathbf{V_p}\right|^{1/2}} \exp\left\{-0.5\left[(\mathbf{dp})^t \mathbf{V_p^{-1}} (\mathbf{dp})\right]\right\} \tag{2.26}$$

$$f(\mathbf{d\theta}) = \frac{1}{(2\pi)^{3/2}\left|\mathbf{V_\theta}\right|^{1/2}} \exp\left\{-0.5\left[(\mathbf{d\theta})^t \mathbf{V_\theta^{-1}} (\mathbf{d\theta})\right]\right\} \tag{2.27}$$

where, $\mathbf{dp}$ is translation vector, $\mathbf{d\theta}$ is rotation vector, $\mathbf{V_p}$ is $3 \times 3$ covariance matrix of $\mathbf{dp}$ translation vector, $\mathbf{V_\theta}$ is $3 \times 3$ covariance matrix of $\mathbf{d\theta}$ rotational vector.

The above statistical method of tri-variate normal probability distribution for approximation of translation and rotation errors was also used by Whitney and his co-workers [21, 22, 27, 74] for analysing 3D variation propagation in mechanical assemblies. The tri-variate normal density functions (Equations (2.26) and (2.27))

give joint distribution of translation $(dX, dY, dZ)$ and rotation $((d\theta_x, d\theta_y, d\theta_z)$ errors of $n^{th}$ transformation frame in the assembly in three-dimensions. In order to calculate the distribution error in a particular degree of freedom (for example $dX$), double integral of Equations (2.26) is needed with respect to $y$ and $z$ that require extensive calculation and is not much accurate. Clearly, there is a need to take into consideration the probabilistic behaviour of the manufacturing processes that produce each feature, and the probability distributions of the resulting assembly response functions.

### 2.7.3 Monte Carlo Simulation (MCS) Method

Traditional Monte Carlo Simulation is widely used in assembly tolerance analysis for assemblies which have linear or explicit non-linear assembly function, that is, each assembly variable must be expressed as a single algebraic function of the manufactured dimensions. The Monte Carlo simulation is very useful when the function of random variables given in Equation (2.20) is complicated in form and the derivation of the statistical moments of given function become challenging.

The MCS method performs repeated assembly simulations based on randomly selected variables. First, the assembly functions are formulated relating the component dimensions to the resultant assembly dimension. Second, the assembly variables are randomly generated based on the appropriate statistical distribution for each manufactured variable. Third, based on the statistical distribution of all contributing variables, the distribution of key assembly parameter is obtained. These values of statistical distribution are combined through the assembly function to determine a series of values of the assembly variable. This series is then used to find the distribution of assembly variation at each assembly stage, and percentage

of assemblies which fall outside the design specifications, or the assembly reject rate [119].

In MCS the sample size must be very large in order to achieve accurate predictions for high-quality levels with small non-conforming fractions. Due to the large sample sizes required, few years ago the solution was considered to be time consuming and computationally expensive [120]. However, due to advanced technology and the high computation speed of personal computers has made it possible to perform Monte Carlo simulation in an affordable time in some cases.

## 2.8 Assembly Error Minimisation

In order to improve the assembly quality it is necessary to control or minimise assembly variation during the assembly. Different error minimisation methods can be applied to different types of assemblies. But the method to control assembly variations must be economical and effective. The research in the area of assembly error minimisation has been given very limited attention in the past. The research in the area of minimising assembly variation is reviewed as follows:

Ceglarek and Shi [121] developed a methodology for reducing dimensional and performing root cause analysis in automotive body assembly. Their methodology is based on diagnostic of fixture fault method, while assuming the automotive body parts as rigid, with single fault and single fixture. Subsequent efforts were made to improve the methodology developed in [121] with more general assumptions, such as multiple faults, compliant components, and multiple fixtures [122, 123]. Hu and Camelio [124] proposed a methodology to reduce dimensional variation in automotive assembly considering component variation due to deformation after assembly. Their methodology to reduce assembly variation applies correction in the

assembly use tooling adjustment technique based on in-line measurements. All above variation reduction methods were used to minimise dimensional variations only for the assembly of compliant parts.

Mantripragada [88, 89] proposed a statistical control theory to minimise assembly errors. The control theory given in this work concentrates on designing the mating features that provide necessary freedom to make possible adjustments during assembly. The proposed control theory can only be applied at the conceptual design stage. Dantan et al. [125] suggested an idea of integrated tolerancing process that provides general methods and tools for reducing geometrical variations in assembled products. Forouraghi [126] focussed on allocating assembly tolerances to minimise total assembly cost. Zhang and Wang [127] developed an analytical model for optimal process sequence selection through planning the dimensions and tolerances for assembly tolerance allocation. None of these methods considered the geometric variations of assembly components in their models.

Another approach of assembling two components based on measurement data of the components known as "selective assembly" is studied by various researchers [128-131]. Selective assembly can only be applied to high-volume assembly products, where mating components are measured and the measurement data collected. The measurement data is then divided into groups. The components are assembled together by randomly selecting components from the grouped data in order to meet the required specifications as closely as possible. The limitation of the selective assembly approach is that it can only be applied to assemblies in mass production or batch production. But for the assembly of low-volume customised products (such as aero-engines, large turbines) the selective assembly approach cannot be applied due to a very limited number of products.

Turner [132] and Li and Roy [133] formulated a mathematical programming approach to find the optimal configuration of parts using a relative positioning technique based on geometric positioning of mating features of the part and neighbouring parts. They consider the variation of existing components in the real world to find the optimal configuration of the two mating parts. However, this approach cannot be applied to assembly where the mating components are only allowed to change the relative angular orientation of the components and where the assembly process is manual.

No work has been presented for assemblies of high-value low-volume customised product of rotating machines with mostly manual operations and considering form tolerances.

## 2.9 Summary and Perceived Knowledge Gaps

In this chapter, the literature has been reviewed in the area of modelling component variation, modelling assembly variation propagation, statistical tolerance analysis, and assembly error minimisation. For modelling component variation, homogeneous transform matrix (HTM) method is a robust method and is capable to capture the component variations along the three degrees of translation errors and the three degrees of rotation errors. HTM method is also compatible with most of the assembly variation propagation modelling approaches reviewed in the literature. For assembly variation modelling, most of the research is carried out at the conceptual stage of design and the models developed are not very accurate. Also, the reviewed methods do not incorporate geometric feature variations, assembly process variations, and the measurement error variations at the same time. In past mainly linear methods and a few non-linear methods have been developed. The linear methods are quicker and computationally simple, whereas non-linear methods are

computationally extensive and time consuming. Among existing linear methods, no method have been proposed that enable the design engineer to quantify major contributing factors in the assembly variation, whereas the existing non-linear methods are not very accurate. Hence, there is a need of assembly variation modelling method(s) that enable the design engineer to quantify major contributing factors and (or) are more accurate in calculating assembly variations with capability of incorporating geometric feature variations, assembly process variations, and the measurement errors.

Tolerance analysis is performed in order to predict the effects of manufacturing variations present in each assembly component on final assembly variation. Various tolerance analysis methods have been reviewed in this chapter, which include; (i) worst-case (WC) criterion based on the arithmetic law (ii) root sum square (RSS) criterion based on the statistical model, (iii) tri-variate normal distribution approach, and, (iv) Monte Carlo Simulation (MCS) method. Both the WC and the RSS approaches are based on unrealistic assumptions and lie on the two extremes of the spectrum. These approaches do not yield accurate results, but can only be used for making a rough estimate of the assembly response. The tri-variate normal probability distribution approach is the method of approximation of translation and rotation errors in an assembly by a joint distribution function. In practice, assembly variations are described in a particular degree of freedom of variation, and a joint tri-variate distribution function is not capable for calculating assembly variation in a required degree of freedom of variation. In order to calculate the distribution of error in a particular degree of freedom, double integral is required that require extensive calculation and is not much accurate. This limits the application of tri-variate joint distribution approach for tolerance analysis in various mechanical assemblies. Monte Carlo simulation (MCS) method is another way of performing tolerance

analysis that requires randomisation of part dimensions. MCS is based on randomly generating variables defining component parts and calculating the manufacturing variations in the resulting assembly. By repeating this procedure the statistical properties and distribution of the manufactured assembly can be determined. The accuracy of MCS depends upon the number of repeated simulations performed. However, to achieve accurate predictions, the large number of simulations can be time consuming and computationally expensive, therefore, analytical methods preferable over MCS. In the literature, no analytical method has been reported that provide more realistic assembly variation analysis efficiently to calculate the assembly variability in a particular degree of freedom.

In high value product assembly of high speed rotating machines, high precision is needed during assembly in order to achieve precise assembly key characteristics. Variation propagation control methods can be used to improve assembly quality to achieve precise assembly key characteristics. Very limited attention has been given in the literature on variation propagation control or assembly optimisation methods. Most of the assembly optimisation methods are focused on assembly of prismatic components. No research has been found in past that focus on error minimisation in assembly of rotating and non-rotating structures (engine rotor and engine casings) of rotating machines. This requires an effective and economical method to minimise error propagation in high speed rotating machines.

## 2.10 Aims and Objectives

The overall aims of the project are to improve understanding of error build-up and variation propagation in mechanical assemblies, especially aero-engines rotors and casings, and to provide means for reducing assembly variations. The measurable objectives are to derive generic mathematical models and implement computer

simulations for complex mechanical assemblies, to develop algorithms for the determination of variation in a final assembly, and to investigate control strategies for in-process adjustments in mechanical assemblies. The objectives of this study are:

- Develop models to calculate variation build-up in mechanical assemblies (in general) more accurately and/or that is capable to quantify major contributing factors in the assembly variation.
- Formulate a method to incorporate the effect of form variation/tolerances in terms of translation and rotation for variation build-up in the rotor and casing assembly of high speed rotating machines.
- Adapt statistical methods to model variation associated with individual parts and to analyse their effects on final assembly variation of high speed rotating machines.
- Propose assembly error minimisation method for assembling axi-symmetric components and uniformly segmented circular components.

# Chapter 3 RESEARCH METHODOLOGY

## 3.1 Introduction

The literature review presented in Chapter 2 predominantly revealed that the field of modelling and controlling variation propagation in mechanical assemblies has been given very less attention in the past. No assembly variation propagation model has been reported in past that produce exact results for calculating assembly variation propagation and is capable of incorporating geometric feature variations, assembly process variations, and the measurement errors. In past mainly linear methods and a few non-linear methods have been developed. The linear methods are quicker and computationally efficient, whereas non-linear methods are computationally extensive and time consuming. Among existing linear methods, no method have been proposed that enable the design engineer to quantify major contributing factors in the assembly variation, whereas the existing non-linear methods are not very accurate. On the other hand, for controlling assembly variations, very limited

research is conducted so far and no any research is reported that focus on controlling variation propagation in the assembly of rotating and non-rotating structure of high speed rotating machines.

This thesis is targeted towards the modelling variation propagations in mechanical assemblies in general to produce accurate results and to enable the design engineer to quantify major contributing factors in the assembly variation, develop method to perform statistical tolerance analysis, and to control variation propagation in the assembly of rotating and non-rotating structure of high speed rotating machines. Two methods are developed to model assembly variation propagation, namely Linear Method and Exact Method. The linear method is developed to precisely approximate assembly variation propagation (providing quick decision making during statistical tolerance analysis) and to enable the design engineer to quantify major contributing factors in the assembly variation. On the other hand, exact method is developed to calculate exact solution for assembly variation propagations and to provide a performance benchmark to verify the accuracy/performance of the simplified (linear) model. Another advantage of the exact model is that the exact model is capable enough to incorporate for assembly process variations and measurement error in assembly variation analysis.

The proposed assembly models (linear and exact) can be used to analyse existing assemblies or the assemblies at conceptual stage of design. In the later case, statistical tolerance analysis is performed in order to predict the effects of manufacturing variations present in each assembly component on final assembly variation. For the linear model, it is possible to derive analytical expressions for the probability density function (pdf) of assembly errors, however for the exact model the statistical tolerance analysis can only be performed by Monte Carlo Simulation method. This highlights the competency of the linear model over the exact model,

because the statistical tolerance analysis performed by analytical expressions of the pdf is much more efficient than the analysis based on the Monte Carlo simulation method that require a very large number of repeated simulations for better prediction. The details are shown in Chapter 7.

The research survey presented in Chapter 2 highlighted knowledge gaps into clearly defined research objectives. In order to achieve the research objectives, this chapter presents an overview of the research methodology adopted in the study. This study is concentrated on the assembly of rigid mechanical components, whereas the possible scope of the proposed methods and models is expected to be much broader. It may also be applied to the assembly of non-rigid components with some modifications.

This chapter provides step-by-step methodology of modelling and controlling variation propagation in assemblies. Each section of this chapter is referring to the relevant chapters of the thesis where a more detailed description is provided. Two assembly case studies of high-value low volume products have been focused throughout the thesis for modelling and controlling assembly variation propagations. The first case study is an example of a rotating part (rotor) from high-speed rotating machines, whereas the second case study is a non-rotating part (stator) of a high-speed rotating machine. The second case study is the assembly example taken from [7, 134].

An overview of the research methodology for calculating and controlling variation propagations in mechanical assemblies is given in next section.

## 3.2 Research Methodology/Research Approach

This research focuses on calculating and controlling variation propagations in mechanical assemblies. The research methodology adopted for calculating and controlling assembly variation propagations comprises four main steps: (i) a complete description of component variations; (ii) transforming component variations into variations along degrees of freedom (VDOF) for each component; (iii) calculating assembly variation propagations and, (iv) controlling or minimising assembly variation propagations. These steps are described by the flow chart given in Figure 3-1.

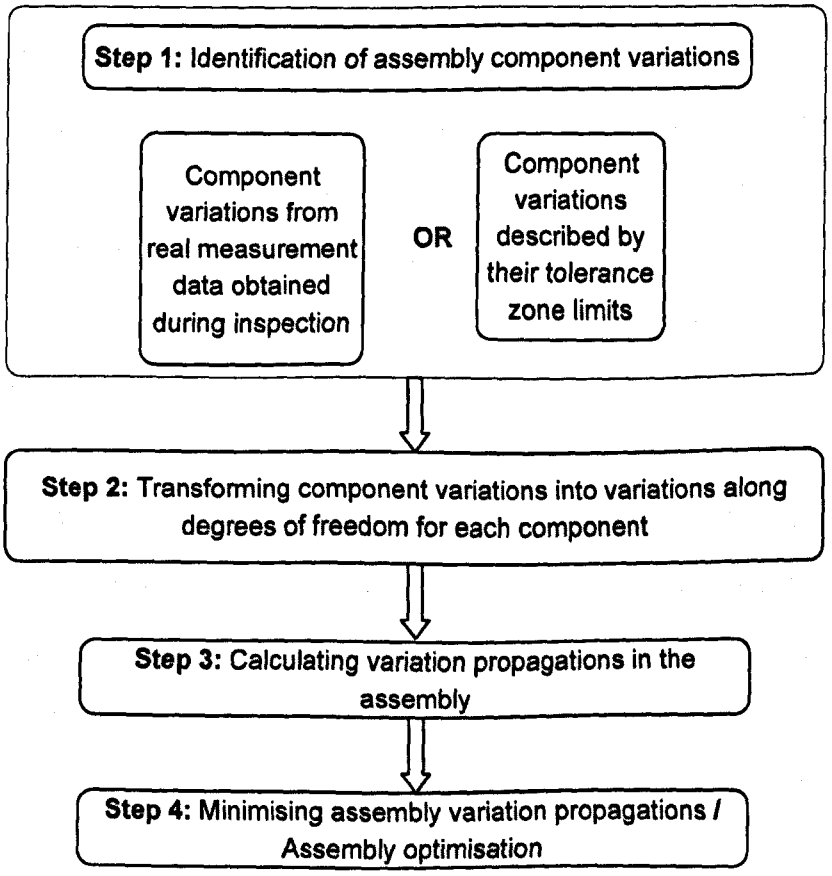


**Figure 3-1: Flow chart of methodology**

### 3.2.1 Step 1: Describing Assembly Components Variations

The first step of calculating and controlling assembly variation requires the knowledge of components variation and identifying key component variations. If the

component variations are known then the variations accumulated after assembling these components can be calculated using a suitable mathematical model. In a manufactured component different types of variation are present such as size (or dimensional), geometrical, form, etc. The assembly variations not only depend on the dimensional variations of individual components, but geometric variations also play a major role in assembly variation propagations. For the purpose of modelling, only those variations are of interest that are critical to assembly variation propagation. These variations are called key component variations and they depend upon the shape, type (rigid/non-rigid) and role of the component part in the assembly. As discussed earlier in Section 3.1, two assembly case studies of rotating part and non-rotating part of high speed rotating machines are studied in this thesis, therefore variations related components of the two case studies are only discussed throughout this thesis. In real assemblies the component variations can be measured during part or product inspection and assembly variation propagations can be calculated using real measurement data. For example in Case Study 1, rotating parts of a rotor are axi-symmetric in shape, and the industries assembling high-value rotating machines, measure the component to check for run-out [135] in axial and radial direction of the mating features from their nominal configuration (see Figure 3-2). The challenge here is to characterise variations present in the axi-symmetric component with respect to its axis of rotation. The task of characterising run-out variations in axi-symmetric component for the purpose of modelling assembly variations has not been carried in the past, but is described next.

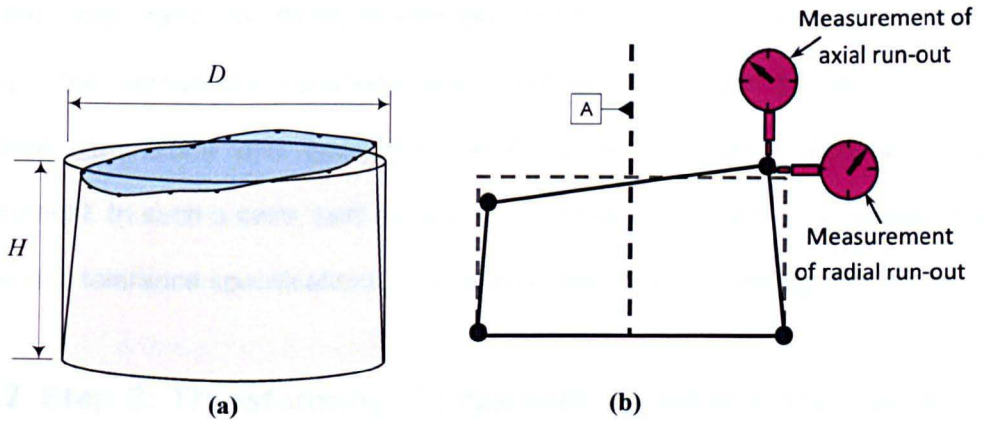


**Figure 3-2: (a) A cylindrical component with its nominal shape and after containing manufacturing variations; (b) Measurement of axial and radial run-out for a cylindrical component (2D view).**

In Figure 3-2(a) a cylindrical component is shown with nominal height $H$ and nominal diameter $D$, whereas, due to manufacturing variations the cylindrical component contains variation that cause a top-surface feature to be mis-positioned and mis-oriented. Figure 3-2 (b) illustrates how to assess the amount of variations present in manufactured component by measuring the component for axial and radial run-outs. Several points can be measured to check the run-out variation at each mating feature of the axi-symmetric component. Mathematically, axial and radial run-out can be defined in polar coordinate system as a function of angle of measurement $\theta$ by the following equation:

$$r(\theta) = R + r_{run-out} \tag{3.1}$$

$$z(\theta) = H + a_{run-out} \tag{3.2}$$

where, $r$ is the actual radius of a point, $R$ is the nominal radius of the circle feature, and $r_{run-out}$ is the measured value of radial run-out with respect to ground reference. Likewise, $z$ is the actual height of a point, $H$ is the nominal height and $a_{run-out}$ is the measured value of axial run-out at that point.

On the other hand, for those assemblies which are at the conceptual stage of design, the component variations are described by design tolerances for the nominal dimensions and geometric variations at the mating feature of each component. In such a case, part variations are modelled based on dimensional and geometric tolerance specifications. This is described in the following section.

### 3.2.2 Step 2: Transforming Component Variations into Variations along Degrees of Freedom

For the purpose of assembly modelling, it is necessary to mathematically describe the geometric variations of each component, using a suitable algorithm that is compatible with the assembly variation propagation model. In this thesis the models used for calculating assembly variation propagation are based on the homogeneous transform matrix (HTM). Using HTM, component variations can be described in terms of three degrees of freedom of translation error $(dX, dY, dZ)$ and three degrees of freedom of rotation error $(d\theta_x, d\theta_y, d\theta_z)$. Therefore, components variations described by real measurement data or described in terms of design tolerances must be transformed into variations along degrees of freedom of components error $(dX, dY, dZ, d\theta_x, d\theta_y, d\theta_z)$. The aim of converting form tolerance into location and orientation tolerance in this research is to represent allowable variation or design intent in a format compatible with the model for calculating variation propagation in an assembly. The review of literature in Chapter 2 has shown that no research has been carried out that transform geometric variation of axi-symmetric components and uniformly segmented components into variations along degrees of freedom. A novel approach has been adopted to represent variations of axi-symmetric and uniformly segmented components (used in assembly Case Study 1 and 2 respectively) into variations along degrees of freedom (As detailed in Chapter 5).

For example, in the case of axi-symmetric component, if the axial and radial run-out data is obtained from the measurements, the data can be evaluated to find the location and orientation error of the actual feature with reference to the corresponding nominal form. The axial run-out and radial run-out is evaluated separately using suitable best-fit algorithms, as discussed in Chapter 5 and Appendix. The radial run-out data is examined to find the location error of the actual mating feature in the direction perpendicular to a datum axis, whereas, the axial run-out data is analysed to evaluate the relative orientation error of actual feature with reference to the nominal feature and the location error in direction along the datum axis.

If the variations are described by design tolerances, the components variations are described by variational constraints based on design tolerances. Variational constraints are the algebraic relations describing the effect of individual tolerance in terms of the resulting translation or rotation error of the corresponding mating feature. Chapter 5 details the variational constraints relations for component variations based on geometric and dimensional tolerances.

### 3.2.3 Step 3: Modelling Assembly Variation Propagations

In order to increase assembly quality it is necessary to know variation propagations in the assembly stage-by-stage. To study and analyse assembly related problems it is essential to develop an appropriate assembly model which enables the representation of an assembly and its components mathematically and to calculate errors accumulated during the assembly. Variation propagation methods are widely used in manufacturing to calculate assembly variation and for tolerance analysis. This thesis presents two novel variation propagation methods based on simple homogeneous matrix transforms, namely a Linear method and an Exact method. The linear model is based on first order perturbation analysis of transformation

matrices and is useful for characterising contributing factors in assembly variations. On the other hand, the exact model uses fully non-linear approach providing exact calculation for assembly variation propagations and is capable to accommodate for assembly process and in-process measurement errors, for calculation of error build-up in an assembly. The details of both variation propagation models can be found in Chapter 4. This chapter only provides the general concept and methodology for calculating assembly variation propagations.

In the proposed variation propagation methods, the components parts are located with respect to each other by transform matrix. A transform relates each feature's location on the part to the part's central coordinate frame. The model assumes that parts are assembled by joining "mating features" to each other [136]. To represent assembly and components Cartesian frames are attached to the mating features and all transformations relate to these frames. The propagation of variation is treated as propagation of errors during transformations of Cartesian frames. The step-by-step methodology of proposed variation propagation models is given in Figure 3-3.

Initially, for preliminary analysis, the proposed variation propagation models (linear and exact model) are designed to calculate the assembly variation propagations while considering components' variation only for 2D and 3D assemblies. No matter the models (linear and exact model) whether applied to 2D or 3D assemblies, the general method for calculating assembly variation propagations is described in Figure 3-3.

Figure 3-3 shows that the first step towards calculating assembly variation is to describe the nominal dimensions and variation of each assembly component using nominal and differential matrix transforms, respectively. Once the nominal and

differential transforms are defined, the actual component containing manufacturing variations is defined using a combination transform by multiplying the nominal transform with the corresponding differential transform. The assembly can now be represented in two ways: nominal assembly, and actual assembly. The nominally assembly is represented by multiplying the nominal transform of $N$ components as a chain of matrix transforms. As parts are added to the assembly, the actual location of the last part in the assembly is calculated by multiplying together all combination transform. The accumulation of error during the assembly is obtained by calculating the difference between the chain of transforms for the actual and nominal assemblies.

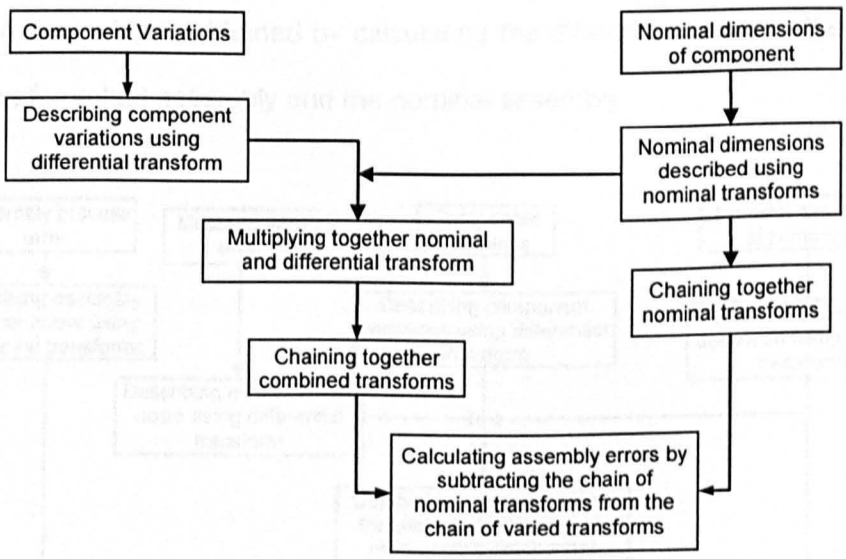


**Figure 3-3: A diagram representing various steps involved in calculating assembly variation propagations while considering component variations only.**

In order to account for assembly process variations and measurement errors in assembly variation analysis, this thesis presents the extension for the exact (non-linear) model to account for measurement and process errors in calculating assembly variation propagations.

Figure 3-4 describes the method of incorporating measurement and process errors in the exact model. It shows that manufacturing variations of components and measurement errors are described by separate differential transform and the net components variations are described by post-multiplying measurement error differential transform with differential transform for manufacturing variations in each component. The nominal transform representing the nominal dimensions of a component is multiplied with a net differential transform to get the net dimensions of each component. Assembly process error are incorporated by pre-multiplying a transform representing assembly process errors with a transform representing net dimensions of each component. The actual assembly can thus be described by chaining together these combined transforms. Finally, the accumulation of error during the assembly is obtained by calculating the difference between the chain of transforms for actual assembly and the nominal assembly.

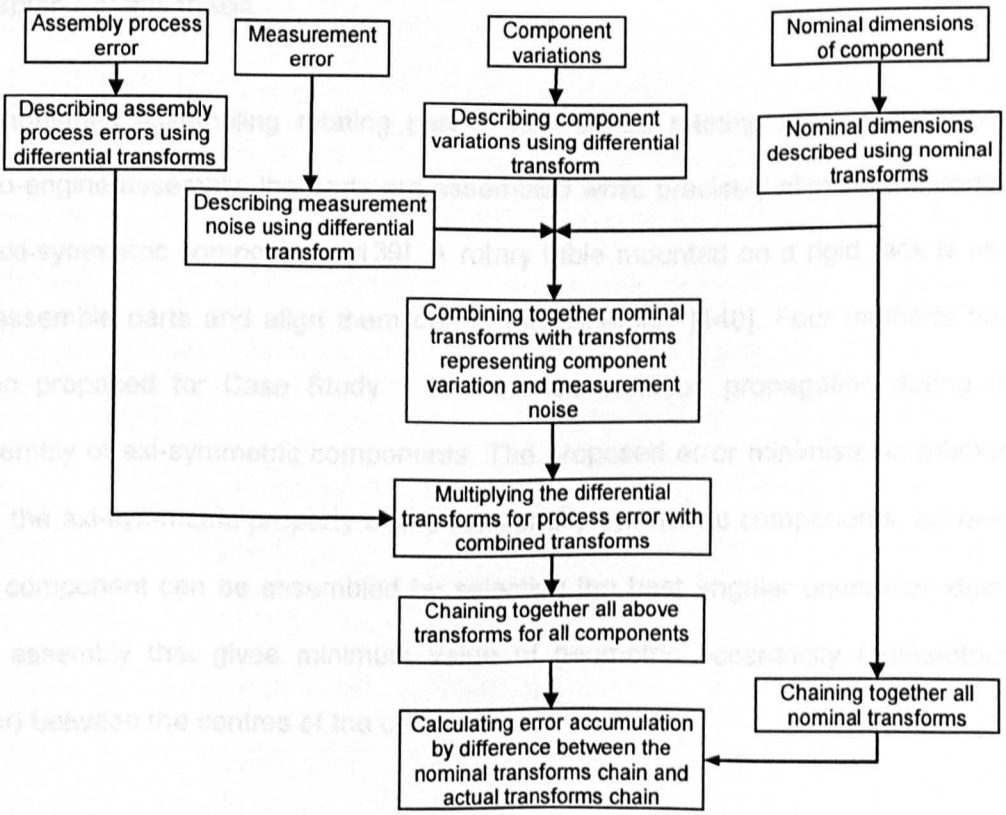

**Figure 3-4: Schematic representation of various steps involved in calculating assembly variation propagations while considering part, process, and measurement errors.**

### 3.2.4 Step 4: Controlling Assembly Variation Propagations

To reduce the chance of assembly failure, it is essential to optimise assembly errors during each assembly stage. Optimisations are used in many fields of engineering to minimise or maximise a function critical to the problem being solved [137, 138]. As discussed in Section 3.1, two assembly case studies are been focused upon in this research for controlling assembly variation propagations. The control strategy for minimising assembly variation propagations can be different for different types of assemblies, however, the model to calculate assembly variation propagations can be general (applied to all types of assemblies). Therefore different control strategies (assembly optimisation methods) are proposed for the case studies of rotating part and non-rotating part of high speed rotating machines, and these are discussed in Chapter 7 of this thesis.

In industries assembling rotating part of high-speed rotating machines, such as aero-engine assembly, the parts are assembled while precisely aligning the centres of axi-symmetric components [139]. A rotary table mounted on a rigid rack is used to assemble parts and align them during the assembly [140]. Four methods have been proposed for Case Study 1 to minimise variation propagation during the assembly of axi-symmetric components. The proposed error minimisation methods use the axi-symmetric property of the rotationally-symmetric components, by which the component can be assembled by selecting the best angular orientation during the assembly that gives minimum value of geometric eccentricity (concentricity error) between the centres of the components.

In Case Study 2, the components are uniformly segmented circular components with nominally identical shape. One optimisation method is proposed for Case Study 2 to minimise assembly variation propagation. The proposed method utilises the property of identical shape for each uniformly segmented components to minimise assembly variation propagations. Using identical shape (nominally) property, each uniformly segmented circular component can be joined in the assembly at different mating sequence. Therefore an optimisation method have been proposed that uses combinatorial approach to find the best mating sequence of all assembly components to get minimum overall assembly variation in radial direction.

## 3.3 Statistical Analysis

This thesis also presents statistical tolerance analysis of Mechanical assemblies. Probabilistic model for assembly variability analysis is developed to perform tolerance analysis based on the linear model. Analytical expressions are determined for the probability density function (pdf) of the position error (along x, y and z direction) for the final component in the assembly based on the manufacturing variations of individual component. Analytical expressions for the pdf are also determined for the Key Characteristics of rotor assembly and casing assembly. For the purposes of validation, comparisons of the derived pdf expressions are made against Monte Carlo simulations. However, in order to perform statistical analysis of assembly variation propagation and evaluate the effect of the proposed optimisation techniques in controlling assembly variation propagations, Monte Carlo simulations are performed. In the Monte Carlo simulation method, the component variations are generated as normally distributed random variables. Further simulations are also performed to analyse the effect of process variation and measurement error on assembly straight-build. The purpose of developing probabilistic model is to propose

an efficient method of estimating assembly variation propagations using analytical method of expressing assembly variations using (pdfs). However, for fully non-linear model it is very difficult to derive pdf expressions for assembly variations, therefore, Monte Carlo Simulation method have been adopted to perform tolerance analysis base on exact solutions. The details of the probabilistic model and the Monte Carlo simulation method are given in Chapter 6.

## 3.4 Summary

This chapter has discussed the different steps involved in calculating and controlling assembly variation propagations. The research methodology has been explained to address the issues discussed with the current knowledge gaps given in the literature review.

The chapter has given a step-by-step methodology for calculating and controlling assembly variation propagations, with the basic concept and ideas behind each step. Various steps of research methodology are described, and how the steps fit together to provide a design tool to the assembly engineer in order to improve the assembly quality of rotating and non-rotating structures of high-speed rotating machines.

Methodology of two assembly models (linear and exact) has been presented and the basic idea, concept and the reason of developing two variation propagation models is briefly described. A general concept of assembly optimisation methodology for minimising assembly errors in the case studies of rotating and non-rotating part of high speed rotating machines have also been described. Finally the methodologies of performing statistical tolerance analysis based on the linear and the fully non-linear method have been described.

# Chapter 4 VARIATION PROPAGATION MODELS

## 4.1 Introduction

Controlling variation propagation requires that the propagation of assembly variation be predicted before assembly takes place. Variation propagation methods are used to predict the error build-up in assembly as the components are assembled together. Once the variation propagations are known for given assembly components and process parameters, control methods can be applied to the assembly process for a given product. One of the aims of this research is to present methods that can predict assembly variation propagation accurately.

The assembly models used in this study are derived from connective assembly models [20]. In a connective assembly model [20], matrix transforms are used to describe the spatial relationship between different components. This method of modelling was first used by Denavit and Hartenberg [77], who applied matrix

transforms to represent kinematic linkages. Using matrix transforms one can capture mathematically the physical way that components are located with respect to each other. The method of representing components and assemblies using matrix transforms has been used by various researchers in the past [74, 89]. Whitney [20] used the approach to represent mechanical assemblies as well as to model variation propagations, and refers to this method as a connective model.

The current study uses the same approach but with some modifications. Two methods to model assembly variations are presented. These methods are referred to as the Exact Method and the Linear Method. This chapter discuss the details of these methods, and describes how the two methods differ. The Exact Method calculates assembly variation using fully non-linear transformation matrices to obtain the exact solution, whereas the Linear Method uses a first order perturbation analysis to approximate the transformations relating to the overall dimensions of the assembly. The Linear Method is developed to enable a design engineer to characterise major contributing factors in assembly variation propagation, which otherwise cannot be identified in the exact method. A fully non-linear model is also proposed to obtain exact results for the assembly variations. Another advantage of the non-linear model is that it is capable of incorporating the effect of assembly optimisation, assembly process error, and measurement error for calculating exact amount of errors accumulated during assembly. The Linear Method also aids the development of a probabilistic approach to analyse assembly variations (see Chapter 6). The probabilistic approach aims to predict variability within the assembly by assuming that the component variations have a known statistical distribution.

Initially, Section 4.2 describes the matrix transform and its types, with Section 4.2.1 describing how to represent the nominal location of components in space using matrix transforms. Section 4.2.2 describes the physical interpretation of matrix

transforms, and Section 4.2.3 demonstrates how to include variations in the location of components using transformation matrices.

Section 4.3 introduces the theory of connective models. Section 4.4 describes the basic assumptions for modelling assembly variations, with Sections 4.4.1 and 4.4.3 referring to the mathematics involved in the Exact and Linear methods for 3D assemblies. Assembly models (Exact and Linear) for 2D assembly are presented in Sections 4.4.2 and 4.4.3. Numerical results obtained using the Exact and Linear methods are given in Section 4.5 and two case studies are analysed to compare results produced by the different methods. Finally, a summary of the chapter along with conclusions based on the results presented in Section 4.5 are given in Section 4.6.

## 4.2 Matrix Transforms

Matrix transformations are used here to describe the movement (translation and rotation) of a coordinate frame in space. In mathematics, the spatial transformation of a coordinate frame is described by a transformation matrix. If a coordinate frame is attached to any surface or object then the movement (translation and rotation) of that object in space can be described by the movement of the coordinate frame attached to that surface using matrix transformations. These transforms are used to locate (*i.e.* position and orient) components and mating features[1] on components. Once the transforms are established, the assembly can be analysed by chaining together the transforms representing individual components and the transformation representing the relationships between mating components.

[1] Mating features also called as assembly features are the places on a part where two components join during their assembly.

Here, matrix transforms are categorised as being nominal transforms and variation transforms. The matrix transforms representing the ideal situation of any feature or component is termed the nominal transform, whilst a transform that represents the variation with respect to the nominal configuration is called the variation transform [20].

### 4.2.1 Nominal Transforms

A matrix transform expresses the spatial relationship of one entire coordinate frame (not simply a point) in terms of another coordinate frame. A matrix transform can be written mathematically as:

$$\mathbf{T}=\begin{bmatrix}\mathbf{R} & \mathbf{p}\\ \mathbf{0}^T & 1\end{bmatrix}. \tag{4.1}$$

In 3D space, a transform matrix represents translation and rotation about the $x$, $y$ and $z$ axes. Therefore, the transform matrix $\mathbf{T}$ (in Equation (4.1)) contains a rotational component represented by a $3\times3$ rotation matrix $\mathbf{R}$, a $3\times1$ translation vector $\mathbf{p}$, and a $3\times1$ null vector $\mathbf{0}$. The superscript $^T$ represents the transpose of a vector. Here, all vectors are assumed to be column vectors, so the transpose of a column vector is a row vector.

For three-dimensional space, a schematic layout representing the function of a matrix transform is given in Figure 4-1. The vector $\mathbf{p}$ represents the translation of an object from location 1 to location 2, and is expressed in the coordinates of the original coordinate frame 1. The rotation of the object about the $x$, $y$ and $z$ axes is represented by $\mathbf{R}$ and is expressed by the direction cosines of frame 2 in terms of frame 1. If $\theta_x$, $\theta_y$ and $\theta_z$ represent the rotation of the object about the $x$, $y$ and $z$

axes, the separate transforms to represent translation and rotation in 3D space are [86] :

$$\mathbf{Trans} = \begin{bmatrix} 1 & 0 & 0 & X \\ 0 & 1 & 0 & Y \\ 0 & 0 & 1 & Z \\ 0 & 0 & 0 & 1 \end{bmatrix}, \tag{4.2}$$

$$\mathbf{Rot}_x = \begin{bmatrix} 1 & 0 & 0 & 0 \\ 0 & \cos\theta_x & -\sin\theta_x & 0 \\ 0 & \sin\theta_x & \cos\theta_x & 0 \\ 0 & 0 & 0 & 1 \end{bmatrix}, \tag{4.3}$$

$$\mathbf{Rot}_y = \begin{bmatrix} \cos\theta_y & 0 & \sin\theta_y & 0 \\ 0 & 1 & 0 & 0 \\ -\sin\theta_y & 0 & \cos\theta_y & 0 \\ 0 & 0 & 0 & 1 \end{bmatrix}, \tag{4.4}$$

and,

$$\mathbf{Rot}_z = \begin{bmatrix} \cos\theta_z & -\sin\theta_z & 0 & 0 \\ \sin\theta_z & \cos\theta_z & 0 & 0 \\ 0 & 0 & 1 & 0 \\ 0 & 0 & 0 & 1 \end{bmatrix}, \tag{4.5}$$

where **Trans** is the pure translation matrix and matrices $\mathbf{Rot}_x$, $\mathbf{Rot}_y$, and $\mathbf{Rot}_z$ represent individual rotations about the $x$, $y$ and $z$ axes, respectively.

If frame 2 (in Figure 4-1) is translated and rotated about the $x$, $y$ and $z$ axes with reference to frame 1, the transform representing the spatial relationship between the two frames can be written as [74]:

$$\mathbf{T} = \mathbf{Trans}\ \mathbf{Rot}_x\ \mathbf{Rot}_y\ \mathbf{Rot}_z = \begin{bmatrix} \mathbf{R} & \mathbf{p} \\ \mathbf{0}^T & 1 \end{bmatrix}. \tag{4.6}$$

Equation (4.6) gives the general form of transformation matrix **T** for transformation from one frame to the next. Substituting Equations (4.2-5) into Equation (4.6) gives the value of rotational matrix **R** and the translational vector **p** such that:

$$\mathbf{R}=\begin{bmatrix} \cos(\theta_y)\cos(\theta_z) & -\cos(\theta_y)\sin(\theta_z) & \sin(\theta_y) \\ \sin(\theta_x)\sin(\theta_y)\cos(\theta_z) \\ +\cos(\theta_x)\sin(\theta_z) & \cos(\theta_x)\cos(\theta_z) \\ & -\sin(\theta_x)\sin(\theta_y)\sin(\theta_z) & -\sin(\theta_x)\cos(\theta_y) \\ \sin(\theta_x)\sin(\theta_z) \\ -\cos(\theta_x)\sin(\theta_y)\cos(\theta_z) & \cos(\theta_x)\sin(\theta_y)\sin(\theta_z) \\ & +\sin(\theta_x)\cos(\theta_z) & \cos(\theta_x)\cos(\theta_y) \end{bmatrix}. \tag{4.7}$$

$$\mathbf{p}=\begin{bmatrix} X \\ Y \\ Z \end{bmatrix}. \tag{4.8}$$

The $3\times 3$ rotational matrix **R** and the $3\times 1$ translational vector **p** are the components of a transformation matrix **T** representing the position and orientation of a new frame relative to a reference frame. The following section provides an example of transformation and interprets its formation stage-by-stage.

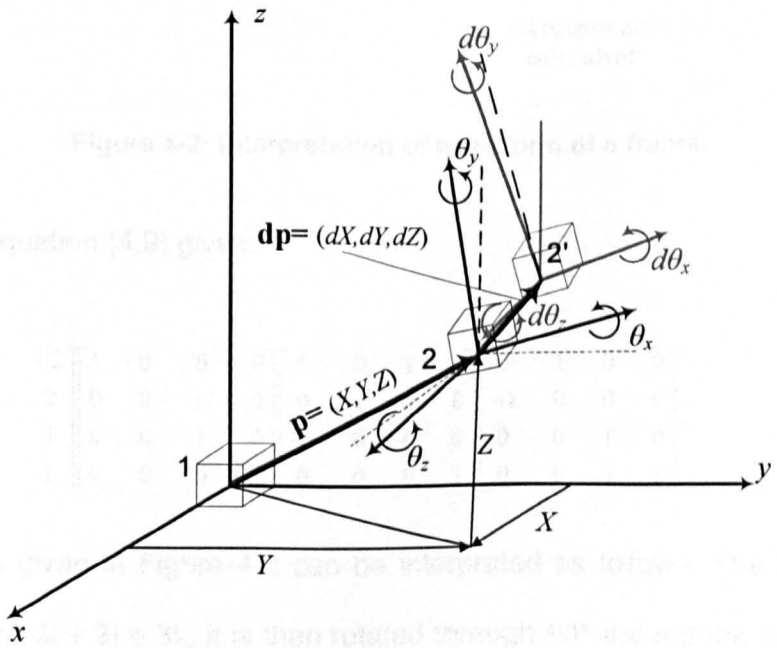


**Figure 4-1: Schematic representation of a transform.**

### 4.2.2 Interpretation of Transforms

Transformation matrices are used to describe position and orientation of an object or a coordinate frame representing an object. Figure 4-2 describes the translation and orientation of a coordinate frame with reference to a Global Coordinate Frame (GCS). A transform **T** describing the translation and orientation of the frame, for the example given in Figure 4-2 with respect to each other can be written mathematically as:

$$\mathbf{T} = \mathbf{Trans}(-2,2,3)\ \mathbf{Rot}_x(\pi/2)\ \mathbf{Rot}_y(\pi/2)\ \mathbf{Rot}_z(-\pi/2). \tag{4.9}$$

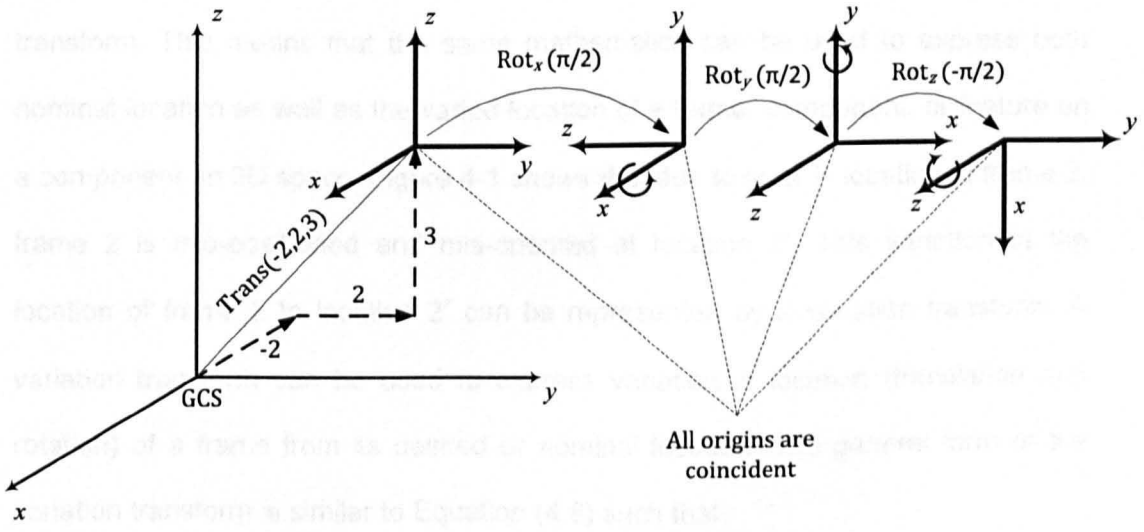


**Figure 4-2: Interpretation of transform of a frame.**

Expanding Equation (4.9) gives:

$$\mathbf{T} = \begin{bmatrix} 1 & 0 & 0 & -2 \\ 0 & 1 & 0 & 2 \\ 0 & 0 & 1 & 3 \\ 0 & 0 & 0 & 1 \end{bmatrix} \begin{bmatrix} 1 & 0 & 0 & 0 \\ 0 & 0 & -1 & 0 \\ 0 & 0 & 1 & 0 \\ 0 & 0 & 0 & 1 \end{bmatrix} \begin{bmatrix} 0 & 0 & 1 & 0 \\ 0 & 1 & 0 & 0 \\ -1 & 0 & 0 & 0 \\ 0 & 0 & 0 & 1 \end{bmatrix} \begin{bmatrix} 0 & 1 & 0 & 0 \\ -1 & 0 & 0 & 0 \\ 0 & 0 & 1 & 0 \\ 0 & 0 & 0 & 1 \end{bmatrix}. \tag{4.10}$$

The example given in Figure 4-2 can be interpreted as follows. The frame is first translated by $-2\mathbf{i} + 2\mathbf{j} + 3\mathbf{k}$, it is then rotated through 90° around the current x-axis, then rotated through 90° around the current y-axis, and finally rotated through $-90°$ around the current z-axis. Expanding Equation (4.10) gives:

$$\mathbf{T}=\begin{bmatrix} 0 & 0 & 1 & -2 \\ 0 & 1 & 0 & 2 \\ -1 & 0 & 0 & 3 \\ 0 & 0 & 0 & 1 \end{bmatrix}. \tag{4.11}$$

Equation (4.11) is the relative transform between two frames, and describes the directions of the three axes and the position of the origin of a coordinate frame rotated and translated away from the reference coordinate frame as shown in Figure 4-2.

### 4.2.3 Variation Transforms

Variation in the transformation of a frame in space can be represented by a matrix transform. This means that the same mathematics can be used to express both nominal location as well as the varied location of a frame, component, or feature on a component. In 3D space, Figure 4-1 shows that due to error in location of frame 2, frame 2 is mis-positioned and mis-oriented at location 2′. This variation in the location of frame 2 to location 2′ can be represented by a variation transform. A variation transform can be used to express variation in location (translation and rotation) of a frame from its desired or nominal location. The general form of the variation transform is similar to Equation (4.6) such that:

$$\mathbf{DT}=\mathbf{dTrans}\ \mathbf{dRot}_x\ \mathbf{dRot}_y\ \mathbf{dRot}_z=\begin{bmatrix} \mathbf{dR} & \mathbf{dp} \\ \mathbf{0}^T & 1 \end{bmatrix}, \tag{4.12}$$

where **dTrans** is the differential transform for translation error indicating the variation in translation of a frame with reference to the corresponding nominal frame. The matrices $\mathbf{dRot}_x$, $\mathbf{dRot}_y$, and $\mathbf{dRot}_z$ are the differential transforms representing the angular orientation error (about the $x$, $y$ and $z$ axes, respectively) of a frame from the nominal configuration (as shown in Figure 4-1). These differential transforms can be written as follows [20]:

$$\mathbf{dTrans} = \begin{bmatrix} 1 & 0 & 0 & dX \\ 0 & 1 & 0 & dY \\ 0 & 0 & 1 & dZ \\ 0 & 0 & 0 & 1 \end{bmatrix}, \tag{4.13}$$

$$\mathbf{dRot}_x = \begin{bmatrix} 1 & 0 & 0 & 0 \\ 0 & \cos d\theta_x & -\sin d\theta_x & 0 \\ 0 & \sin d\theta_x & \cos d\theta_x & 0 \\ 0 & 0 & 0 & 1 \end{bmatrix}, \tag{4.14}$$

$$\mathbf{dRot}_y = \begin{bmatrix} \cos d\theta_y & 0 & \sin d\theta_y & 0 \\ 0 & 1 & 0 & 0 \\ -\sin d\theta_y & 0 & \cos d\theta_y & 0 \\ 0 & 0 & 0 & 1 \end{bmatrix}, \tag{4.15}$$

and,

$$\mathbf{dRot}_z = \begin{bmatrix} \cos d\theta_z & -\sin d\theta_z & 0 & 0 \\ \sin d\theta_z & \cos d\theta_z & 0 & 0 \\ 0 & 0 & 1 & 0 \\ 0 & 0 & 0 & 1 \end{bmatrix}, \tag{4.16}$$

where $dX, dY$ and $dZ$ represent the translation error in the location of a frame, and $d\theta_x, d\theta_y$ and $d\theta_z$ represent the error in rotation of a frame about the $x$, $y$ and $z$ axes, respectively. If the nominal transform describing the relationship between frame 1 and frame 2 is given by Equation (4.6), the final transform after considering the variation in location (as shown in Figure 4-3) can be obtained by multiplying the nominal transform by the varied transform as [20, 74]:

$$\mathbf{T}' = \mathbf{T}\,\mathbf{DT}. \tag{4.17}$$

In Equation (4.17), the order of multiplication is important. Equation (4.17) reveals that the transform T is accomplished first and then the error **DT** is applied. However,

if the error **DT** occurs before transform **T** is accomplished, then Equation (4.17) can be written as:

$$\mathbf{T}' = \mathbf{DTT}. \tag{4.18}$$

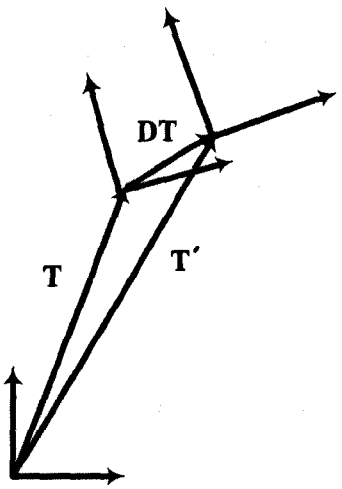


**Figure 4-3: Properties of error transform.**

## 4.3 Connective Models

A Connective Assembly Model is a type of assembly model in which the components are joined by connecting them together at their assembly features. A connective assembly model can represent components, assembly features, and surfaces individually and can indicate the variation present in them. This helps to model different kinds of variation correctly and to distinguish between different sources of error in the assembly model. An assembly model can be developed by placing feature frames on components and joining components using feature frames. The connective model of assembly defines a component as having a central coordinate frame plus one or more assembly features (mating surface), each feature having its own frame of reference. The features are placed on a component by defining a transform from the central coordinate frame for the component to the

feature frame. The transform matrices are also used to locate components with respect to each other during assembly.

In connective models, each component is modelled as a chain of nominal transforms representing the nominal or error free dimensions and a linearised variation transform representing the component variations from nominal or designed dimensions. A connective model assumes that the component variations are very small, meaning that a linearised matrix transform can be used to represent the component variations. The varied transform representing the difference between the nominal and varied situation of a frame is given in a linear form as [20]:

$$\mathbf{DT}=\begin{bmatrix} 1 & -d\theta_z & d\theta_y & dX \\ d\theta_z & 1 & -d\theta_x & dY \\ -d\theta_y & d\theta_x & 1 & dZ \\ 0 & 0 & 0 & 1 \end{bmatrix}=\begin{bmatrix} \mathbf{I}+\boldsymbol{\delta}\mathbf{R} & \mathbf{dp} \\ \mathbf{0}^T & 1 \end{bmatrix}, \tag{4.19}$$

where $\mathbf{I}$ is an identity matrix, and $\boldsymbol{\delta}\mathbf{R}$ and $\mathbf{dp}$ are given as:

$$\boldsymbol{\delta}\mathbf{R}=\begin{bmatrix} 0 & -d\theta_z & d\theta_y \\ d\theta_z & 0 & -d\theta_x \\ -d\theta_y & d\theta_x & 0 \end{bmatrix}, \tag{4.20}$$

$$\mathbf{dp}=\begin{bmatrix} dX \\ dY \\ dZ \end{bmatrix}. \tag{4.21}$$

Equation (4.19) is a reduced form of Equation (4.12), obtained by multiplying the differential transforms , $\mathbf{dRot}_x$, $\mathbf{dRot}_y$, and $\mathbf{dRot}_z$ together and using small angle approximations such that $\sin d\theta \cong d\theta$ and $\cos d\theta \cong 1$.

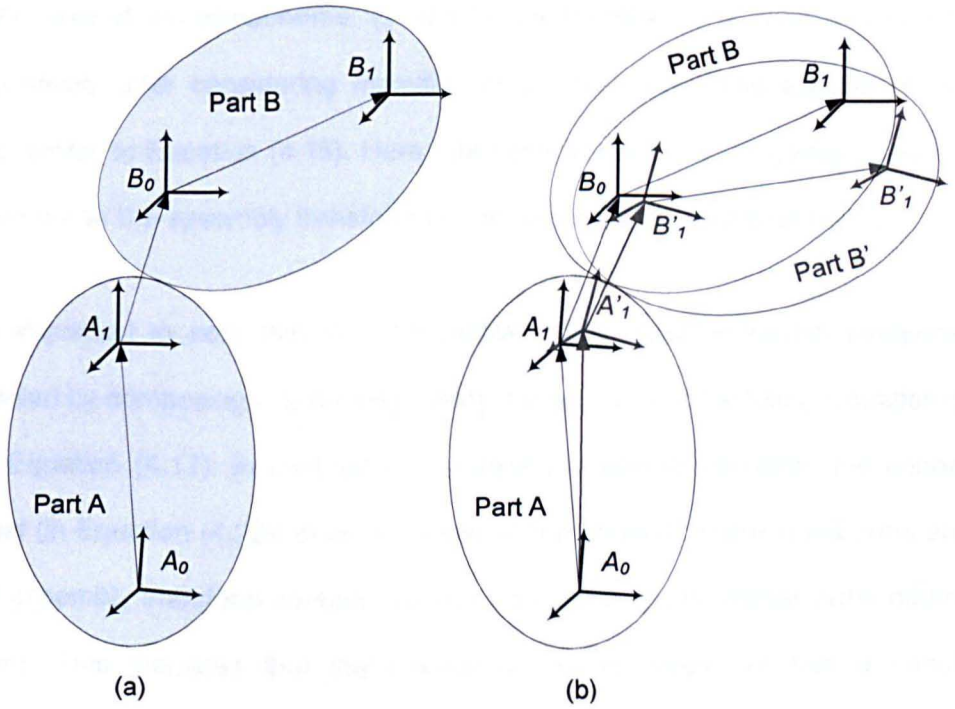


**Figure 4-4: Two components assembled by a connective assembly model; (a) nominal situation, (b) varied situation**

Figure 4-4 shows two components joined using the connective method. The nominal situation is shown in Figure 4-4(a) and a varied situation is shown in Figure 4-4(b). In Figure 4-4(b), feature $A_1$ on component A is mis-positioned and mis-oriented, causing component B to be in an incorrect location. In connective assembly models, during the assembly of two components, the assembly feature on one component is made to coincide with the assembly feature on another component [20]. A feature interface transform is defined to relate the frame on one component's assembly feature to the frame on the other component's assembly feature. Therefore to model an assembly using a connective model, the chain of matrix transforms representing the assembly components is composed as:

$$\mathbf{A}_{A-B} = \mathbf{T}'_A \, \mathbf{T}_{A-B} \, \mathbf{T}'_B , \tag{4.22}$$

where transform $\mathbf{A}_{A-B}$ represents the assembly of components A and B (shown in Figure 4-4(b)), $\mathbf{T}_{A-B}$ is the feature interface transform representing the mating

relationship of two components, $T_A'$ and $T_B'$ are transforms for components A and B, respectively after considering manufacturing error, and these transforms have a form similar to Equation (4.18). Here, the base frame $A_0$ is the global frame for the assembly so the assembly transform is with reference to the global frame.

It is important to note that in a connective model each individual component is modeled by composing a linearised matrix transform by substituting Equation (4.19) into Equation (4.17). In contrast for modelling assembly variation, the connective model (in Equation (4.22)) does not linearise the chain of matrix transforms and the final assembly transform contains various non-linear terms (higher order differential terms). This indicates that the Connective Model does not use a consistent mathematical approach of linearising matrix transforms during assembly modelling. To overcome this discrepancy, this chapter presents two assembly models (in Section 4.4) that use a consistent mathematical approach to determine the resulting variation in assembly dimensions. The proposed models are: (i) a fully non-linear model to obtain the exact assembly variations, and (ii) a linear model for approximating assembly variation propagation. In a later chapter the linear model is used to express assembly uncertainties in terms of statistical distributions which can be used to statistically validate the assembly design and analyse the achievability of assembly KC.

## 4.4 Variation Propagation Models

Two variation propagation models are presented in this section based on the principle of connective assembly models. The first model, termed the Exact Method, uses a fully non-linear approach for considering manufacturing variation throughout the assembly, whereas, the second model, termed the Linear Method, uses a linear approach.

For modelling variation propagation, the following assumptions are made about the assembly:

- The assembly is composed of rigid components.
- The assembly is performed stage-by-stage, one stage at a time.
- Each component is fully constrained with respect to existing components during the assembly.
- Cartesian frames are attached to a specified point on the surface of a component.
- The propagation of variations in three dimensional space is treated as propagation of errors through transformations of Cartesian frames.
- The general form of a transformation matrix between two frames is given by Equation (4.6), where the order of multiplication of rotation matrices is important and consistency must be maintained through the process of assembling all components.

### 4.4.1 Exact Model for 3D assemblies

The Exact Model uses a similar approach to that developed for connective assembly models, to represent assemblies in space as well as to calculate assembly variation propagation. The exact model is different from a connective model as it does not reduce the differential transform given in Equation (4.12) to the linearised form given in Equation (4.19). Also for the calculation of assembly variation, exact model consistently uses fully non-linear approach during the multiplication of transforms. This means that variation propagation can be calculated exactly no matter if the variations are large or small. The Exact Method is relatively straight forward and capable of accounting for assembly process and measurement errors (details are given Chapter 8).

To describe the Exact Method, a two-component assembly taken from [20] (as shown in Figure 4-5) is considered. For this example, the assembly consists of joining two components at their mating features, and composing matrix transforms to represent each component and to express the component-to-component relationship.

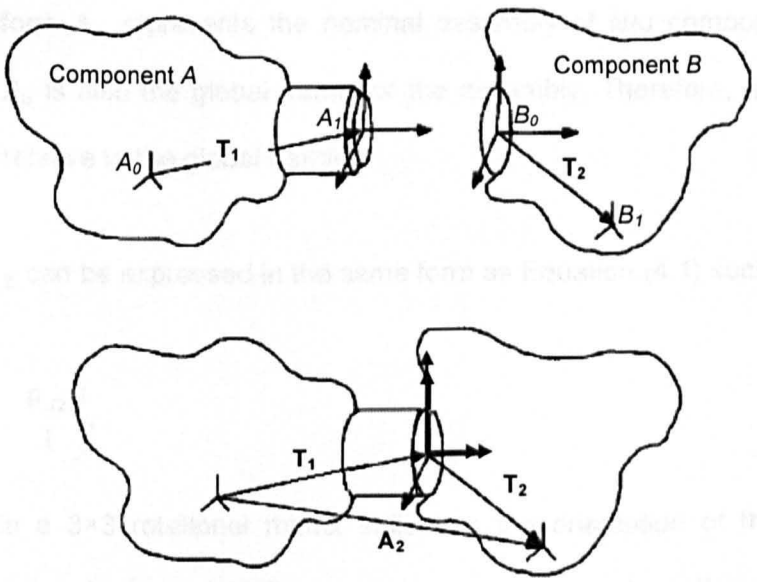


**Figure 4-5: Two components assembled by a joining at assembly features [20].**

Figure 4-5 shows that two frames are attached to each component (component A and component B). Frame $A_0$ is the global frame for component A and frame $A_1$ is the frame attached to the mating feature on the same component. Similarly, $B_0$ is the global frame for component B that is attached to its mating feature, and frame $B_1$ is another frame attached to component B. The assembly of two components consists of joining the components together at their mating features. To represent assembly of two components, the transforms are composed by representing each component and the intermediate transform describing the mating relationship between two components. If the transform $\mathbf{T}_1$ represents the nominal transformation between frames $A_0$ and $A_1$ on component A, transform $\mathbf{T}_2$ represents the nominal transformation between frames $B_0$ and $B_1$ on component B, and transform $\mathbf{T}_{1-2}$ is

the feature interface transform representing the nominal transformation at the mating of two components between frames $A_1$ and $B_0$. Therefore, the transform between frames $A_0$ and $B_1$ representing the nominal assembly of two components can be obtained by multiplying the transforms together as follows:

$$\mathbf{A}_2 = \mathbf{T}_1 \mathbf{T}_{1-2} \mathbf{T}_2 , \tag{4.23}$$

where transform $\mathbf{A}_2$ represents the nominal assembly of two components. Here, base frame $A_0$ is also the global frame for the assembly. Therefore, the assembly transform is relative to the global frame.

Transform $\mathbf{A}_2$ can be expressed in the same form as Equation (4.1) such that:

$$\mathbf{A}_2 = \begin{bmatrix} \mathbf{R}_{A2} & \mathbf{p}_{A2} \\ \mathbf{0}^T & 1 \end{bmatrix}, \tag{4.24}$$

where $\mathbf{R}_{A2}$ is a 3×3 rotational matrix indicating the orientation of the frame $B_1$ relative to global frame $A_0$ of the assembly, $\mathbf{p}_{A2}$ is a 3×1 displacement vector indicating the position of the $B_1$ frame relative to global frame $A_0$.

If there are '$N$' components in the assembly, the transform representing the ideal relationship between the last feature of the '$i^{th}$' assembly component relative to the base feature of the first component in the assembly is given by:

$$\mathbf{A}_i = \mathbf{T}_1 \mathbf{T}_{1-2} \mathbf{T}_2 \mathbf{T}_{2-3} \ldots \mathbf{T}_i \tag{4.25}$$

If during the mating process, the coordinate frames attached to the mating features of both components are co-incident and co-axial, the feature interface transforms $\mathbf{T}_{1-2}, \mathbf{T}_{2-3}, \ldots \mathbf{T}_{(i-1)-i}$ will be identity matrices, otherwise the feature interface transforms can be used to represent assembly process error. If the assembly is

performed with no error during the mating process, in such circumstances, Equation (4.25) can be written as:

$$\mathbf{A}_i = \mathbf{T}_1 \mathbf{T}_2 \mathbf{T}_3 ... \mathbf{T}_i = \prod_{i=1}^{N} \mathbf{T}_i = \begin{bmatrix} \mathbf{R}_{Ai} & \mathbf{p}_{Ai} \\ \mathbf{0}^T & 1 \end{bmatrix} \tag{4.26}$$

In order to account for manufacturing variations in each component, the nominal transform for each component is multiplied by the error transform (given by Equation (4.12)), describing the position and orientation error between the two mating features of each component. If the transforms $\mathbf{T}_1'$ and $\mathbf{T}_2'$ represent the transformation for components A and B after taking into account manufacturing variation, the transform matrix representing the actual assembly of two manufactured components can be expressed as:

$$\mathbf{A}_2' = \mathbf{T}_1' \mathbf{T}_{1-2} \mathbf{T}_2', \tag{4.27}$$

where transforms $\mathbf{T}_1'$ and $\mathbf{T}_2'$ have a similar form to that of Equation (4.17), and transform $\mathbf{T}_{1-2}$ is an identity matrix, as the mating between two components is assumed to be ideal and co-incident. The transform $\mathbf{T}_{1-2}$ in Equation (4.27) can also be used as an expression for considering assembly process error in assembly variation analysis (for details see Chapter 8). Equation (4.27) can be expressed in the same form as Equations (4.1) and (4.24) such that:

$$\mathbf{A}_2' = \begin{bmatrix} \mathbf{R}_{A2}' & \mathbf{p}_{A2}' \\ \mathbf{0}^T & 1 \end{bmatrix}, \tag{4.28}$$

where $\mathbf{R}_{A2}'$ is a 3×3 rotational matrix indicating the orientation of final component in the assembly of manufactured components, $\mathbf{p}_{A2}'$ is a 3×1 displacement vector indicating the position of final component in the assembly of manufactured components.

If there are '*N*' components in the assembly, the transform representing assembly of the manufactured components can be written as:

$$\mathbf{A}_i' = \mathbf{T}_1' \mathbf{T}_2' ... \mathbf{T}_i' = \prod_{i=1}^{N} \mathbf{T}_i' = \begin{bmatrix} \mathbf{R}_{Ai}' & \mathbf{p}_{Ai}' \\ \mathbf{0}^T & 1 \end{bmatrix}. \tag{4.29}$$

Here, the assembly variations are expressed as position errors in the location of the coordinate frames attached to each assembly feature, and are described as the translation error between the actual assembly and the nominal assembly. The calculated translation error can be used to quantify the influence of component manufacturing variation on the assembly, where the translational error vector $(dp_2^X,\ dp_2^Y,\ dp_2^Z)$ for the assembly of two components is given by:

$$\begin{bmatrix} dp_2^X \\ dp_2^Y \\ dp_2^Z \end{bmatrix} = \mathbf{p}_{A2}' - \mathbf{p}_{A2}. \tag{4.30}$$

Similarly the error vector for an assembly consisting of $i$ manufactured components can be expressed as:

$$\begin{bmatrix} dp_i^X \\ dp_i^Y \\ dp_i^Z \end{bmatrix} = \mathbf{p}_{Ai}' - \mathbf{p}_{Ai}. \tag{4.31}$$

This is the general form of the equation for calculating assembly variation propagations. Equation (4.31) will be used for assembly examples given in this chapter and in later chapters to calculate assembly variation propagations.

### 4.4.2 Exact Model for 2D assemblies

The Exact Method for calculating assembly variation propagations for two-dimensional assemblies is the same as that for 3D assemblies except for the size

and form of the basic transforms. For two-dimensional assemblies, the transform matrix **T** (see Equation(4.24)) contains a rotational component represented by a $2 \times 2$ rotation matrix **R**, a $2 \times 1$ translation vector **p**, and a $2 \times 1$ null vector **0**.

Figure 4-6 illustrates the geometric relationship between any two coordinate frames. The relationship between coordinate frames $O_0$ and $O_1$ can be represented by translation $(X, Y)$ along two reference axes, and rotation of the frame by angle θ. Thus, the transform matrix to describe the relationship of coordinate frames $O_0$ to $O_1$ can be written as:

$$\mathbf{T} = \begin{bmatrix} \cos\theta & -\sin\theta & X \\ \sin\theta & \cos\theta & Y \\ 0 & 0 & 1 \end{bmatrix} \tag{4.32}$$

Comparing equations (4.1) and (4.32) gives:

$$\mathbf{R} = \begin{bmatrix} \cos\theta & -\sin\theta \\ \sin\theta & \cos\theta \end{bmatrix}, \tag{4.33}$$

$$\mathbf{p} = \begin{bmatrix} X \\ Y \end{bmatrix}. \tag{4.34}$$

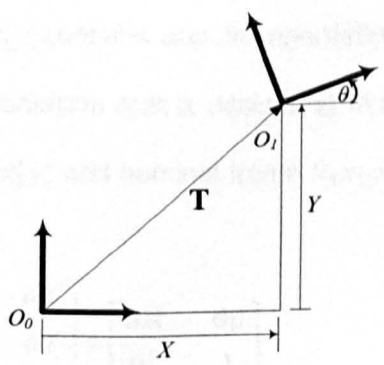


**Figure 4-6: Geometric relationship between two coordinate frames**

For 2D assemblies Figure 4-7(a) shows the nominal geometry of a 2D component. Feature frames are attached to the nominal mating features. Equation (4.32) can be used to represent the transformation between feature frames $O_0$ and $O_1$. Figure 4-7(b) shows the manufactured component containing (exaggerated) deviations from nominal geometry.

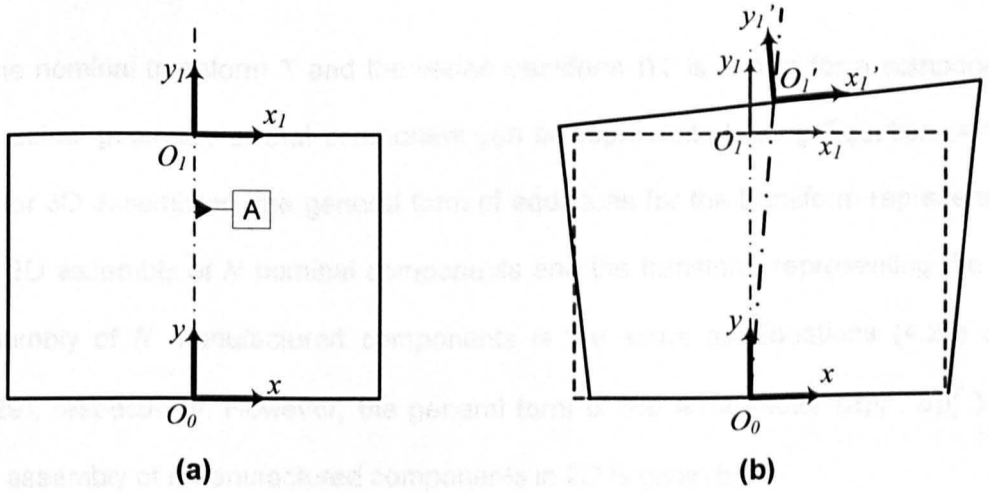


**Figure 4-7: (a) Nominal rectangular component symmetric about axis A; (b) Manufactured "rectangular" component**

Figure 4-8 shows as enlarged view of the top mating feature of the manufactured component shown in Figure 4-7(b). It can be seen from this figure that the coordinate frame $O_1'x_1'y_1'$ is mis-positioned from coordinate frame $O_1x_1y_1$ by $(dX, dY)$. Also coordinate frame $O_1'x_1'y_1'$contains angular orientation error $d\theta$ from coordinate frame $O_1x_1y_1$. Thus, the transform matrix describing the relative situation between varied coordinate frame $O_1'x_1'y_1'$ and nominal frame $O_1x_1y_1$can be written as:

$$\mathbf{DT} = \begin{bmatrix} \cos d\theta & -\sin d\theta & dX \\ \sin d\theta & \cos d\theta & dY \\ 0 & 0 & 1 \end{bmatrix} = \begin{bmatrix} \mathbf{dR} & \mathbf{dp} \\ \mathbf{0}^T & 1 \end{bmatrix} \tag{4.35}$$

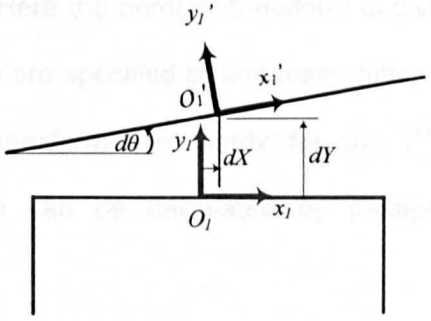


**Figure 4-8: Enlarged view of top surface variation in Figure 4-7(b)**

If the nominal transform **T** and the varied transform **DT** is known for a component, the actual geometry of that component can be represented using Equation (4.17). As for 3D assemblies, the general form of equations for the transform representing the 2D assembly of $N$ nominal components and the transform representing the 2D assembly of $N$ manufactured components is the same as Equations (4.25) and (4.29), respectively. However, the general form of the error vector $(dp_i^X,\ dp_i^Y)$ for the assembly of $i$ manufactured components in 2D is given by:

$$\begin{bmatrix} dp_i^X \\ dp_i^Y \end{bmatrix} = \mathbf{p}_i' - \mathbf{p}_i \tag{4.36}$$

Equations (4.31) and (4.36) show that assembly variations using the exact model are obtained by subtracting the nominal position of the desired assembly stage from the actual position for the same assembly stage. The Exact method provides the exact calculations for assembly variations, but it is difficult to interpret the dominant factors for assembly variation propagation from the resulting equations ((4.31) and (4.36)).

### 4.4.3 Linear Assembly Model

The Linear Model initially uses the same approach of connective models to represent individual components as a chain of nominal transform and linearised variation transform, but with a consistent linear approach during the multiplication of

the chain of transforms. Here the nominal transform is given by Equation (4.6) and the component variations are specified by linearised differential transforms given by Equation (4.19). The transformation matrix for the $i^{th}$ component containing manufacturing variations can be calculated by multiplying Equation (4.6) by Equation (4.19) to give:

$$\mathbf{T}_i^{'} = \mathbf{T}_i\ \mathbf{DT}_i = \begin{bmatrix} \mathbf{R}_i + \mathbf{R}_i\delta\mathbf{R}_i & \mathbf{p}_i + \mathbf{R}_i\mathbf{dp}_i \\ \mathbf{0}^T & 1 \end{bmatrix}, \tag{4.37}$$

where $\mathbf{R_i}$, $\mathbf{p_i}$, $\delta\mathbf{R_i}$ and $\mathbf{dp_i}$ are given by Equations (4.7), (4.8), (4.20) and (4.21), respectively.

If two components are assembled together, the transform representing the assembly of two manufactured components under ideal mating conditions such that:

$$\mathbf{A}_2^{'} = \mathbf{T}_1^{'}\ \mathbf{T}_2^{'} = \begin{bmatrix} \mathbf{R}_1 + \mathbf{R}_1\delta\mathbf{R}_1 & \mathbf{R}_1\mathbf{dp}_1 + \mathbf{p}_1 \\ \mathbf{0}^T & 1 \end{bmatrix}\begin{bmatrix} \mathbf{R}_2 + \mathbf{R}_2\delta\mathbf{R}_2 & \mathbf{R}_2\mathbf{dp}_2 + \mathbf{p}_2 \\ \mathbf{0}^T & 1 \end{bmatrix}. \tag{4.38}$$

After ignoring the terms involving products of differential errors (such as $\delta\mathbf{R}_1\delta\mathbf{R}_2$ and $\delta\mathbf{R}_1\mathbf{dp}_2$) and keeping only first order terms, it can be shown easily that $\mathbf{A}_2'$ is given by:

$$\mathbf{A}_2^{'} = \begin{bmatrix} \mathbf{R}_1\mathbf{R}_2 + \mathbf{R}_1\delta\mathbf{R}_1\mathbf{R}_2 + \mathbf{R}_1\mathbf{R}_2\delta\mathbf{R}_2 & \mathbf{p}_1 + \mathbf{R}_1\mathbf{p}_2 + \mathbf{R}_1\mathbf{dp}_1 + \mathbf{R}_1\delta\mathbf{R}_1\mathbf{p}_2 + \mathbf{R}_1\mathbf{R}_2\mathbf{dp}_2 \\ \mathbf{0}^T & 1 \end{bmatrix}. \tag{4.39}$$

Similarly, the transform matrix representing the assembly of '$N$' components can be written as:

$$\mathbf{A}'_N = \begin{bmatrix} \mathbf{R}_1\mathbf{R}_2\mathbf{R}_3 & \left(\mathbf{p}_1 + \mathbf{R}_1\mathbf{p}_2 + \ldots + \mathbf{R}_1\ldots\mathbf{R}_{N-1}\mathbf{p}_N\right) \\ +\mathbf{R}_1\delta\mathbf{R}_1\mathbf{R}_2\mathbf{R}_3 & +\left(\mathbf{R}_1\mathbf{dp}_1 + \mathbf{R}_1\mathbf{R}_2\mathbf{dp}_2 + \ldots + \mathbf{R}_1\ldots\mathbf{R}_{N-1}\mathbf{dp}_N\right) \\ +\mathbf{R}_1\mathbf{R}_2\delta\mathbf{R}_2\mathbf{R}_3 & \\ +\mathbf{R}_1\mathbf{R}_2\mathbf{R}_3\delta\mathbf{R}_3 & +\begin{pmatrix} \mathbf{R}_1\delta\mathbf{R}_1\mathbf{p}_2 + \mathbf{R}_1\delta\mathbf{R}_1\mathbf{R}_2\mathbf{p}_3 + \ldots + \mathbf{R}_1\delta\mathbf{R}_1\mathbf{R}_2\ldots\mathbf{R}_{N-1}\mathbf{p}_N \\ +\mathbf{R}_1\mathbf{R}_2\delta\mathbf{R}_2\mathbf{p}_3 + +\mathbf{R}_1\mathbf{R}_2\delta\mathbf{R}_2\mathbf{R}_3\mathbf{p}_4 + \ldots + \mathbf{R}_1\mathbf{R}_1\delta\mathbf{R}_2\mathbf{R}_3\ldots\mathbf{R}_{N-1}\mathbf{p}_N \\ \vdots \\ \mathbf{R}_1\mathbf{R}_1\ldots\delta\mathbf{R}_{N-1}\mathbf{p}_N \end{pmatrix} \\ \mathbf{0}^T & 1 \end{bmatrix} \quad (4.40)$$

Equation (4.40) can be generalised in a summation for as:

$$\mathbf{A}'_i = \begin{bmatrix} \prod_{i=1}^{N}\mathbf{R}_i & \sum_{i=1}^{N}\left(\prod_{j=0}^{i-1}\mathbf{R}_j\right)\mathbf{p}_i \\ +\sum_{i=1}^{N-1}\left(\left(\prod_{j=1}^{i}\mathbf{R}_j\right)\delta\mathbf{R}_i\left(\prod_{k=i+1}^{N-1}\mathbf{R}_k\right)\right) & +\sum_{i=1}^{N}\left[\prod_{j=1}^{i}\left(\mathbf{R}_j\right)\mathbf{dp}_i\right] \\ +\left(\prod_{i=1}^{N}\mathbf{R}_i\right)\delta\mathbf{R}_N & +\sum_{i=1}^{N-1}\left(\left(\prod_{j=1}^{i}\mathbf{R}_j\right)\delta\mathbf{R}_i\sum_{l=i+1}^{N}\left(\prod_{\substack{k=l-1\\k\neq i}}^{N-1}\mathbf{R}_k\right)\mathbf{p}_l\right) \\ \mathbf{0}^T & 1 \end{bmatrix}, \quad (4.41)$$

Here $\mathbf{A}'_i$ is the transform matrix relating the location and orientation of the coordinate frame at the top of $i^{th}$ component in the assembly to the coordinate frame at the base of component 1 after taking into account manufacturing variations in each component. Using Equation (4.41), it can be shown that the translation errors accumulated after the assembly of '$N$' components are given by:

$$\begin{bmatrix} dp_i^X \\ dp_i^Y \\ dp_i^Z \end{bmatrix} = \left[\sum_{i=1}^{N}\left[\prod_{j=1}^{i}\left(\mathbf{R}_j\right)\mathbf{dp}_i\right] + \sum_{i=1}^{N-1}\left(\left(\prod_{j=1}^{i}\mathbf{R}_j\right)\delta\mathbf{R}_i\sum_{l=i+1}^{N}\left(\prod_{\substack{k=l-1\\k\neq i}}^{N-1}\mathbf{R}_k\right)\mathbf{p}_l\right)\right], \quad (4.42)$$

where $dp_i^X$, $dp_i^Y$ and $dp_i^Z$ are the translation error accumulated after the assembly of $i^{th}$ component.

Equation (4.42) is the generalised form of linear model for calculating translation error accumulated in 3D assemblies, whereas, for 2D assemblies Equation (4.42) can be reduced to calculated translation error in x and y-direction as:

$$\begin{bmatrix} dp_i^X \\ dp_i^Y \end{bmatrix} = \left[ \sum_{i=1}^{N} \left[ \prod_{j=1}^{i} \left( \mathbf{R}_j \right) \mathbf{dp}_i \right] + \sum_{i=1}^{N-1} \left( \left( \prod_{j=1}^{i} \mathbf{R}_j \right) \boldsymbol{\delta} \mathbf{R}_i \sum_{l=i+1}^{N} \left( \prod_{\substack{k=l-1 \\ k \neq i}}^{N-1} \mathbf{R}_k \right) \mathbf{p}_l \right) \right], \tag{4.43}$$

where $\mathbf{R}_i$, $\mathbf{p}_i$ are given by Equations (4.33) and (4.34), respectively, and $\boldsymbol{\delta}\mathbf{R}_i$ and $\mathbf{dp}_i$ can be obtained by reducing Equation (4.35) using small angle approximation such that $\sin d\theta \cong d\theta$ and $\cos d\theta \cong 1$. Therefore $\boldsymbol{\delta}\mathbf{R}_i$ and $\mathbf{dp}_i$ can be written as:

$$\boldsymbol{\delta}\mathbf{R}_i = \begin{bmatrix} 0 & -d\theta_i \\ d\theta_i & 0 \end{bmatrix}, \tag{4.44}$$

$$\mathbf{dp}_i = \begin{bmatrix} dX_i \\ dY_i \end{bmatrix}. \tag{4.45}$$

In Equations (4.42) and (4.43), assembly variations are a function of nominal rotation matrices $\mathbf{R}_i$, nominal translation vectors $\mathbf{p}_i$, differential rotation matrices $\boldsymbol{\delta}\mathbf{R}_i$ and translation error vectors $\mathbf{dp}_i$ of each assembly component. This indicates that assembly variations not only depend upon individual part variations ($dX_i, dY_i, dZ_i, d\theta_{xi}, d\theta_{yi}, d\theta_{zi}$ for 3D and $dX_i, dY_i, d\theta_i$ for 2D), but also individual part dimensions ($X_i, Y_i, Z_i$, for 3D and $X_i, Y_i$ for 2D) and rotations ($\theta_{xi}, \theta_{yi}, \theta_{zi}$ for 3D and $\theta_i$ for 2D) between the frames attached to mating features for each part. As a result, for fixed values of part tolerance, assembling parts with larger dimension will accumulate greater variations compared to the assembly of parts with smaller dimensions.

## 4.5 Analysis of Linear and Exact Models

The aim of the analysis in this section is to analyse the performance of the linear model under a range of values of angular orientation error, to identify the limitations of the linear model. The analysis is based on the worst possible variations for components in the assembly. Two case studies are analysed and these are referred to as Case Study 1 and Case Study 2. Case Study 1 consists of parts with axi-symmetric shape, whilst Case Study 2 consists of parts with uniformly segmented circular shape. In order to investigate the accuracy and efficiency of the proposed linear method, numerical results obtained using the linear method are compared with results obtained using the exact method for each case study. Both case studies are analysed in 2D as well as 3D. The purpose of the 2D analysis is to provide a clearer representation of the assembly process and to improve understanding of the modelling technique for assembly variation propagation. Throughout the analysis, variations in each component are specified for position errors ($dX$, $dY$ and $dZ$ for 3D components (see Figure 4-11(b)), and $dX$ and $dY$ for 2D component as shown in Figure 4-10(b)) and the orientation error ($d\theta_x$, $d\theta_y$ and $d\theta_z$ in 3D, and $d\theta$ in 2D).

### 4.5.1 Analysis of Case Study 1

Case Study 1 consists of assembling four axially symmetric components (rectangles in 2D and cylinders in 3D). During the assembly, the components are stacked one on top of another to build a tower, as shown in Figure 4-9.

To illustrate the assembly process and effects of variation propagation, a 2D example is presented in Figure 4-9. At the first stage of assembly, the first component is placed on the assembly table with its base concentric to the geometric centre of the assembly table (as shown in Figure 4-9). At each subsequent stage, the assembly process consists of "stacking" one rectangular component on top of

another to build a tower, and during the stacking process, it is assumed that the coordinate frame located at the centre of the base of one component is placed co-incident and co-axial (with no mating error) with the coordinate frame attached to the centre of the top of the previous component (see Figure 4-9).

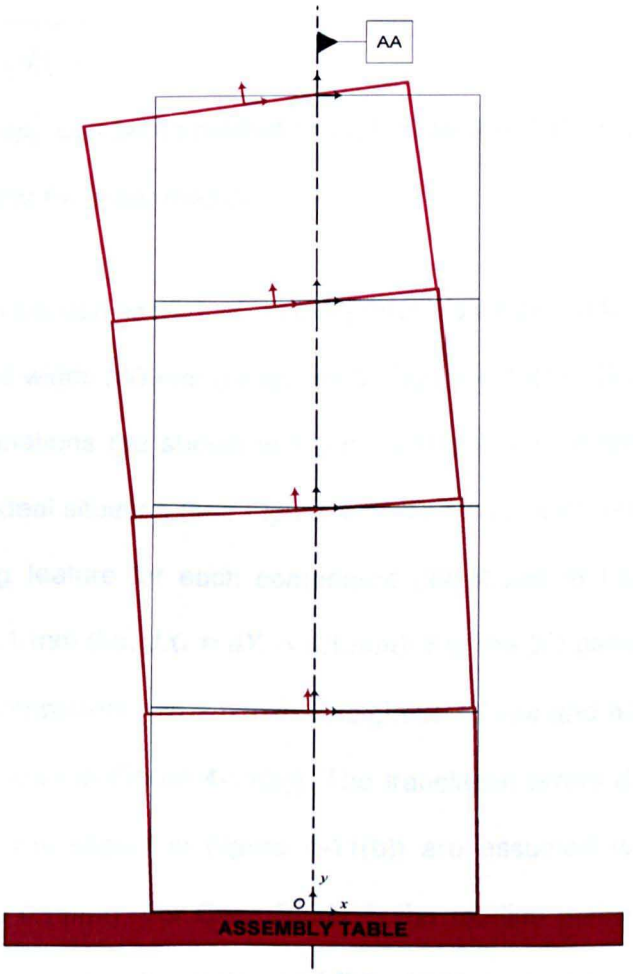


**Figure 4-9: Assembly of ideal and non-ideal axisymmetric components (case study 1)**

The Key Characteristic (KC) for the assembly of axi-symmetric structures as in case of rotating machines is the eccentricity error. In the assembly of rotating machines, eccentricity error at each assembly stage is the measure of the perpendicular distance from the datum axis AA to the centre of the component feature. Figure 4-9 shows that datum axis AA passes through the centre of the base of the first component and is oriented normal to the base. For the assembly of 2D rectangular

components, the eccentricity error after assembling the $i^{th}$ component is the error in the global $x$-direction and is referred to $|dp_i^X|$ that can be calculated using Equation (4.36) (for the exact model) and Equation (4.43) (for the linear model). Similarly, the eccentricity error for the 3D example can be calculated as:

$$e_i^{Ecc} = \sqrt{\left(dp_i^X\right)^2 + \left(dp_i^Y\right)^2} \tag{4.46}$$

where $dp_i^X$, and $dp_i^Y$ can be calculated using Equation (4.31) for exact method and Equation (4.42) and for linear method.

For the 2D assembly considered, each component is assumed to be a rectangle of height 70 mm and width 100 mm (as shown in Figure 4-10(a)). Due to the presence of component variations (as shown in Figure 4-10(b)), the assembly may deviate from its nominal/ideal situation (see Figure 4-9). The translation errors ($dX_i$ and $dY_i$) of the top mating feature for each component (as shown in Figure 4-10(b)) are assumed to be 0.1 mm (i.e. $dX_i = dY_i = 0.1\,mm$). For the 3D assembly considered, each cylindrical component has a nominal height of 70 $mm$ and a nominal diameter of 100 $mm$ (as shown in Figure 4-11(a)). The translation errors $dX_i, dY_i$ and $dZ_i$ in each component (as shown in Figure 4-11(b)) are assumed to be $0.1\,mm$ (i.e. $dX_i = dY_i = dZ_i = 0.1\,mm$). For Case Study 1, the rotation matrix $\mathbf{R}_i$ in Equations (4.42) and (4.43) is an identity matrix and the vector $\mathbf{p}_i$ is given by $[0, Y_i]^T$ (in 2D) and $[0,0,Z_i]^T$ (in 3D). The analysis presents the worst case assembly of components. When analysing the worst-case, each variable for translation and rotation error is assumed to be at its maximum limit so that the worst possible assembly variations are obtained.

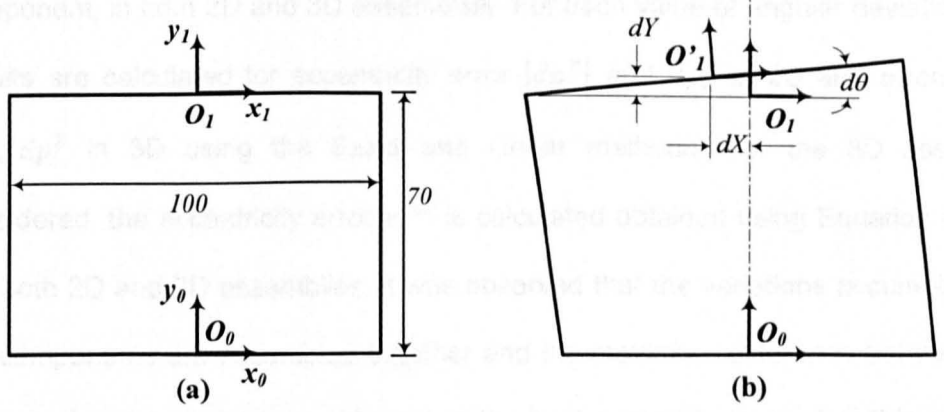


**Figure 4-10: A typical example of 2D component variation**

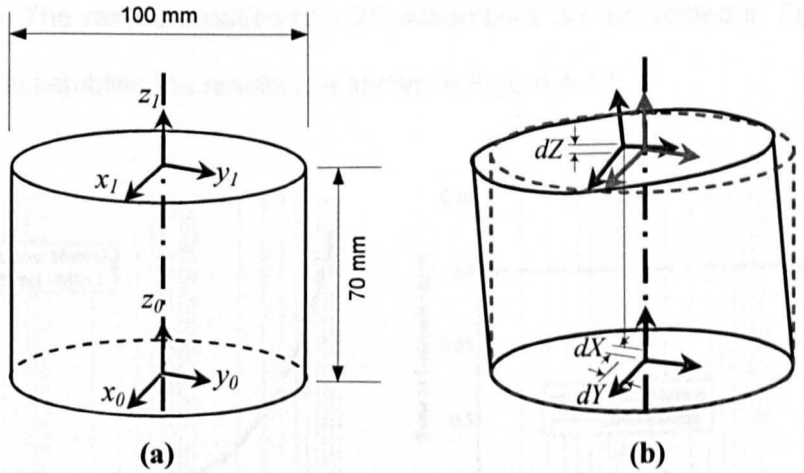


**Figure 4-11: Axisymmetric cylindrical component: (a) Nominal dimensions; (b) deviation form nominal geometry.**

For the purpose of analysing the performance of the linear model, a range of angular orientation errors in degrees ($d\theta_i$ for 2D components, and $d\theta_{xi}$, $d\theta_{yi}$ $d\theta_{zi}$ for 3D components) are considered in Equation (4.47). These are:

$$\begin{aligned} d\theta_{xi} = d\theta_{yi} = d\theta_{zi} = [\,&0.001, 0.005, 0.01, 0.05, 0.10, 0.15, 0.20, 0.25, 0.30, 0.35, \\ &0.40, 0.45, 0.50, 0.55, 0.60, 0.65, 0.70, 0.75, 0.80, 0.85, 0.90, 0.95, 1.00]\ \text{deg} \\ d\theta_i = [\,&0.001, 0.005, 0.01, 0.05, 0.10, 0.15, 0.20, 0.25, 0.30, 0.35, 0.40, 0.45, \\ &0.50, 0.55, 0.60, 0.65, 0.70, 0.75, 0.80, 0.85, 0.90, 0.95, 1.00]\ \text{deg} \end{aligned} \tag{4.47}$$

Assembly variations are calculated for stated values of angular orientation error, while keeping the translation errors constant (at 0.1 mm) for each assembly

component, in both 2D and 3D assemblies. For each value of angular deviation, the results are calculated for eccentricity error $|dp_i^X|$ and $dp_i^Y$ in 2D and errors $dp_i^X$, $dp_i^Y$, $dp_i^Z$ in 3D using the Exact and Linear methods. For the 3D assembly considered, the eccentricity error $e_i^{Ecc}$ is calculated obtained using Equation (4.46). For both 2D and 3D assemblies, it was observed that the variations accumulate as the components are assembled together and the maximum difference between the linear and exact methods is obtained at the final assembly stage. For this reason, the results are only compared for the final assembly stage for both 2D and 3D assemblies. The results produced for 2D assemblies are presented in Figure 4-12, and for 3D assemblies the results are shown in Figure 4-13.

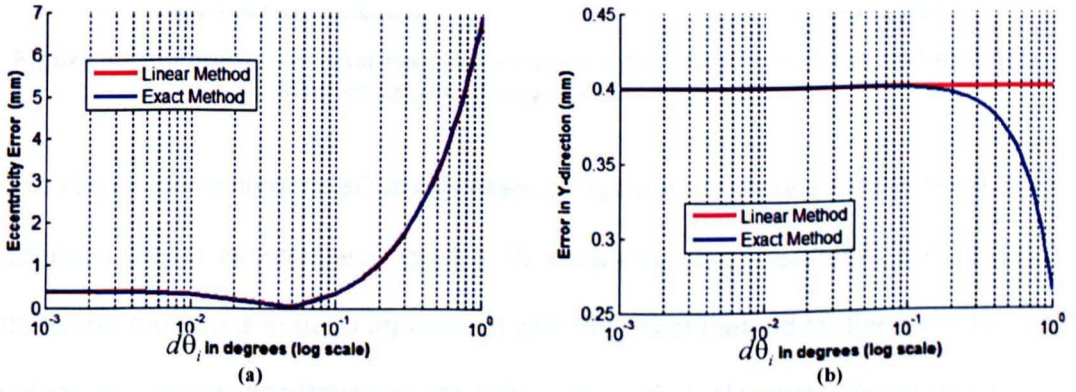


**Figure 4-12: The effect of changing orientation error on translation error (2D assembly).**

Figure 4-12 shows that the linear method produces results in good agreement with the exact method for error $|dp_i^X|$ (eccentricity error in the direction perpendicular to the datum axis), for the given range of values for $d\theta_i$. Similar levels of agreement are obtained for error $dp_i^Y$ (error along the datum axis), when $d\theta_i \leq 0.1°$. However, for $d\theta_i$ greater than $0.1°$, the linear and exact methods diverge for error $dp_i^Y$.

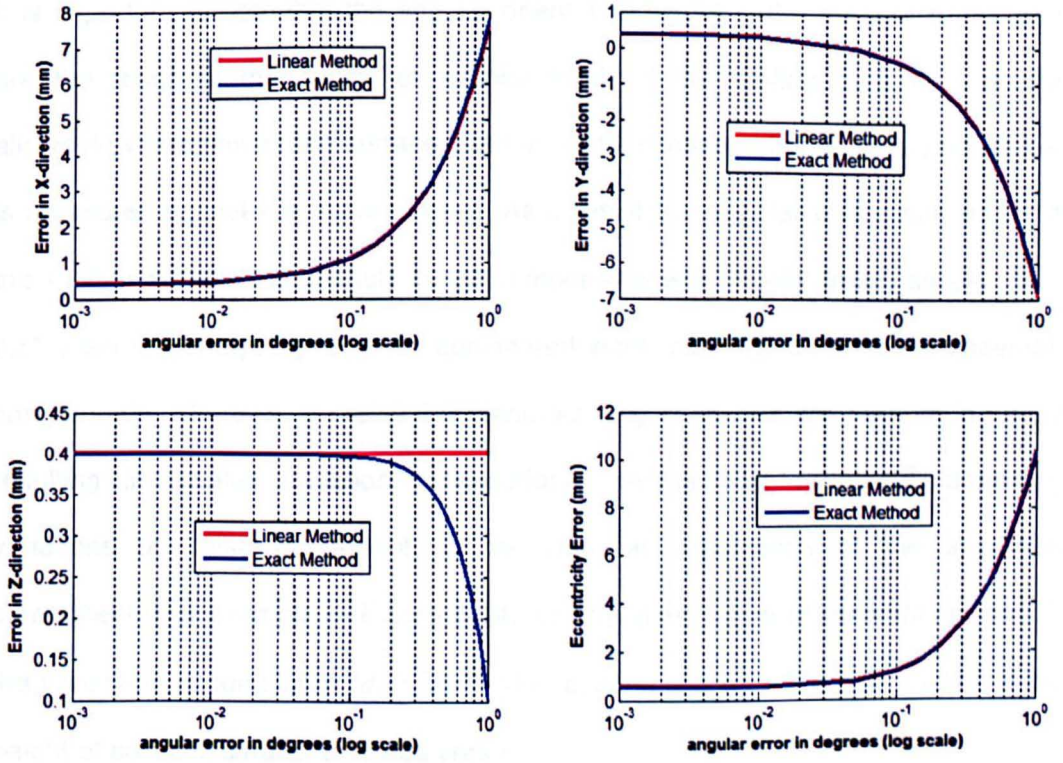


**Figure 4-13: Variation in final stage of an assembly of four cylindrical components at different values of angular orientation errors.**

The results presented for 3D assemblies in Figure 4-13 show a similar trend to that obtained for 2D assemblies. Figure 4-13 shows that for errors $dp_i^X$, $dp_i^Y$ and $e_i^{Con}$, the linear method is in good agreement with the exact method for the given range of values for angular orientation errors ($d\theta_{xi}$, $d\theta_{yi}$, $d\theta_{zi}$). However, for errors $dp_i^Z$, the results are in good agreement only when $d\theta_{xi}, d\theta_{yi}, d\theta_{zi}$ are less than $0.1°$. For values of $d\theta_{xi}, d\theta_{yi}, d\theta_{zi}$ greater than $0.1°$, the linear and exact methods diverge for error $dp_i^Z$. If the manufacturer is only interested in accurate prediction of assembly KC ($e_i^{Con}$), then linear method produce good results in all cases as shown in Figure 4-13, else linear method produce results in good agreement with the exact model for angular orientation errors as large as $0.1°$. In this Chapter the comparison of the linear and exact methods is focus for all translation errors and the assembly KC.

It is important to note that the angular orientation errors in the manufactured parts are the result of the quality of surface finish at the mating features, and the allowable variations for the surface finish in complex assemblies is quite precise and is measured typically in microns ($\mu m$). As a result the angular orientation errors at the mating surfaces of manufactured components are usually much smaller than 0.1°. Also the analysis presented considered worst case variation in the assembly components, whereas, in reality the manufacturing variations are random in nature resulting in smaller variation propagations. Beside part variations, assembly variations are also dependent on the nominal dimensions of the assembly component. For example in Figure 4-14, for any given value of error $d\theta_1$ in part 1, the variations accumulated ($dp_2^X$, $dp_2^Y$) after assembling part 2 will be smaller if the height of part 2 is smaller and vice versa.

The main finding for the above example is that the application of the linear method for calculating assembly variation propagations is limited to angular orientation errors less than 0.1°. The observed divergence between the linear and exact methods arises because the linear method is based on the assumptions that the angular orientation errors are small and the products of differential errors are negligible. This is further explained by considering the two-component assembly example shown in Figure 4-14.

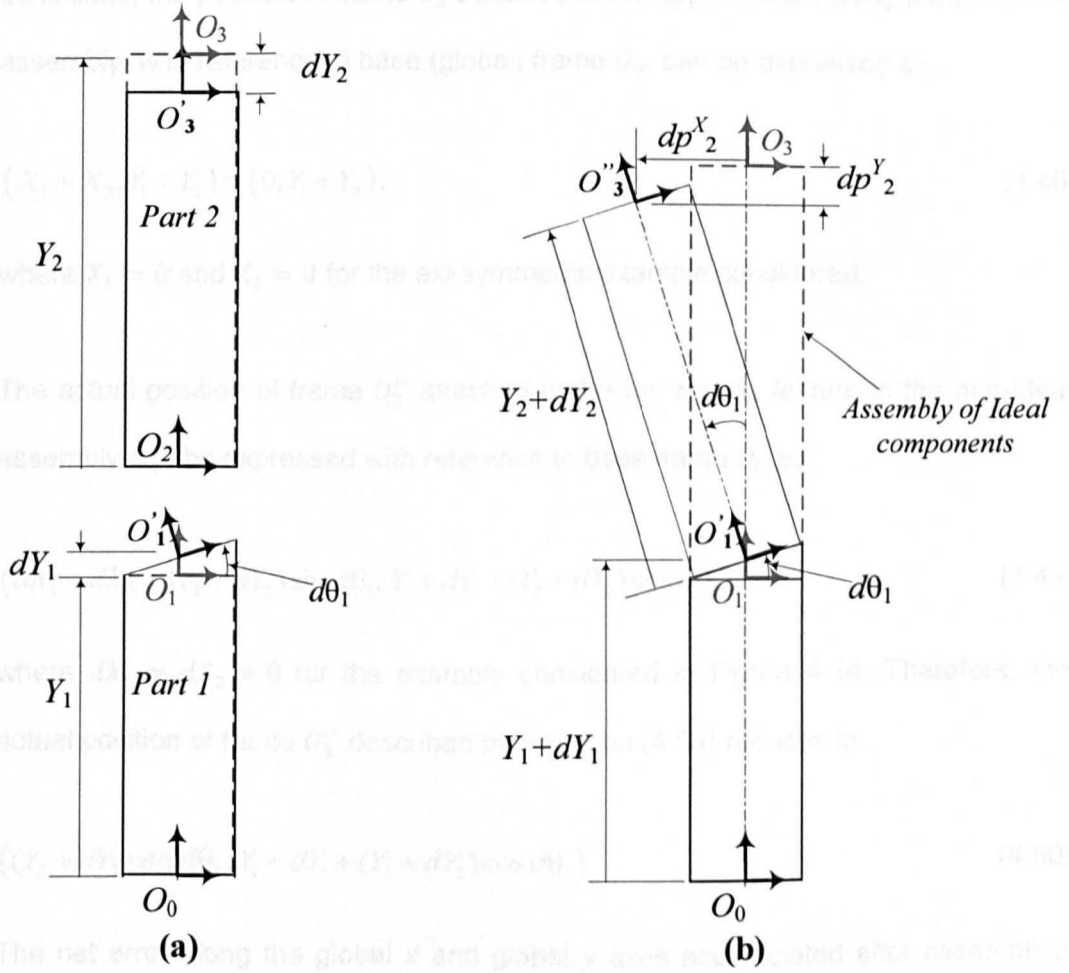


**Figure 4-14: (a) A typical example of ideal and non-ideal geometry of two rectangular components, (b) assembly of two components to demonstrate error accumulation after assembly.**

Figure 4-14 shows the assembly errors for a two-component assembly composed of rectangular shaped components with nominal heights $Y_1$ and $Y_2$. Figure 4-14(a) details the geometry of the two components under the nominal situation, as well as non-perfect situation. Due to variations in the manufacturing process, coordinate frame $O_1$ on part 1 is mis-positioned (by $dY_1$) and mis-oriented (by $d\theta_1$) to $O'_1$. Similarly, frame $O_3$ on part 2 is mis-positioned (by $dY_2$ only) to $O'_3$. Figure 4-14(b) shows the ideal assembly and the assembly when the two components contain variations from the nominal geometry. Due to the effect of $d\theta_1$, component 2 is mis-positioned and mis-oriented such that $O'_3$ has moved to location $O''_3$. Under ideal

conditions, the position of frame $O_3$ attached to the upper most mating feature in the assembly, with reference to base (global) frame $O_0$, can be expressed as:

$$(X_1 + X_2, Y_1 + Y_2) = (0, Y_1 + Y_2), \tag{4.48}$$

where $X_1 = 0$ and $X_2 = 0$ for the axi-symmetric example considered.

The actual position of frame $O_3''$ attached to the top mating feature in the non-ideal assembly can be expressed with reference to base frame $O_0$ as:

$$\left(dX_1 + dX_2 + (Y_2 + dY_2)\sin d\theta_1, Y_1 + dY_1 + (Y_2 + dY_2)\cos d\theta_1\right), \tag{4.49}$$

where $dX_1 = dX_2 = 0$ for the example considered in Figure 4-14. Therefore, the actual position of frame $O_3''$ described by Equation (4.53) reduces to:

$$\left((Y_2 + dY_2)\sin d\theta_1, Y_1 + dY_1 + (Y_2 + dY_2)\cos d\theta_1\right) \tag{4.50}$$

The net error along the global $x$ and global $y$ axes accumulated after assembling the two components ($dp_2^X$, $dp_2^Y$) can be calculated by subtracting the position of nominal assembly $(0, Y_1 + Y_2)$ to give:

$$\begin{aligned} dp_2^X &= (Y_2 + dY_2)\sin d\theta_1, \\ dp_2^Y &= \left(Y_1 + dY_1 + (Y_2 + dY_2)\cos d\theta_1\right) - \left(Y_1 + Y_2\right) = dY_1 + Y_2\left(\cos d\theta_1 - 1\right) + dY_2 \cos d\theta_1 \end{aligned} \tag{4.51}$$

Equation (4.51) represents the variations accumulated after assembling the two components. However, in the linear model, it is assumed that $d\theta_1$ is sufficiently small, that $\cos d\theta_1 \cong 1$ and $\sin d\theta_1 \cong d\theta_1$ and the product $dY_2.d\theta_1 = 0$. Using this approximation the variations accumulated after linearisation can be expressed as:

$$\begin{aligned} dp_2^X &= Y_2 d\theta_1 + dY_2 d\theta_1 = Y_2 d\theta_1 + 0 = Y_2 d\theta_1, \\ dp_2^Y &= dY_1 + Y_2\left(1 - 1\right) + dY_2\left(1\right) = dY_1 + dY_2. \end{aligned} \tag{4.52}$$

Equation (4.52) shows that if linearisation is performed, it does not account for effects of variations caused by angular error $d\theta_1$ when calculating variation propagation in the vertical $y$-direction and the product $dY_2 d\theta_1$ when calculating variation propagation in the $x$-direction. Comparing Equations (4.51) and (4.52), it is observed that the difference between the results obtained using the linear and exact methods for assembly variation $dp_2^Y$, depends upon the value of $d\theta_1$ and the height $Y_2$. This observation can be generalised to a general axi-symmetric assembly (as $dp_i^Y$ depend on $d\theta_{i-1}$ and $Y_i$). Comparing Equations (4.51) and (4.52), it is also observed that despite neglecting the product $dY_2.d\theta_1$ for assembly variation $dp_2^X$, the linear and exact methods are in good agreement. This indicates that product $dY_2.d\theta_1$ is much smaller than $Y_2(\cos d\theta_1 - 1)$ in Equation (4.52), particularly when $Y_2$ is large.

### 4.5.2 Analysis of Case Study 2

Case Study 2 considers the assembly of a casing used for a rotating machine. Such casings are either made as a single unit by casting, or fabricated from circular segments having nominally identical dimensions. The case considered consists of four uniformly segmented circular components. In order to investigate the performance of the proposed linear method, 2D (see Figure 4-15) and 3D uniformly segmented components (see Figure 4-16) are analysed.

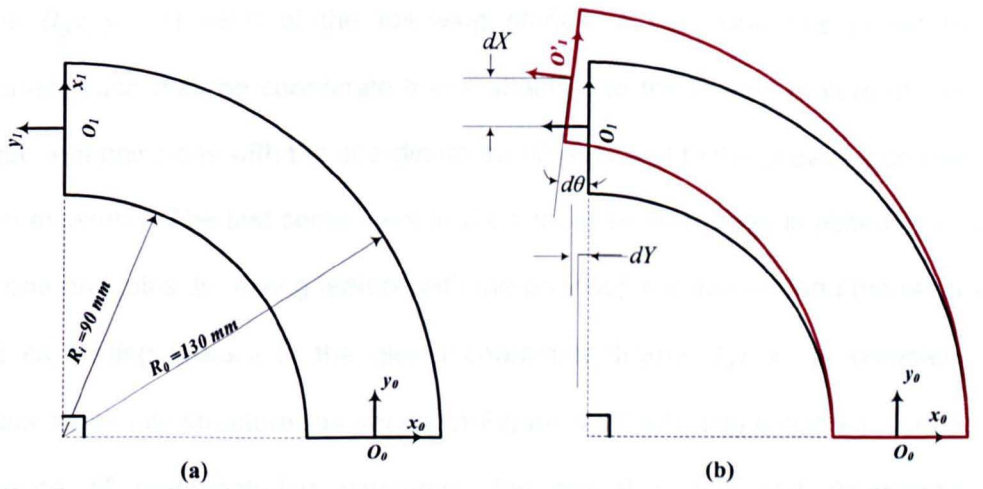


**Figure 4-15: (a) Nominal dimensions of a 2D uniformly segmented circular component; (b) A typical example of a 2D uniformly segmented circular component.**

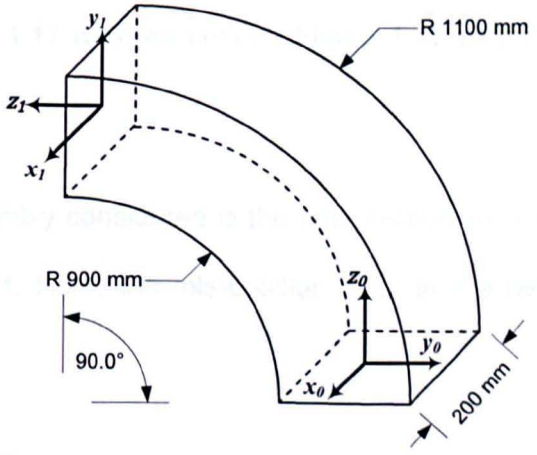


**Figure 4-16: Nominal dimensions of 3D uniformly segmented circular component.**

For assembly modelling, it is assumed that a coordinate frame is attached at the centre of each mating feature for each component, and the components are assembled by joining the mating surfaces of two mating components such that coordinate frames attached at the centre of mating surfaces are placed co-incident with no mating error. A 2D example is shown in Figure 4-17 to illustrate the assembly process and variation propagation. The first stage of assembly for ideal components represents the relationship between reference frames $O_0x_0y_0$ and $O_1x_1y_1$ attached to the first component (as shown in Figure 4-17). The centre of the base of the first component is considered as the origin of the global coordinate

frame $O_0x_0y_0$. At each of the following stages, a component is joined to the assembly such that the coordinate frame attached to the mating feature of the new component coincides with the coordinate frame attached to the previous component in the assembly. The last component in the final assembly stage is assembled such that one end joins its mating feature with the previous component and the other end joins its mating feature to the global coordinate frame $O_0x_0y_0$ to complete the circular assembly structure (as shown in Figure 4-17 with black colour). Due to the presence of manufacturing variations, the actual shape and dimensions of components vary from the nominal shape and dimensions. If manufactured components are assembled together, they do not form a perfect circular structure (as shown in Figure 4-17 with red colour). Figure 4-17 demonstrates this for a 2D assembly.

The KC for the assembly considered is the mis-position error in the radial direction of the $i^{th}$ component. Here, the mis-position error in the radial direction can be calculated as:

$$e_i^R = \sqrt{\left(dp_i^X\right)^2 + \left(dp_i^Y\right)^2} \qquad (for\ 2D\ assembly) \tag{4.53}$$

$$e_i^R = \sqrt{\left(dp_i^Y\right)^2 + \left(dp_i^Z\right)^2} \qquad (for\ 3D\ assembly) \tag{4.54}$$

where $dp_i^X$, and $dp_i^Y$ for the 2D assembly can be calculated using Equation (4.36) for the exact method and Equation (4.43) for the linear method, and $dp_i^Y$ and $dp_i^Z$ for the 3D assembly can be calculated using Equation (4.31) for the exact method and Equation (4.42) for the linear method.

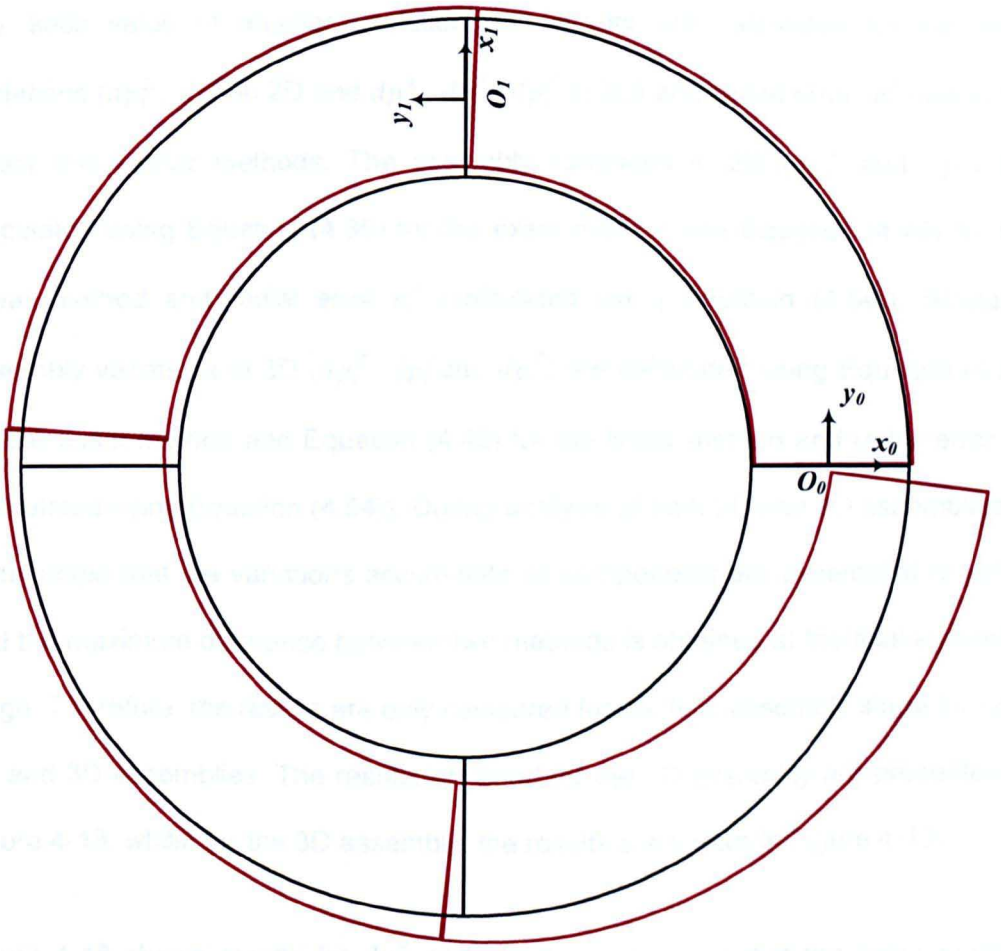


**Figure 4-17: Assembly of four ideal and non-ideal uniformly segmented circular components (case study 2).**

The nominal dimensions for each of the 2D assembly components are given in Figure 4-15 and nominal dimensions for each of the 3D assembly components are given in Figure 4-16. For the 2D assembly, the translation errors ($dX$ and $dY$) for each 2D component (as shown in Figure 4-15(b)) are taken to be 0.1 mm (i.e. $dX = dY = 0.1$) and for the 3D assembly, the translation errors for each 3D component are taken as 0.1 $mm$ (i.e. $dX = dY = dZ = 0.1\ mm$). In order to analyse the performance of the linear model compared to the exact model (in both 2D and 3D assemblies), results are calculated for a range of 23 values of angular orientation errors (as given in Equation (4.47)), while keeping the translation errors constant (at 0.1 mm) for each assembly component.

For each value of angular deviation, the results are calculated for assembly variations ($dp_i^X$, $dp_i^Y$ in 2D and $dp_i^X$, $dp_i^Y$, $dp_i^Z$ in 3D) and radial error ($e_i^R$) using the Exact and Linear methods. The assembly variations in 2D ($dp_i^X$ and $dp_i^Y$) are calculated using Equation (4.36) for the exact method and Equation (4.43) for the linear method and radial error $e_i^R$ (calculated using Equation (4.54)). Similarly, assembly variations in 3D ($dp_i^X$, $dp_i^Y$and $dp_i^Z$) are calculated using Equation (4.31) for the exact method and Equation (4.42) for the linear method and radial error $e_i^R$ (calculated using Equation (4.54)). During analysis of both 2D and 3D assemblies, it is observed that the variations accumulate as components are assembled together and the maximum difference between two methods is obtained at the final assembly stage. Therefore, the results are only compared for the final assembly stage for both 2D and 3D assemblies. The results obtained for the 2D assembly are presented in Figure 4-18, whilst for the 3D assembly, the results are shown in Figure 4-19.

Figure 4-18 shows results for $dp_i^Y$ and $e_i^R$. It can be seen that the linear method produces results in good agreement to the exact method for all values of $d\theta_i$. However for $dp_i^X$ (see Figure 4-18(a)), the linear method produces results in good agreement to the exact method only for $d\theta_i$ as large as 0.1°. These findings are identical to those obtained for Case Study 2 (in 2D) and are identical to Case Study 1 (in 2D), as the linear and exact method are in good agreement for the value of $d\theta_i$ as large as 0.1°.

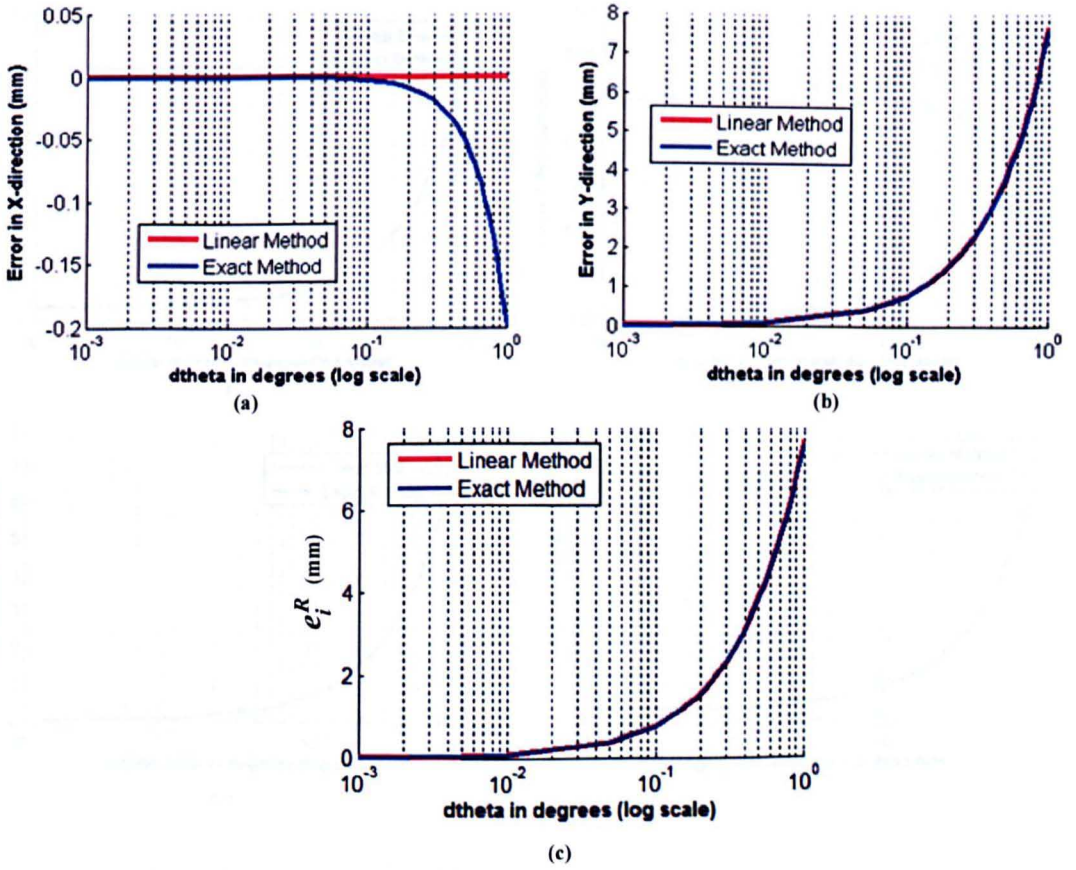


**Figure 4-18: : Variation at final stage in the 2D assembly of uniformly segmented circular components for different values of angular orientation errors.**

Similarly comparing the results in 3D (in Figure 4-19), it is found that for the given range of values for angular orientation error ($d\theta_{xi}$, $d\theta_{yi}$, $d\theta_{zi}$), the linear method is in good agreement with the exact method for errors $dp_i^X$, $dp_i^Z$ and $e_i^{Con}$. However, for error $dp_i^Y$, the results are in good agreement only when $d\theta_{xi}, d\theta_{yi}, d\theta_{zi} \leq 0.1°$. These results further confirm that the linear model can provide satisfactory results for calculating assembly variations even when component angular orientation errors are as large as $0.1°$.

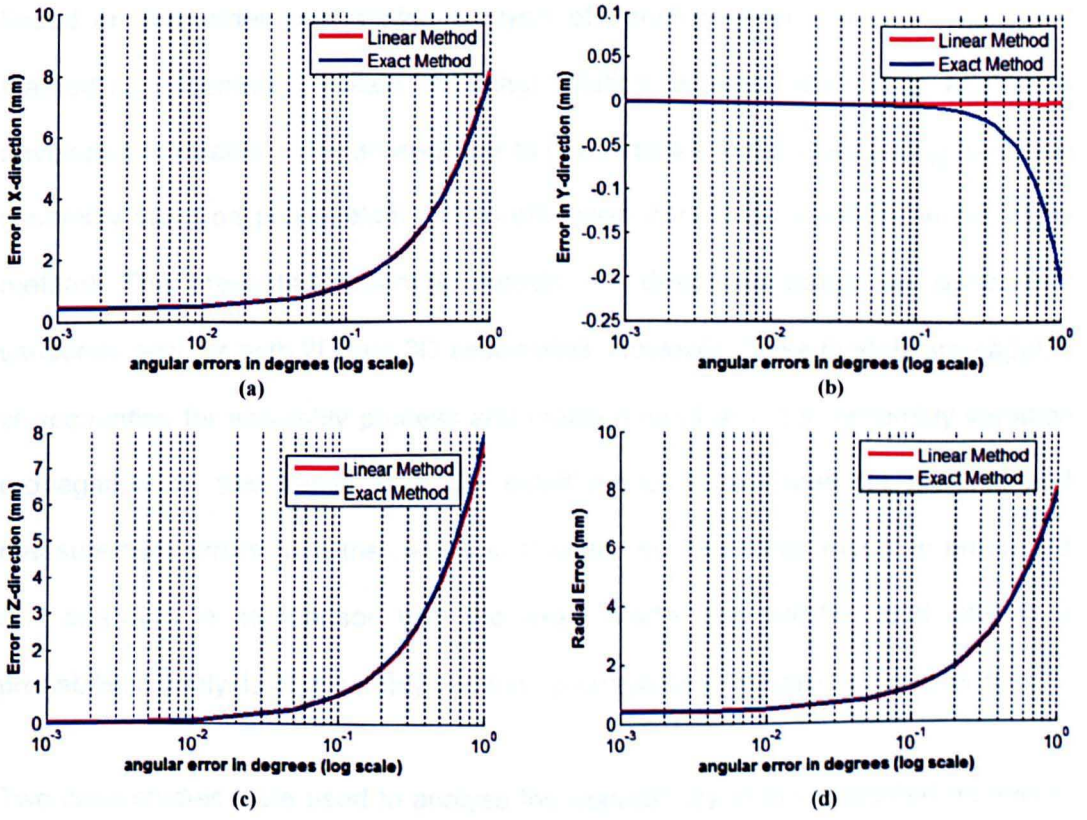


**Figure 4-19: Variation at final stage in the 3D assembly of uniformly segmented circular components for different values of angular orientation errors.**

## 4.6 Summary

This chapter gives an overview of assembly modelling and presents two models for calculating assembly variation propagations. The assembly models are based on transformation matrices and use a similar approach to connective assembly models to calculate variation propagation. The connective assembly is mathematically inconsistent because it uses linearised approach to model individual component but for modelling an assembly, connective model does not linearise the chain of matrix transform representing each assembly component. To overcome this discrepancy, the proposed models use consistent approach (either linear or fully non-linear) for modelling individual component or the assembly. The presented models are: i) Exact Model, based on fully non-linear matrix transforms; and ii) Linear Model,

based on first order perturbation analysis of transformation matrices. The Exact Method is presented to obtain the exact solution, whereas the Linear Method is developed to enable a design engineer to characterise major contributing factors in assembly variation propagation, which otherwise cannot be identified in the exact method. The presented assembly models are described based on component variations only for both 2D and 3D assemblies. However, these models are capable of accounting for assembly process and measurement errors in assembly variation propagation. In this thesis, only the exact model is extended for process and measurement errors (see the details in Chapter 8). The linear model is presented and analysed in comparison with the exact model and will be used later in a probabilistic analysis of assembly variation propagations (detailed in Chapter 6).

Two case studies were used to analyse the applicability of the presented models in 2D as well as 3D assemblies. Both case studies are typical examples of real assemblies for complex mechanical systems. The first case study comprises joining axially symmetric components together to build an up-right shaft. The second case study consists of uniformly segmented circular components, when assembled together they form a circular structure (such as the casing for a rotor used in high speed rotating machinery).

The performance of the linear model was compared to the exact model based on a range of values for angular orientation errors and worst case assembly of components. The numerical results indicate that the linear model can calculate results with good accuracy, if angular orientation errors ($d\theta_i$ in 2D and $d\theta_{xi}$, $d\theta_{yi}$, $d\theta_{zi}$ in 3D) are not larger than 0.1°. The analysis presented is based on worst case component variations, however in real world the manufactured parts are produced with random errors. For such cases of parts with random variations, the linear and

exact method may have good agreement for angular orientation errors greater than 0.1°.

It is also observed that the trends of results presented for 2D assemblies are similar to those for 3D assemblies in both case studies. The above finding are based on the given assembly examples, whereas, the results may vary depending upon the dimensions of the components.

The presented assembly models are quite simple, and yield accurate (exact) predictions efficiently. Although the Exact Model is the most accurate, it is not well suited to understanding the factors that contribute to the assembly variations. In contrast, the linear model provides an approximation that is in good agreement with the exact model, and results in equations that are easier to interpret and can be used in a probabilistic analysis of assembly variations. The presented models can be used to perform detailed assembly variation propagation analysis and minimise variation propagation in mechanical assemblies. However in this thesis, only exact model is extended for the detailed analysis and minimising variation propagations.

# Chapter 5 MODELLING GEOMETRIC VARIATIONS IN AXISYMMETRIC AND UNIFORMLY SEGMENTED CIRCULAR COMPONENTS

## 5.1 Introduction

Variations in manufacturing processes result in dimensional and geometric errors in components. Component variability is not only dependant on the inherent nature of the manufacturing process but also on inner properties of the component such as material properties, inner discontinuities of the material, and on chemical, mechanical, and geometrical properties of the component [141]. To take account of these variations from the nominal, the design engineer specifies a tolerance (i-e. the extent of acceptable deviation) for every component feature. A tolerance can be assigned for a dimension (size) or a feature describing the extent of geometric variation in the shape. Geometric variations refer to variation in shape, form, profile or location of a feature representing line plane or a surface.

Variations are different from tolerances. Component variations arise due to presence of manufacturing defects and the amount of variation present in a manufactured component can be quantified by inspecting the component using suitable measurement systems. In contrast, tolerance is the amount by which a specific feature or dimension is permitted to vary. The variations (dimensional and geometric) in a component can contribute significantly to the performance of an assembly or a product. These variations propagate and accumulate as the parts are assembled together, causing critical feature of the final assembly to vary. Variation propagation analysis is performed to predict the accumulation of variations in an assembly. If the parts are production parts, actual measurement data are preferred to be used to perform variation propagation analysis. In the case where parts are not in production and the measurement data is not available, data on similar parts and processes can be used [142]. In case when variation data is not available, part tolerances are substituted in place of its variations, assuming that the variations are within the tolerance limits.

The Exact and the Linear assembly models presented in Chapter 4 calculate assembly variations based on part variations described in terms of variations along degree of freedom (VDOF) (i.e. $dX, dY, dZ, d\theta_x, d\theta_y, d\theta_z$ in 3D and $dX, dY, d\theta$ in 2D). In practice, part variations or tolerances are not described in terms of VDOF, and require component variations (or tolerances) to be described in terms of VDOF (a form compatible with presented assembly models). The review of literature in show that good amount of work have been carried out in past on. Most of the work in literature review (see Chapter 2) is reported for describing part variations into VDOF for assembly components with prismatic shape. None of the researchers have attempted to describe geometric variation of axi-symmetric components and uniformly segmented components in terms of VDOF. This chapter thus aims to

model geometric variation (or tolerances) in axi-symmetric components and uniformly segmented components in terms of VDOF (a form compatible with assembly variation models presented in Chapter 4). VDOF methods are described in 2D as well as 3D based on the dimensional and geometric tolerances (run-out tolerances for Case Study 1 and flatness tolerances for Case Study 2) associated with components for Case Studies 1 and 2 considered in Chapter 4. This chapter also demonstrates a method for modelling component variations based on measured run-out data of production parts considered for Case Study 1. This data is used to demonstrate practical consideration of metrology for axi-symmetric components.

In Chapter 4 the performance of the linear model compared to the exact model was investigated without considering the effect of variation caused by geometric tolerances in the components. However, assembly variation propagations were calculated based on consideration of worst case variations along DOF in each component. In contrast, this chapter analyse the effect of variations caused by geometric tolerances (run-out tolerances for axi-symmetric components and flatness tolerances for uniformly segmented components) on assembly variation propagations. This chapter also investigates the performance of Linear model compared to Exact model based on range of values for geometric tolerance in two assembly case studies given in Chapter 4.

Initially this chapter describes geometric variations and their types in Section 5.2. This thesis focus on the assembly Case Study 1 containing axi-symmetric components and Case Study 2 containing uniformly segmented circular components The geometric variations and their tolerances associated with axi-symmetric components are normally expressed as run-out variations or their tolerances and for uniformly segmented circular components are usually expressed

as flatness variations or their tolerances. Therefore this chapter only describes run-out and flatness variations and their tolerances in Subsections 5.2.1 and 5.2.2, respectively. A description of geometric features along with the method of representing geometric variations in components using geometric feature techniques are described in Section 5.3. Section 5.4 describes a method of modelling geometric variations based on the tolerance zone limits and presents variational constraints algebraically for variation along degree of freedom (VDOF) based on run-out and flatness tolerance limits. Results are produced for incorporating geometric variations in components for assembly variation analysis. Also an analysis based on variational constraints is performed to investigate the effect of geometric feature variation on assembly variation using the linear and exact models in Section 5.4. A method for processing run-out measurement data in a form compatible with assembly variation models is described in Section 5.5. A summary of the chapter together with conclusions is presented in Section 5.6.

## 5.2 Component Variations and Their Types

Component variations are the deviation in the size or geometry of a component with respect to the nominal dimensions. Component variations can be divided into two types: dimensional variations and geometric variations. Dimensional variations refer to variation in the size of a particular dimension (such as length, width, diameter etc), whereas, geometric variations refer to the variation in the shape or form of a component feature from its nominal form [143]. In order to specify geometric variations in a component, the component is considered to be composed of features (geometric elements) such as planes, lines, etc. [141]. Geometric variations can be classified based on Geometric Dimensioning and Tolerancing (GD&T) specifications. GD&T is a symbolic language for communicating engineering design

specifications. It is used to specify the size, shape, form, orientation, and location of features on a part [135]. Figure 5-1 gives the classification of geometric variations (or corresponding tolerances) as given in [135, 141, 143].

Figure 5-1 shows that in general, geometric variations can be classified into four main categories: form, orientation, location, and run-out variations. The details of each of these geometric variations and their corresponding tolerances can be found [141]. This chapter only describes run-out variations and flatness as a form variation and their tolerance specifications because these specifications are associated with components present in Case Study 1 and Case Study 2, respectively.

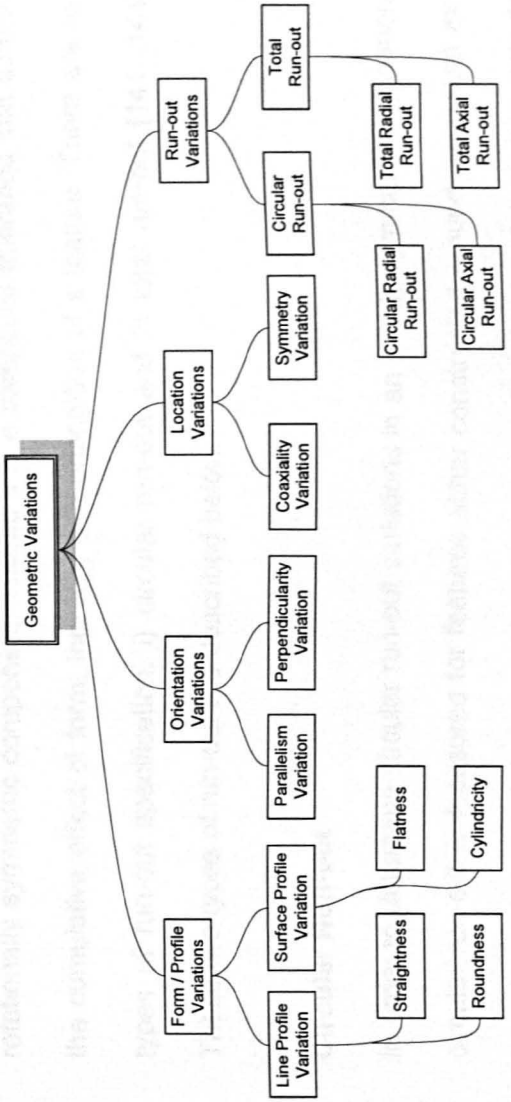


**Figure 5-1: Classification of geometric variations**

### 5.2.1 Run-out Tolerances

Run-out can be considered to be a measure of geometric uniformity of a surface, constructed symmetrically around an axis (radial run-out of cylindrical and conical surfaces), or constructed symmetrically perpendicular to the axis of symmetry (axial run-out of flat surfaces). Excessive run-out in rotating parts such as motor shafts and turbine rotors can lead to rotation imbalance problems and rejection of the final assembly due to mis-alignment [52].

The run-out tolerance associated with run-out variation does not control the size of rotationally symmetric component. Instead it is a composite tolerance that controls the cumulative effect of form, location, and orientation of a feature. There are two types of run-out specification: i) circular run-out and ii) total run-out [141, 144]. These two types of run-out are described below.

**Circular Run-out**

In order to determine circular run-out variations in an axially symmetric component, circular run-out is measured for features either constructed around the datum axis (circular radial run-out) or constructed at right angles to the datum axis (circular axial run-out). The circular run-out is measured in terms of the Full Indicator Movement (FIM), while the gauge probes over a single circular element on the surface of the component (see Figure 5-2(a)). FIM can be defined as the difference between the maximum and minimum reading of the probe as the part makes one complete revolution around the datum axis.

Circular radial run-out controls composite error effect of circularity[2][145, 146] and concentricity[3][147] (eccentricity error), and circular axial run-out controls profile variation in circular elements of a plane surface [148, 149].

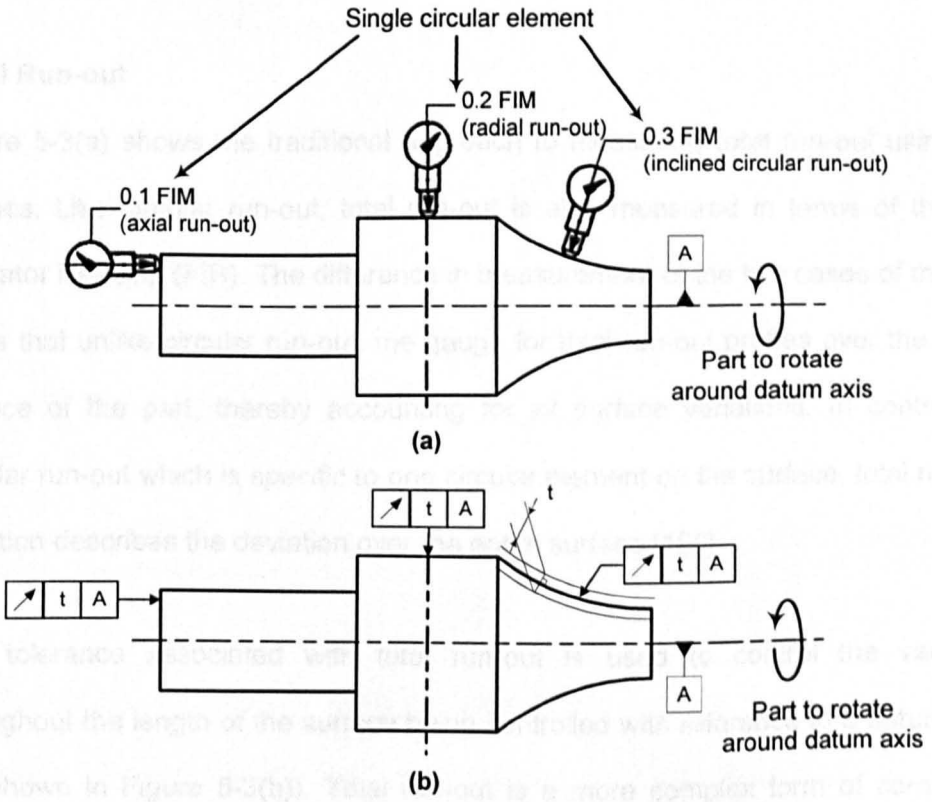


**Figure 5-2: (a) Traditional approach of measuring circular run-out using dial gauges; (b) Symbolic representation of circular run-out tolerance as per design standard BS EN ISO 1101:2005 [37]**

Figure 5-2(b) shows the standard representation of circular run-out tolerance in axial, radial, and inclined directions. For axial run-out, the tolerance zone is limited at any radial position by two adjacent circles a distance "t" apart, lying in a cylinder of measurement, the axis of which coincides with the datum axis A. The tolerance zone for radial run-out is limited by two concentric circles a distance "t" apart, the centre of which coincides with the datum axis A (as shown in Figure 5-2(b)).

[2] Circularity error also known as roundness error describes the variation in shape of a circular feature.

[3] Concentricity error can be described as eccentricity of geometric centre of a real circular feature with respect to datum axis or ideal centre.

Similarly, for inclined surfaces, the run-out in the direction perpendicular to the tangent of a curved surface shall not be greater than distance "t" during one revolution about the datum axis A. According to [36, 37], run-out not only applies to complete features but can also be applied to a restricted area of the feature.

**Total Run-out**

Figure 5-3(a) shows the traditional approach to measuring total run-out using dial gauges. Like circular run-out, total run-out is also measured in terms of the Full Indicator Reading (FIR). The difference in measurement of the two cases of the run-out is that unlike circular run-out, the gauge for total run-out probes over the entire surface of the part, thereby accounting for all surface variations. In contrast to circular run-out which is specific to one circular element on the surface, total run-out variation describes the deviation over the entire surface [150].

The tolerance associated with total run-out is used to control the variation throughout the length of the surface being controlled with reference to a datum axis (as shown in Figure 5-3(b)). Total run-out is a more complex form of composite tolerance and represents the higher level of run-out control. If total radial run-out tolerance is applied to surfaces constructed around the datum axis, it controls cumulative variations of cylindricity [151, 152], straightness, coaxiality, angularity, taper, and the profile of a surface. Also, when applied to surfaces at right angles to a datum axis, total run-out controls cumulative variations of perpendicularity (to detect wobble) and flatness (to detect concavity or convexity).

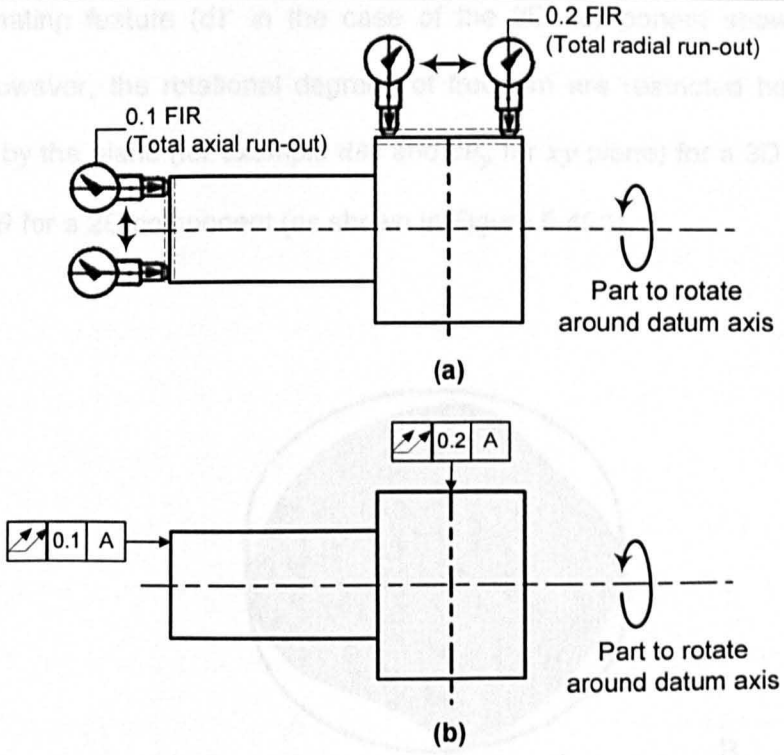


**Figure 5-3: (a) Traditional approach of measuring total run-out using dial gauges; (b) Symbolic representation of total run-out as per design standard BS EN ISO 1101:2005 [37]**

### 5.2.2 Flatness Variation and its Tolerance

Flatness variation is the form variation that describes the deviation in a feature from its geometrically ideal form. The specification of the flatness is described by a tolerance zone defined by two parallel planes within which the surface must lie [153]. Figure 5-4(a) shows an example of a flatness tolerance zone for a cylindrical object. It illustrates that the flatness tolerance zone is bounded by offsetting two planes parallel to the nominal. Figure 5-4(b) is taken from [72], and illustrates how flatness error affects the profile of a mating surface when viewed in 2D. As a result, the flatness error affects the orientation and position of the mating part.

The flatness tolerance has both rotational and translational degrees of freedom restricted within the flatness tolerance zone boundary. The translation degree of freedom due to flatness tolerance is restricted along the direction normal to the

nominal mating feature ($dY$ in the case of the 2D component shown in Figure 5-4(c)). However, the rotational degrees of freedom are restricted between axes contained by the plane (for example $d\theta_x$ and $d\theta_y$ for $xy$ plane) for a 3D component, or angle $d\theta$ for a 2D component (as shown in Figure 5-4(c)).

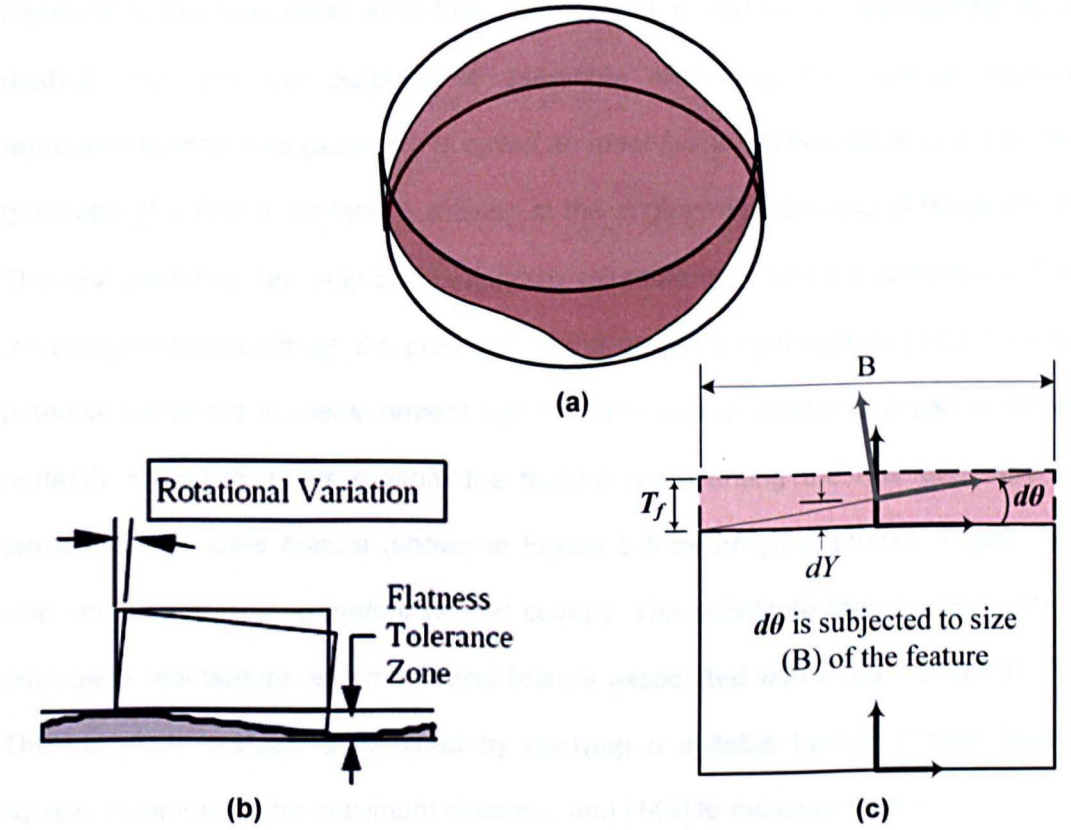


**Figure 5-4: (a) flatness tolerance zone of a cylindrical object; (b) effect of flatness error on mating component [72]; (c) effect of flatness error in terms of translation and rotation degrees of freedom error.**

## 5.3 What are Geometric Features?

Geometric features (also known as assembly features) are basically building blocks that provide convenient geometric operations and parameters for building assemblies [81]. A geometric feature represents the shape or geometry of the surface, line, or object. Geometric features are distinguished by their nature such

as: point feature, line feature, surface feature, or volume feature. According to international design standards DD CEN ISO/TS 17450-1:2007 [154], features can be classified by three types: ideal, non-ideal (real), and substitute feature.

Figure 5-5 shows the difference between ideal, non-ideal, and substitute feature. Consider a surface feature representing circular plane (as shown in Figure 5-5). In Figure 5-5, the theoretical error-free geometry of a surface is represented by a dashed line. For the purpose of assembly modelling, the surface feature representing error-free geometry is called an *ideal feature*. Theoretical or error-free geometry of a part or surface is defined in the engineering drawing of the product. The real geometry can only be obtained by measurement and the accuracy of the measurement depends on the precision of the measurement system [143]. Due to potential variations in measurement systems, the real geometry of a part is never perfectly known. For this reason, the feature representing the real geometry is termed as *non-ideal feature* (shown in Figure 5-5 by irregular profile). Figure 5-5 also shows a *substitute feature* (in red colour). The substitute feature, also called equivalent real feature, is a theoretical feature associated with a real surface [155]. The substitute surface is obtained by applying a suitable best-fit criteria (least-square, minimum of the maximum distance, etc) [143] to measured data.

For the purpose of modelling component variations, the relative variation between ideal and substitute features need to be described in terms of translation errors $(dX, dY, dZ)$ and rotation errors $(d\theta_x, d\theta_y, d\theta_z)$. For this purpose, Cartesian frames are attached to both ideal and substitute features (as shown in Figure 5-5). Figure 5-5 shows that a local coordinate frame $O'X'Y'Z'$ is attached to the substitute feature and a reference coordinate frame $OXYZ$ is rigidly attached to the ideal feature. These coordinate frames have the degrees of freedom of the corresponding features or surfaces. Therefore, the relative position (error) between coordinate

frame $O'X'Y'Z'$ and coordinate frame $OXYZ$ can be described using matrix transforms. Matrix transform expressed by Equation (4.12) can be used when the analysis is based on exact method, and transform given by Equation (4.19) can be used for the linear methods.

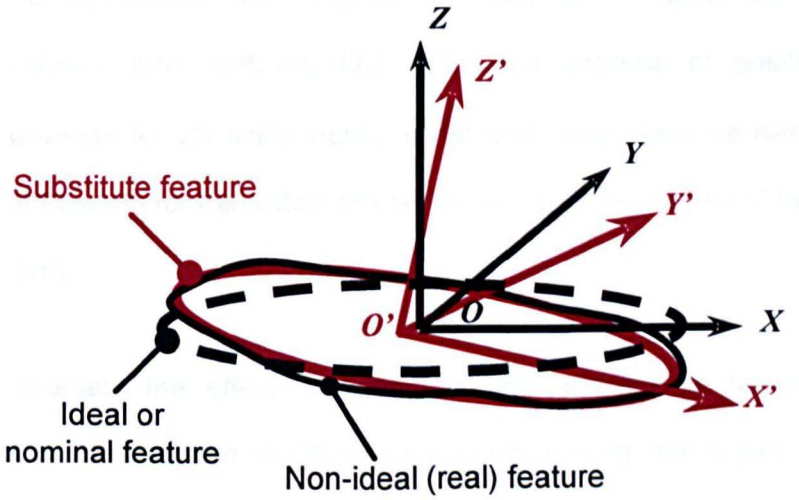


**Figure 5-5: Representation of ideal, non-ideal, and substitute feature.**

Similarly, the matrix transformations for 2D components for the relative position (error) between a coordinate frame, attached to the substitute feature, and a reference coordinate frame attached to ideal feature can be expressed using Equations (4.35) for the exact method and similarly for linear method.

## 5.4 Modelling Component Variations Based on Tolerance Zone Limits

The effect of the geometric tolerances associated with the corresponding surface feature may result in mis-position and mis-orientation of the associated feature [72]. The errors caused by geometric tolerances are usually smaller than the size tolerances on the same part [156]. These deviations can be regarded as deviations of the nominal surface. To model component variations based on tolerance zone

limits, variational constraints are described along possible degrees of freedom of error for a toleranced feature. Such deviation of a surface/feature can be described accurately by VDOF-based representation. This approach for modelling component variations is also referred as variations along degree of freedom (VDOF) modelling [84]. For a 3D component, the variational constraints are described as three degrees of rotation error $(d\theta_x, d\theta_y, d\theta_z)$ and three degrees of position error $(dX, dY, dZ)$, whereas for 2D components, variational constraints are described in two degrees of freedom for translation errors $(dX, dY)$ and one degree of freedom of rotation error $(d\theta)$.

In order to evaluate the effect of geometric and dimensional tolerances on component variability here, the VDOF for axi-symmetric components given in Case Study 1 and uniformly-segmented circular components Case Study 2 are considered. Algebraic relations for VDOFs are derived separately for axi-symmetric components and uniformly-segmented circular components for both 2D and 3D assemblies.

## 5.4.1 Modelling VDOF for Axi-Symmetric Components in Case Study 1

In this section, the variational constraints for 2D and 3D components are evaluated separately based on size and run-out tolerance zones applied to axi-symmetric components.

### *5.4.1.1 Evaluating VDOF for 2D Axi-Symmetric Components*

A 2D axi-symmetric component, taken from Case Study 1 in Chapter 4 is considered here under the effect of dimensional (size) tolerance and circular run-out tolerances in the axial and radial directions for the evaluation of VDOF. Figure

5-6(a) shows the symbolic representation of the tolerance zone limits. The tolerance zone limits are specified for variations in size (height) by $\pm T_s$, and run-out variations in radial and axial directions by $T_{rr}$ and $T_{ar}$, respectively.

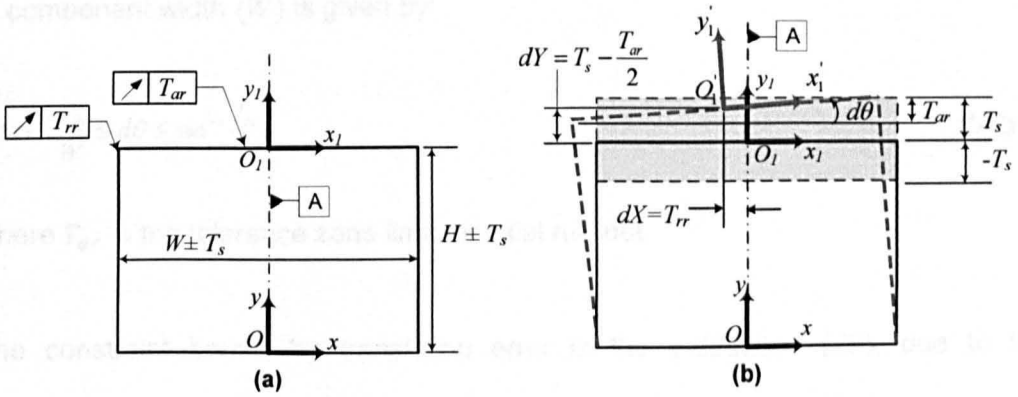


**Figure 5-6: A typical example showing the effect of axial and radial circular run-out on 2D rectangular component.**

Figure 5-6(b) shows that due to the effect of radial run-out ($T_{rr}$), axial run-out ($T_{ar}$), and size variation ($T_s$), the feature frame $O_1x_1y_1$ is mis-positioned and mis-oriented by $dX, dY$ and $d\theta$ to new position $O_1'x_1'y_1'$. Based on design standards [37], it is found (see Figure 5-6(b)) that the radial run-out only contributes to mis-position of feature frame $O_1x_1y_1$ in the direction perpendicular to the datum axis A (i-e. $dX$), whereas axial run-out contributes to both mis-position (in y-direction) and mis-orientation of $O_1x_1y_1$. The mis-position of frame $O_1x_1y_1$ in the y-direction ($dY$) is due to the combined effect of axial run-out $T_{ar}$ and size tolerance $T_s$. The orientation error $d\theta$ for the top feature is solely influenced by the axial run-out. Therefore variations along degrees of freedom for the rectangular component considered under the effect of size and run-out tolerances can be derived for the constraint bounds as shown below.

From Figure 5-6 (b) the constraint bound of translation error $dX$ as a result of radial run-out is depicted as:

$$-T_{rr} \le dX \le T_{rr}, \tag{5.1}$$

where $T_{rr}$ is the range of the radial run-out tolerance zone.

The constraint bound for rotation error as a result of axial run-out after ignoring error in component width ($W$) is given by:

$$-\tan^{-1}\frac{T_{ar}}{W} \le d\theta \le \tan^{-1}\frac{T_{ar}}{W}, \tag{5.2}$$

where $T_{ar}$ is the tolerance zone limit for axial run-out.

The constraint bound for translation error in the y-direction ($dY$), due to the combined effect of axial run-out tolerance $T_{ar}$ and size tolerance $T_s$ can be written as:

$$-(T_s - \frac{dY_{ar}}{2}) \le dY \le (T_s - \frac{dY_{ar}}{2}). \tag{5.3}$$

The constraints for translation and orientation errors in a 2D component using VDOF are:

$$(dX, dY, d\theta)^T \tag{5.4}$$

### *5.4.1.2 Evaluating VDOF for 3D Axi-Symmetric Components*

A 3D axially symmetric cylindrical component taken from Case study 1 in Chapter 4 is considered here under the effect of dimensional (size) and run-out tolerances. Industries assembling axi-symmetric components for high-speed rotating machines designate axial run-out and radial run-out as key tolerances for components that rotate about their axis or rotation. Therefore, it is necessary to derive algebraic constraints describing VDOF resulting from joint effect of size and run-out tolerances. The limits for VDOF for a 3D axi symmetric component are evaluated based on given tolerance limits. Figure 5-7(a) shows a 3D axi-symmetric cylindrical

component subjected to the effect of radial run-out $T_{rr}$ for the feature constructed around the datum axis, axial run-out $T_{ar}$ for top feature constructed normal to the datum axis and dimensional tolerance $\pm T_s$ showing the limits for variation in size.

For the purpose of modelling geometric variations, it is assumed that the geometric tolerance (axial run-out) $T_{ar}$ is contained within the size tolerance zone limit $\pm T_s$. Figure 5-7(b) shows how the tolerance zone limit for axial run-out is contained by the size tolerance zone. The given example shows the exaggerated tolerance zone limits for axial run-out and size tolerances. The net effect of dimensional and axial run-out tolerances is described in Figure 5-7(d), the enlarged view of toleranced part of top feature of Figure 5-7(b).Figure 5-7(d) shows that axial run-out contributes to a position error in z-direction as well as orientation errors about axes contained by the feature (i-e. $d\theta_x$ and $d\theta_y$). However, size tolerance only contributes to mis position error in the z-direction.

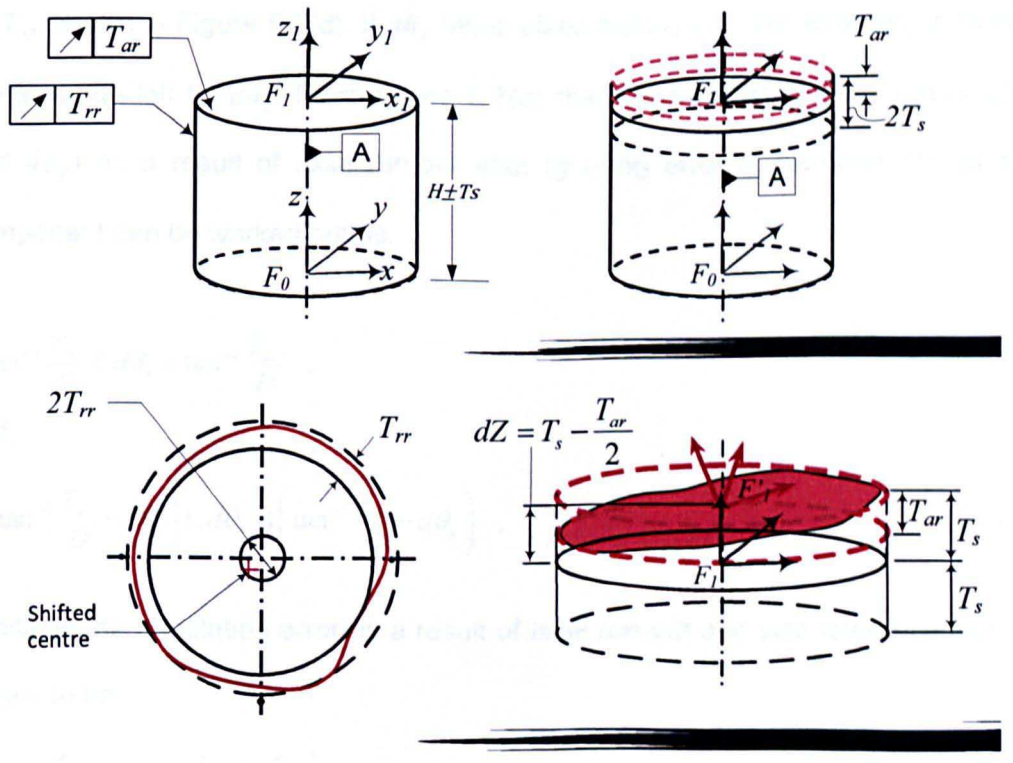


**Figure 5-7: Effect of axial and radial circular run-out on 3D component**

The tolerance zone limit for radial run-out is described in Figure 5-7(c), which shows a top view of the cylindrical component. The radial run-out zone is represented by a circle (dashed) concentric to the nominal circle (solid) with a difference in radius of $T_{rr}$. Figure 5-7(c) shows that due to the effect of radial run-out, the actual profile of the circular segment is mis-located causing eccentricity (geometric shift by $dX, dY$) of the actual centre with respect to the ideal centre. The maximum eccentricity caused by radial run-out is contained within the zone defined by a small circle of radius $T_{rr}$ concentric to the nominal circle, as shown in Figure 5-7(c). Using this information the constraint bounds can be obtained as described below.

From Figure 5-7(c) the translation error constraint as a result of radial run-out is depicted as:

$$-T_{rr} \le dX \le T_{rr} \quad and \quad -T_{rr} \le dY \le T_{rr}, \tag{5.5}$$

The orientation errors $d\theta_x$ and $d\theta_y$ are constrained to lie within the region bounded by $T_{ar}$ shown in Figure 5-7(d). If $d\theta_x$ takes place before $d\theta_y$, the error $d\theta_y$ is limited to the range left by $d\theta_x$. From Figure 5-7(d) the constraint on rotation errors ($d\theta_x$ and $d\theta_y$) as a result of axial run-out after ignoring error in diameter ($D$) of the component can be worked out as:

$$-\tan^{-1}\frac{T_{ar}}{D} \le d\theta_x \le \tan^{-1}\frac{T_{ar}}{D} \ , \tag{5.6}$$

and,

$$-\left(\tan^{-1}\frac{T_{ar}}{D} - d\theta_x\right) \le d\theta_y \le \left(\tan^{-1}\frac{T_{ar}}{D} - d\theta_x\right) \ , \tag{5.7}$$

Similarly, the translation error as a result of axial run-out and size tolerance can be shown to be:

$$-\left(T_s - \frac{T_{ar}}{2}\right) \le dZ \le \left(T_s - \frac{T_{ar}}{2}\right) \tag{5.8}$$

If the constraints for translation and orientation errors in 3D component due to combined effect of size and run-out tolerances are described, then the vector representing VDOF for a 3D component can be written as:

$$(dX, dY, dZ, d\theta_x, d\theta_y, d\theta_z)^T, \quad where \quad d\theta_z = 0 \tag{5.9}$$

### *5.4.1.3 Analysis of Case Study 1*

The analysis is performed for 2D as well as 3D assemblies based on a range of values for run-out tolerance zone limits while assuming worst possible variations for each component in the assembly.The purpose of analysis here is to evaluate the performance of the linear model compared to the exact model based on a range of values for run-out tolerances and to determine the threshold value for run-out tolerances at which there is significant difference between the results produced by linear and exact model.

Case Study 1 consists of four identical axi-symmetric rigid components and four assembly stages. For 2D assembly, each component is nominally a rectangle of height 70 mm and width 100 $mm$, whereas, for 3D assembly, the components are ideally cylinders of identical size with nominal height of 70 $mm$ and nominal diameter of 100 $mm$. Variations along degrees of freedom are calculated based on the tolerance zone limits for 2D component (as described in 5.4.1.1) and 3D axi-symmetric components (as described in 5.4.1.2) to calculate assembly variations. The tolerance zone limit for size variation ($T_s$) is taken as 0.1 $mm$ for both 2D and 3D assembly components, whereas, the range of tolerance zone limits for both axial and radial run-out ($T_{ar}$and $T_{rr}$) is given by following series:

$$T_{ar} = T_{rr} = [0.001, 0.005, 0.01, 0.02, ...0.10, 0.15, 0.20, 0.25, 0.30, 0.35, 0.40, 0.45, 0.50, 0.55, 0.60, 0.65, 0.70, 0.75, 0.80, 0.85, 0.90, 0.95, 1.00]\ mm \tag{5.10}$$

For each value of run-out tolerance, the results are calculated for assembly variations (in 2D and in 3D) using the Exact and Linear methods as described in Chapter 4. For the 2D assembly considered, the results are calculated for error $dp_i^Y$ and assembly KC (the eccentricity error $|dp_i^X|$), whereas for the 3D assembly considered, the results are calculated for errors $dp_i^X$, $dp_i^Y$, $dp_i^Z$ and the eccentricity error (the KC) $e_i^{Con}$ (calculated using Equation (4.46)).

For both 2D and 3D assemblies, it was observed that the variations accumulate as the components are assembled together and the maximum difference between the linear and exact methods is obtained at the final assembly stage. For this reason, the results are only compared for final assembly stage for both 2D and 3D assemblies. The results produced for 2D assemblies are presented in Figure 5-8, and for 3D assemblies the results are shown in Figure 5-9.

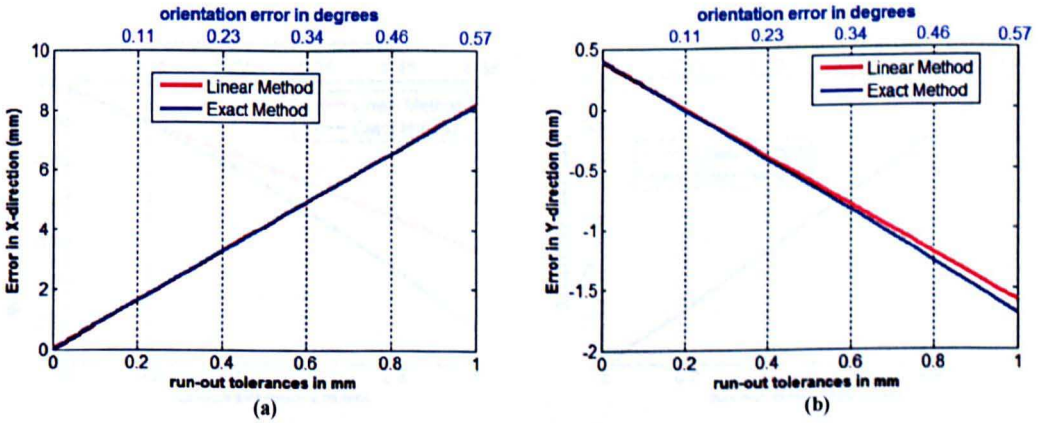


**Figure 5-8: Variations at final assemble stage for the assembly of 2D axi-symmetric rectangular components using exact and linear model.**

Figure 5-8 shows that the linear method produce results in good agreement with the exact method for the assembly KC $|dp_i^X|$ (eccentricity error), for the given range of values for run-out tolerances. Similar levels of agreement are obtained for error $dp_i^Y$ (error along the datum axis), when run-out $\leq 0.4\ mm$. However, for run-out greater than $0.4\ mm$, there is a small difference between the results obtained using the

linear and exact methods for error $dp_i^Y$. In Figure 5-8 the results are also compared for equivalent value of orientation error in degrees. The results show a similar trend to those obtained in Chapter 4 for 2D rectangular components. In industrial applications the run-out tolerance assigned to axi-symmetric components is much smaller than $0.4\,mm$ (usually expressed in microns). This shows that the linear model produce results in good agreement compared with the exact model even if the run-out tolerance are as large as $0.4\,mm$.

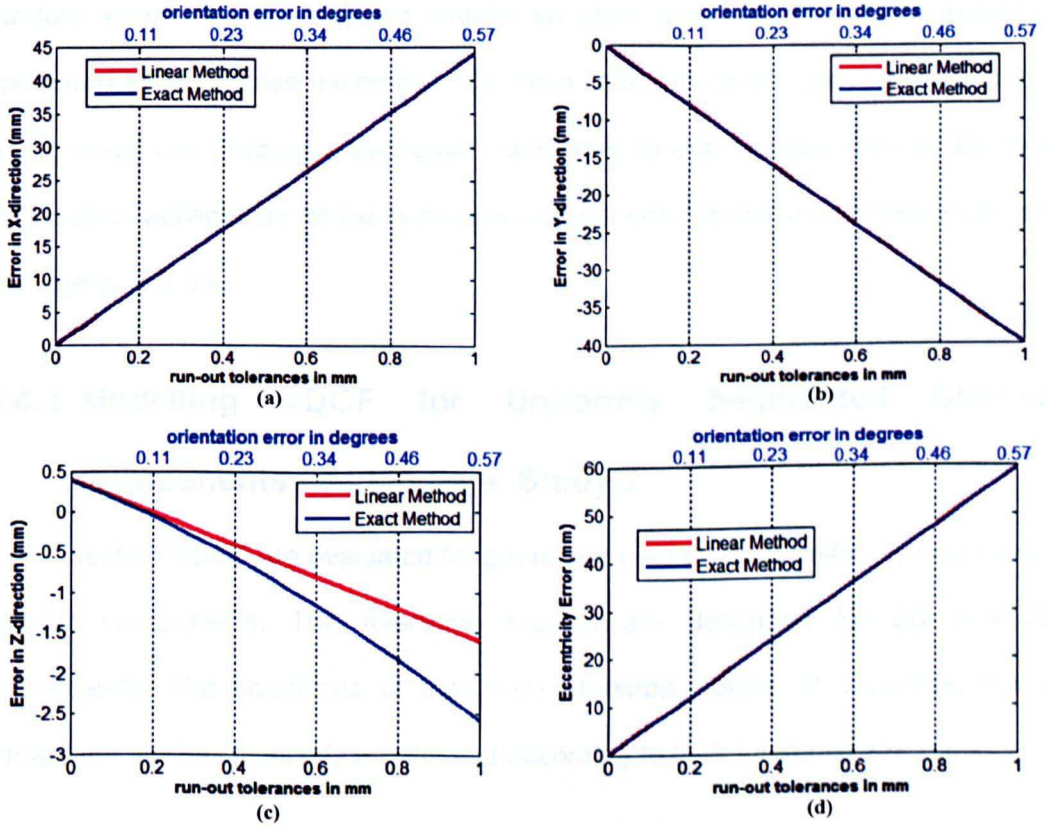


**Figure 5-9: Variations at final assemble stage for the assembly of 3D axi-symmetric cylindrical components using exact and linear model.**

The results presented for 3D assemblies shown in Figure 5-9 show a similar trend to that obtained for 2D assemblies. Figure 5-9 shows that for errors $\mathrm{dp_i^X}$, $\mathrm{dp_i^Y}$ and $\mathrm{e_i^{Con}}$, the linear method is in good agreement with the exact method for the given range of values for angular orientation errors ($d\theta_{xi}$, $d\theta_{yi}$, $d\theta_{zi}$). However, for errors

$dp_i^z$, the results are also in good agreement even when run-out tolerances are large as 0.2 $mm$. Also based on the comparison for angular orientation error equivalant to run-out tolerance it can be seen that the linear model produce results with agreement. These results show a similar trend to those obtained in Chapter 4 for 3D axi-symmetric cylindrical components.

It is important to note that the analysis presented considered worst case variation in the assembly components, whereas, in reality the manufacturing variations are random in nature thus resulting smaller variation propagations in real assembly compared to worst case assembly. The main finding from the above results is that linear model can produce good results compared to exact model and can be used for practical applications of axi-symmetric components where run-out tolerances are as large as 0.2 $mm$.

### 5.4.2 Modelling VDOF for Uniformly Segmented Circular Components used in Case Study 2

In this section VDOF are evaluated for geometric tolerances of uniformly segmented circular components. The tolerance bounds are described for 2D and 3D components. The conditions of maximum allowable values of variations that a variant feature has to satisfy are derived according to their tolerance zone limits.

#### *5.4.2.1 Evaluating VDOF for a 2D Uniformly-Segmented Circular Component*

A 2D uniformly segmented circular component under the influence of size tolerance and form tolerance is shown in Figure 5-10 (a). The nominal relationship of feature frame $O_1x_1y_1$ with respect to feature frame $O_0x_0y_0$ can be represented by vector $(X, Y, \pi/2)^T$. Figure 5-10 (b) shows that due to effect of size and form variations the

feature frame $O_1x_1y_1$ is mis-positioned and mis-oriented to feature frame $O_1'x_1'y_1'$. The size tolerances only contribute in mis-position of feature frame $O_1x_1y_1$ in $x$-direction by $dX$ to new position $O_1'x_1'y_1'$. However, the form variations contribute in mis-position and mis-orientation of feature frame $O_1x_1y_1$ by $dY$ and $d\theta$, respectively. Thus following constraint bounds can be obtained for VDOF within given tolerance zones.

From Figure 5-10 (b) the constraint of translation error $dX$ as a result of size tolerance $T_s$ can be depicted as:

$$-T_s \le dX \le T_s. \tag{5.11}$$

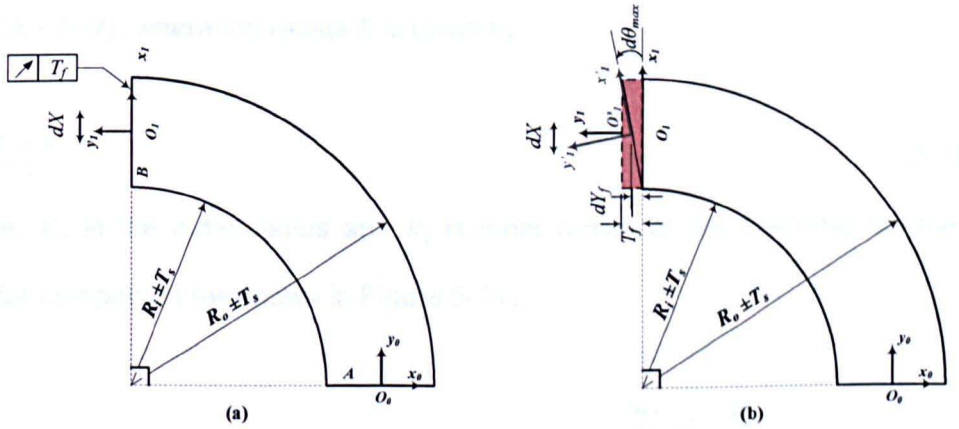


**Figure 5-10: Effect of size and form tolerance on 2D uniformly segmented circular component.**

The constraint of rotation errors $d\theta$ and translation error $dY$ as a result of form tolerance $T_f$ can be worked out from Figure 5-10 (b) as:

$$-\tan^{-1}\left(\frac{T_f}{R_o - R_i}\right) \le d\theta \le \tan^{-1}\left(\frac{T_f}{R_o - R_i}\right), \tag{5.12}$$

$$-\frac{T_f}{2} \le dY \le \frac{T_f}{2}, \tag{5.13}$$

where, $R_o$ is the outer radius and $R_i$ is inner radius of the segmented circular component (as shown in Figure 5-10). If the constraints for translation and

orientation errors in 2D component are described, vector representing VDOF for a 2D component can be written as:

$$(dX, dY, d\theta)^T. \tag{5.14}$$

### 5.4.2.2 Evaluating VDOF for a 3D Uniformly-Segmented Circular Component

A 3D uniformly segmented rigid circular component is considered here under the effect of dimensional (size) and form tolerance (as shown in Figure 5-11). Under ideal situations, coordinate frames $x_0y_0z_0$ and $x_1y_1z_1$ are attached at the centres of the two mating features to define the location and orientation in 3D space. For a nominal component, the co-ordinates of frame $x_1y_1z_1$ with reference to frame $x_0y_0z_0$ are: $(0, -R, R)$, where the radius $R$ is given by:

$$R = \frac{R_o + R_i}{2}, \tag{5.15}$$

where, $R_o$ is the outer radius and $R_i$ is inner radius of the uniformly segmented circular component (as shown in Figure 5-11).

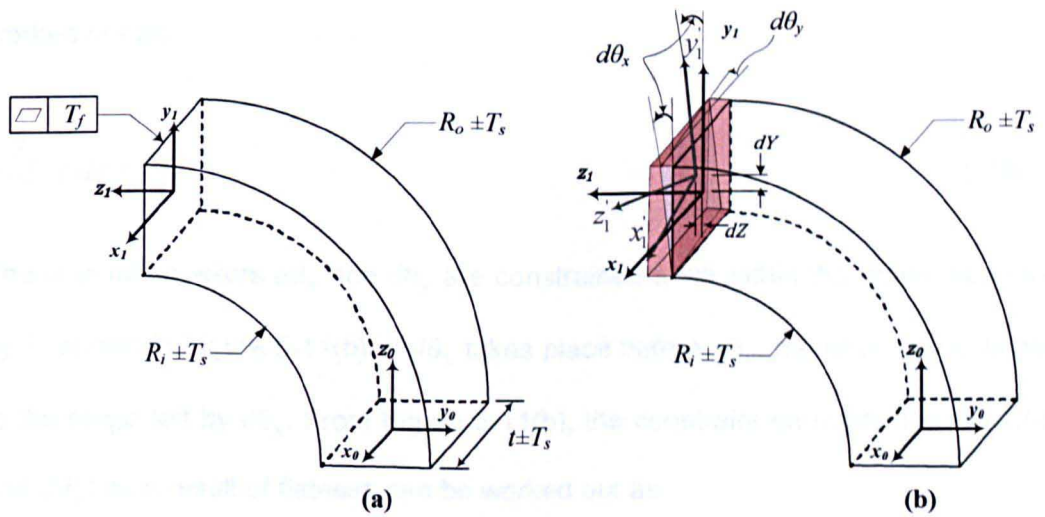


**Figure 5-11: Effect of size and form tolerance on 3D uniformly segmented circular component.**

Figure 5-11(a) shows the symbolic representation of tolerance zone limits. Size tolerance zone limits are specified for variation in radii ($R_o$ and $R_i$) and thickness ($t$) of the component by $\pm T_s$. Size tolerances for radii contribute in position error of frame $x_1y_1z_1$ along $y$-axis (by $dY$). Size tolerances for thickness $t$ contributes in position error $dX$. Flatness tolerance zone $T_f$ is specified for the surface containing feature frame $x_1y_1z_1$. Due to effect of form tolerance, the feature frame $x_1y_1z_1$ is mis-positioned (along $z$-axis by $dZ$) and mis-oriented (by $d\theta_x$ and $d\theta_y$) to new location $x_1'y_1'z_1'$ (see Figure 5-11(b)). Therefore following constraint bounds can be obtained for VDOF within given tolerance zones.

From Figure 5-11(b) the constraint of translation error $dX$ and $dY$ as a result of size tolerance $T_s$ can be depicted as:

$$-T_s \le dX \le T_s, \tag{5.16}$$

$$-T_s \le dY \le T_s, \tag{5.17}$$

The constraint of translation error $dZ$ as a result of flatness tolerance $T_f$ can be worked out as:

$$-\frac{T_f}{2} \le dZ \le \frac{T_f}{2}. \tag{5.18}$$

The orientation errors $d\theta_x$ and $d\theta_y$ are constrained to lie within the region bounded by $T_f$ shown in Figure 5-11(b). If $d\theta_x$ takes place before $d\theta_y$, the error $d\theta_y$ is limited to the range left by $d\theta_x$. From Figure 5-11(b), the constraint on rotation errors ($d\theta_x$ and $d\theta_y$) as a result of flatness can be worked out as:

$$-\tan^{-1}\left(\frac{T_f}{R_o - R_i}\right) \le d\theta_x \le \tan^{-1}\left(\frac{T_f}{R_o - R_i}\right), \tag{5.19}$$

$$-\left(\tan^{-1}\left(\frac{T_f}{t}\right)-d\theta_x\right)\leq d\theta_y\leq\left(\tan^{-1}\left(\frac{T_f}{t}\right)-d\theta_x\right), \tag{5.20}$$

If the constraints for translation and orientation errors in 3D component due to combined effect of size and flatness tolerances are described, then vector representing VDOF for a 3D component can be written as:

$$(dX,dY,dZ,d\theta_x,d\theta_y,d\theta_z)^T, \tag{5.21}$$

Here the angular orientation error $d\theta_z$ represents the angular twist between the two mating surfaces of the uniformly segmented circular component. As in this thesis, the components are assumed to be rigid, therefore due to assumption of rigid material, angular twist $d\theta_z$ can be neglected (i-e. $d\theta_z = 0$).

### 5.4.2.3 Analysis of Case Study 2

Case Study 2 considered here for analysis is same as described in Chapter 4 and consists of four uniformly segmented circular components for both 2D and 3D assembly examples. Ideally, all four components have same nominal dimensions. The nominal dimensions for 2D and 3D components are shown in Figure 5-12.

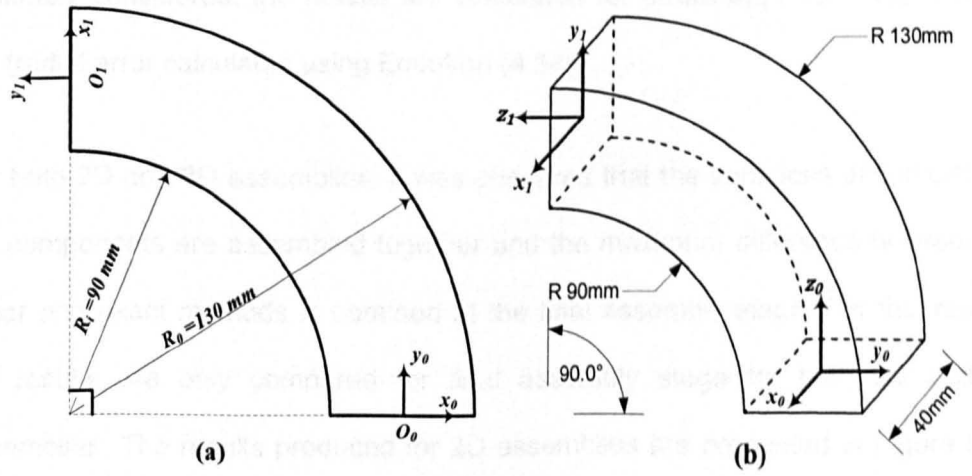


**Figure 5-12: (a) Nominal dimensions uniformly segmented 2D circular component; (b) Nominal dimensions uniformly segmented 3D circular component.**

The purpose of analysis here is to evaluate the performance of the linear model compared to the exact model and to determine the threshold value for run-out tolerances at which there is significant difference between the results produced by linear and exact model. The analysis is performed for 2D as well as 3D assemblies while assuming tolerance zone limit for size variation ($T_s = 0.1\,mm$). The analysis is based on a range of values for run-out tolerances while assuming worst possible variations for each component in the assembly for both 2D and 3D assembly components. The range of values for form tolerance zone limits is as follows:

$$T_f = [\,0.001, 0.005, 0.01, 0.02, \ldots 0.10, 0.15, 0.20, 0.25, 0.30, 0.35, 0.40, 0.45, 0.50, 0.55, 0.60, 0.65, 0.70, 0.75, 0.80, 0.85, 0.90, 0.95, 1.00\,]\,mm \quad (5.22)$$

For each value from given range of form tolerance $T_f$, the variations along degrees of freedom are calculated for 2D components (as described in 5.4.2.1) and 3D components (as described in 5.4.2.2). Assembly variation propagations are then calculated (for both 2D and 3D) using the Exact and Linear methods. For the 2D assembly considered, the results are calculated for errors $dp_i^X$, $dp_i^Y$ and the assembly KC (radial error calculated using Equation (4.54)), whereas for the 3D assembly considered, the results are calculated for errors $dp_i^X$, $dp_i^Y$, $dp_i^Z$ and the KC (radial error calculated using Equation (4.54)).

For both 2D and 3D assemblies, it was observed that the variations accumulate as the components are assembled together and the maximum difference between the linear and exact methods is obtained at the final assembly stage. For this reason, the results are only compared for final assembly stage for both 2D and 3D assemblies. The results produced for 2D assemblies are presented in Figure 5-13, and for 3D assemblies the results are shown in Figure 5-14.

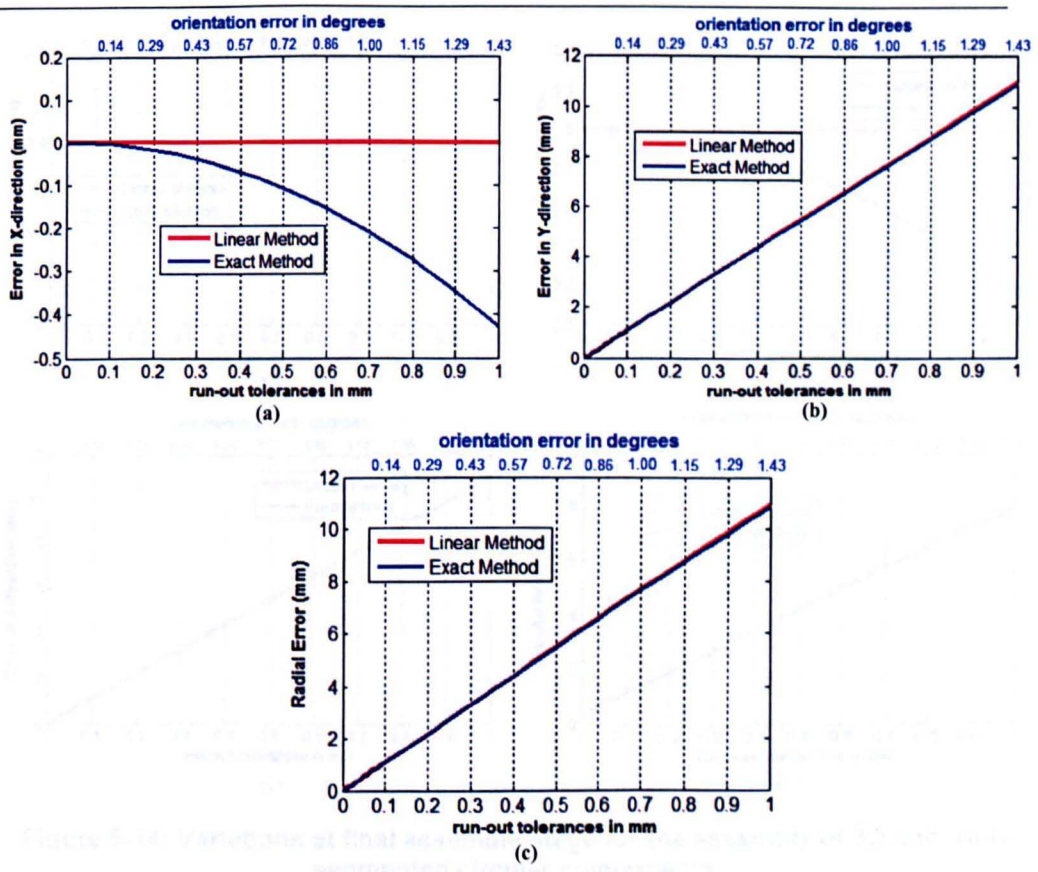


**Figure 5-13: Variations at final assemble stage for the assembly of 2D uniformly segmented circular components.**

Figure 5-13 shows that for $dp_i^Y$ and $e_i^R$, the linear method produces results in good agreement compared to the exact method for all values of form tolerances. However for $dp_i^X$ (see Figure 5-13 (a)), the linear method produces results with good agreement to exact method for value of form tolerance as large as $0.1\ mm$. The results are also compared for equivalent orientation error (for form tolerance) in degrees. It is observed that for given dimensions of assembly components, the linear model provides good agreement results compared to exact model for angular orientation error as large as $0.1^\circ$. These findings are identical to those obtained in Chapter 4 for Case Study 2 (in 2D).

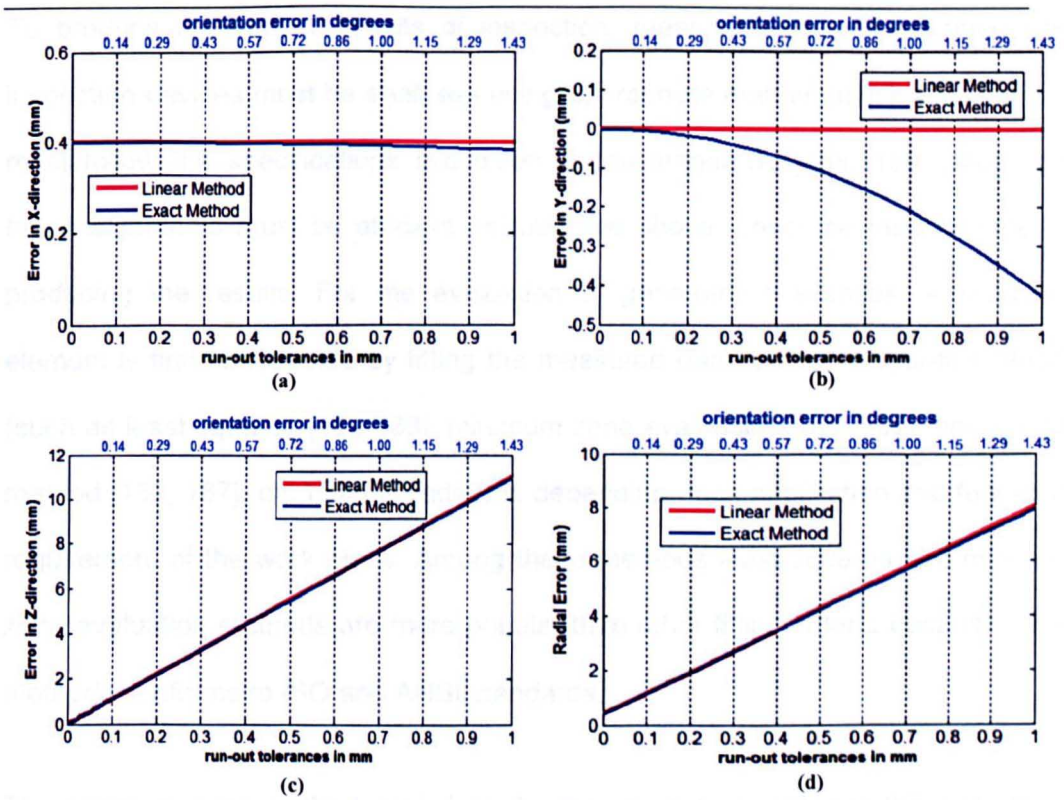


**Figure 5-14: Variations at final assemble stage for the assembly of 3D uniformly segmented circular components.**

Similarly comparing the results in 3D (in Figure 5-14), it is found that for the given range of values of form tolerance, the linear method is in good agreement with the exact method for errors $dp_i^X$, $dp_i^Z$ and the assembly KC $e_i^{Con}$. However, for error $dp_i^Z$, the results are in good agreement only when run-out tolerances are as large as $0.1\,mm$ (or equivalent angular orientation error of $0.14^{\circ}$) These results further confirm that linear model can provide satisfactory results for calculating assembly variations.

## 5.5 Evaluation of Run-out Variations Using Measurement Data

In industries assembling high-value low-volume products, the geometry of parts is inspected to verify the deviation of the real overall shape from nominal shape [157].

To produce the desired results of inspection, measurement data obtained from inspection devices must be analysed using appropriate mathematical algorithm that must follow the specifications laid down in the standards [158, 159]. Moreover, these algorithms must be efficient, robust, and should consume minimal time for producing the results. For the evaluation of geometric tolerances, a substitute element is first constructed by fitting the measured data. Different best-fit methods (such as least-squares [160-163], minimum zone evaluation [164, 165], convex hull method [166, 167], etc.) can be adopted depending upon application and functional requirement of the work piece. Among these methods least-squares and minimum zone evaluation methods are more popular than other fitting criteria because these methods conforms to ISO and ANSI standards.

The minimum zone method minimises the maximum error between the data points and a reference feature [168]. The minimum zone method also conforms to the ANSI and ISO standards for geometric variations, but it is very sensitive to asperities (such as those caused by dirt or scratches on the surface), which may lead to inaccurate results if these asperities are not detected [169]. Algorithms for minimum-zone methods can be found in [161, 170], where it can be seen that all the measurement points does not contribute to the best-fit result.

Least-square best-fit minimises the sum of squared errors, and is mathematically well defined and widely accepted in practical applications. In the least-square method, all the measurement points contribute to the best-fit result, thus the fitted feature is very stable and much less sensitive to the effects of asperities [171]. The current study also uses a least-square method for the evaluation of run-out variations using discrete data.

In order to measure run-out variation in an axi-symmetric component, the component is placed on rotary table with its base concentric to the table axis. Circular run-out of axi-symmetric component in axial and radial direction can be measured using a measurement probe during a complete revolution of the rotary table [140], see also Figure 5-2.

### 5.5.1 Evaluation of Radial Run-Out

The purpose of evaluating radial run-out variations here is to calculate the resulting shift of rotation centre in terms of $x$ and $y$ coordinates. Each mating feature of the axi-symmetric component is measured separately for radial run-out (as shown in Figure 5-15). Several points are measured at each surface feature. Each of the measured point gives a reading of distance along the radial direction at given angle about the axis of rotation. For radial run-out, the radial values are usually measured in $\mu m$ and the rotation of component using rotating table of measuring instrument is described in degrees or radians. Mathematically, the radial run-out can be expressed by Equation (3.1) in polar coordinates and is re-produced as follows:

$$R(\varphi) = R_n + r_{run-out}(\varphi), \tag{5.23}$$

where $R$ is the radius of a point on the measured surface at component orientation $\varphi$, $R_n$ is the nominal radius, and $r_{run-out}$ is the measured run-out in the radial direction.

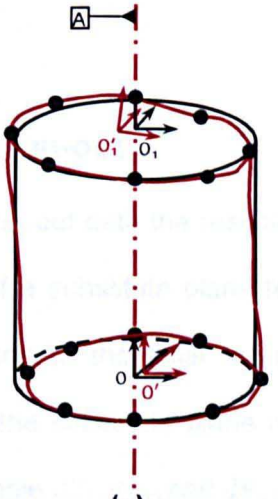


(a)

**Figure 5-15: Representation of points measured to check the run-out tolerances at mating features of a cylindrical component.**

In order to calculate assembly variation propagations using discrete data of run-out measurement, the discrete data need to be described in terms of VDOF-based representation. Therefore, the purpose of evaluating discrete data of radial run-out measurement here is to calculate the resulting shift of rotation centre in $x$ and $y$ coordinates. The resultant shift of lower base of the component from datum axis (as shown in Figure 5-15) can be expressed by $(dX_1, dY_1)$ and the mis-location of the top feature can be expressed by $(dX_2, dY_2)$, respectively. The translation errors $dX_1, dY_1, dX_2$, and $dY_2$ are not shown in Figure 5-15.

Once the radial run-out value of a mating feature is measured, the values of resulting translation errors $(dX_1, dY_1)$ and $(dX_2, dY_2)$ of the corresponding mating feature can be calculated with respect to the datum axis 'A' using a least-square best-circle-fit method (see Appendix for details). In order to incorporate translation errors $(dX_1, dY_1)$ and $(dX_2, dY_2)$ evaluated from radial run-out data in assembly variation modelling, it is desired to find the relative mis-location between the centres of the two surfaces. Therefore, the resultant shift of the centre of top feature relative to base feature can be calculated as:

$$(dX, dY) = (dX_2 - dX_1, dY_2 - dY_1). \quad (5.24)$$

### 5.5.2 Evaluation of axial run-out

In order to evaluate the axial run-out data the resulting variations of the feature are represented by the variation of a substitute plane feature. The substitute plane is obtained by best fitting a plane to the axial run-out data of the manufactured component. The variations of the substitute plane represent the resulting position and orientation errors (for example $dZ_1, d\theta_{x1}$ and $d\theta_{y1}$ for the base feature of the axi-symmetric component shown in Figure 5-15) of the actual feature with respect to nominal feature of the manufactured component. The substitute plane that equally represents the real geometric feature can be evaluated from discrete data using best fit plane method (detailed in Appendix of this thesis). Once the resulting position and orientation errors are obtained by best fit algorithm for the two surfaces of the cylindrical component, the net position and orientation errors ($dZ, d\theta_x$ and $d\theta_y$) of the component due to axial run-out can be calculated as:

$$dZ = dZ_2 - dZ_1, \quad (5.25)$$

$$(d\theta_x, d\theta_y) = (d\theta_{x2} - d\theta_{x1}, \quad d\theta_{y2} - d\theta_{y1}). \quad (5.26)$$

Once all six degrees of freedom of error ($dX$, $dY$, $dZ$, $d\theta_x$, $d\theta_y$, $d\theta_z$) are evaluated from radial and axial run-out measurement data for two mating surfaces of the axi-symmetric component, the overall components variations can be represented by differential homogeneous matrix transform equations. For linear assembly variation propagation method, the overall component variations can be represented by Equation (4.19) given in Chapter 4, whereas, Equation (4.12) can be used for exact method.

### 5.5.3 Assembly Variation Analysis Based on Run-out Measurement Data

In this section, variation propagation analysis based on run-out measurement data is performed for the assembly example given in Case study 1 of Chapter 4. The assembly example consists of four identical rigid cylindrical components and four assembly stages.

| Measurements of Top Surface Feature | | | | | | | | | |
|---|---|---|---|---|---|---|---|---|---|
| Part | Reading | 1 | 2 | 3 | 4 | 5 | 6 | 7 | 8 |
| 1 | Radial Run-out | 0.0040 | 0.0006 | 0.0029 | 0.0021 | -0.0049 | 0.0038 | -0.0033 | -0.0030 |
| 2 | | -0.0038 | -0.0028 | 0.0028 | -0.0028 | -0.0045 | -0.0020 | -0.0008 | 0.0020 |
| 3 | | -0.0015 | -0.0035 | 0.0042 | -0.0035 | -0.0023 | 0.0044 | 0.0022 | 0.0045 |
| 4 | | 0.0021 | -0.0015 | -0.0045 | 0.0032 | 0.0003 | -0.0009 | 0.0015 | 0.0049 |
| 1 | Axial Run-out | -0.0029 | -0.0042 | 0.0043 | 0.0024 | 0.0015 | 0.0021 | 0.0002 | -0.0047 |
| 2 | | -0.0008 | 0.0006 | 0.0025 | -0.0002 | -0.0023 | 0.0030 | -0.0006 | 0.0040 |
| 3 | | 0.0023 | -0.0013 | -0.0015 | -0.0019 | -0.0028 | -0.0047 | -0.0003 | -0.0029 |
| 4 | | -0.0024 | 0.0014 | 0.0049 | 0.0050 | 0.0033 | -0.0003 | -0.0031 | 0.0011 |
| Measurements of Bottom Surface Feature | | | | | | | | | |
| 1 | Radial Run-out | 0.0022 | 0.0041 | 0.0043 | 0.0045 | -0.0035 | -0.0007 | 0.0005 | 0.0027 |
| 2 | | 0.0007 | 0.0039 | -0.0032 | 0.0032 | 0.0016 | -0.0021 | -0.0036 | 0.0031 |
| 3 | | -0.0046 | -0.0037 | -0.0020 | 0.0049 | -0.0027 | -0.0008 | 0.0033 | 0.0027 |
| 4 | | 0.0009 | 0.0005 | 0.0046 | -0.0018 | -0.0012 | -0.0009 | 0.0012 | -0.0042 |
| 1 | Axial Run-out | 0.0043 | -0.0035 | 0.0022 | 0.0005 | 0.0041 | 0.0027 | 0.0045 | -0.0007 |
| 2 | | -0.0032 | 0.0016 | 0.0007 | -0.0036 | 0.0039 | 0.0031 | 0.0032 | -0.0021 |
| 3 | | -0.0020 | -0.0027 | -0.0046 | 0.0033 | -0.0037 | 0.0027 | 0.0049 | -0.0008 |
| 4 | | 0.0046 | -0.0012 | 0.0009 | 0.0012 | 0.0005 | -0.0042 | -0.0018 | -0.0009 |

**Table 5-1: Run-out Values for four rotationally symmetric components.**

| | $dX$ | $dY$ | $dZ$ | $d\theta_x$ | $d\theta_y$ | $d\theta_z$ |
|---|---|---|---|---|---|---|
| Part 1 | 0.000769 | 0.001870 | 0.001778 | 0.000012 | -0.000014 | 0.00 |
| Part 2 | 0.000889 | -0.000095 | 0.000457 | 0.000017 | -0.000011 | 0.00 |
| Part 3 | 0.000209 | -0.002309 | -0.000360 | 0.000012 | -0.000025 | 0.00 |
| Part 4 | 0.000665 | -0.001900 | -0.000103 | -0.000011 | 0.000015 | 0.00 |

**Table 5-2: Six degrees of freedom of component variations obtained from run-out data.**

Ideally, each cylinder has a nominal height of 70 mm and nominal diameter of 100 mm. An example of run-out measurement data is given in Table 5-1. The values of run-out variations (given in Table 5-1) are not real values but are selected randomly.

Eight measurement values are given for each reading of radial and axial run-out for two mating surfaces (upper and lower) of each cylindrical component. The run-out measurement data given in Table 5-1 is converted into six degrees of freedom of error ($dX$, $dY$, $dZ$, $d\theta_x$, $d\theta_y$, $d\theta_z$) using least square methods given in Appendix at the end of this thesis. Table 5-2 shows the converted values of variations along six degrees of freedom.

Once all the six model variables for the run-out tolerance zone are obtained, these model variables can directly be used in assembly variation propagation models given in Chapter 4 of this thesis. Here the assembly variation propagations $dp_i^X$, $dp_i^Y$, $dp_i^Z$ and the eccentricity error (the KC) $e_i^{Con}$ (calculated using Equation (4.46)) are calculated using the Linear and the Exact model. The calculated results are given in Figure 5-16. Results given in Figure 5-16 give the demonstration of calculating assembly variation when discrete data of run-out measurement is given. The results also show that the results produced by two methods (Exact and Linear) are in very good agreement with each other.

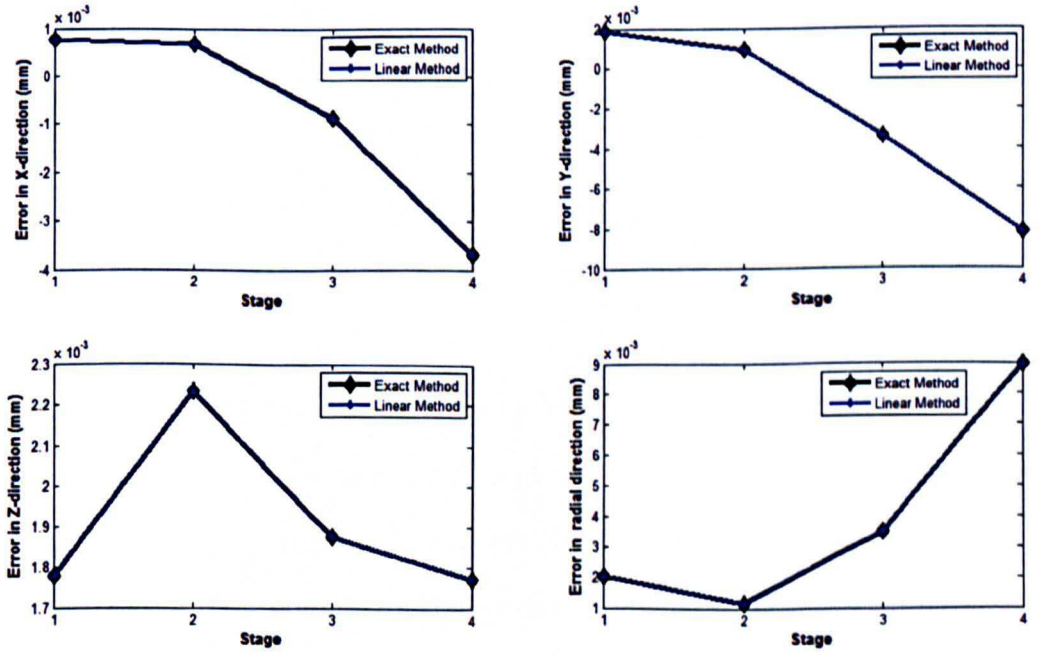


**Figure 5-16: Stage-by-stage assembly variations.**

## 5.6 Summary

A methodology of representing geometric variation using geometric features is discussed. Variational constraints for three degrees of translation error ($dX$, $dY$, $dZ$) and three degrees of rotation error ($d\theta_x$, $d\theta_y$, $d\theta_z$) are derived from dimensional and geometric (run-out and form) tolerances specified for axi-symmetric components and uniformly segmented circular components. The analysis is performed for Case Studies 1 and 2 in 2D as well as 3D based on a series of values for run-out tolerance and form tolerance respectively. The analysis for Case Study 1 show that Linear model can produce results in good agreement with exact model if run-out tolerances are as large as $0.4\ mm$. For Case Study 2 it was also observed that the linear model can produce results with good agreement to exact method for form tolerance value of as large as $0.1\ mm$. Finally the method of evaluating translation ($dX$, $dY$, $dZ$) and rotation error ($d\theta_x$, $d\theta_y$, $d\theta_z$) from run-out inspection data is described to demonstrate the consideration of in-line measurement in calculating assembly variation propagations in metrology assisted mechanical assemblies.

# Chapter 6 PROBABILISTIC ANALYSIS OF ASSEMBLY VARIATIONS

## 6.1 Introduction

In Chapters 4 and 5 assembly variations were analysed based on worst case component variations. Whilst these variations are unlikely to occur in practice, the worst case analysis is useful for calculating the extreme limits of assembly variations based on the worst combination of parts. In practice, the physical dimensions of manufactured components are random and lie within a range of permissible variation [172]. In order to evaluate the effect of realistic part or subassembly variations on the resulting assembly, a model based on a probabilistic approach is required. The probabilistic model developed in this chapter calculates the variability of an assembly based on the tolerances of individual components and can be used at the conceptual design stage to assess assembly variation for different tolerances.

The proposed probabilistic model assumes the individual component variations are Gaussian random variables. This assumption is used widely in assembly tolerance analysis[4] [173] to represent individual component variations [174-176], and complements the linear assembly model developed in Chapter 4. To evaluate the performance of the presented model, numerical results are obtained and compared with Monte Carlo Simulation (MCS) results obtained using the exact fully non-linear approach presented in Chapter 4, and a comparison of results is performed for assembly Case Studies 1 and 2 (as given in Chapter 4). The main advantage of the presented probabilistic method is that it is efficient and accurate in comparison to MCS. The method also has the capability to aid tolerance allocation in assembly components. However, this is not considered here.

Section 6.2 describes the basics of the Monte Carlo Simulation method. Section 6.3 describes the detailed mathematics behind the proposed probabilistic model, and Section 6.4 presents numerical results comparing the two methods. Finally Section 6.5 summarises the contribution of the Chapter.

## 6.2 Monte Carlo Simulation

Monte Carlo Simulation (MCS) is a general numerical method for assessing the statistical behaviour of systems incorporating random variables [177, 178]. It is an established method for tolerance analysis [179, 180] and is based on randomly generating variables defining component parts and calculating the manufacturing variations in the resulting assembly. By repeating this procedure the statistical properties and distribution of the manufactured assembly can be determined. The accuracy of MCS depends upon the number of repeated simulations performed,

[4] Assembly tolerance analysis refers to evaluating the effect of variations of individual part or subassembly dimensions on designated dimensions or functions of the resulting assembly.

where the larger the number of simulations, the more accurate the predicted distribution of dimensions [181].

## 6.3 Probabilistic Model

In mechanical assemblies, random variations can be modelled and analysed using the principles of statistics [116, 182]. In this work, a probabilistic model is presented that can be used to predict the influence of part and sub-assembly variations on product variation. This model can be used to investigate how well the assembly tolerances and functional requirements [183] are achieved in the final product.

The proposed method is presented as a general analytical method for analysing 3D mechanical assemblies. The analysis is based on the linear model presented in Chapter 4 while assuming input component variations $(dX_i, dY_i, dZ_i, d\theta_{xi}, d\theta_{yi}, d\theta_{zi})$ are statistically independent, zero-mean Gaussian random variables with known standard deviation.

In Section 4.4.3 of Chapter 4, it was shown that the translation errors accumulated after assembly of '$N$' components (in Equation (4.42)) are given by:

$$\begin{bmatrix} dp^X \\ dp^Y \\ dp^Z \end{bmatrix} = \left[ \sum_{i=1}^{N} \left[ \prod_{j=1}^{i} (\mathbf{R}_j) \mathbf{dp}_i \right] + \sum_{i=1}^{N-1} \left( \left( \prod_{j=1}^{i} \mathbf{R}_j \right) \delta \mathbf{R}_i \sum_{l=i+1}^{N} \left( \prod_{\substack{k=l-1 \\ k \neq l}}^{N-1} \mathbf{R}_k \right) \mathbf{p}_l \right) \right] = \Delta_1 + \Delta_2, \qquad (6.1)$$

where $\mathbf{R}_i$ and $\delta\mathbf{R}_i$ are rotation matrices, $\mathbf{p}_i$ and $\mathbf{dp}_i$ are translation vectors, $\Delta_1 = \sum_{i=1}^{N} \left[ \left( \prod_{j=1}^{i} \mathbf{R}_j \right) \mathbf{dp}_i \right]$ is a $3 \times 1$ vector representing the combined effect of nominal rotation and translation error of individual component on the assembly and

$\Delta_2 = \sum_{i=1}^{N-1}\left(\left(\prod_{j=1}^{i}\mathbf{R}_j\right)\delta\mathbf{R}_i\sum_{l=i+1}^{N}\left(\prod_{\substack{k=l-1\\k\neq i}}^{N-1}\mathbf{R}_k\right)\mathbf{p}_l\right)$ is a 3 × 1 vector representing the combined effect of rotational error, nominal rotation and nominal dimensions of individual component on the assembly.

The expansion for $\Delta_1$ in Equation (6.1) can be written as follows:

$$\Delta_1 = \left[\mathbf{R}_1\mathbf{dp}_1 + \mathbf{R}_1\mathbf{R}_2\mathbf{dp}_2 + \ldots + \mathbf{R}_1\ldots\mathbf{R}_{N-1}\mathbf{dp}_N\right], \tag{6.2}$$

where $\mathbf{dp}_1, \mathbf{dp}_2, \mathbf{dp}_3, \ldots \mathbf{dp}_N$ are 3 × 1 vectors each representing translational error in individual assembly components, and $\mathbf{R}_1, \mathbf{R}_2, \mathbf{R}_3, \ldots \mathbf{R}_N$ are 3 × 3 rotation matrices each representing the nominal orientation (rotation) between two mating features of each component. In Equation (6.2), $\Delta_1$ consists of a linear sum of statistically independent random vectors, each containing a trivariate random vector $\mathbf{dp}_i$, where,

$$\mathbf{dp}_i = \begin{bmatrix} dX_i \\ dY_i \\ dZ_i \end{bmatrix}, \tag{6.3}$$

The random vector $[dX_i, dY_i, dZ_i]^T$ represents the mis-location error in three dimensions for the $i^{th}$ component. Using Equations (6.2) and (6.3) it can be shown that:

$$\Delta_1 = \begin{bmatrix} \Delta_1^X \\ \Delta_1^Y \\ \Delta_1^Z \end{bmatrix} = \sum_{i=1}^{N}\mathbf{M}_i\begin{bmatrix} dX_i \\ dY_i \\ dZ_i \end{bmatrix}, \tag{6.4}$$

$$\text{where } \mathbf{M}_i = \left( \prod_{j=1}^{i} \mathbf{R}_j \right) = \begin{bmatrix} m_{(1,1)i} & m_{(1,2)i} & m_{(1,3)i} \\ m_{(2,1)i} & m_{(2,2)i} & m_{(2,3)i} \\ m_{(3,1)i} & m_{(3,2)i} & m_{(3,3)i} \end{bmatrix}. \tag{6.5}$$

Expanding Equation (6.4), $\Delta_1^X$ , $\Delta_1^Y$ , and $\Delta_1^Z$ are given by:

$$\Delta_1^X = \sum_{i=1}^{N} \left( m_{(1,1)i}\, dX_i + m_{(1,2)i}\, dY_i + m_{(1,3)i}\, dZ_i \right), \tag{6.6}$$

$$\Delta_1^Y = \sum_{i=1}^{N} \left( m_{(2,1)i}\, dX_i + m_{(2,2)i}\, dY_i + m_{(2,3)i}\, dZ_i \right), \tag{6.7}$$

$$\Delta_1^Z = \sum_{i=1}^{N} \left( m_{(3,1)i}\, dX_i + m_{(3,2)i}\, dY_i + m_{(3,3)i}\, dZ_i \right). \tag{6.8}$$

Equations (6.6) to (6.8) represent the x, y and z components of error $\Delta_1$ , and each of $\Delta_1^X$ , $\Delta_1^Y$ and $\Delta_1^Z$ consist of a linear sum of statistically independent random variables $dX_i$, $dY_i$, $dZ_i$.

The expansion for $\Delta_2$ in Equation (6.1) can be written as follows:

$$\Delta_2 = \begin{bmatrix} \mathbf{R}_1 \delta \mathbf{R}_1 \mathbf{p}_2 + \mathbf{R}_1 \delta \mathbf{R}_1 \mathbf{R}_2 \mathbf{p}_3 + \ldots + \mathbf{R}_1 \delta \mathbf{R}_1 \mathbf{R}_2 \ldots \mathbf{R}_{N-1} \mathbf{p}_N \\ + \mathbf{R}_1 \mathbf{R}_2 \delta \mathbf{R}_2 \mathbf{p}_3 + + \mathbf{R}_1 \mathbf{R}_2 \delta \mathbf{R}_2 \mathbf{R}_3 \mathbf{p}_4 + \ldots + \mathbf{R}_1 \mathbf{R}_1 \delta \mathbf{R}_2 \mathbf{R}_3 \ldots \mathbf{R}_{N-1} \mathbf{p}_N \\ \vdots \\ \mathbf{R}_1 \mathbf{R}_1 \ldots \delta \mathbf{R}_{N-1} \mathbf{p}_N \end{bmatrix}, \tag{6.9}$$

where $\mathbf{p}_2, \mathbf{p}_3, \mathbf{p}_4, \ldots \mathbf{p}_N$ are $3 \times 1$ vectors each representing the nominal position between two mating features for each component and $\delta \mathbf{R}_1, \delta \mathbf{R}_2, \delta \mathbf{R}_3, \ldots \delta \mathbf{R}_{N-1}$ are $3 \times 3$ matrices each representing the orientation error between two mating features for each component, as given by Equation (4.20).

Equation (6.9) consists of a linear sum of terms involving independent random matrices $\delta\mathbf{R}_i$, deterministic matrices $\mathbf{R}_j$, and deterministic translation vectors $\mathbf{p}_l$. In general, the random matrix $\delta\mathbf{R}_i$ can be written as:

$$\delta\mathbf{R}_i = \mathbf{D}_x d\theta_{xi} + \mathbf{D}_y d\theta_{yi} + \mathbf{D}_z d\theta_{zi} \quad , \tag{6.10}$$

where $\mathbf{D}_x = \begin{bmatrix} 0 & 0 & 0 \\ 0 & 0 & -1 \\ 0 & 1 & 0 \end{bmatrix}$, $\mathbf{D}_y = \begin{bmatrix} 0 & 0 & 1 \\ 0 & 0 & 0 \\ -1 & 0 & 0 \end{bmatrix}$ and $\mathbf{D}_z = \begin{bmatrix} 0 & -1 & 0 \\ 1 & 0 & 0 \\ 0 & 0 & 0 \end{bmatrix}$.

Substituting Equation (6.10) into the definition of $\Delta_2$ it can be shown that:

$$\Delta_2 = \sum_{i=1}^{N-1} \left( d\theta_{xi}\,\mathbf{L}_x + d\theta_{yi}\,\mathbf{L}_y + d\theta_{zi}\,\mathbf{L}_z \right), \tag{6.11}$$

where $\mathbf{L}_x$, $\mathbf{L}_y$ and $\mathbf{L}_z$ are $3 \times 1$ deterministic vectors given by:

$$\mathbf{L}_x = \left( \prod_{j=1}^{i} \mathbf{R}_j \right) \mathbf{D}_x \sum_{l=i+1}^{N} \left( \prod_{\substack{k=l-1 \\ k \neq i}}^{N-1} \mathbf{R}_k \right) \mathbf{p}_l, \tag{6.12}$$

$$\mathbf{L}_y = \left( \prod_{j=1}^{i} \mathbf{R}_j \right) \mathbf{D}_y \sum_{l=i+1}^{N} \left( \prod_{\substack{k=l-1 \\ k \neq i}}^{N-1} \mathbf{R}_k \right) \mathbf{p}_l, \tag{6.13}$$

$$\mathbf{L}_z = \left( \prod_{j=1}^{i} \mathbf{R}_j \right) \mathbf{D}_z \sum_{l=i+1}^{N} \left( \prod_{\substack{k=l-1 \\ k \neq i}}^{N-1} \mathbf{R}_k \right) \mathbf{p}_l . \tag{6.14}$$

To determine the statistical distribution for vector $\Delta_2$ it is convenient to re-write Equation (6.11) as the product of a $3 \times 3$ deterministic matrix $\mathbf{Q}_i$ and an independent random vector $\left[ d\theta_{xi}, d\theta_{yi}, d\theta_{zi} \right]^T$ such that:

$$\Delta_2 = \begin{bmatrix} \Delta_2^X \\ \Delta_2^Y \\ \Delta_2^Z \end{bmatrix} = \sum_{i=1}^{N-1} \left( \mathbf{Q}_i \begin{bmatrix} d\theta_{xi} \\ d\theta_{yi} \\ d\theta_{zi} \end{bmatrix} \right). \tag{6.15}$$

where,

$$\mathbf{Q}_i = \begin{bmatrix} \mathbf{L}_x & \mathbf{L}_y & \mathbf{L}_z \end{bmatrix} = \begin{bmatrix} q_{(1,1)i} & q_{(1,2)i} & q_{(1,3)i} \\ q_{(2,1)i} & q_{(2,2)i} & q_{(2,3)i} \\ q_{(3,1)i} & q_{(3,2)i} & q_{(3,3)i} \end{bmatrix}. \tag{6.16}$$

Equation (6.15) contains a tri-variate random vector $[d\theta_{xi}, d\theta_{yi}, d\theta_{zi}]^T$ representing the orientation error for the $i^{th}$ component in three dimensions and has an identical form to Equation (6.4) for $\Delta_1$. Each of the errors $\Delta_2^X$, $\Delta_2^Y$, and $\Delta_2^Z$ in Equation (6.15) can be expressed separately as a linear sum of random errors $d\theta_{xi}$, $d\theta_{yi}$ and $d\theta_{zi}$ such that:

$$\Delta_2^X = \sum_{i=1}^{N-1} \left( q_{(1,1)i} d\theta_{xi} + q_{(1,2)i} d\theta_{yi} + q_{(1,3)i} d\theta_{zi} \right), \tag{6.17}$$

$$\Delta_2^Y = \sum_{i=1}^{N-1} \left( q_{(2,1)i} d\theta_{xi} + q_{(2,2)i} d\theta_{yi} + q_{(2,3)i} d\theta_{zi} \right), \tag{6.18}$$

$$\Delta_2^Z = \sum_{i=1}^{N-1} \left( q_{(3,1)i} d\theta_{xi} + q_{(3,2)i} d\theta_{yi} + q_{(3,3)i} d\theta_{zi} \right), \tag{6.19}$$

Using Equations (6.6) to (6.8) and (6.17) to (6.19), the components of the vector representing the variations accumulated after assembly of the $N^{th}$ component (see Equation (6.1)) can be written as:

$$dp^X = \sum_{i=1}^{N} \left( m_{(1,1)i} dX_i + m_{(1,2)i} dY_i + m_{(1,3)i} dZ_i \right) + \sum_{i=1}^{N-1} \left( q_{(1,1)i} d\theta_{xi} + q_{(1,2)i} d\theta_{yi} + q_{(1,3)i} d\theta_{zi} \right), \tag{6.20}$$

$$dp^Y = \sum_{i=1}^{N}\left(m_{(2,1)i}dX_i + m_{(2,2)i}dY_i + m_{(2,3)i}dZ_i\right) + \sum_{i=1}^{N-1}\left(q_{(2,1)i}d\theta_{xi} + q_{(2,2)i}d\theta_{yi} + q_{(2,3)i}d\theta_{zi}\right), \quad (6.21)$$

$$dp^Z = \sum_{i=1}^{N}\left(m_{(3,1)i}dX_i + m_{(3,2)i}dY_i + m_{(3,3)i}dZ_i\right) + \sum_{i=1}^{N-1}\left(q_{(3,1)i}d\theta_{xi} + q_{(3,2)i}d\theta_{yi} + q_{(3,3)i}d\theta_{zi}\right), \quad (6.22)$$

where $dp^X$, $dp^Y$ and $dp^Z$ are the translation errors accumulated after the assembly of $N^{\text{th}}$ component in the $x$, $y$ and $z$ directions, respectively.

Equations (6.20) to (6.22) show that the assembly errors $dp^X$, $dp^Y$ and $dp^Z$ consist of a linear sum of statistically independent random variables $dX_i$, $dY_i$, $dZ_i$, $d\theta_{xi}$, $d\theta_{yi}$ and $d\theta_{zi}$ each having a uni-variate normal distribution with zero mean and variances $\sigma^2_{dX_i}$, $\sigma^2_{dY_i}$, $\sigma^2_{dZ_i}$, $\sigma^2_{d\theta_{xi}}$, $\sigma^2_{d\theta_{yi}}$ and $\sigma^2_{d\theta_{zi}}$, respectively. It can be shown that $dp^X$, $dp^Y$ and $dp^Z$ are zero-mean and have variances $\sigma^2_{dp^X}$, $\sigma^2_{dp^Y}$ and $\sigma^2_{dp^Z}$, where:

$$\sigma^2_{dp^X} = \left\{\begin{array}{l}\sum_{i=1}^{N}\left(m^2_{(1,1)i}\sigma^2_{dX_i} + m^2_{(1,2)i}\sigma^2_{dY_i} + m^2_{(1,3)i}\sigma^2_{dZ_i}\right) \\ +\sum_{i=1}^{N-1}\left(q^2_{(1,1)i}\sigma^2_{d\theta_{xi}} + q^2_{(1,2)i}\sigma^2_{d\theta_{yi}} + q^2_{(1,3)i}\sigma^2_{d\theta_{zi}}\right)\end{array}\right\}, \quad (6.23)$$

$$\sigma^2_{dp^Y} = \left\{\begin{array}{l}\sum_{i=1}^{N}\left(m^2_{(2,1)i}\sigma^2_{dX_i} + m^2_{(2,2)i}\sigma^2_{dY_i} + m^2_{(2,3)i}\sigma^2_{dZ_i}\right) \\ +\sum_{i=1}^{N-1}\left(q^2_{(2,1)i}\sigma^2_{d\theta_{xi}} + q^2_{(2,2)i}\sigma^2_{d\theta_{yi}} + q^2_{(2,3)i}\sigma^2_{d\theta_{zi}}\right)\end{array}\right\}, \quad (6.24)$$

$$\sigma^2_{dp^Z} = \left\{\begin{array}{l}\sum_{i=1}^{N}\left(m^2_{(3,1)i}\sigma^2_{dX_i} + m^2_{(3,2)i}\sigma^2_{dY_i} + m^2_{(3,3)i}\sigma^2_{dZ_i}\right) \\ +\sum_{i=1}^{N-1}\left(q^2_{(3,1)i}\sigma^2_{d\theta_{xi}} + q^2_{(3,2)i}\sigma^2_{d\theta_{yi}} + q^2_{(3,3)i}\sigma^2_{d\theta_{zi}}\right)\end{array}\right\}. \quad (6.25)$$

As Equations (6.20) to (6.22) consist of a linear sum of normally distributed random variables, it can be concluded that errors $dp^X$, $dp^Y$ and $dp^Z$ also normally distributed such that:

$$f\left(dp^X\right)=\frac{1}{\sqrt{2\pi}\sigma_{dp^X}}e^{-\frac{1}{2}\left(\frac{dp^X-\mu_{dp^X}}{\sigma_{dp^X}}\right)^2}, \tag{6.26}$$

$$f\left(dp^Y\right)=\frac{1}{\sqrt{2\pi}\sigma_{dp^Y}}e^{-\frac{1}{2}\left(\frac{dp^Y-\mu_{dp^Y}}{\sigma_{dp^Y}}\right)^2}, \tag{6.27}$$

$$f\left(dp^Z\right)=\frac{1}{\sqrt{2\pi}\sigma_{dp^Z}}e^{-\frac{1}{2}\left(\frac{dp^Z-\mu_{dp^Z}}{\sigma_{dp^Z}}\right)^2}, \tag{6.28}$$

where $\mu_{dp^X}$, $\mu_{dp^Y}$ and $\mu_{dp^Z}$ are zero, and $\sigma_{dp^X}$, $\sigma_{dp^Y}$ and $\sigma_{dp^Z}$ .are given in Equations (6.23) to (6.25).

Equations (6.26) to (6.28) are the statistical distributions of the assembly errors $dp^X$, $dp^Y$ and $dp^Z$, respectively and can be used to predict variability in the position of any component in a mechanical assembly in three dimensions. The probability that the errors $dp^X$, $dp^Y$ and $dp^Z$ exceed value $x, y$ and $z$ respectively, are given by:

$$P(x)=\int_x^{\infty}\frac{1}{\sqrt{2\pi}\sigma_{dp^X}}e^{-\frac{1}{2}\left(\frac{dp^X-\mu_{dp^X}}{\sigma_{dp^X}}\right)^2}dp^X, \tag{6.29}$$

$$P(y)=\int_y^{\infty}\frac{1}{\sqrt{2\pi}\sigma_{dp^Y}}e^{-\frac{1}{2}\left(\frac{dp^Y-\mu_{dp^Y}}{\sigma_{dp^Y}}\right)^2}dp^Y, \tag{6.30}$$

$$P(z)=\int_{z}^{\infty}\frac{1}{\sqrt{2\pi}\sigma_{dp^Z}}e^{-\frac{1}{2}\left(\frac{dp^Z-\mu_{dp^Z}}{\sigma_{dp^Z}}\right)^2}dp^Z, \tag{6.31}$$

In complex assemblies, variability in the key characteristics (KCs) must be calculated to evaluate the quality of an assembly. The KCs depend upon the type and application of an assembly and can vary depending upon practical application. Two assembly examples are studied throughout this thesis. Case Study 1 represents assembly of a rotating part (rotor) for a high-speed rotating machine and Case Study 2 represents the assembly of a non-rotating part (casing) for a high-speed rotating machines. The following sections consider modelling the KC for each of these case studies.

### 6.3.1 Modelling Variability of Assembly KC for Case Study 1

The KC for Case Study 1 (as discussed in Chapters 4) is the eccentricity error $e_i^{Ecc}$ given by Equation (4.46). In Equation (4.46), the eccentricity error $\left(e_i^{Ecc}=\sqrt{(dp^X)^2+(dp^Y)^2}\right)$ is determined by errors $dp^X$ and $dp^Y$ as described by Equations (6.20) and (6.21), respectively. In these equations, $dp^X$ and $dp^Y$ are expressed in a general form and it is important to realise that they are correlated.

For the case of rotationally symmetric components errors $dp^X$ and $dp^Y$ can be reduced to a simplified form that aids the development of an equation to estimate the variability of eccentricity error $e_i^{Ecc}$. For Case Study 1 (as described in chapter 4), matrix $\mathbf{R}_i$ represents the nominal rotation between mating features for each axisymmetric component and is the identity matrix. In addition, the nominal translation between the mating features of each axi-symmetric component is given by $\mathbf{p}_i = [0\ 0\ Z_i]^T$. Therefore Equation (6.1) can be simplified as:

$$\begin{bmatrix} dp^X \\ dp^Y \\ dp^Z \end{bmatrix} = \left[ \sum_{i=1}^{N} \mathbf{dp}_i + \sum_{i=1}^{N-1} \left( \delta \mathbf{R}_i \sum_{j=i+1}^{N} \mathbf{p}_j \right) \right], \tag{6.32}$$

From Equation (6.32) assembly errors $dp^X$, $dp^Y$ and $dp^Z$ can be deduced as:

$$dp^X = \sum_{i=1}^{N} dX_i + \sum_{i=1}^{N-1} d\theta_{yi} \sum_{j=i+1}^{N} Z_j, \tag{6.33}$$

$$dp^Y = \sum_{i=1}^{N} dY_i + \sum_{i=1}^{N-1} d\theta_{xi} \sum_{j=i+1}^{N} Z_j, \tag{6.34}$$

$$dp^Z = \sum_{i=1}^{N} dZ_i. \tag{6.35}$$

where $dX_i$, $dY_i$, $dZ_i$, $d\theta_{xi}$, $d\theta_{yi}$ and $d\theta_{zi}$ are statistically independent zero mean normally distributed random numbers having variance $\sigma^2_{dX_i}$, $\sigma^2_{dY_i}$, $\sigma^2_{dZ_i}$, $\sigma^2_{d\theta_{xi}}$, $\sigma^2_{d\theta_{yi}}$ and $\sigma^2_{d\theta_{zi}}$, respectively.

Taking into account that the components of $dp^X$, $dp^Y$ and $dp^Z$ are statistically independent zero-mean Gaussian variables, it can be concluded that for Case Study 1, errors $dp^X$, $dp^Y$ and $dp^Z$ have zero mean Gaussian distributions (given by Equations (6.26) to (6.28), respectively) with variances $\sigma^2_{dpx}$, $\sigma^2_{dpY}$ and $\sigma^2_{dpz}$, respectively, such that:

$$\sigma^2_{dp^X} = \sum_{i=1}^{N} \sigma^2_{dX_i} + \sum_{i=1}^{N-1} \sigma^2_{d\theta_{yi}} \sum_{j=i+1}^{N} Z_j, \tag{6.36}$$

$$\sigma^2_{dp^Y} = \sum_{i=1}^{N} \sigma^2_{dY_i} + \sum_{i=1}^{N-1} \sigma^2_{d\theta_{xi}} \sum_{j=i+1}^{N} Z_j \tag{6.37}$$

$$\sigma_{dp^Z}^2 = \sum_{i=1}^{N} \sigma_{dZ_i}^2 . \tag{6.38}$$

Substituting equations (6.33) and (6.34) for $dp^X$ and $dp^Y$ in Equation (4.46) gives:

$$e_i^{Ecc} = \sqrt{\left(dp^X\right)^2 + \left(dp^Y\right)^2} = \sqrt{\left(\sum_{i=1}^{N} dX_i + \sum_{i=1}^{N-1} d\theta_{yi} \sum_{j=i+1}^{N} Z_j\right)^2 + \left(\sum_{i=1}^{N} dY_i + \sum_{i=1}^{N-1} d\theta_{xi} \sum_{j=i+1}^{N} Z_j\right)^2} , \tag{6.39}$$

In Equation (6.39) the eccentricity error $e_i^{Ecc}$ is determined by two statistically independent, zero-mean Gaussian random variables $dp^X$ and $dp^Y$. It follows that $e_i^{Ecc}$ has a Rayleigh distribution [184-186]. Assuming that $d\theta_{xi}$ and $d\theta_{yi}$ have equal variance, it can be shown that $dp^X$ and $dp^Y$ are of equal variance ($\sigma^{dp^X} = \sigma^{dp^Y}$). Therefore pdf of eccentricity error $e_i^{Ecc}$ for the final component in an assembly consisting of $n$ axi-symmetric components is given by:

$$f\left(e^{Ecc}\right) = \frac{e^{Ecc}}{\sigma_{e^{Ecc}}^2} \exp\left[\frac{-\left(e^{Ecc}\right)^2}{2\sigma_{e^{Ecc}}^2}\right], \quad e^{Ecc} \geq 0 \tag{6.40}$$

where $\sigma_{e^{Ecc}}$ is the standard deviation of eccentricity error and is given by:

$$\sigma_{e^{Ecc}} = \sqrt{\sum_{i=1}^{N} \sigma_{dX_i}^2 + \sum_{i=1}^{N-1} \sigma_{d\theta_{yi}}^2 \sum_{j=i+1}^{N} Z_j} \tag{6.41}$$

Using Equation (6.40), the probability that the eccentricity is less than a particular value $\alpha$ is given by:

$$P(\alpha) = \int_0^{\alpha} \frac{e^{Ecc}}{\sigma_{e^{Ecc}}^2} \exp\left[\frac{-\left(e^{Ecc}\right)^2}{2\sigma_{e^{Ecc}}^2}\right] de^{Ecc} . \tag{6.42}$$

This equation is used later for calculating the assembly yield to perform variation analysis for Case Study 1 in Section 6.4.1.

### 6.3.2 Modelling Variability of Assembly KC for Case Study 2

The KC for Case Study 2 is the error in radial direction $\left(e_i^R = \sqrt{(dp^Y)^2 + (dp^Z)^2}\right)$ given by Equation (4.54). Error $e_i^R$ have a similar form to $e_i^{Ecc}$ in Case Study 1 but involve zero mean correlated Gaussian random variables $dp^Y$ and $dp^Z$ given by Equations (6.21) and (6.22), respectively. Since $dp^Y$ and $dp^Z$ are correlated, the Rayleigh distribution function cannot be applied to determine the distribution of the radial error $e_i^R$. However by using a change of variables in terms of two uncorrelated normal random variables $u_1$ and $u_2$ (as shown in Figure 6-1) having zero mean and non-identical variance [187, 188]. The relationship between the coordinates $(y, z)$ and $(u_1, u_2)$ is a rotation transformation, as shown in Figure 6-1.

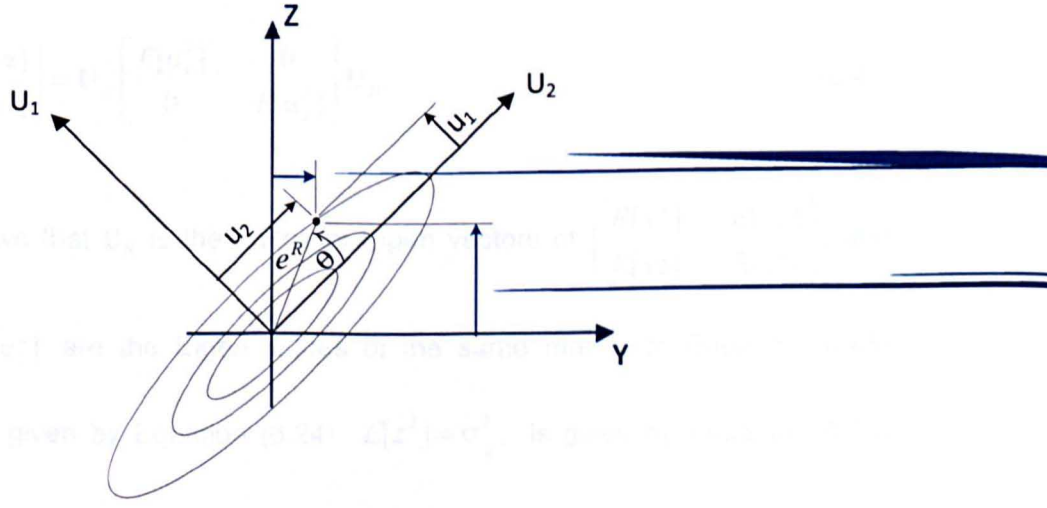


**Figure 6-1:Transformation of radial error along principal axes of the distribution.**

The joint probability density function for $u_1$ and $u_2$ can be expressed as [189]:

$$f(u_1,u_2)=\frac{1}{2\pi\sigma_{u_1}\sigma_{u_2}}\exp\left[-\frac{1}{2}\left\{\left(u_1/\sigma_{u_1}\right)^2+\left(u_2/\sigma_{u_2}\right)^2\right\}\right],\quad -\infty<u_1,u_2<\infty \tag{6.43}$$

where $\sigma_{u_1}$ and $\sigma_{u_2}$ are the standard deviations of $u_1$ and $u_2$, respectively.

The relationship between the coordinates $(y,z)$ and $(u_1,u_2)$ can be expressed as:

$$\begin{bmatrix} y \\ z \end{bmatrix}=\mathbf{U}_R\begin{bmatrix} u_1 \\ u_2 \end{bmatrix}, \tag{6.44}$$

where $\mathbf{U}_R$ is the rotation matrix that transforms coordinate axes Y and Z to principal axes $U_1$ and $U_2$ of the distribution.

The correlation matrix $\mathbf{U}_R$ can be obtained from the covariance matrix of $[y,z]^T$ by post multiplying the entries of Equation (6.44) by transpose of Equation (6.44) and taking the expected values [190], this gives:

$$\begin{bmatrix} E[y^2] & E[yz] \\ E[yz] & E[z^2] \end{bmatrix}=\mathbf{U}_R\begin{bmatrix} E[u_1^2] & 0 \\ 0 & E[u_2^2] \end{bmatrix}\mathbf{U}_R^T. \tag{6.45}$$

It can be shown that $\mathbf{U}_R$ is the matrix of Eigen vectors of $\begin{bmatrix} E[y^2] & E[yz] \\ E[yz] & E[z^2] \end{bmatrix}$, and $E[u_1^2]$ and $E[u_2^2]$ are the Eigen values of the same matrix. In Equation (6.45) $E[y^2]=\sigma^2_{dp^Y}$ is given by Equation (6.24), $E[z^2]=\sigma^2_{dp^Z}$ is given by Equation (6.25) and $E[yz]$ is given by:

$$E[yz]=E[dp^Y dp^Z]=\left\{\begin{array}{l}\sum_{i=1}^{N}\left(m_{(2,1)i}m_{(3,1)i}\sigma^2_{dX_i}+m_{(2,2)i}m_{(3,2)i}\sigma^2_{dY_i}+m_{(2,3)i}m_{(3,3)i}\sigma^2_{dZ_i}\right)\\ +\sum_{i=1}^{N}\left(q_{(2,1)i}q_{(3,1)i}\sigma^2_{d\theta_{xi}}+q_{(2,2)i}q_{(3,2)i}\sigma^2_{d\theta_{yi}}+q_{(2,3)i}q_{(3,3)i}\sigma^2_{d\theta_{zi}}\right)\end{array}\right\} \tag{6.46}$$

Equation (6.43) can be expressed in polar coordinated as [189]:

$$\left(e^R,\theta\right)=\frac{\left(e^R\right)^2}{2\pi\sigma_{u_1}\sigma_{u_2}}\exp\left[-a\left(e^R\right)^2\right]\exp\left[b\left(e^R\right)^2\cos 2\theta\right]\quad \begin{matrix}0<e^R<\infty\\ 0<\theta<2\pi\end{matrix} \tag{6.47}$$

where

$$a=\left(\sigma_{u_2}^2+\sigma_{u_1}^2\right)/\left(2\sigma_{u_1}\sigma_{u_2}\right)^2, \text{ and} \tag{6.48}$$

$$b=\left(\sigma_{u_2}^2-\sigma_{u_1}^2\right)/\left(2\sigma_{u_1}\sigma_{u_2}\right)^2 \tag{6.49}$$

Integrating Equation (6.47) with respect to $\theta$ from 0 to $2\pi$, it can be shown that the distribution function for $e^R$ is given by [191]:

$$f\left(e^R\right)=\frac{e^R}{\sigma_{u_1}\sigma_{u_2}}\exp\left[-a\left(e^R\right)^2\right]I_0\left(b\left(e^R\right)^2\right),\quad 0<e^R<\infty \tag{6.50}$$

where $I_0(x)$ is the modified Bessel function of the First Kind and Zero Order.

Equation (6.50) is the generalised form for calculating stochastic variability of radial error for two correlated Gaussian random variables. To calculate the probability that the radial error is less than a particular value $\alpha$ it is necessary to integrate over Equation (6.50) from 0 to $\alpha$ to give:

$$P\left(e^R\right)=\int_0^{\alpha}\frac{e^R}{\sigma_{u_1}\sigma_{u_2}}\exp\left[-a\left(e^R\right)^2\right]I_0\left(b\left(e^R\right)^2\right)de^R \tag{6.51}$$

This equation is used later to find the assembly yield during the variation analysis of Case Study 2 in Section 6.4.2.

## 6.4 Results and Discussion

To investigate the accuracy and efficiency of the above probabilistic method to perform a variation analysis, two assembly examples (Case Studies 1 and 2 as discussed in Chapter 4) are considered. The results obtained using the proposed method are compared with results obtained using the standard Monte Carlo Simulation (MCS) method incorporating the exact method described in Equation (4.31), rather than the linearised model derived in Equation (4.42). Convergence studies have been performed to determine the number of simulations required by Monte Carlo simulation to obtain accurate results. For the examples considered, it was found that 10,000 simulations are required.

In the examples, it is assumed that there are four components and four assembly stages. Each component in the two case studies has two mating features and two coordinate frames. The assembly is performed by joining components together at their mating features. The coordinate frame attached at the base of the first component is considered to be the global coordinate system for the assembly. The influence of different component tolerances on the component is specified in terms of the location ($dX_l$,$dY_l$, and $dZ_l$) and orientation ($d\theta_{xl}$, $d\theta_{yl}$, and $d\theta_{zl}$) error of the coordinate frames attached to the mating feature for each component on its upper surface relative to its lower surface. The variations are assumed to be zero-mean Gaussian random variables, where the standard deviation (σ) is taken to be one third of the specified tolerance. Results are compared for assembly errors ($dp^X$, $dp^Y$ and $dp^Z$) and the corresponding assembly key characteristic (KC) for the case studies considered. The details of the analysis performed for each case study are given in following subsections.

### 6.4.1 Example 1: Assembly of four Cylindrical Components

An assembly case study of four axi-symmetric (cylindrical) components is considered for the analysis. All components are identical in dimensions with nominal height $H = 70$ mm and nominal diameter $D = 100$ mm. These dimensions ensure the nominal mating feature on the upper surface has coordinates [0,0,70] relative to the mating feature on the lower surface (as shown in Figure 6-2), i.e. $X_i = 0$ mm, $Y_i = 0$ mm, $Z_i = 70$ mm.

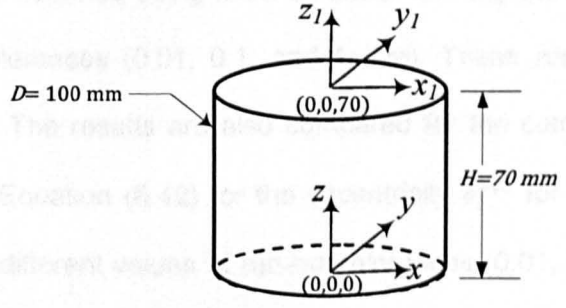


**Figure 6-2:Nominal dimensions of cylindrical components.**

The location and orientation errors for each component are extracted from the dimensional and geometric (axial and radial run-out) tolerances (as described in Chapter 5) specified for each axi-symmetric component. The translation tolerances considered are taken to be $dX_i = dY_i = \pm T_{rr}$ and $dZ_i = \pm(T_s + T_{ar}/2)$, and orientation errors are taken to be $d\theta_{xi} = \pm \tan^{-1}(T_{ar}/D)$ radians, $d\theta_{yi} = \pm(\tan^{-1}(T_{ar}/D) - d\theta_{xi})$ radians and $d\theta_{zi} = 0$ radians. Here, $T_s$, $T_{ar}$, and $T_{rr}$ refer to the size tolerance, tolerance for axial run-out and radial run-out, respectively (as shown in Figure 5-7).

For the purpose of analysing the performance of the probabilistic model, comparisons are made between the analytical and MCS methods at different component tolerance values. The run-out tolerances ($T_{ar}$,and $T_{rr}$) are selected to

take three different small to large values: 0.01, 0.1, and 1 mm, while the size tolerances $T_s$ is kept fixed at $0.1$ mm.

To perform the analysis, variances $\sigma^2_{dpX}$, $\sigma^2_{dpY}$, $\sigma^2_{dpZ}$ and $\sigma_{e^{Ecc}}$ are calculated using Equations (6.36), (6.37), (6.38) and (6.41), respectively . Based on the calculated values of covariance, the probability density functions (pdfs) are plotted separately for assembly errors ($dp_i^X, dp_i^Y, dp_i^Z$) and eccentricity error ($e_i^{Ecc}$) for final assembly component using Equations (6.26), (6.27), (6.28) and (6.40), respectively and compared with those obtained using MCS on linear and log scale at three different values of run-out tolerances (0.01, 0.1, and 1 mm). These results are shown in Figures 6-3 to 6-14. The results are also compared for the cumulative distribution function (cdf) using Equation (6.42) for the eccentricity $e_i^{Ecc}$ for the final assembly component at three different values of run-out tolerances (0.01, 0.1, and 1 mm) as given in Figures 6-15 to 6-17.

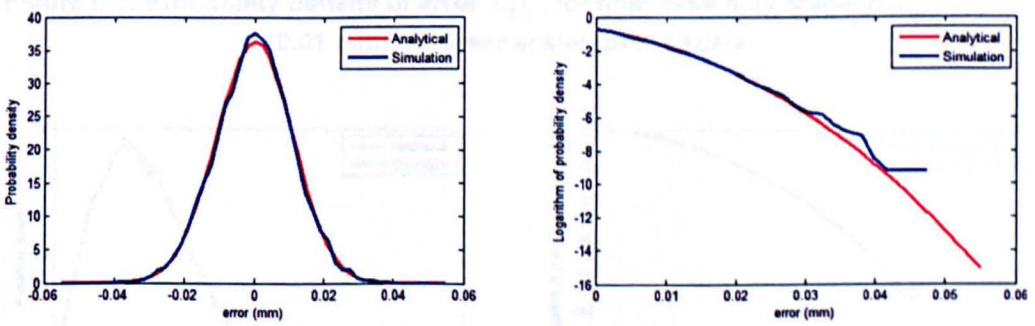


**Figure 6-3: Probability density of error $dp_i^X$ for final assembly stage at $T_{ar} = T_{rr} =$ 0.01 mm: (a) linear scale; (b) log scale.**

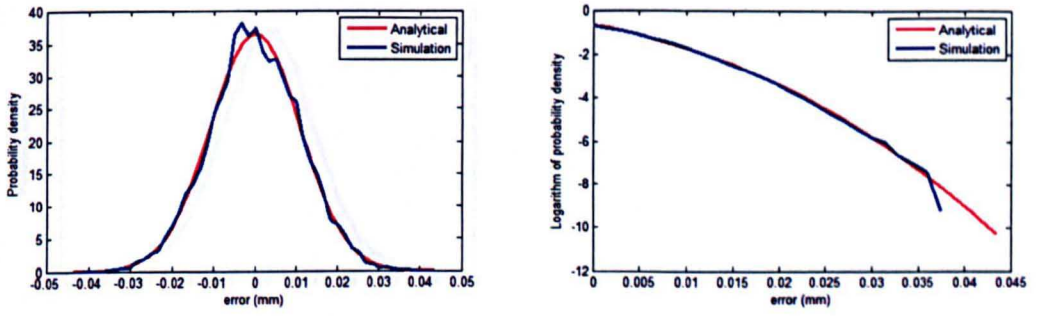


(a) (b)

**Figure 6-4: Probability density of error $dp_i^Y$ for final assembly stage at $T_{ar} = T_{rr} =$ 0.01 mm: (a) linear scale; (b) log scale.**

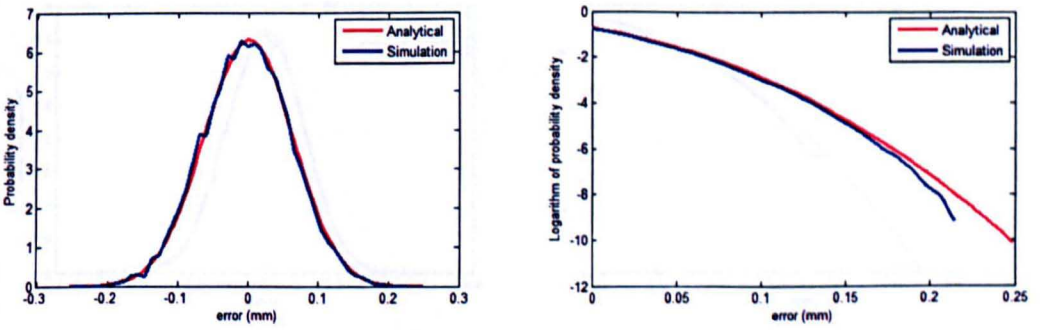


(a) (b)

**Figure 6-5: Probability density of error $dp_i^Z$ for final assembly stage at $T_{ar} = T_{rr} =$ 0.01 mm: (a) linear scale; (b) log scale.**

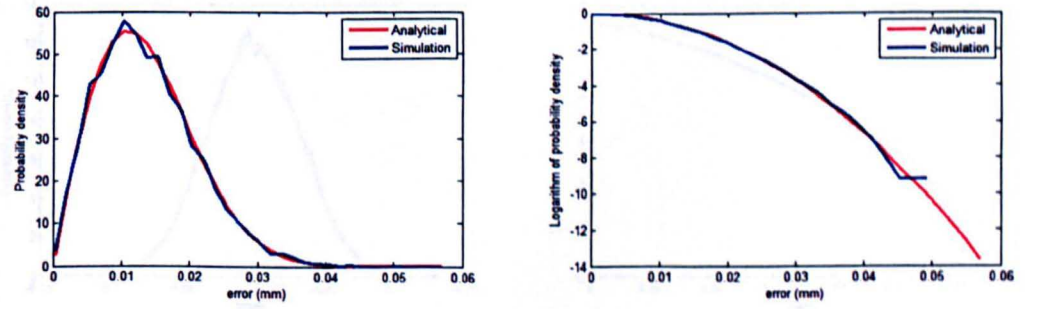


(a) (b)

**Figure 6-6: Probability density of eccentricity error for final assembly stage at $T_{ar} = T_{rr} =$ 0.01 mm: (a) linear scale; (b) log scale.**

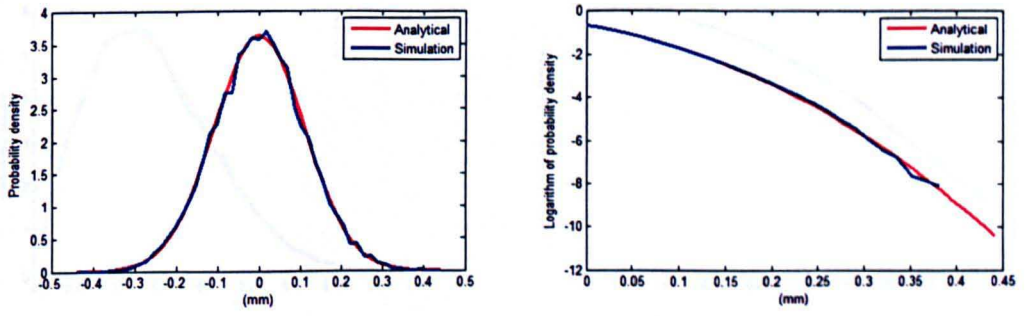


(a) (b)

**Figure 6-7: Probability density of error $dp_i^X$ for final assembly stage at $T_{ar} = T_{rr} = 0.1$ mm: (a) linear scale; (b) log scale.**

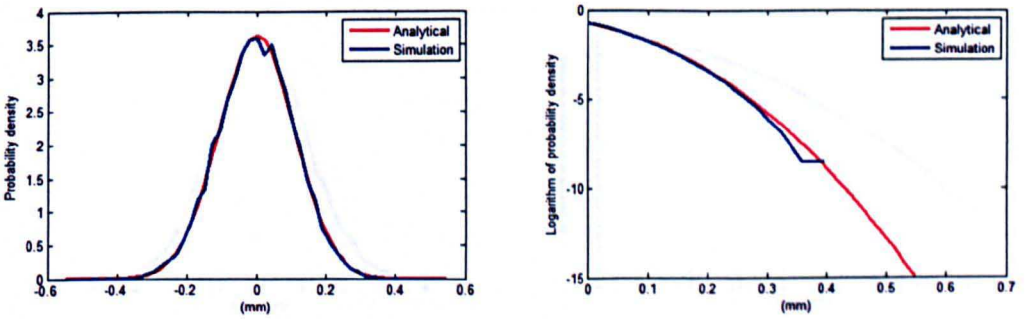


(a) (b)

**Figure 6-8: Probability density of error $dp_i^Y$ for final assembly stage at $T_{ar} = T_{rr} = 0.1$ mm: (a) linear scale; (b) log scale.**

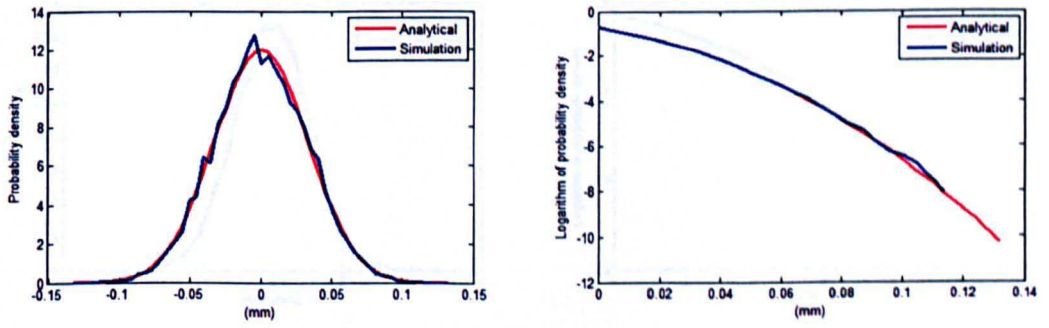


(a) (b)

**Figure 6-9: Probability density of error $dp_i^Z$ for final assembly stage at $T_{ar} = T_{rr} = 0.1$ mm: (a) linear scale; (b) log scale.**

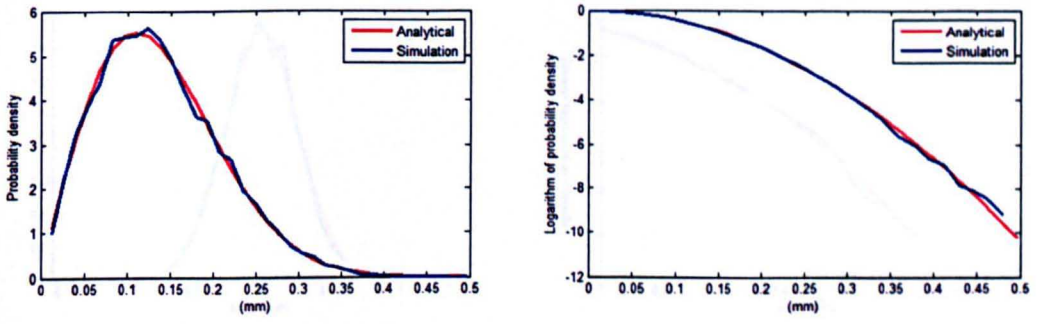


(a) (b)

**Figure 6-10: Probability density of eccentricity error for final assembly stage at $T_{ar} = T_{rr} =$ 0.1 mm: (a) linear scale; (b) log scale.**

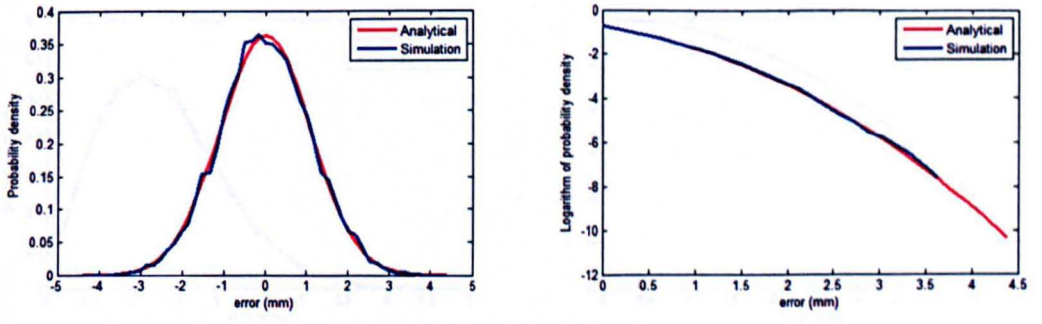


(a) (b)

**Figure 6-11: Probability density of error $dp_i^X$ for final assembly stage at $T_{ar} = T_{rr} =$ 1 mm: (a) linear scale; (b) log scale.**

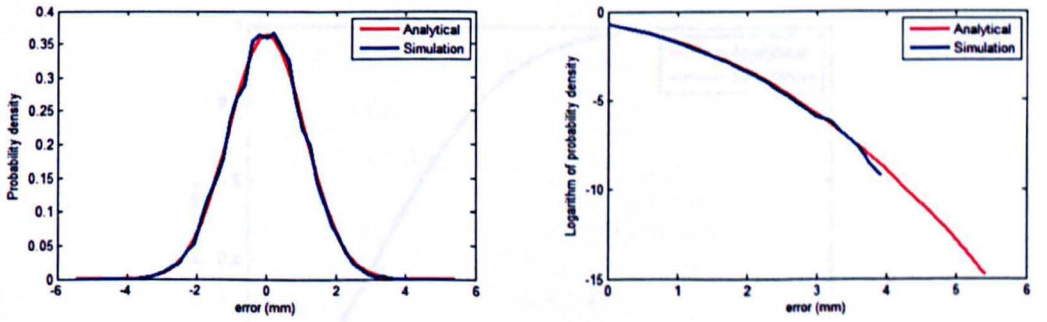


(a) (b)

**Figure 6-12: Probability density of error $dp_i^Y$ for final assembly stage at $T_{ar} = T_{rr} =$ 1 mm: (a) linear scale; (b) log scale.**

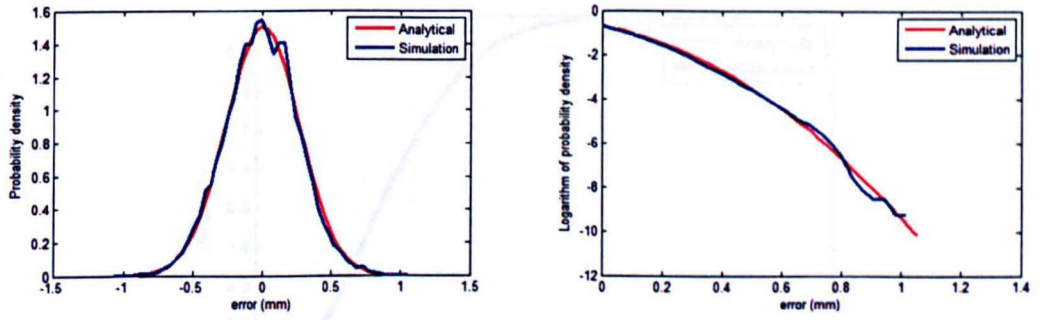


**Figure 6-13: Probability density of error $dp_i^z$ for final assembly stage at $T_{ar} = T_{rr} =$ 1 mm: (a) linear scale; (b) log scale.**

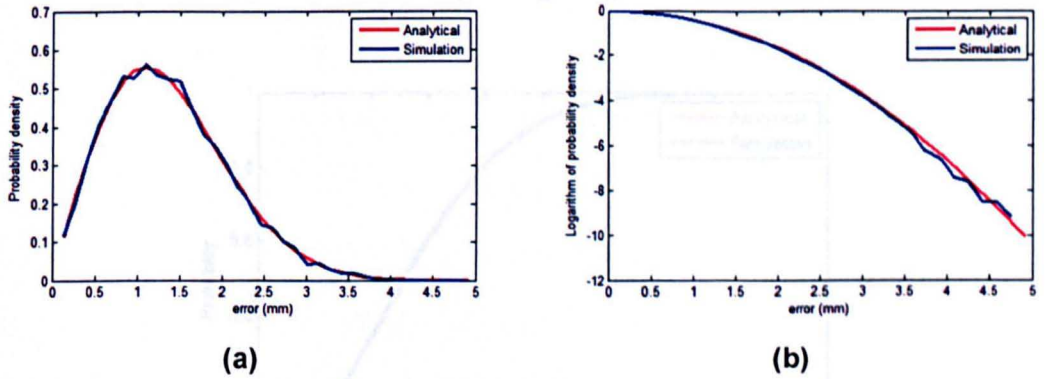


**Figure 6-14: Probability density of eccentricity error for final assembly stage at $T_{ar} = T_{rr} =$ 1 mm: (a) linear scale; (b) log scale.**

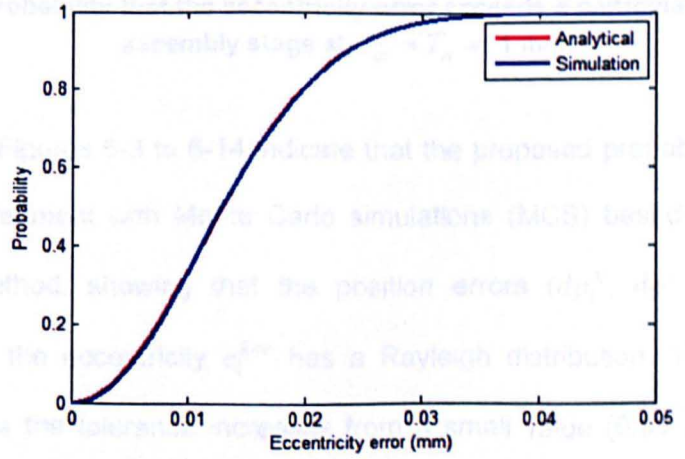


**Figure 6-15: Probability that the eccentricity error exceeds a particular value for final assembly stage at $T_{ar} = T_{rr} =$ 0.01 mm.**

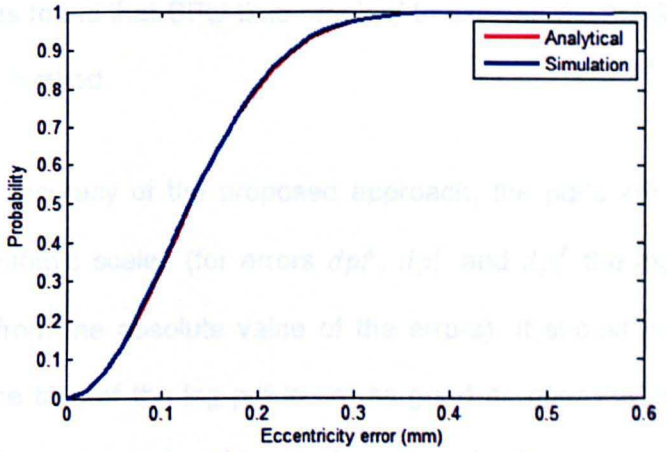


**Figure 6-16: Probability that the eccentricity error exceeds a particular value for final assembly stage at $T_{ar} = T_{rr} =$ 0.1 mm.**

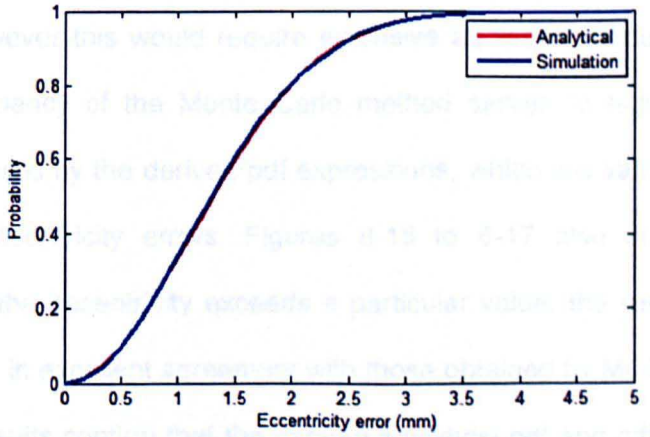


**Figure 6-17: Probability that the eccentricity error exceeds a particular value for final assembly stage at $T_{ar} = T_{rr} =$ 1 mm.**

The results in Figures 6-3 to 6-14 indicate that the proposed probabilistic approach is in good agreement with Monte Carlo simulations (MCS) based on exact (fully non-linear) method, showing that the position errors ($dp_i^X$, $dp_i^Y$ and $dp_i^Z$) are Gaussian and the eccentricity $e_i^{Ecc}$ has a Rayleigh distribution. The results also indicate that as the tolerance increases from a small value (0.01 mm) to a large value (1.0 mm), the magnitude of the position errors and the eccentricity increase and the general shape of the distributions remains relatively unchanged. The efficiency of the probabilistic methods is assessed by comparing the execution times required to perform the calculations with results obtained using Monte Carlo

simulation. It was found that CPU-time required to execute the MCS is 124.58 times the probabilistic method.

To confirm the accuracy of the proposed approach, the pdf's are plotted on both linear and logarithmic scales (for errors $dp_i^X$, $dp_i^Y$ and $dp_i^Z$ the logarithmic results are calculated from the absolute value of the errors). It should be noted that the agreement at the tails of the log-pdf is not as good as over the main body of the distributions. The reason for this is that the simulations are less accurate (statistically) for high position and eccentricity errors. Monte Carlo simulations would produce accurate results at the tails if a larger number of simulations was performed. However this would require extensive additional calculations and CPU time. This deficiency of the Monte Carlo method serves to highlight one of the advantages offered by the derived pdf expressions, which are valid for all values of position and eccentricity errors. Figures 6-15 to 6-17 also show that for the probability that the eccentricity exceeds a particular value, the results obtained by Probabilistic are in excellent agreement with those obtained by MCS based on exact method. The results confirm that the derived analytical pdf and cdf expressions are valid.

A similar comparison between the linear and the exact assembly models was made in Chapter 5, where, it was found that for assembly example considered, linear and exact methods are in good agreement only if run-out values are less than 0.2 mm. The example in chapter 5 considered worst case component variations as well as worst case combinations of components during their assembly, which in practice is very unlikely. However, the assembly variation analysis presented here represents more realistic assembly example and can be used for statistical tolerance analysis of mechanical assemblies.

### 6.4.2 Example 2: Assembly of Four Uniformly Segmented Components

For example 2, an assembly of four uniformly segmented circular components is considered, (as shown in Figure 6-18). All components have identical nominal dimensions with outer radius $R_o = 130\,\text{mm}$ and inner radius $R_i = 90\,\text{mm}$. These dimensions ensure that the nominal mating features on the upper surface have coordinates [0,-110,110] relative to the mating feature on the lower surface (as shown in Figure 6-18). However, the nominal orientation of feature frame $(x_1, y_1, z_1)$ relative to base frame $(x_o, y_o, z_o)$ can be expressed as $(d\theta_x, d\theta_y, d\theta_z) = (90°, 0°, 0°)$.

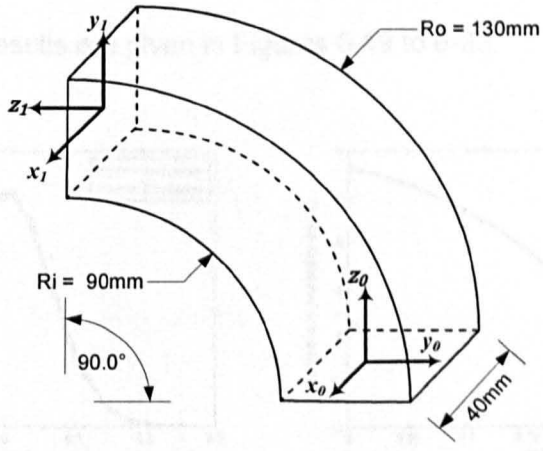


**Figure 6-18:Nominal dimensions of a uniformly segmented circular component.**

In order to investigate the performance of the proposed analytical model, and to evaluate the effect of changing form tolerance $T_f$ for each component on the resulting assembly variations, three analyses are presented. For each of these analyses, the value of size tolerance $T_s$ for each component is fixed as $0.1\,\text{mm}$, and the flatness tolerance is selected to take the following values: 0.01 mm, 0.1 mm and 1 mm.

Based on the specified tolerance zone limits, the location and orientation error of the upper surface relative to the lower surface for each component are extracted using variational constraints described in Chapter 5 for Case Study 2. These constraints are $dX_i = dY_i = \pm T_s$, $dZ_i = \pm T_f/2$ , $d\theta_{Xi} = \pm \tan^{-1}(T_f/(R_o - R_i))$, $d\theta_{Yi} = \pm\left(\tan^{-1}(T_f/(R_o - R_i)) - \text{abs}(d\theta_{Xi})\right)$ and $d\theta_{Zi} = \pm \tan^{-1}(T_f/40)$.

To confirm the accuracy of the proposed approach, pdfs have been plotted for output errors $dp_i^X, dp_i^Y$ and $dp_i^Z$ using Equations (6.26), (6.27) and (6.28), and radial error using Equation (6.50) for the final component in the assembly. The pdfs and cdfs obtained using the analytical (linear) method are compared with those obtained using Monte Carlo Simulations based on exact (non-linear) model (as described in Chapter 4) and the results are given in Figures 6-19 to 6-33.

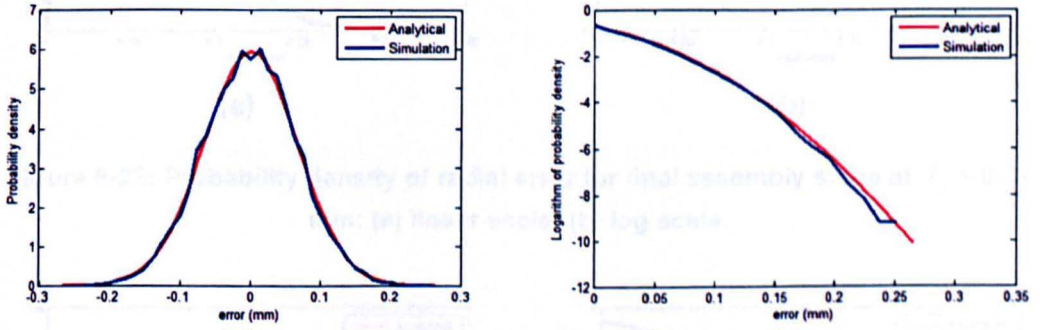


**Figure 6-19: Probability density of error $dp_i^X$ for final assembly stage at $T_f$ = 0.01 mm: (a) linear scale; (b) log scale.**

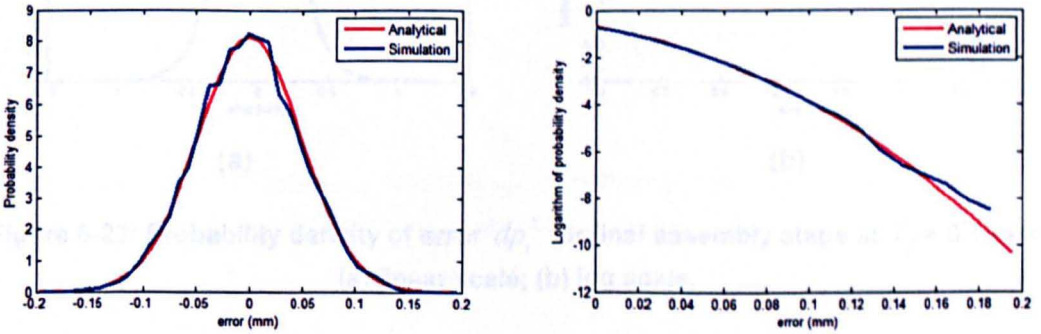


**Figure 6-20: Probability density of error $dp_i^Y$ for final assembly stage at $T_f$ = 0.01 mm: (a) linear scale; (b) log scale.**

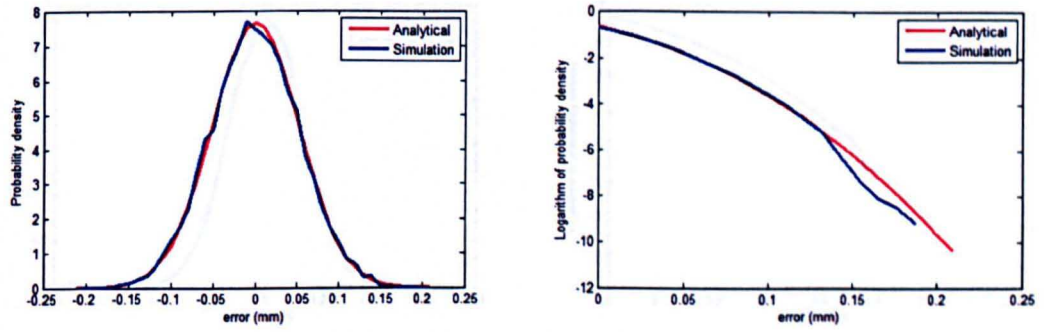


(a) (b)

**Figure 6-21: Probability density of error $dp_i^z$ for final assembly stage at $T_f$ = 0.01 mm: (a) linear scale; (b) log scale.**

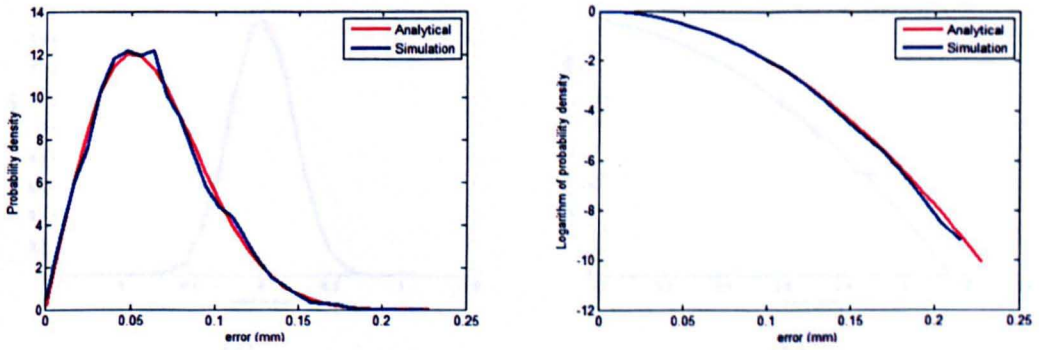


(a) (b)

**Figure 6-22: Probability density of radial error for final assembly stage at $T_f$ = 0.01 mm: (a) linear scale; (b) log scale.**

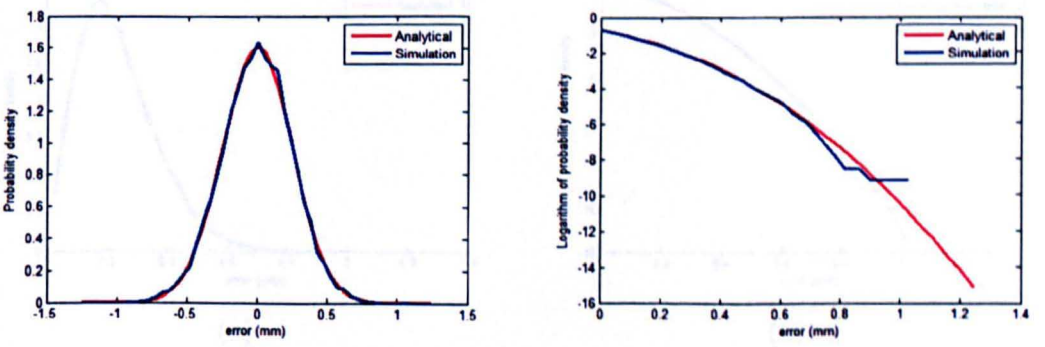


(a) (b)

**Figure 6-23: Probability density of error $dp_i^x$ for final assembly stage at $T_f$ = 0.1 mm: (a) linear scale; (b) log scale.**

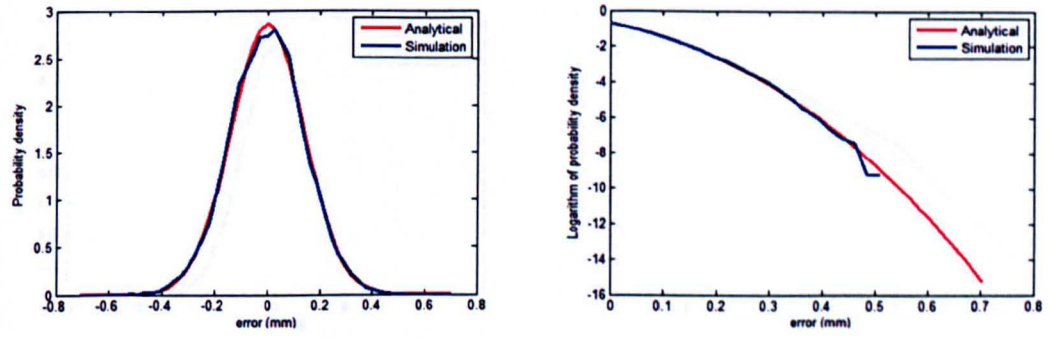


(a) (b)

**Figure 6-24: Probability density of error $dp_i^Y$ for final assembly stage at $T_f$ = 0.1 mm: (a) linear scale; (b) log scale.**

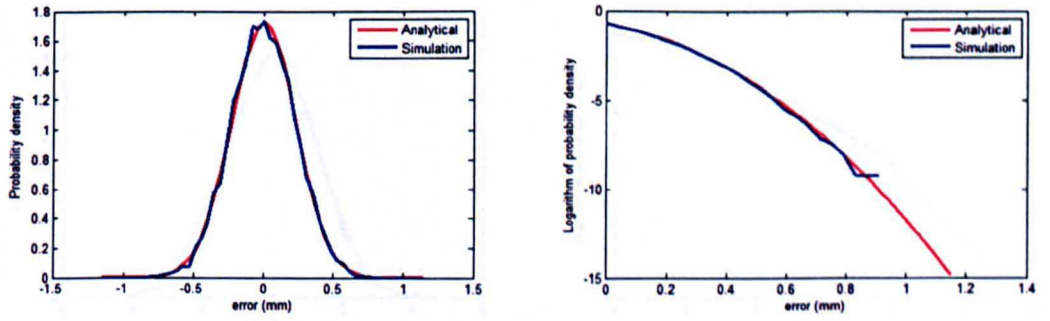


(a) (b)

**Figure 6-25: Probability density of error $dp_i^Z$ for final assembly stage at $T_f$ = 0.1 mm: (a) linear scale; (b) log scale.**

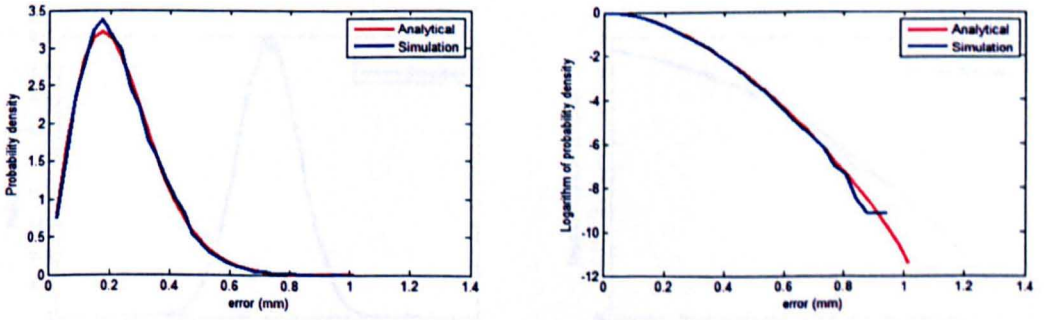


(a) (b)

**Figure 6-26: Probability density of radial error for final assembly stage at $T_f$ = 0.1 mm: (a) linear scale; (b) log scale.**

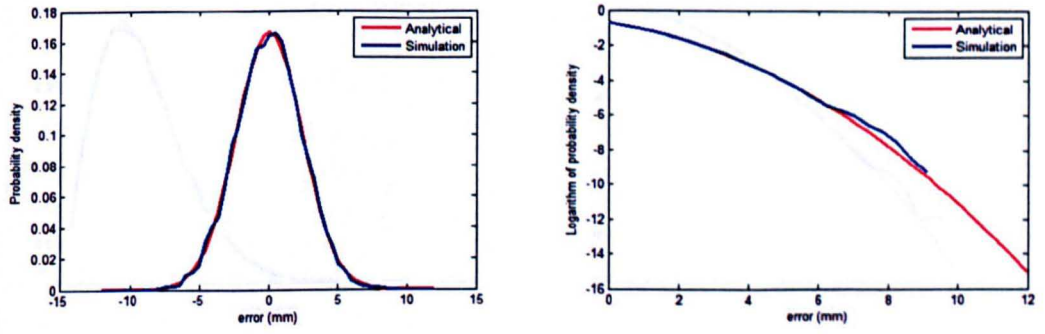


(a) (b)

**Figure 6-27: Probability density of error $dp_i^X$ for final assembly stage at $T_f$ = 1 mm: (a) linear scale; (b) log scale.**

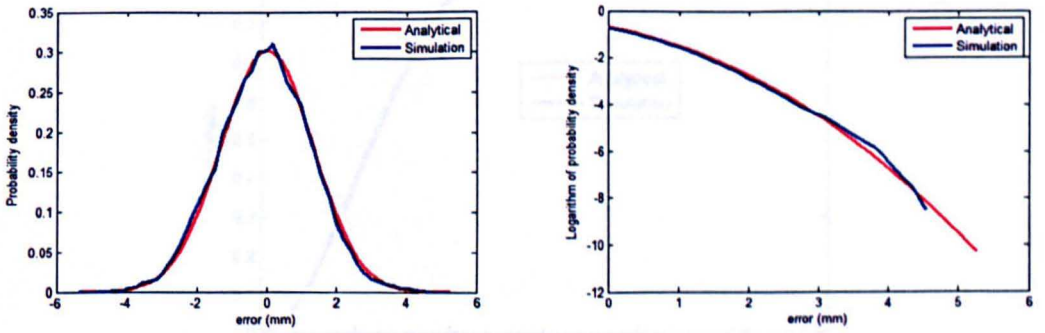


(a) (b)

**Figure 6-28: Probability density of error $dp_i^Y$ for final assembly stage at $T_f$ = 1 mm: (a) linear scale; (b) log scale.**

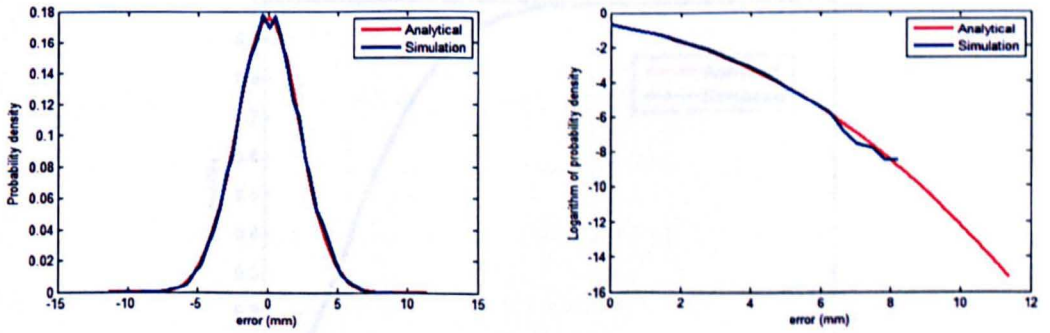


(a) (b)

**Figure 6-29: Probability density of error $dp_i^Z$ for final assembly stage at $T_f$ = 1 mm: (a) linear scale; (b) log scale.**

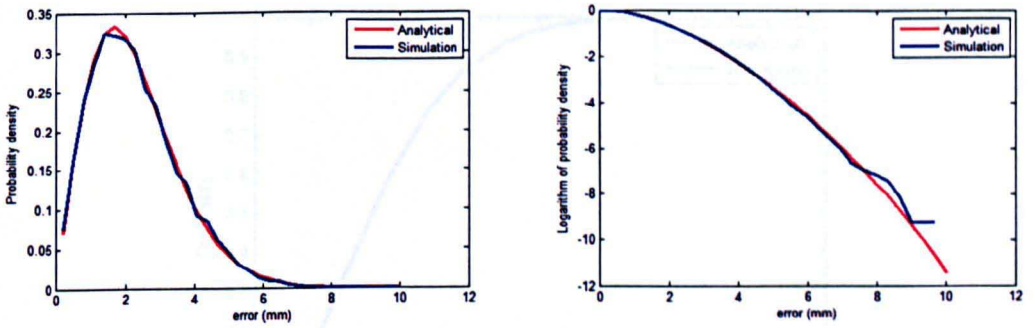


**Figure 6-30: Probability density of radial error for final assembly stage at $T_f$ = 1 mm: (a) linear scale; (b) log scale.**

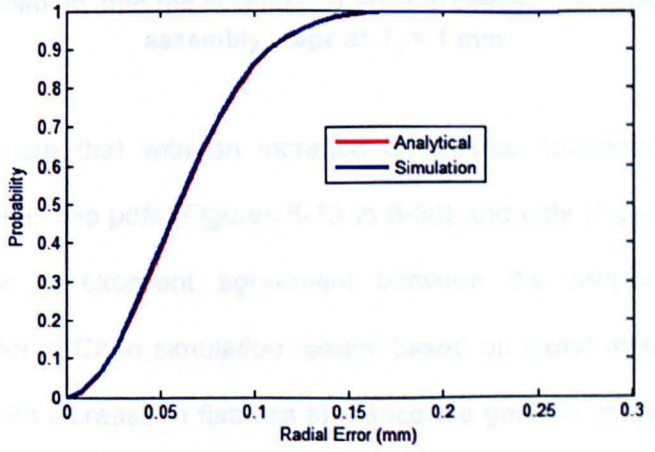


**Figure 6-31: Probability that the eccentricity error exceeds a particular value for final assembly stage at $T_f$ = 0.01 mm.**

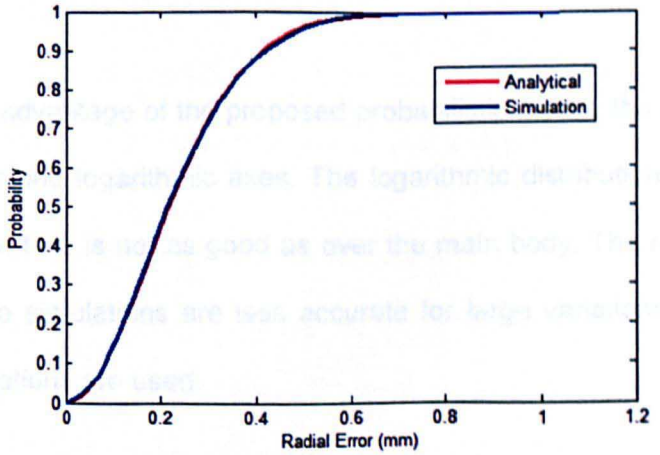


**Figure 6-32: Probability that the eccentricity error exceeds a particular value for final assembly stage at $T_f$ = 0.1 mm.**

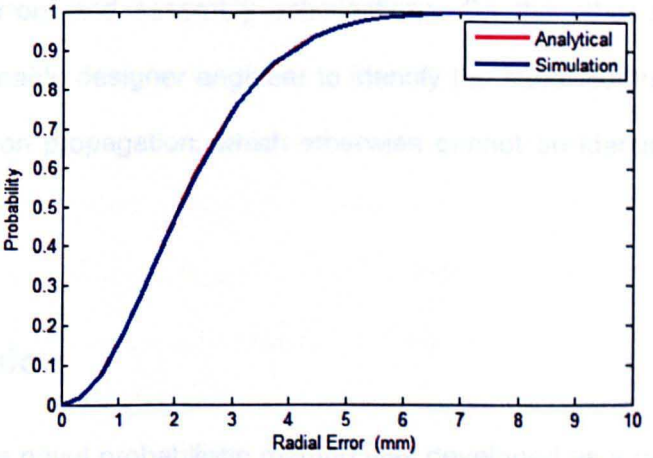


**Figure 6-33: Probability that the eccentricity error exceeds a particular value for final assembly stage at $T_f$ = 1 mm.**

The results indicate that with an increase of flatness tolerance, the assembly variations increase. The pdfs (Figures 6-19 to 6-30) and cdfs (Figures 6-31 to 6-33) show that there is excellent agreement between the proposed probabilistic approach and Monte Carlo simulation results based on exact method. The results also show that with increase in flatness tolerance the general shape of distributions remain unchanged. For errors $dp_i^X$, $dp_i^Y$, and $dp_i^Z$, the distributions are Gaussian, whilst the radial error is highly non-Gaussain and the expression derived for pdf is valid.

To highlight the advantage of the proposed probabilistic model, the distributions are plotted on linear and logarithmic axes. The logarithmic distributions show that the agreement at the tails is not as good as over the main body. The reason for this is that Monte Carlo simulations are less accurate for large variations unless a large number of simulations are used.

It is also important to highlight the advantages of Monte Carlo method over the linear model that it can use a fully non-linear (exact) method for calculating assembly variations and can also incorporate assembly process errors,

measurement errors and assembly optimisations. On the other hand, the linear approximation enable designer engineer to identify the major contributing factors in assembly variation propagation, which otherwise cannot be identified in the exact method.

## 6.5 Conclusion

In this Chapter, a novel probabilistic method was developed as a general analytical method for analysis of 3D mechanical assemblies based on the linear model for calculating assembly variation propagation presented in Chapter 4. Probability density functions were derived for position errors in an assembly ($dp_i^X$, $dp_i^Y$, and $dp_i^Z$) and can be used to analyse a general mechanical assembly. Separate probability functions were derived for the Key Characteristics (KCs) for assembly Case studies 1 and 2. The derived expressions are based on assumptions that the component variations are independent zero-mean Gaussian random variables. The probability density functions are used to calculate the probability that the eccentricity will exceed a particular value, and are useful for industrial applications and academic research in tolerance assignment and assembly process design. The proposed method is used to analyse the influence of different component tolerances on the build quality of an example originating in aero-engine subassembly.

Results obtained using the proposed method, based on linear connective modelling, is compared with those calculated using Monte Carlo simulation method based on the exact non-linear model described in Equation. (4.29). The results are calculated in terms of probability density function for translation error and assembly KCs (eccentricity error for Case Study 1 and radial error for Case Study 1) for the final component in the assembly based on specified size and geometric tolerances (run-out tolerances in Case Study 1 and form tolerances in Case Study 2). The results

show that for the case studies analysed, the statistical distributions obtained using the proposed approach are in excellent agreement with those obtained using Monte Carlo simulation based on exact solution. One of the advantages of the probabilistic model is that it is more accurate than Monte Carlo simulation, particularly if large variations at the tails of the distributions are considered. The linear approximations used in the proposed model also enable the design engineer to identify the main contributing factors in the assembly variation propagations.

The analysis was performed at different values of geometric tolerances (small to large) for each component in both case studies and the results were found to be in excellent agreement even with the larger component tolerances. It was observed that with increase of geometric tolerances assembly variations increase and the shape of the distribution remained unchanged maintaining good agreement between the two approaches. It should be noted that the results produced are only valid for the case studies studied and may vary depending upon the components dimensions, type of the assembly and number of components in the assembly.

Another advantage the proposed probabilistic model over MCS is that it is computationally much more efficient than Monte Carlo simulation as the CPU-time required by Monte Carlo simulations is much longer than the proposed method and can be used in tolerance synthesis problem. On the other hand, MCS can be used for tolerance analysis for assemblies considering assembly error minimisation or any other factor such as assembly process and measurement error. However MCS is not suitable for tolerance allocation in mechanical assemblies because results calculated by MCS will be computationally extensive.

# Chapter 7 VARIATION PROPAGATION CONTROL IN ASSEMBLIES

## 7.1 Introduction

The assembly of mechanical components has a significant impact on manufacturing cost and plays an important role in the quality of the final product. The manufacturing processes always result in variations among the same parts and assemblies. The quality of the assembly is greatly influenced by the presence of manufacturing variations in its constituent parts. If effective measures are taken to minimise error build-up in the assembly before the components are assembled in shop floor, this will reduce the assembly time and cost of product. Controlling the propagation of variations in assembly forms the main theme of this chapter. The methods to minimise assembly variation depend upon the type of product and the assembly process. This implies that different types of assemblies need different control strategies to minimise assembly variation. It is not possible to develop a

generalised method to minimise assembly variation that can be applied to all type of assemblies. Therefore, this chapter proposes control strategies to minimise assembly variation propagation only for Case Studies 1 and 2 discussed in earlier chapters.

The first case study is an example of the assembly of high-speed rotating machines that consists of rigid axi-symmetric components. In high-speed rotating machines, the components are assembled together in a form of stack to build an upright shaft (as described in [140]). In such products, the assembly is aimed to be built as straight as possible. Four optimisation methods are proposed to control variation propagations in the assembly of rotating machines and the proposed methods for Case Study 1 are referred as ***"Straight-build"*** assembly optimisation methods. The second case study consists of components in the shape of round segments, where the components are assembled together to build a circular structure. The assembly example considered in Case Study 2, can be found in the large casing that forms the main non-rotating structure (stator part) of large high-speed rotating machines. The assembly of such round-shaped segmented components is targeted to build the structure with precise circular shape to accommodate the rotor. One error minimisation method is proposed for Case Study 2 and is referred to here as ***"Circular-build"*** assembly optimisation method.

This chapter is divided into two parts, each part describing optimisation strategies proposed for Case Study 1 of straight-build assemblies (in Section 7.2) and Case Study 2 of circular-build assemblies (in Section 7.4). Section 7.3 presents the results based on straight-build assembly optimisation method for 2D assemblies and Section 7.5 presents the results for circular-build assembly optimisation in 2D as well as 3D. The results for 3D circular-build assemblies are also presented to analyse the probabilistic model proposed in Chapter 6 based on increasing the

number of components in an assembly without considering optimisation. Finally, Section 7.6 presents a summary of the chapter and conclusions based on the presented results.

## 7.2 Case Study 1: Straight-Build Assemblies

Parts here are geometrically symmetric about their central axis (axi-symmetric components). Axi-symmetric components are widely used in rotating machines. Applications of such parts cover all facets of manufacturing from large turbo-machinery to miniature precision assemblies of rotating components. It is essential that rotating machines are assembled as straight as possible in order to satisfy the vibration and functional requirements of the rotor.

The optimisation techniques proposed in this research use the axi-symmetric property of the rotationally-symmetric components, by which the component can be assembled by selecting the best angular orientation during the assembly that gives minimum value of geometric eccentricity (concentricity error) between the centres of the components.

### 7.2.1 Optimisation Methods

For the purpose of error minimisation, it is assumed that the manufacturing variations of all assembly components are known. A key characteristic here is to give the best 'straight line' between the centres of the parts during the assembly process.

The current study suggests four optimisation methods to control error propagation in straight-build assemblies based on known variation of each assembly component. Each method uses relative orientation technique to minimise error propagation in

the assembly. The relative orientation technique is a unique approach of error minimisation in the assembly of rotationally symmetric components, where each part is oriented relative to its adjacent part by rotating it about its axis of symmetry. An optimal relative orientation between the mating components is selected based on the objective function for each optimisation method. The proposed optimisation methods are describes using pictorial examples of two-dimensional assemblies for simplicity and better representation of the concepts. The mathematics behind each optimisation strategy is described for both 2D and 3D assemblies. The proposed optimisation methods are given as under:

#### *7.2.1.1 Method 1- Table-Axis-Build Assembly (Stage-by-Stage Error Minimisation)*

Figure 7-1 shows an assembly example of two rectangular 2D components. The first component is placed on the assembly table with its base concentric to the table axis (as shown in Figure 7-1). Part 2 is placed concentric to the top centre of part 1 (as shown in Figure 7-1(a)). Due to the axi-symmetric property of both components, part 2 can be re-oriented (flipped) about its axis of symmetry relative to part 1 without affecting the assembly characteristics. In Figure 7-1 part 2 is shown at two different configurations of its orientation relative to part 1. At both configurations, the eccentricity error of the top centre C2 from table axis has different value (as observed from Figure 7-1). Figure 7-1 also shows that the deviation of the component centre 'C2' from table axis can be minimised by rotating components about their axis of symmetry. Therefore, the table-axis-build assembly method is aimed to minimise table-axis error at each assembly stage by rotating the upper most component about its axis of symmetry and finding the best configuration that gives minimum eccentricity error after assembly.

For 2D component, the upper component has two possible orientations at 0 and 180 degrees. However, a 3D component may have various indexing orientations relative to previous component depending upon the method of assembly of components. For example, if two components are assembled by bolting together, then the number of indexing orientation depends upon the number of bolting holes (as shown in Figure 7-2).

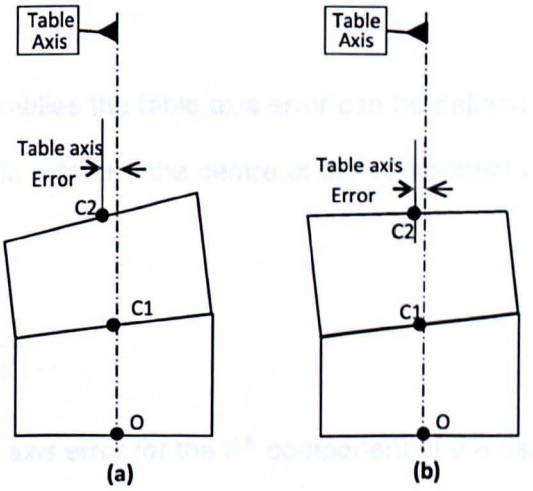


**Figure 7-1: Optimisation Method 1: Two component assembly with upper component in: (a) Orientation 1, (b) Orientation 2**

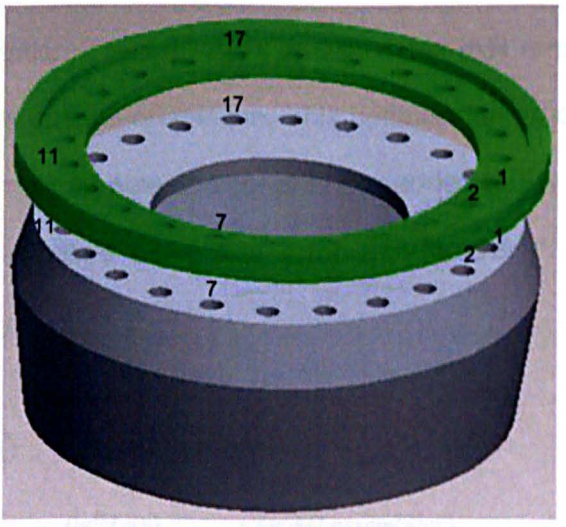


**Figure 7-2: A 3D example to demonstrate number of indexing orientations between two components (the number of indexing orientations is equal to the number of bolting holes).**

For 2D assemblies, the table-axis error is the horizontal component of the translation error vector (given by Equation (4.36)) such that:

$$\varepsilon_i^{ta} = dp_i^X \tag{7.1}$$

where $\varepsilon_i^{ta}$ is the table axis error for the $i^{th}$ component of the assembly and $dp_i^X$ is the horizontal component of the translation error vector given by Equation (4.36) in Chapter 4.

Similarly, for 3D assemblies the table axis error can be defined as the perpendicular distance between table axis and the centre of the component (radial error) as given by following equation:

$$\varepsilon_i^{ta} = \sqrt{(dp_i^X)^2 + (dp_i^Y)^2}, \tag{7.2}$$

where $\varepsilon_i^{ta}$ is the table axis error for the $i^{th}$ component of the assembly, $dp_i^X$ and $dp_i^Y$ are the $x$ and $y$ components of translation error vector given by Equation (4.31) in Chapter 4.

In Figure 7-1, orientation 2 has a visibly smaller table axis error than orientation 1 and is chosen as the optimal orientation. This optimisation process is performed at each stage of assembly as new components are added to the assembly. Applying this process, the optimised table axis error $\varepsilon_i^{ota}$ for the $i^{th}$ component of the assembly is given by:

$$\varepsilon_i^{ota} = \min_{\varphi=0^\circ,180^\circ} \left(\left|dp_i^X(\varphi)\right|\right) \qquad (for\ 2D\ assemblies) \tag{7.3}$$

$$\varepsilon_i^{ota} = \min_{\varphi=0^\circ,\frac{360^\circ}{N}\times 1,\frac{360^\circ}{N}\times 2\ldots,\frac{360^\circ}{N}\times N} \left(\left|\varepsilon_i^{ta}(\varphi)\right|\right) \qquad (for\ 3D\ assemblies) \tag{7.4}$$

where $dp_i^X$ and $\varepsilon_i^{ta}$ is the table axis error for 2D and 3D assemblies, respectively, for the $i^{th}$ component at orientation $\varphi$.

#### 7.2.1.2 Method 2: Table-Axis-Build Assembly (Minimising Error at Two Consecutive Stages)

In Method 2 the table axis error is predicted for two subsequent stages by calculating the eccentricity for all possible orientations of the two components. The optimal orientation is chosen as the configuration that minimises the combined error for the two stages considered. Using the notation introduced in Method 1, the combined table-axis error is expressed as the Root-Mean-Square (RMS) error for the two stages ($i^{th}$ and $(i+1)^{st}$ stage).

Applying this method, the optimised combined table axis error $\varepsilon_i^{octa}$ for the $i^{th}$ component of the assembly is given by:

$$\varepsilon_i^{octa} = \min_{\substack{\varphi_i=0^\circ,180^\circ \\ \varphi_{i+1}=0^\circ,180^\circ}} \left( \sqrt{\frac{\left|dp_i^X(\varphi_i)\right|^2 + \left|dp_{i+1}^X(\varphi_{i+1})\right|^2}{2}} \right) \quad (for\ 2D\ assemblies) \tag{7.5}$$

$$\varepsilon_i^{octa} = \min_{\substack{\varphi_i=0^\circ,\frac{360^\circ}{N}\times 1,\frac{360^\circ}{N}\times 2\ldots,\frac{360^\circ}{N}\times N \\ \varphi_{i+1}=0^\circ,\frac{360^\circ}{N}\times 1,\frac{360^\circ}{N}\times 2\ldots,\frac{360^\circ}{N}\times N}} \left( \sqrt{\frac{\left|\varepsilon_i^{ta}(\varphi_i)\right|^2 + \left|\varepsilon_{i+1}^{ta}(\varphi_{i+1})\right|^2}{2}} \right) \quad (for\ 3D\ assemblies) \tag{7.6}$$

The orientation $\varphi_i = \alpha_1$ that satisfies Equations (7.5) and (7.6), define the optimal configuration. Using these values, the optimised table axis error $\varepsilon_i^{ota}$ for the $i^{th}$ component of the assembly is given by:

$$\varepsilon_i^{ota} = \left| dp_i^X(\alpha_1) \right| \quad (for\ 2D\ assemblies) \tag{7.7}$$

$$\varepsilon_i^{ota} = \left| \varepsilon_i^{ta}(\alpha_1) \right| \quad (for\ 3D\ assemblies) \tag{7.8}$$

#### 7.2.1.3 Method 3: Table-Axis Based Combinatorial Approach

In Method 3, all possible orientations of all components in the assembly are considered, and the configuration of components that yields the minimum table-axis

error for the whole assembly is chosen to be optimal. Applying this method, the optimised table axis error $\varepsilon^{otaa}$ for the whole assembly is calculated as:

$$\varepsilon^{otaa} = \min_{\substack{\varphi_1=0°,180° \\ \varphi_2=0°,180° \\ \cdots \\ \varphi_N=0°,180°}} \left( \sqrt{\frac{\sum_{i=1}^{N} \left| dp_i^X(\varphi_i) \right|^2}{N}} \right) \quad (for\ 2D\ assemblies) \tag{7.9}$$

$$\varepsilon^{otaa} = \min_{\substack{\varphi_1=0°,\frac{360°}{N}\times 1,\frac{360°}{N}\times 2\ldots,\frac{360°}{N}\times N \\ \varphi_2=0°,\frac{360°}{N}\times 1,\frac{360°}{N}\times 2\ldots,\frac{360°}{N}\times N \\ \cdots \\ \varphi_N=0°,\frac{360°}{N}\times 1,\frac{360°}{N}\times 2\ldots,\frac{360°}{N}\times N}} \left( \sqrt{\frac{\sum_{i=1}^{N} \left| \varepsilon_i^{ta}(\varphi_i) \right|^2}{N}} \right) \quad (for\ 3D\ assemblies) \tag{7.10}$$

The orientations $\varphi_i = \beta_i$ that satisfy Equations (7.9) and (7.10) define the optimal configuration. Using these values, the optimised table axis error $\varepsilon_i^{ota}$ for the $i^{th}$ component of the assembly is given by:

$$\varepsilon_i^{ota} = \left| dp_i^X(\beta_i) \right| \quad (for\ 2D\ assemblies) \tag{7.11}$$

$$\varepsilon_i^{ota} = \left| \varepsilon_i^{ta}(\beta_i) \right| \quad (for\ 3D\ assemblies) \tag{7.12}$$

#### *7.2.1.4 Method 4: Final-Assembly Axis Based Combinatorial Approach*

In Method 4, a similar approach is applied to Method 3, but instead of minimising the table-axis error for the whole assembly, Method 4 minimises the final-assembly axis error. Final-assembly axis refers to the axis passing through the centre of the base of the first component and the centre of top of the upper-most component in the assembly.

### 7.2.2 Direct Build Assembly

To investigate any potential improvements in straight-build assembly, the above four optimisation methods are compared with each other, and direct-build assembly.

Direct-build assembly includes component variations but does not use any optimisation methods to control variation propagation.

## 7.3 Results and Discussion

Here, results are calculated for straight-build assembly. The analysis is presented for two-dimensional assemblies. However, results for three dimensional assemblies are given in Chapter 8. The results are calculated to investigate the performance of the proposed optimisation methods for improving the assembly quality. The assembly examples considered consists of axi-symmetric rigid components and the following assembly stages. The first stage of assembly is to place the first component on the table with its base concentric to the geometric centre of the table. As stated earlier, the point of coincidence of the centre of the base of the first component and the geometric centre of the table axis is considered as the origin of the global coordinate frame. At each subsequent stage, a component is joined to the assembly by locating the mating features for the component so that it is concentric with the reference frame attached to the assembly feature.

Each component is assumed to contain variation in size and geometric variations (axial and radial run-out) at the mating features. The presence of geometric variations causes mis-alignment and mis-orientation of the mating features of the component relative to the nominal situation. These variations accumulate as the parts are assembled together. In order to improve assembly quality, the four different optimisation methods are analysed.

The performance of the optimisation methods is investigated using the standard Monte Carlo simulation approach. In this approach, the nominal dimensions of each assembly component are known. Only the size tolerance and the axial and radial

run-outs for each component are selected to be independent zero-mean Gaussian random variables with known standard deviation ($\sigma$). First size and run-out tolerances are randomly generated based on '$\pm 3\sigma$ principle' within prescribed tolerance zone for each component, then using Equations (5.1), (5.2) and (5.3), these values are transformed into translation ($dX, dY$) and rotation ($d\theta$) errors for each assembly component. Assembly variation propagations are calculated based on these transformed values of translation ($dX, dY$) and rotation ($d\theta$) errors of individual component. The Exact Method described in Section 4.4.1 (in Chapter 4) is used to calculate assembly variations. In the variation propagation model used, it has been assumed that there is no mating error at the mating between any two components. Each assembly is repeated 10,000 times using the proposed optimisation methods and direct-build assembly, and statistical data for the resulting assembly errors are generated.

The simulation results are computed to compare the Root Mean Square (RMS) of eccentricity error from the final assembly axis as well as the nominal assembly axis. The final assembly axis refers to the axis passing from the centre of the base of the first component to the centre of the top of the final component in the assembly. The nominal assembly axis is the axis of assembly that is achieved under ideal conditions with no error present in the assembly. The nominal assembly axis can also be defined as the axis perpendicular to the base of the first component and passing through its centre. For an assembly consisting of N components, the RMS assembly variation from the table axis $\varepsilon_{ta}^{RMS}$ is calculated as follows:

$$\varepsilon_{ta}^{RMS} = \sqrt{\frac{\sum_{i=1}^{N}\left(\varepsilon_i^{ota}\right)^2}{N}} \tag{7.13}$$

The RMS assembly variation from the final assembly axis is calculated in a similar way, by replacing the table-axis error for each component by the final-assembly axis error in Equation (7.13). In what follows, the statistical distribution, mean, and standard deviation of the assembly variation (Mean of RMS for 10,000 repeated assemblies) are presented for the complete assembly and at different stages of assembly. In order to investigate the performance of the proposed optimisation methods for straight-build assemblies, two examples are considered. Example 1 is the simple case of 2D rectangular components with identical dimension, and Example 2 is more realistic example of non-identical 2D components. These examples are analysed as under:

### 7.3.1 Example 1: Identical Components Assembly

This example investigates assemblies consisting of identical components. To analyse the performance of the straight-build optimisation methods, assemblies with 4, 6 and 8 identical components are considered. Each component has a nominal width of 100 mm and a nominal height of 70 mm. The geometric feature tolerances for axial and radial run-out of each component are assumed to be 0.01 mm and 0.05 mm, respectively, and size tolerance of ±0.1 mm (as shown in Figure 7-3).

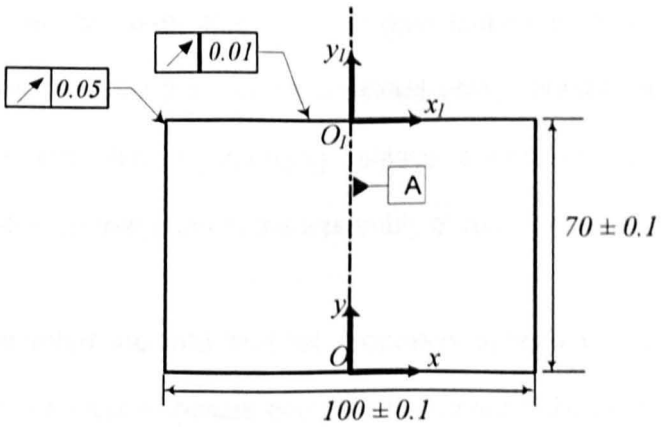


**Figure 7-3: Dimensions and tolerances of 2D rectangular component**

Figures 7-4 to 7-6 present results for the mean of RMS assembly variation from the table axis (using Equation (7.13)) and the final axis based on 10,000 repeated assemblies using the proposed optimisation methods and direct-build assembly, for 4, 6 and 8 component assemblies, respectively. Also, Tables 7-1, 7-3 and 7-5 present numerical results for stage-by-stage mean and standard deviations of table-axis error for 4, 6 and 8 component assemblies, respectively. Tables 7-2, 7-4 and 7-6 present numerical results for stage-by-stage mean and standard deviations of final assembly axis error for 4, 6 and 8 component assemblies, respectively. Tables 7-1, 7-3 and 7-5 show that the average and the standard deviation of error from table-axis increase with the stage for each procedure. As final assembly axis passes through the center of the base of first component and the center of the top of the uppermost component in the assembly, this implies that the eccentricity error for final assembly axis will be zero at the base of the first component and the top of the uppermost component. Therefore Tables 7-2, 7-4 and 7-6 does not include error at stage 4 (error at the top of the uppermost component) and from these tables it can be found that the averages and the standard deviations of error from final-assembly axis increase at each following stage. Not surprisingly these results show that the errors accumulate as parts are assembled together.

In all cases it can be seen that all four optimisation methods yield assembly variations that are smaller than those obtained using direct-build assembly. This shows that the approach of changing relative orientation is very effective in minimising variation propagation in the assembly of axi-symmetric components.

The results presented indicate that all proposed optimisation methods produce significantly improved eccentricities compared to direct build (without optimisation). The combinatorial approaches (Methods 3 and 4) are fully "global" and consider all assembly stages simultaneously and always yield the smallest possible

eccentricities. However, practical complexities, including potentially large numbers of calculations, make them unsuitable for practical implementation currently. Method 1 is a "local" method based only on the errors for the component being considered. Method 2 considers errors in two adjacent components at a time, meaning that it makes some allowances for errors in subsequent stages of assembly. Although, Methods 1 and 2 are not as effective as Method-3 for reducing table-axis variations, they have been shown to produce good improvements compared to direct build, with Method-2 always producing smaller eccentricities than Method-1. It is also interesting to note that for all cases considered the variations obtained using Method 2 are only slightly larger than those obtained using Method 3.

For an assembly with two components, Methods 2 and 3 are of course equivalent, and this suggests that these methods will yield similar results for components with a small number of components. However, the results shown indicate that this trend also applies when the number of components is increased. Method 4 consistently produces the smallest variation from the final assembly axis for the different number of components. This is expected, because this optimisation method is based on minimising the final assembly axis variation.

As the number of components increases, the proposed optimisation methods reduce assembly variation more significantly, compared to direct-build assembly. For example, from Figure 7-4, Methods 1 and 2 reduce the variation by 29.2% and 50.3% respectively, for the 4-component assembly; while for the 6-components assembly from Figure 7-5, Methods 1 and 2 reduce the variation by 32.3% and 68.2%, respectively; for the 8-components assembly from Figure 7-6, Methods 1 and 2 reduce the variation by 36.2% and 77.4%, respectively. These results indicate that the optimisation methods are effective for any number of components in an assembly.

The above findings can be confirmed by considering the probability that the table or final-axis error for the final component in the assembly exceeds certain threshold values. The analysis performed to assess this probability is similar for assemblies with different numbers of components, and the findings are also similar. For this reason, only the results obtained for the 4-component assembly are presented here. The threshold values from the table axis considered are: 0.05 mm, 0.1 mm, 0.15 mm, and 0.2 mm. Results for the probabilities that these threshold variations are exceeded are shown in Figure 7-7(a), where it can be seen that all optimisation methods are more effective than direct-build assembly. In addition, Method 3 is superior to Method 2, and Method 2 is superior to Method 1. Figure 7-7(b) shows results for the probability that the assembly variation from the final axis assembly exceeds 0.02 mm, 0.04 mm, 0.06 mm and 0.08 mm. These results indicate that Method 4 is the most effective at reducing variation from final axis than all other methods, as expected. However, it should be noticed that Methods 3 and 4 are based on a combinatorial approach which are potentially much less efficient than Methods 1 and 2 in terms of computation time, particularly as the numbers of components and configurations increase. In practice, Methods 1 and 2 have the potential to control the propagation of component variation since they are easily implementable and have been shown to yield significant improvements, compared to direct-build assembly, as described above. Furthermore, in all cases considered, the results obtained using Method 2 are close to those obtained using the combinatorial approach (Method 3), as shown in Figures 7-4, 7-5 and 7-6.

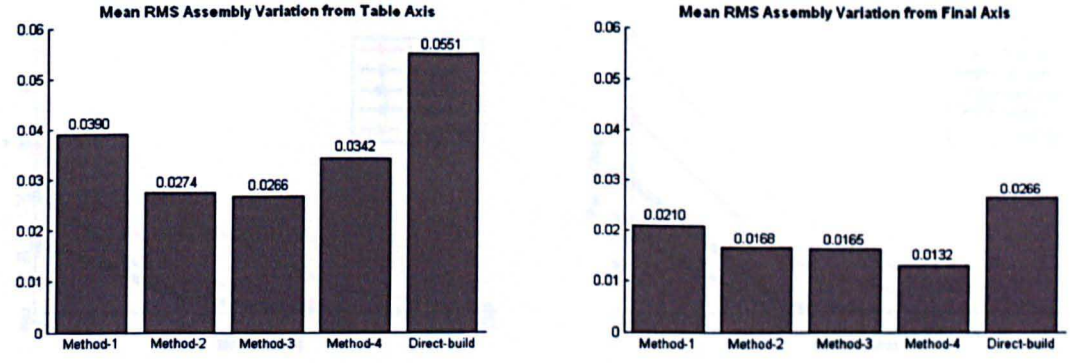


(a) (b)

**Figure 7-4: Mean of RMS assembly variation (equation (7.13)) based on 10,000 repeated assemblies for four-component assembly: (a) table-axis variation; (b) final-axis variation.**

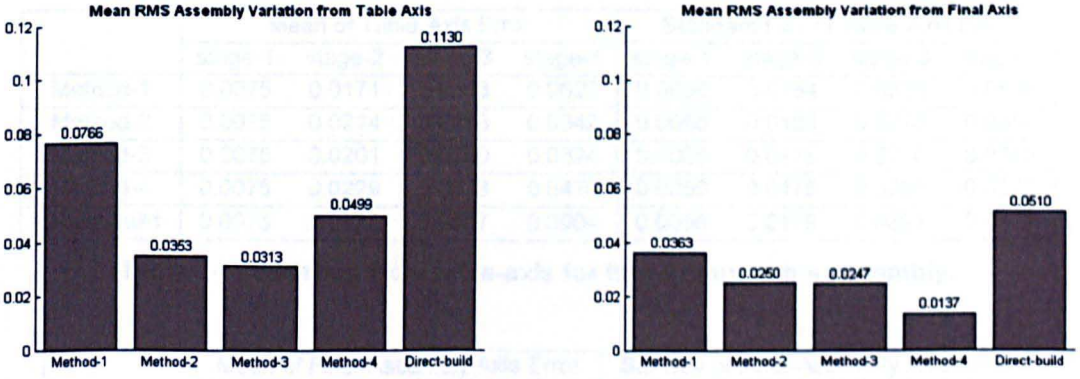


(a) (b)

**Figure 7-5: Mean of RMS assembly variation (equation (7.13)) based on 10,000 repeated assemblies for six-component assembly: (a) table-axis variation; (b) final-axis variation.**

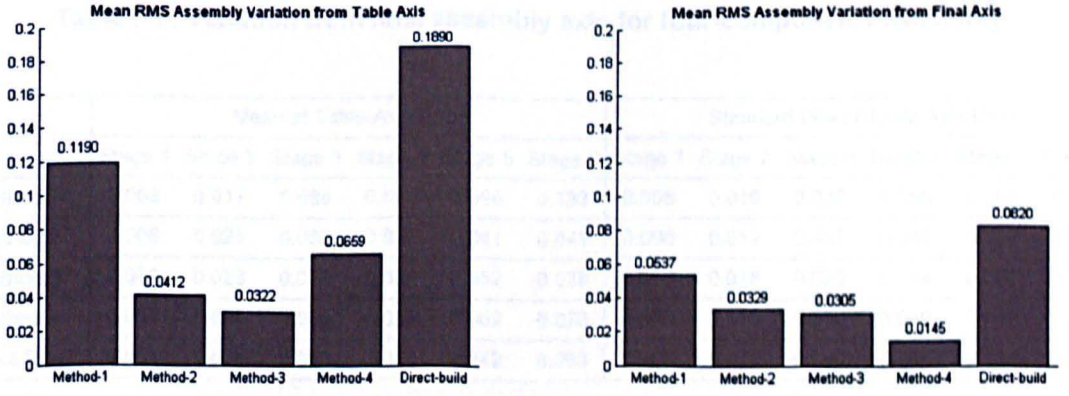


(a) (b)

**Figure 7-6: Mean of RMS assembly variation (equation (7.13)) based on 10,000 repeated assemblies for eight-component assembly:(a) table-axis variation; (b) final-axis variation.**

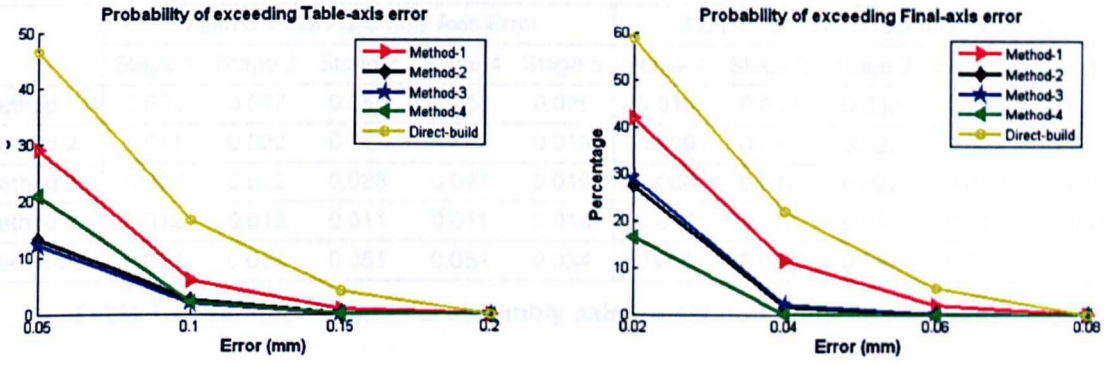


(a) (b)

**Figure 7-7: (a) Probability of the table-axis error exceeding 0.05 mm, 0.1 mm, 0.15 mm, and 0.2 mm; (b) Probability of the final-axis error exceeding 0.02 mm, 0.04 mm, 0.06 mm and 0.08 mm, for four identical components assembly.**

| | Mean of Table-Axis Error | | | | Standard Dev of Table-Axis Error | | | |
|---|---|---|---|---|---|---|---|---|
| | stage-1 | stage-2 | stage-3 | stage-4 | stage-1 | stage-2 | stage-3 | stage-4 |
| Method-1 | 0.0075 | 0.0171 | 0.0363 | 0.0620 | 0.0056 | 0.0154 | 0.0326 | 0.0546 |
| Method-2 | 0.0075 | 0.0214 | 0.0293 | 0.0342 | 0.0056 | 0.0168 | 0.0273 | 0.0350 |
| Method-3 | 0.0075 | 0.0201 | 0.0290 | 0.0324 | 0.0056 | 0.0173 | 0.0270 | 0.0348 |
| Method-4 | 0.0075 | 0.0229 | 0.0378 | 0.0478 | 0.0056 | 0.0175 | 0.0294 | 0.0373 |
| Direct-build | 0.0075 | 0.0234 | 0.0517 | 0.0904 | 0.0056 | 0.0179 | 0.0391 | 0.0671 |

**Table 7-1: Variation from table-axis for four-components assembly.**

| | Mean of Final-Assembly Axis Error | | | Std Dev of Final-Assembly Axis Error | | |
|---|---|---|---|---|---|---|
| | stage-1 | stage-2 | stage-3 | stage-1 | stage-2 | stage-3 |
| Method-1 | 0.0172 | 0.0228 | 0.0182 | 0.0138 | 0.0182 | 0.0141 |
| Method-2 | 0.0114 | 0.0173 | 0.0155 | 0.0094 | 0.0136 | 0.0122 |
| Method-3 | 0.0112 | 0.0171 | 0.0150 | 0.0093 | 0.0133 | 0.0117 |
| Method-4 | 0.0112 | 0.0117 | 0.0109 | 0.0094 | 0.0112 | 0.0092 |
| Direct Build | 0.0232 | 0.0305 | 0.0233 | 0.0172 | 0.0226 | 0.0173 |

**Table 7-2: Variation from final assembly axis for four-components assembly.**

| | Mean of Table-Axis Error | | | | | | Standard Dev of Table-Axis Error | | | | | |
|---|---|---|---|---|---|---|---|---|---|---|---|---|
| | Stage 1 | Stage 2 | Stage 3 | Stage 4 | Stage 5 | Stage 6 | Stage 1 | Stage 2 | Stage 3 | Stage 4 | Stage 5 | Stage 6 |
| Method 1 | 0.008 | 0.017 | 0.038 | 0.064 | 0.096 | 0.133 | 0.006 | 0.016 | 0.033 | 0.056 | 0.082 | 0.111 |
| Method 2 | 0.008 | 0.021 | 0.030 | 0.036 | 0.041 | 0.041 | 0.006 | 0.017 | 0.027 | 0.036 | 0.042 | 0.047 |
| Method 3 | 0.008 | 0.023 | 0.033 | 0.035 | 0.032 | 0.028 | 0.006 | 0.018 | 0.028 | 0.034 | 0.037 | 0.037 |
| Method 4 | 0.008 | 0.024 | 0.039 | 0.052 | 0.062 | 0.073 | 0.006 | 0.018 | 0.030 | 0.040 | 0.048 | 0.056 |
| Direct-Build | 0.008 | 0.024 | 0.053 | 0.092 | 0.142 | 0.203 | 0.006 | 0.018 | 0.040 | 0.068 | 0.104 | 0.145 |

**Table 7-3: Variation from table axis for six-components assembly.**

| | Mean of Final Assembly Axis Error | | | | | Std Dev of Final Assembly Axis Error | | | | |
|---|---|---|---|---|---|---|---|---|---|---|
| | Stage 1 | Stage 2 | Stage 3 | Stage 4 | Stage 5 | Stage 1 | Stage 2 | Stage 3 | Stage 4 | Stage 5 |
| Method 1 | 0.023 | 0.037 | 0.042 | 0.038 | 0.025 | 0.019 | 0.030 | 0.033 | 0.030 | 0.019 |
| Method 2 | 0.011 | 0.022 | 0.028 | 0.027 | 0.019 | 0.009 | 0.017 | 0.022 | 0.022 | 0.015 |
| Method 3 | 0.009 | 0.022 | 0.028 | 0.027 | 0.019 | 0.008 | 0.016 | 0.022 | 0.022 | 0.015 |
| Method 4 | 0.012 | 0.012 | 0.011 | 0.011 | 0.010 | 0.010 | 0.011 | 0.011 | 0.010 | 0.008 |
| Direct-Build | 0.034 | 0.054 | 0.061 | 0.054 | 0.034 | 0.025 | 0.038 | 0.043 | 0.038 | 0.024 |

**Table 7-4: Variation from final assembly axis for six-components assembly.**

| | Mean of Table-Axis Error | | | | | | | |
|---|---|---|---|---|---|---|---|---|
| | Stage 1 | Stage 2 | Stage 3 | Stage 4 | Stage 5 | Stage 6 | Stage 7 | Stage 8 |
| Method 1 | 0.008 | 0.018 | 0.037 | 0.064 | 0.095 | 0.131 | 0.170 | 0.213 |
| Method 2 | 0.008 | 0.021 | 0.030 | 0.036 | 0.040 | 0.044 | 0.046 | 0.045 |
| Method 3 | 0.008 | 0.023 | 0.033 | 0.037 | 0.036 | 0.031 | 0.025 | 0.021 |
| Method 4 | 0.008 | 0.024 | 0.040 | 0.053 | 0.065 | 0.077 | 0.088 | 0.100 |
| Direct-Build | 0.008 | 0.024 | 0.053 | 0.092 | 0.142 | 0.203 | 0.274 | 0.356 |
| Standard Dev of Table-Axis Error | | | | | | | | |
| Method 1 | 0.006 | 0.015 | 0.033 | 0.055 | 0.081 | 0.111 | 0.143 | 0.178 |
| Method 2 | 0.006 | 0.017 | 0.027 | 0.036 | 0.042 | 0.048 | 0.052 | 0.056 |
| Method 3 | 0.006 | 0.018 | 0.028 | 0.035 | 0.038 | 0.037 | 0.035 | 0.031 |
| Method 4 | 0.006 | 0.018 | 0.031 | 0.041 | 0.050 | 0.060 | 0.069 | 0.078 |
| Direct-Build | 0.006 | 0.018 | 0.040 | 0.068 | 0.102 | 0.142 | 0.188 | 0.238 |

**Table 7-5: Variation from table axis for eight-components assembly.**

| | Mean of Final Assembly Axis Error | | | | | | |
|---|---|---|---|---|---|---|---|
| | Stage 1 | Stage 2 | Stage 3 | Stage 4 | Stage 5 | Stage 6 | Stage 7 |
| Method 1 | 0.028 | 0.047 | 0.060 | 0.065 | 0.061 | 0.050 | 0.030 |
| Method 2 | 0.010 | 0.024 | 0.033 | 0.038 | 0.037 | 0.032 | 0.021 |
| Method 3 | 0.008 | 0.023 | 0.033 | 0.036 | 0.034 | 0.028 | 0.018 |
| Method 4 | 0.012 | 0.013 | 0.012 | 0.012 | 0.012 | 0.012 | 0.010 |
| Direct-Build | 0.045 | 0.076 | 0.095 | 0.101 | 0.095 | 0.076 | 0.045 |
| Std Dev of Final Assembly Axis Error | | | | | | | |
| Method 1 | 0.022 | 0.038 | 0.048 | 0.051 | 0.048 | 0.039 | 0.023 |
| Method 2 | 0.009 | 0.019 | 0.027 | 0.032 | 0.032 | 0.027 | 0.017 |
| Method 3 | 0.007 | 0.018 | 0.027 | 0.031 | 0.031 | 0.026 | 0.016 |
| Method 4 | 0.010 | 0.011 | 0.011 | 0.010 | 0.011 | 0.010 | 0.009 |
| Direct-Build | 0.030 | 0.051 | 0.064 | 0.068 | 0.064 | 0.052 | 0.031 |

**Table 7-6: Variation from final assembly axis for eight-component assembly**

### 7.3.2 Example 2: Non-Identical Components Assembly

The dimensions of the components considered in Example 2 are provided in Table 7-7 and represent scaled versions of components forming part of an aero-engine assembly used in industry.

| | Part 1 | Part 2 | Part 3 | Part 4 |
|---|---|---|---|---|
| Height (*H*) (mm) | 9 | 202 | 32 | 390 |
| Width (*B*) (mm) | 206 | 572 | 572 | 310 |

**Table 7-7: Dimensions of four components of the assembly**

For this example, the tolerances used for size (height) are again of ±0.1 mm, and the axial and radial run-outs in each component are 0.1 mm and 0.05 mm, respectively.

Figure 7-8 presents results for the mean assembly variation from the table axis and final-assembly axis. These were obtained using 10,000 simulations in conjunction with the proposed optimisation methods and direct-build assembly. Similarly, Table 7-8 and Table 7-9 present numerical results for the mean and standard deviations of table-axis error and final assembly axis error for each assembly stage.

In all cases, the four optimisation methods produce lower variations than direct-build assembly. From Tables 7-8 and 7-9, it is found that the mean and standard deviation of the variation increases with stage for all methods for both table-axis and final-axis measures. Comparing all these results, identical trends to those indicated for Example 1 are found, with Method 3 producing the smallest variation from the table axis and Method 4 producing the smallest variation from the final-assembly axis. Further confirmation of these findings is presented in Figure 7-9, which plots the probability that the assembly variation from the table axis and final assembly axis exceeds particular values. Figure 7-9 shows that for table-axis error, Method 3 always produce the lowest error, Method 2 producing results lower than Methods 1

and 4 and slightly higher than Method 3. For final-axis error, Method 4 produces the lowest variations with Method 2 always producing errors with lower probability than Method 1 and 3 and higher probability than Method 4 for the given values of errors. This shows that Method 2 produce lower variations from both table-axis and the final-axis results at the same time compared to other methods.

In summary, the proposed optimisation methods have demonstrated good potential to reduce variation propagation in axi-symmetric mechanical assemblies. Although Methods 3 and 4 produce the smallest variations, it is important to realise that these methods are based on a combinatorial approach which is potentially much less efficient than the other proposed methods, particularly as the number of components increases. For example, for a *N*-component assembly, the total number of combinations of the complete assembly to be computed is $2^{N-1}$. In spite Methods 3 and 4 are computationally extensive; the results presented by these methods are useful because they provide the best possible outcome, which is useful for comparison when considering the performance of other methods. On the other hand, Method 2 provides results that are very close to those obtained using Method 3 for table-axis error and at the same time reasonably close to Method 4 for final assembly axis with less computational efforts. Although Method 1 provide results with relatively higher variations compared to Methods 2, 3 and 4, Method 1 has the potential to control the variation propagation and significant improvements to assembly variations are possible compared to direct-build assembly in all of the cases considered. In addition to this, Methods 1 is very simple, provides good understanding of minimising eccentricity error in the assembly of rotationally symmetric components.

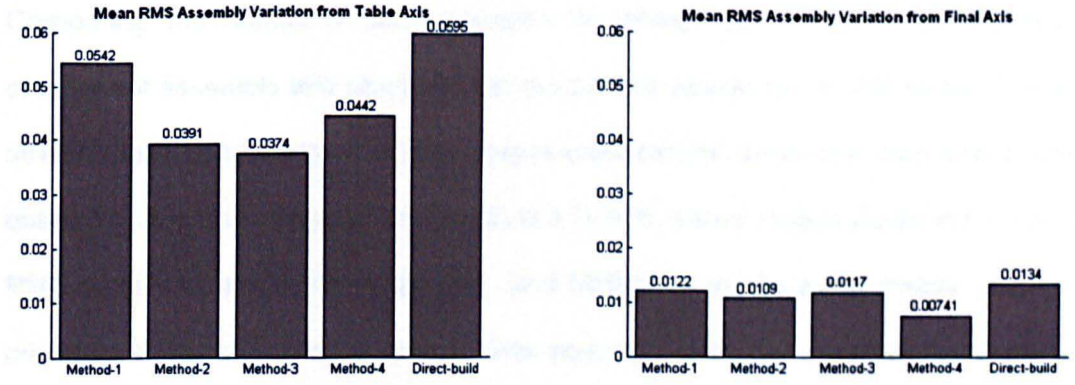


(a) (b)

**Figure 7-8: (a) Assembly variations from table axis, (b) Assembly variations from final assembly axis**

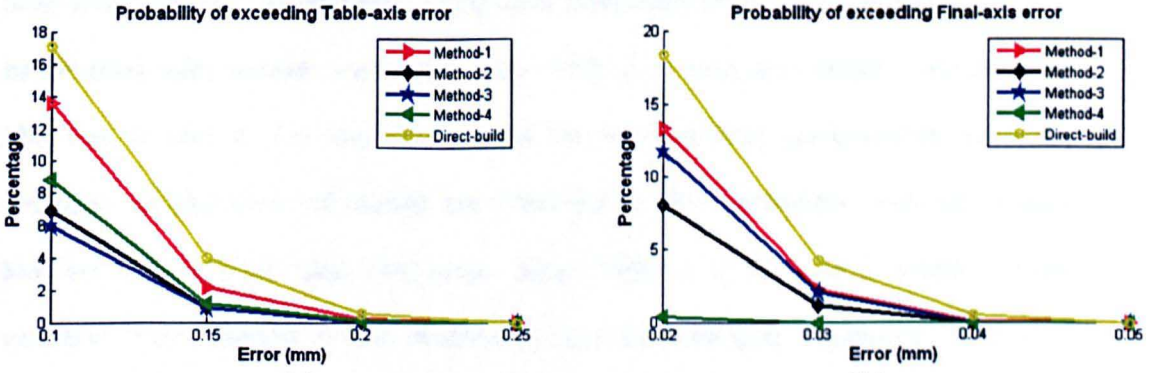


(a) (b)

**Figure 7-9: (a) Probability of the table-axis error exceeding 0.1 mm, 0.15 mm, 0.2 mm, and 0.25 mm; (b) Probability of the final-axis error exceeding 0.02 mm, 0.03 mm, 0.4 mm and 0.5 mm.**

| | Mean of Table-Axis Error | | | | Standard Dev of Table-Axis Error | | | |
|---|---|---|---|---|---|---|---|---|
| | stage-1 | stage-2 | stage-3 | stage-4 | stage-1 | stage-2 | stage-3 | stage-4 |
| Method-1 | 0.0076 | 0.0315 | 0.0367 | 0.0952 | 0.0057 | 0.0235 | 0.0273 | 0.0706 |
| Method-2 | 0.0076 | 0.0248 | 0.0274 | 0.0647 | 0.0057 | 0.0215 | 0.0246 | 0.0632 |
| Method-3 | 0.0076 | 0.0278 | 0.0293 | 0.0584 | 0.0057 | 0.0227 | 0.0254 | 0.0596 |
| Method-4 | 0.0076 | 0.0247 | 0.0241 | 0.0790 | 0.0057 | 0.0215 | 0.0234 | 0.0678 |
| Direct Build | 0.0076 | 0.0314 | 0.0369 | 0.1054 | 0.0057 | 0.0235 | 0.0276 | 0.0790 |

**Table 7-8: Variation from table-axis at each assembly stage for four non-identical components' assembly.**

| | Mean of Final Assembly Axis Error | | | Std Dev of Final Assembly Axis Error | | |
|---|---|---|---|---|---|---|
| | stage-1 | stage-2 | stage-3 | stage-1 | stage-2 | stage-3 |
| Method-1 | 0.0076 | 0.0124 | 0.0125 | 0.0057 | 0.0095 | 0.0096 |
| Method-2 | 0.0076 | 0.0102 | 0.0113 | 0.0057 | 0.0079 | 0.0086 |
| Method-3 | 0.0076 | 0.0114 | 0.0126 | 0.0057 | 0.0088 | 0.0097 |
| Method-4 | 0.0074 | 0.0057 | 0.0060 | 0.0056 | 0.0048 | 0.0050 |
| Direct Build | 0.0076 | 0.0139 | 0.0145 | 0.0057 | 0.0105 | 0.0110 |

**Table 7-9: Variation from final-assembly axis for four non-identical components assembly.**

Comparing the results of two examples for straight-build assemblies (identical component assembly and non-identical component assembly), it is observed that all straight-build optimisation methods always yield smaller variations than direct-build assembly. It is also observed that Method 3 in both cases always yields in minimum RMS error with respect to table-axis, and Method 3 in all cases always yields in minimum RMS error with respect to final-assembly-axis. For identical components assembly, Method 2 yields smaller variation than Method 1 and Method 4 for table axis measures, and slightly larger variations than Method 3. The results comparing final-axis measures for identical component assembly shows that Method 2 produce assemblies with smaller variations than method 1 only and larger variation than Methods 3 and 4. On the other hand for non-identical components assembly example, similar trend of results are obtained for all optimisation methods except Method 2. For table axis measures, after Method 3, Method 2 yields smaller variation than Method 1 and Method 4 and for final-axis measures, Method 2 produce assemblies with smaller variations than Methods 1 and 3 and larger variation than Method 4 only. It is important to note that in practice, assembly components for rotating machines are not identical in dimensions but they vary in size with respect to each other. Also the manufacturers are not always interested in minimising assembly variations based on table-axis measures only or final axis measures only but may also be interested for method that closely satisfy both table-axis and final axis measures (Such as Method 2). Therefore it will be quite early to decide among proposed straight-build optimisation methods for their suitability.

## 7.4 Case Study 2: Circular-Build Assembly

Uniformly segmented circular components (as described earlier in Chapter 4 in Case Study 2) when assembled form the main non-rotating structures (stator) of the

rotating machines. In high-speed rotating machines such as jet engines, a precise clearance between a rotor and a non-rotating structure (stator or casing) is required. The assembly of these uniformly segmented circular components play the main role in maintaining the precise clearance between the rotor and the casing (stator). In circular-build assemblies, all uniformly segmented components are ideally identical in shape and dimensions. During the assembly of uniformly segmented circular components, geometric variation at the mating feature of the components plays a major role in the overall assembly variations. The KC for such an assembly is to have minimum radial variation throughout the assembly to build a precise circular structure.

### 7.4.1 Optimisation Method (Combinatorial Approach)

An optimisation method based on combinatorial approach is proposed in this section to control variation propagation in the assembly of uniformly-segmented circular components. In the proposed optimisation method, optimum assembly sequence is identified from all possible combinations of mating sequence of the assembly components. The three steps, involved in the proposed optimisation strategy for the assembly of nominally identical uniformly-segmented circular components, are:

1. Determine possible combinations of mating sequence of assembly components.

$$Total\ mating\ combinations = (N-1)! \tag{7.14}$$

where, $N$= number of assembly components.

2. Calculate the overall assembly variation, root-mean-square (RMS) of radial error ($e_i^R$) at all assembly stages. The RMS error is calculated as:

$$\varepsilon^{RMS} = \sqrt{\frac{\sum_{i=1}^{N} \left(e_i^R\right)^2}{N}} \tag{7.15}$$

where, error $\varepsilon^{RMS}$ is the over assembly variation in radial direction and $e_i^R$ is the error in radial direction at $i^{th}$ assembly stage given by Equation (4.53) for 2D assemblies and Equation (4.54) for 3D assemblies.

3. Evaluate the mating sequence of components that gives minimum assembly error.

In order to evaluate the best mating sequence of all assembly components the RMS error is calculated for all $(N-1)!$ mating combination of assembly components. Once RMS errors for all $(N-1)!$ combinations are calculated, the best mating sequence that gives minimum assembly error can be calculated as:

$$\varepsilon^{opt} = \min_{combi=1}^{(N-1)!} \left(\varepsilon^{RMS}\right) \text{ (Provided there is no interference fit at the end)} \tag{7.16}$$

where, $\varepsilon^{opt}$ is the optimum overall assembly error evaluated from all mating combinations of assembly components.

It is important to note that the best mating sequence is that which has the minimum error among those that do not result in interference between the last and the first component in the circular-build assembly. Such interference may cause fit-up problems in the circular-build assembly.

### 7.4.2 Direct-Build Assembly

To investigate any potential improvements in circular-build assembly, the results obtained by the error minimisation method based on the combinatorial based approach are compared with direct-build assembly. Direct-build assembly includes

component variations but does not use any optimisation methods to control variation propagation.

## 7.5 Results and Discussion

Here the results are calculated for assembly examples of two-dimensional and three-dimensional uniformly-segmented circular components. To analyse the performance of the proposed methods, assemblies with 4, 6 and 8 identical components are considered. In the cases of 4, 6 and 8 identical components assembly, the nominal dimensions of the components are different in each case. Each component is assumed under influence of dimensional and form tolerances. The nominal dimensions and size tolerances of 2D uniformly segmented circular components for 4, 6 and 8 identical component assembly are shown in Figure 7-10. Also, the nominal dimensions and size tolerances of 3D uniformly segmented circular components for 4, 6 and 8 identical component assembly are shown in Figure 7-11.

From Figure 7-10, coordinates of the feature containing frame $O_1x_1y_1$ relative to the base feature for each component of 4, 6 and 8 component assembly are $[-R_m, R_m]$, $\left[-R_m\left(1-\cos\left(\frac{\pi}{3}\right)\right), R_m\sin\left(\frac{\pi}{3}\right)\right]$ and $\left[-R_m\left(1-\cos\left(\frac{\pi}{4}\right)\right), R_m\sin\left(\frac{\pi}{4}\right)\right]$, respectively. Similarly from Figure 7-11, coordinates of the feature containing frame $x_1y_1z_1$ relative to the base feature for each component of 4, 6 and 8 component assembly are $[0, -R_m, R_m]$, $\left[0, -R_m\left(1-\cos\left(\frac{\pi}{3}\right)\right), R_m\sin\left(\frac{\pi}{3}\right)\right]$ and $\left[0, -R_m\left(1-\cos\left(\frac{\pi}{4}\right)\right), R_m\sin\left(\frac{\pi}{4}\right)\right]$, respectively, where $R_m = (R_o + R_i)/2$. A 3D components given in Figure 7-11 have similar shape and dimensions to that of a 2D component (Figure 7-10), except that 2D component has three degrees of freedom

of variation (translation error along $x$ and $y$ ($dX$ and $dY$), and rotation error $d\theta$) and 3D component have six degrees of freedom of error ($dX, dY, dZ, d\theta_x, d\theta_y$ and $d\theta_z$).

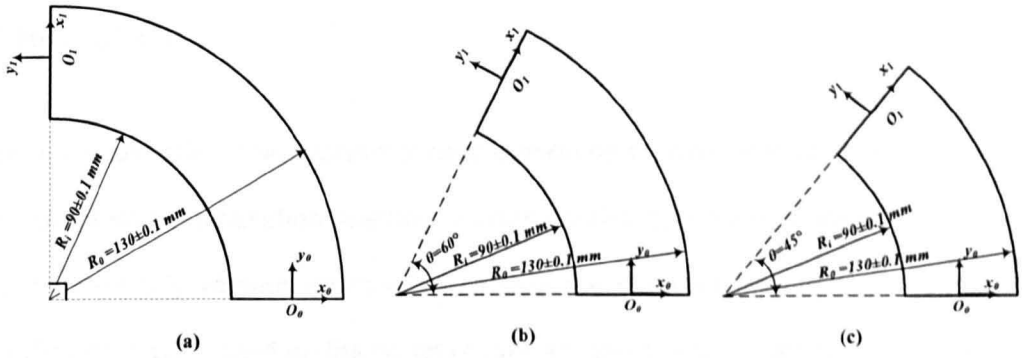


**Figure 7-10: Nominal dimensions of a uniformly segmented 2D circular component: (a) for four component assembly; (b) for six component assembly; (c) for eight component assembly.**

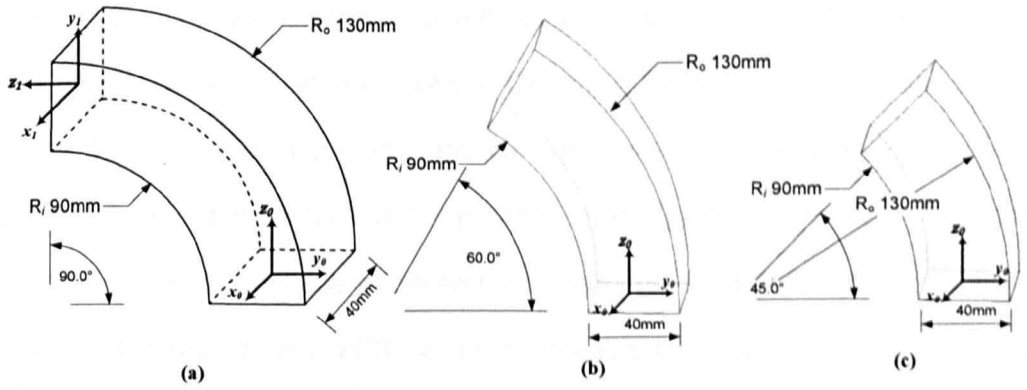


**Figure 7-11: Nominal dimensions of a uniformly segmented 3D circular component: (a) for four component assembly; (b) for six component assembly; (c) for eight component assembly**

The form tolerance limits at the mating features in all cases are assumed to be 0.01 mm and the size tolerances are taken as ±0.1mm for all dimensions. The circular assembly structure is obtained by joining the components together at their mating surfaces. It is assumed that the components are rigid components and there is no error at the mating between two components. During analysis, the size and form variations for each component are selected to be independent zero-mean Gaussian random variables with ±3σ standard deviation for specified tolerance limit. For 2D components, the values of size and form tolerance are transformed into translation

errors $(dX, dY)$ and rotation error $(d\theta)$ using Equations (5.11), (5.12) and (5.13). For 3D assemblies the values of size and form tolerances are transformed into translation errors $(dX, dY, dZ)$ and rotation error $(d\theta_x, d\theta_y, d\theta_z)$ using Equations (5.16) to (5.20).

For 2D assemblies, the analysis is only presented to investigate the performance of the proposed optimisation method (combinatorial approach) compared to direct-build (assembly without optimisation) using the standard Monte Carlo Simulation (MCS) approach based on the exact model, as described in Chapter 4. The analysis of 2D uniformly-segmented circular components assembly is based on 4, 6 and 8 components. For 3D assemblies, the analysis is initially performed to compare the results of the probabilistic model developed in Chapter 6 with MCS based on the exact model, as described in Chapter 4. Chapter 6 investigates the performance of the developed probabilistic model and compared the results with MCS at different values of form tolerance for our-component assembly only. However, this Chapter investigates the performance of the probabilistic model for direct-build assembly and compares the results with MCS based on the exact model at different number of assembly components (4, 6 and 8 components). The results for 3D assemblies are also presented to evaluate the performance of the proposed optimisation method (combinatorial approach) compared with direct-build assembly. The performance of the proposed optimisation method (combinatorial approach) is investigated using the standard MCS approach based on exact model (as described in Chapter 4).

### 7.5.1 2D Example of Uniformly Segmented Circular Components

Assembly variation propagations are calculated based on translation and rotation errors of individual component using the exact method described in Section 4.4.1 (in Chapter 4). Each assembly is repeated 10,000 times using the optimisation method

and direct-build assembly, and statistical data for the resulting assembly errors are generated. Figures 7-12 and 7-13 present results for mean and standard deviation of stage-by-stage radial error (i.e. mean and STD value of Equation (4.53)) based on 10,000 repeated assemblies using the optimisation method and direct-build assembly, for 4, 6 and 8 component assemblies. Also, Figure 7-14 compare the results of RMS assembly error $\varepsilon^{RMS}$ for direct build assembly and the optimised assembly error $\varepsilon^{opt}$ for combinatorial approach based on 10,000 repeated assemblies, for 4, 6 and 8 component assemblies. In all cases it can be seen that the optimisation method yield assembly variations that are smaller than those obtained using direct build assembly, as expected.

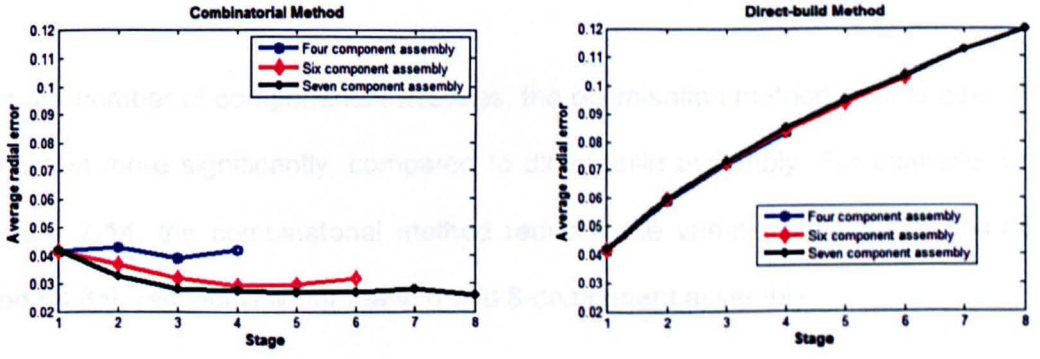


(a) (b)

**Figure 7-12: Mean of stage-by-stage radial error based on 10,000 repeated assemblies.**

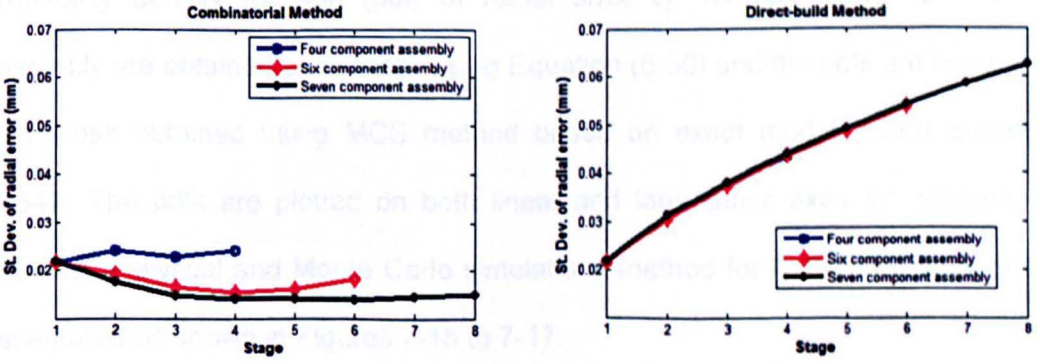


(a) (b)

**Figure 7-13: Standard deviation of stage-by-stage radial error based on 10,000 repeated assemblies.**

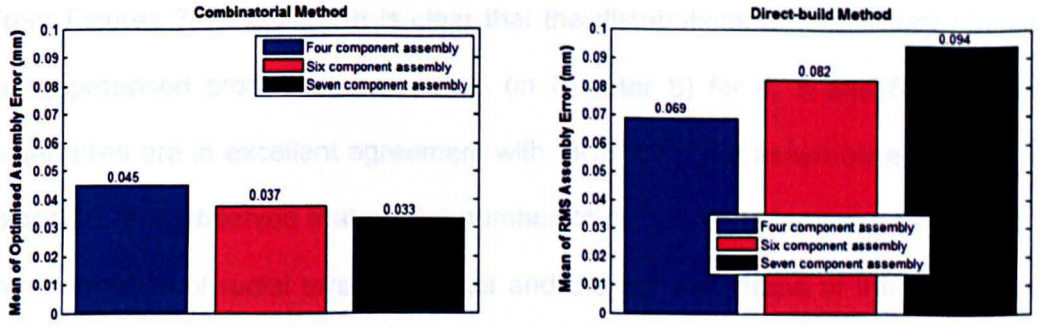


(a) (b)

**Figure 7-14: Mean of overall assembly error based on 10,000 repeated assemblies.**

From Figures 7-12 and 7-13 it can be observed that the optimised solution produces assemblies with smaller stage-by-stage variations than direct build. This is not surprising because combinatorial method considers all possible mating sequence of assembly components.

As the number of components increases, the optimisation method reduce assembly variation more significantly, compared to direct-build assembly. For example, from Figure 7-14, the combinatorial method reduces the variations by 34.7%, 54.85% and 64.8%, respectively, for the 4, 6 and 8-component assembly.

### 7.5.2 3D Example of Uniformly Segmented Circular Components

To confirm the accuracy of the probabilistic model developed in Chapter 6, the probability density function (pdf) of radial error $e_i^R$ for last component in the assembly are obtained analytically using Equation (6.50) and the pdfs are compared with those obtained using MCS method based on exact model (using Equation (4.54)). The pdfs are plotted on both linear and logarithmic axes for comparison between analytical and Monte Carlo simulations method for 4, 6 and 8 component assemblies as shown in Figures 7-15 to 7-17.

From Figures 7-15 to 7-17, it is clear that the distributions of radial error obtained using proposed probabilistic approach (in Chapter 6) for 4, 6 and 8 component assemblies are in excellent agreement with MCS for given assembly examples. As expected, it is observed that as the number of components increase (from 4 to 8) the magnitude of radial error increases and the general shape of the distributions remain relatively unchanged. The probabilistic approach is much more efficient in terms of calculation time and as the number of components is increased, the MCS method takes more and more time to compute the distributions. This is because the pdfs can be calculated easily using Equation (6.40) for any number of components. The average CPU time ratio (for 4, 6 and 8 component assemblies) for analytical method Vs Monte Carlo Simulations was 1:117.5. The results in Figures 7-15 to 7-17 also indicate that the agreement at the tails of the log-pdf are not matching well and as the number of components is increased the disagreement at the tails of log-pdf is increased. This shows that the Monte Carlo Simulations are less accurate for high radial errors. The results also confirm that the derived analytical pdf expressions (Equation (6.40) is valid.

In order to evaluate the effectiveness of the proposed optimisation method for minimising variations in uniformly segmented component assembly, the results of mean RMS assembly error $\varepsilon^{RMS}$ for direct-build assembly and optimised assembly error $\varepsilon^{opt}$ for combinatorial approach are compared. Figure 7-18 presents results obtained by Monte Carlo Simulation based on the exact model for 10,000 repeated assemblies using the proposed optimisation method and direct build assembly for 4, 6 and 8 component assemblies. In all cases it can be seen that the optimisation method yield assembly variations that are smaller than those obtained using direct build assembly.

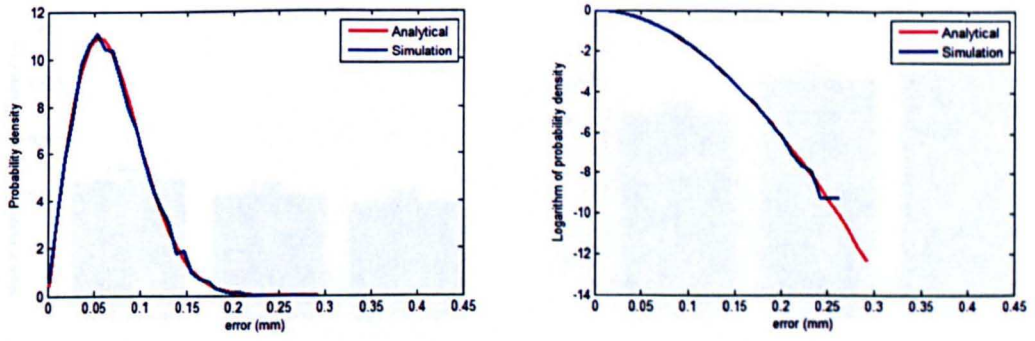


(a) (b)

**Figure 7-15: Probability density of radial error of last component in 4 component assembly: (a) linear scale; (b) log scale.**

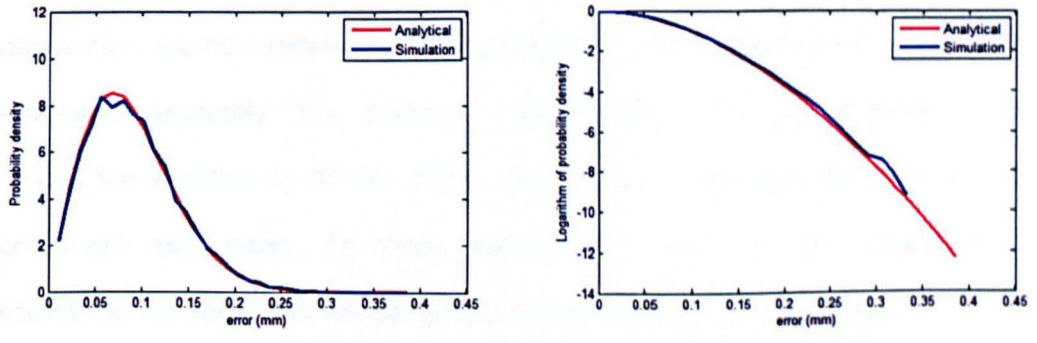


(a) (b)

**Figure 7-16: Probability density of radial error of last component in 8 component assembly: (a) linear scale; (b) log scale.**

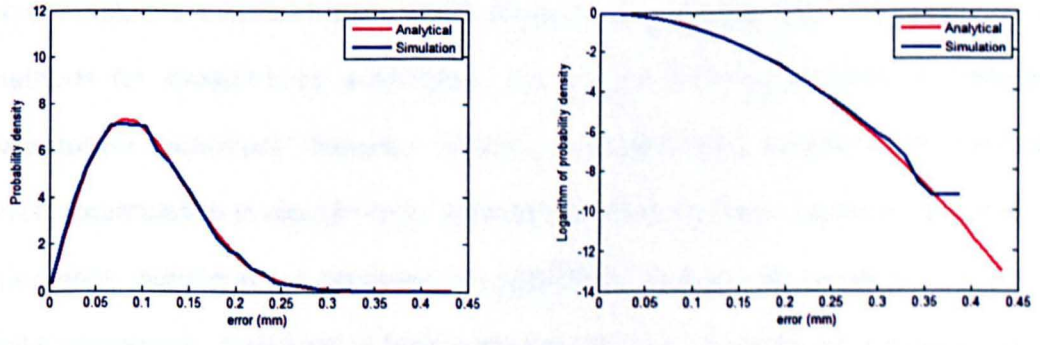


(a) (b)

**Figure 7-17: Probability density of radial error of last component in 8 component assembly: (a) linear scale; (b) log scale.**

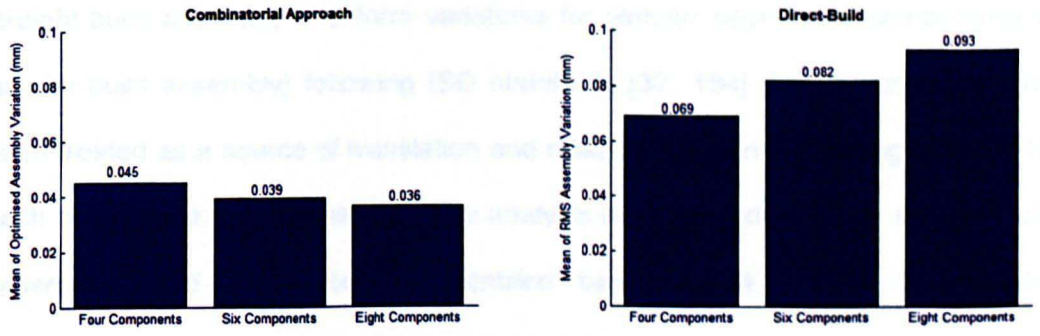


(a) (b)

**Figure 7-18: Mean of overall assembly error based on 10,000 repeated assemblies**

Figure 7-18 also show that as the number of components increases, the proposed optimisation method reduce assembly variation more significantly, compared to direct-build assembly. For example, from Figure 7-18, combinatorial method reduces the variation by 34.7%, 52.4% and 60.2%, respectively for the 4, 6 and 8-component assemblies. All these results also show that the results for 3D assemblies are very much similar to those calculated by 2D assemblies.

## 7.6 Summary

This chapter is a core chapter of the thesis that proposes assembly optimisation methods for straight-build assemblies and circular-build assemblies. A ***"relative orientation technique"*** between mating components was introduced to minimise error accumulation in straight-build assemblies. Four methods based on the relative orientation technique are proposed for controlling variation propagation in straight-build assemblies. A method of finding the best mating sequence for the assembly of uniformly segmented components is proposed to minimise error accumulation in circular-build assemblies.

The variations considered for each component are expressed in terms of the size and geometric variations (radial and axial run-outs for axi-symmetric components in

straight-build assembly and form variations for circular segmented components in circular-build assembly) following ISO standards [37, 154]. These variations have been treated as a source of translation and rotation errors in the mating features for each component in the assembly. The analysis is presented in 2D for straight-build assemblies and circular-build assemblies based on 4, 6 and 8 assembly components. 3D analysis is presented for circular-build assemblies only based on 4, 6 and 8 assembly components. In 2D analysis, Monte Carlo simulations have been used to investigate the statistical performance of proposed straight-build optimisation methods and the circular-build optimisation method. For 3D analysis, initially the results of circular-build assemblies are compared to confirm the accuracy and efficiency of probabilistic model developed in Chapter 6 with Monte Carlo simulations based on direct-build assembly (assembly without optimisation). The circular-build assemblies are further analysed in 3D to evaluate the performance of circular-build optimisation method compared to direct-build assembly using Monte Carlo simulations based on 10,000 repeated assemblies.

The results presented for straight-build assemblies indicate that the *relative orientation technique* is very efficient in minimising accumulation of eccentricity error in straight-build assemblies. It was also found that all proposed optimisation methods produce significantly improved eccentricities compared to direct build (without optimisation). The combinatorial approaches (Methods 3 and 4) are fully "global" and consider all assembly stages simultaneously. Methods 3 always yield the smallest possible eccentricities from table-axis (not from final assembly axis) and Methods 4 always yield the smallest possible eccentricities only from final-assembly axis. However, practical complexities, including potentially large numbers of calculations, make Methods 3 and 4 unsuitable for practical implementation currently. For the examples considered it was found that Method 2 is always

producing small eccentricities (with respect to table-axis) compared to Methods 1 and 4, and slightly larger eccentricities compared to Method 3. Also for final-axis measures, Method 2 produce small eccentricities compared to Methods 1 and 3 in case of assembly example considered for non-identical components. Method 2 is also computationally more efficient than Methods 3 and 4 and suitable for practical implementation. Although, Methods 1 is not as effective as Methods 2, 3 and 4 for reducing assembly variations, it has been shown to produce good improvements compared to direct build. Method 1 gives a clearer picture and helps the reader in better understanding the concept of the *relative orientation technique*.

For circular-build assembly a combinatorial approach based optimisation method has been proposed that selects the best mating sequence of assembly components from all possible combinations of component mating sequences. The results were presented for both 2D and 3D assemblies based on 4, 6, and 8 component assemblies. The results presented show that the combinatorial approach produces better results than direct-build assembly in all cases of 4, 6, and 8 component assemblies. It was also observed that the results produced for 2D assemblies are very much similar to those produced by 3D assemblies. The 3D circular-build assembly was also analysed to evaluate the performance of probabilistic model developed in Chapter 6 for 4, 6, and 8 component assemblies. The results of distributions obtained by probabilistic method proposed in Chapter 6 are compared with those calculated by Monte Carlo simulation method based on the exact model described in Chapter 4. The results validate the efficiency and accuracy of proposed probabilistic method and show that probability distributions obtained by analytical method are in excellent agreement with those obtained by Monte Carlo simulation method.

# Chapter 8 3D CASE STUDY OF STRAIGHT-BUILD ASSEMBLY

## 8.1 Introduction

Earlier in Chapter 7, optimisation methods to control variation propagation in two assembly case studies were described. The results were calculated using 2D assembly models for both case studies, and 3D assembly examples were only analysed for the case study of circular-build assemblies. For the case study of straight-build assemblies, results for 3D assembly will be produced in this chapter to show the effectiveness of proposed straight-build optimisation methods. Initially the 3D tolerance analysis based on probabilistic model (proposed in Chapter 6) is presented for straight-build assemblies without considering assembly optimisations in Section 8.2.

This chapter applies the proposed straight-build optimisation methods to the assembly of nominally identical cylindrical components and to more realistic non-

identical axi-symmetric components. This initially requires some calculations to find out the optimum number of indexing orientations of each assembly component during the optimisation process. The results of finding optimum number of indexing orientations are presented in Section 8.3. In order to check the effectiveness of optimisation methods for straight-build assembly, Monte Carlo simulations based on 10,000 repeated assemblies are performed in Section 8.4.

Further in this chapter, the effect of measurement and assembly process noise on the propagation of assembly variations is analysed. Section 8.5 describes the modelling technique for incorporating measurement and assembly process variations in assembly variation propagation model. Detailed results to analyse the effect of measurement uncertainty and assembly process variations on assembly variations are produced in Section 8.5.1. In Sections 8.3, 8.4 and 8.5 the analysis presented is based on the exact method for calculating assembly variation propagations as described in Chapter 4 of the thesis.

## 8.2 Probabilistic Tolerance Analysis

In Chapter 6, the results of probabilistic method were compared to those obtained by Monte Carlo Simulation results (based on the exact method derived in Chapter 4) at different values of run-out tolerances. The analysis was performed for assembly of four axi-symmetric components with identical dimensions. The accuracy of the analytical method not only depends on the different values of component tolerances, but also depends upon the nominal dimensions of components and the number of components in the assembly. Therefore this section compares the results of the probabilistic model with Monte Carlo simulation method based on the exact method, when the number of components is large and when the components have different dimensions. The results are produced for the assembly of 4, 6 and 8

components with nominally identical cylindrical shape. Each cylindrical component has a nominal diameter of 100 mm and nominal height 70 mm. The results are also produced for a more realistic assembly example with four non-identical components, the dimensions of each components represent scaled version of components forming part of an aero-engine assembly. The dimensions of the components considered in realistic assemble example are provided in Table 8-1.

| Component | 1 | 2 | 3 | 4 |
|---|---|---|---|---|
| Height (*H*) (mm) | 9 | 202 | 32 | 390 |
| Dia of base (mm) | 206 | 228 | 572 | 572 |
| Dia of top surface (mm) | 228 | 572 | 572 | 310 |

**Table 8-1: Dimensions of four components of the assembly.**

The geometric feature tolerances for axial and radial run-out of each component in all cases are assumed to be 0.05 mm (for both axial and radial run-out) and the size tolerance is assumed to be $\pm 0.1$ mm. Components variations in all cases are selected from independent zero-mean Gaussian random variables for size, axial and radial run-out variation with known standard deviation based on specified tolerance limits. The component variations are transformed into variations along degrees of freedom (VDOF) as described in Section 5.4.1.2 of Chapter 5. Assembly variation propagations are then calculated based on VDOF of each assembly component using Equation (4.31) while assuming that there is no variation at the mating between any two components.

To confirm the accuracy of the probabilistic method derived in Chapter 6, the probability density functions (pdfs) of eccentricity error $e_i^{Ecc}$ for last component in the assembly are plotted on both linear and logarithmic axes. Figures 8-1 to 8-3 present the comparison of pdf obtained analytically (using Equation (6.40) on linear scale and logarithmic scale) and using MCS method for assembly of 4, 6 and 8 identical

components. Also Figure 8-4 presents the results of the more realistic assembly example of four non-identical axi-symmetric components.

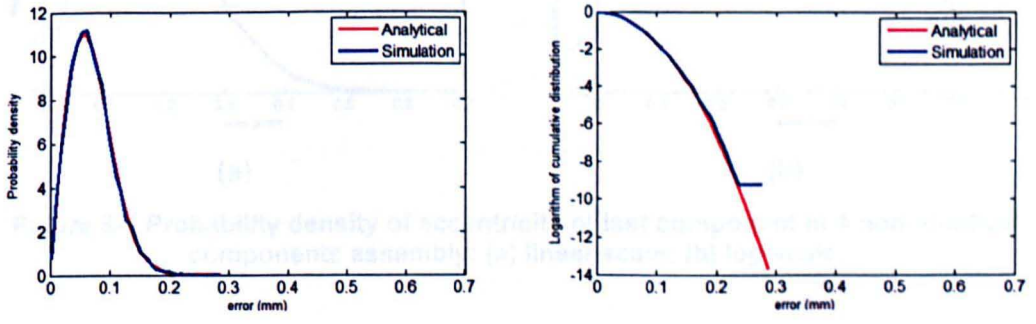


(a) (b)

**Figure 8-1: Probability density of eccentricity of last component in 4 identical components assembly: (a) linear scale; (b) log scale.**

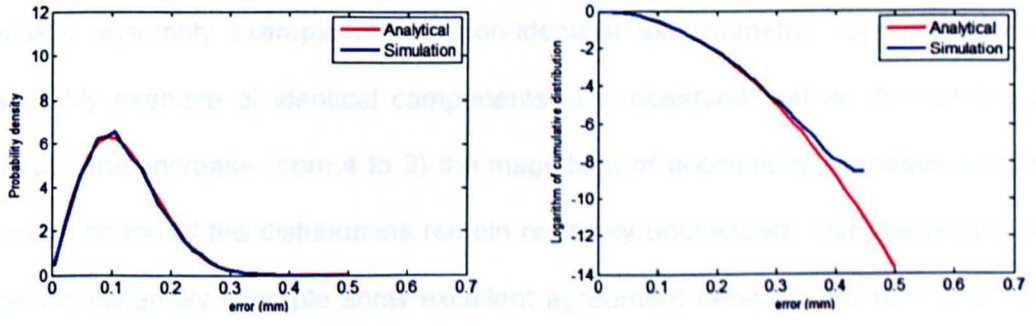


(a) (b)

**Figure 8-2: Probability density of eccentricity of last component in 6 identical components assembly: (a) linear scale; (b) log scale.**

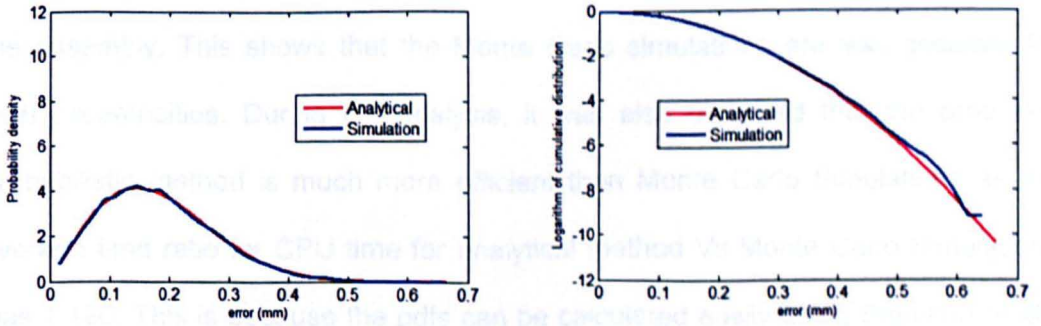


(a) (b)

**Figure 8-3: Probability density of eccentricity of last component in 6 identical component assembly: (a) linear scale; (b) log scale.**

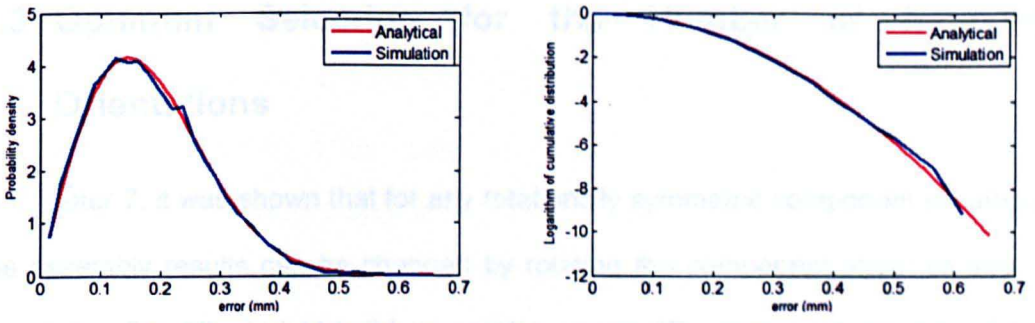


**Figure 8-4 Probability density of eccentricity of last component in 4 non-identical components assembly: (a) linear scale; (b) log scale.**

All above results show that the distributions of eccentricity error obtained using the probabilistic approach of Chapter 6 are in excellent agreement with MCS for 4, 6 and 8 component assemblies of identical cylindrical components and the more realistic assembly example of four non-identical axi-symmetric components. For assembly example of identical components, it is observed that as the number of components increase (from 4 to 8) the magnitude of eccentricity increases and the general shape of the distributions remain relatively unchanged. Also the results for realistic assembly example show excellent agreement between two methods. The above results also indicate that the agreement at the tails of the log-pdf is not as good in all cases. It was observed that for assembly of identical components, the disagreement at the tails of log-pdf is increased with the increase of components in the assembly. This shows that the Monte Carlo simulations are less accurate for high eccentricities. During the analysis, it was also observed that the proposed probabilistic method is much more efficient than Monte Carlo Simulations as the average time ratio for CPU time for analytical method Vs Monte Carlo Simulations was 1:120. This is because the pdfs can be calculated easily using Equation (6.40) for any number of components. The results also confirm that the derived analytical pdf expressions (Equation (6.40) is valid.

## 8.3 Optimum Selection for the Number of Indexing Orientations

In Chapter 7, it was shown that for any rotationally symmetric component assembly, the assembly results can be changed by rotating the component about its axis of symmetry. For 2D straight-build assemblies, each 2D component can be rotated (flipped) at two orientations only. However, for 3D components, the assembly results can be changed by rotating each component (theoretically at any angle from 0° to 360°) about the axis of symmetry. This technique of minimising assembly error by rotating (indexing) components about its axis of symmetry is termed here as relative orientation technique. The number of indexing orientations depends upon the method of joining two components in the assembly. If the components are joined together using bolts, the total number of indexing orientations depend upon the number of bolting holes in each component. Similarly, if the components are joined together by welding, the two component can be theoretically indexed (rotated about the axis of symmetry) with respect to each other at an infinite number of orientation (between 0° and 360°). Therefore it is necessary, to find out the optimum number of orientations that a component may be rotated about its axis of symmetry during error minimisation process. Here, the optimum number of indexing orientations refers to selection of a suitable indexing number that is viable in terms of calculating minimum error and is not computationally extensive.

In order to find out the optimum number for indexing orientation of an axi-symmetric component, an assembly example of four identical cylindrical components is considered. Each cylindrical component has a nominal diameter of 100 mm and nominal height 70 mm. The Components variations and the process of calculating assembly variations is same as described in Section 8.2.

Monte Carlo simulation is performed for 10,000 repeated assemblies using four optimisation methods (as proposed in Chapter 7). The simulations are performed based on various equi-spaced indexing orientations such as; 4, 8, 16, 24, 32, 40, 48, and 56. RMS assembly error is calculated for four optimisation methods (using Equation (7.13)) at each equi-spaced indexing orientations. Statistical results are calculated for mean and standard deviation of Root Mean Square (RMS) assembly error for 10,000 repeated assemblies based on table-axis and final assembly axis (as shown in Figure 8-5 and Figure 8-6). The optimum number of equi-spaced indexing orientation is selected based on the criteria where the mean, standard and deviation are accurate within $\pm 1\%$. The results show that for all four optimisation methods, assembly variations are reduced as the number of indexing orientations are increased. However, if the number of indexing orientations is increased from 24, there is no significant difference observed for mean and standard deviation of RMS assembly variation with reference to table-axis as well as final-assembly-axis. From the convergent analysis presented in Figures 8-1 and 8-2, the optimum number for indexing orientation is selected as 24. If the number of indexing orientations is increased, it will result in unnecessary increase of calculation time with no significant difference in the results.

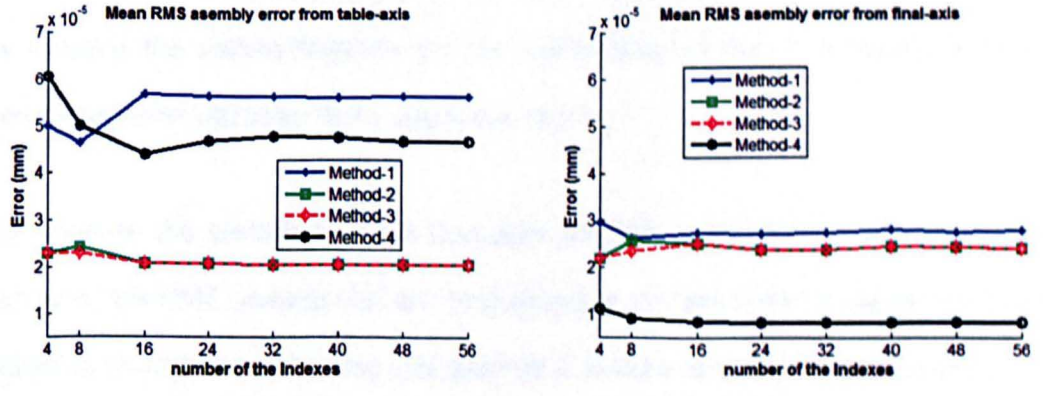


**Figure 8-5: Mean of RMS assembly variation based on 10,000 repeated assemblies for four optimisation methods at different indexing orientations: (a) table-axis variation; (b) final-axis variation.**

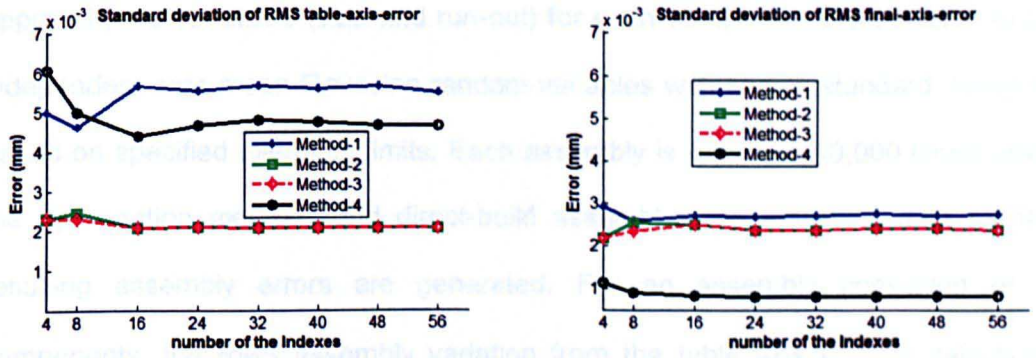


**Figure 8-6: Standard deviation of RMS assembly variation based on 10,000 repeated assemblies for four optimisation methods at different indexing orientations: (a) table-axis variation; (b) final-axis variation.**

## 8.4 Assembly Variation Analysis for 3D Straight-build Assemblies

Two examples are considered to investigate the performance of the optimisation methods (proposed in Chapter 7) to improve straight-build assembly. Each of the assembly examples consists of axi-symmetric rigid components and the following assembly stages. The first stage of assembly is to place the first component on the assembly table with its base concentric to the geometric centre of the table. The point of coincidence of the centre of the base of the first component and the geometric centre of the table axis is considered as the origin of the global coordinate frame. At each subsequent stage, a component is joined to the assembly by locating the mating features for the component so that it is aligned with the reference frame attached to the assembly feature.

To measure the variations in the complete (or part) assembly for each assembly example, the RMS variation for all components in the assembly is calculated (using Equation (7.13)) based on size and geometric feature tolerances for axial and radial run-out of each component. The error minimisation in assembly is based on 24 indexing orientations of each component during the optimisation processes. In this

approach, the variations (size and run-out) for each component are selected to be independent zero-mean Gaussian random variables with known standard deviation based on specified tolerance limits. Each assembly is repeated 10,000 times using the optimisation methods and direct-build assembly, and statistical data for the resulting assembly errors are generated. For an assembly consisting of $N$ components, the RMS assembly variation from the table axis $\varepsilon_{ta}^{RMS}$ is calculated using Equation (7.13). The RMS assembly variation from the final assembly axis is calculated in a similar way, by replacing the table-axis error for each component by the final-assembly axis error in Equation (7.13).

### 8.4.1 Example 1: Assembly of Four Identical Components

This example investigates assembly consisting of four identical components. Each component is ideally a perfect cylinder with nominal diameter of 100 mm and nominal height 70 mm. The geometric feature tolerances for axial and radial run-out of each component are assumed to be 0.01 mm and 0.05 mm, respectively, and size tolerance of $\pm 0.1$ mm. The results are presented to compare the proposed optimisation methods in 3D compared with direct-build assembly and the assembly variations are calculated using exact method (as described in Chapter 4). Figure 8-7 presents results for the mean assembly variation from the table axis and final-assembly axis for 10,000 repeated assemblies using the proposed optimisation methods and direct build assembly.

Figure 8-7 shows that a similar trend of results is obtained for 3D assemblies compared to those obtained for 2D assemblies in Chapter 7. In Figure 8-7, it can be seen that all four optimisation methods yield assembly variations that are smaller than those obtained using direct-build assembly. Method 3 produces assemblies with the smallest variations from table axis and Method 4 consistently produces the

smallest variation from the final-assembly axis. This is because Methods 3 and 4 use fully "global" approaches that consider all assembly stages simultaneously to minimise variations from table axis and final-assembly axis, respectively. The 3D analysis also confirms that the analysis presented for 2D straight-build assemblies in Chapter 7 is a good representation of straight-build assembly optimisation and provide good understanding of the proposed methods.

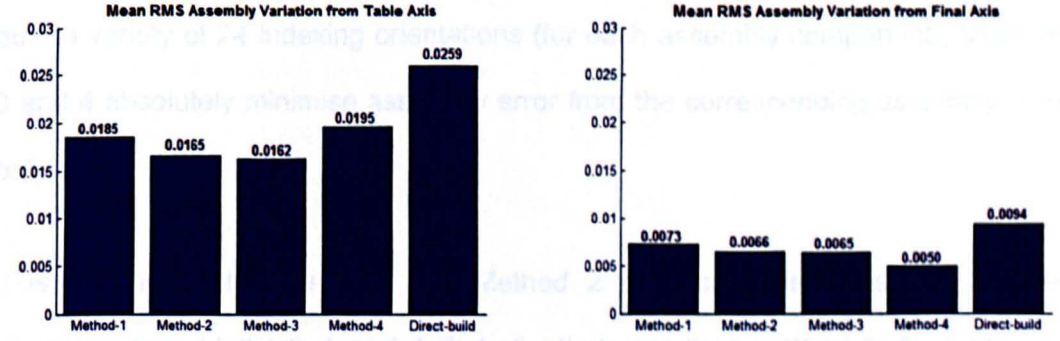


**Figure 8-7: Mean of RMS assembly variation (equation (7.13)) based on 10,000 repeated assemblies for four-identical-component assembly: (a) table-axis variation; (b) final-axis variation.**

### 8.4.2 Example 2: Assembly of Four Non-Identical Components

The dimensions of the components considered in Example 2 are provided in Table 8-1 and represent scaled versions of components forming part of an aero-engine assembly used in industry. For this example, the tolerances used for size (height) are $\pm 0.1$ mm, and the axial and radial run-outs in each component are taken as 0.1 mm and 0.05 mm, respectively.

Figure 8-8 presents results for the mean of RMS assembly variation from the table axis and the final-assembly axis for 10,000 repeated assemblies using the proposed optimisation methods and direct-build assembly.

Similarly to the 2D analysis of the given assembly example in Chapter 7, Figure 8-8 shows that the four optimisation methods produce lower variations than direct-build

assembly with Method 3 producing the smallest variation from the table-axis and Method 4 producing the smallest variation from the final-assembly-axis. On the other hand, it is also found that unlike the 2D analysis, Method 4 produces assemblies with larger variations than Methods 1, 2 and 3 for table axis measures and Method 3 produce assemblies with larger variations than Methods 1, 2 and 4 for final-assembly axis measures. This can be explained by noting that Methods 3 and 4 consider all assembly stages simultaneously for minimising assembly error, and due to variety of 24 indexing orientations (for each assembly component), Methods 3 and 4 absolutely minimise assembly error from the corresponding assembly axes only.

It is also interesting to note that Method 2 produce assemblies with smaller variations than Methods 1 and 4 (but slightly larger than method 3) for table-axis measures and smaller variations than Methods 1 and 3 (but larger than method 4) for final-assembly-axis measures. This trend shows the superiority of Method 2 over all other optimisation method in minimising variations in straight-build assemblies. In addition to this, Methods 2 is simple and efficient compared to Methods 3 and 4 and can easily be implemented in real practice than Methods 3 and 4.

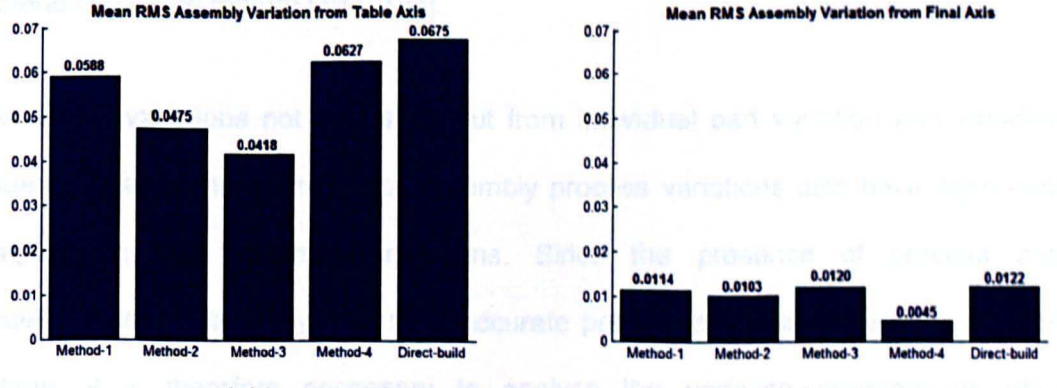


**Figure 8-8: Mean of RMS assembly variation (equation (7.13)) based on 10,000 repeated assemblies for four non-identical-components assembly: (a) table-axis variation; (b) final-axis variation.**

## 8.5 Modelling for Measurement and Process Noise

The assembly process can also be considered as a variation stack up process due to interaction of parts that contain variation, variation in fixtures used for assembly, various random errors in the assembly process, and measurement errors at each assembly stage [95, 96, 155]. The analysis presented in Sections 8.3 and 8.4 was based on tolerance limits for components features. These sections did not consider the measurement uncertainty and process variations in the assembly variation propagation analysis. In real practice, the validity of the predictions of assembly variation propagation depends on the accuracy of the measured variations during the inspection process and variations in the assembly process.

Every measurement has errors which result in a difference between the measured value and the true value. This difference between the measured value and the true value is the total measurement error. Due to inherent variability in any measurement system the true value cannot be known and thus the total measurement error also cannot be known. Therefore, only the limit of total measurement error can be estimated. It must be noted that the total measurement error due to the measurement uncertainty is always significantly smaller than the specified tolerances of the feature [192, 193].

Assembly variations not only stem out from individual part variation and variation due to measurement errors, but assembly process variations also have significant impact on final assembly variations. Since the presence of process and measurement noise may lead to in-accurate prediction of assembly error at each stage, it is therefore necessary to analyse the variation propagations after considering process and measurement noise in the assembly modelling. The

simulations of assembly variation after considering process and measurement noise will help in better prediction of actual assembly error.

This section describes modelling for incorporating assembly process and measurement error in the variation propagation model (Exact Model) described in Chapter 4 of this thesis.

In Chapter 4 Equation (4.23) describes the nominal assembly (assembly without any error) of two components, and the assembly of two components considering part manufacturing variations is given by Equation (4.27). These equations are re-produced in Equations (8.1) and (8.2), respectively,

$$\mathbf{A}_2 = \mathbf{T}_1 \, \mathbf{T}_{1-2} \, \mathbf{T}_2 , \tag{8.1}$$

$$\mathbf{A}_2^{'} = \mathbf{T}_1^{'} \, \mathbf{T}_{1-2} \, \mathbf{T}_2^{'} , \tag{8.2}$$

where $\mathbf{T}_1$ and $\mathbf{T}_2$ are the nominal transforms representing the nominal geometry of components, $\mathbf{T}_{1-2}$ is the feature interface transform describing the mating relationship between the two components, $\mathbf{T}_1^{'} = \mathbf{T}_1 \mathbf{DT}_1$ considering the manufacturing variations in component 1, $\mathbf{T}_2^{'} = \mathbf{T}_2 \mathbf{DT}_2$ considering the manufacturing variations in component 2 and $\mathbf{DT}_1$ and $\mathbf{DT}_2$ are the transforms associated with manufacturing variations in each component.

If the measurement error is considered in the component error, therefore the assembly of two components after considering manufacturing and the measuring uncertainty can be written as:

$$\mathbf{A}_2^{''} = \mathbf{T}_1^{'} \mathbf{V}_1 \, \mathbf{T}_{1-2} \, \mathbf{T}_2^{'} \mathbf{V}_2 , \tag{8.3}$$

where $\mathbf{A}_2^{''}$ is the transform representing the assembly of two components after considering measurement uncertainty and manufacturing variations in the components, $\mathbf{V}_1$ and $\mathbf{V}_2$ are the transforms representing the measuring error in each component. Transforms $\mathbf{V}_1$ and $\mathbf{V}_2$ have a form similar to Equation (4.12).

Similarly the transform representing the assembly of $i$ components can be written as:

$$\mathbf{A}_i^{''} = \mathbf{T}_1^{'}\mathbf{V}_1\,\mathbf{T}_{1-2}\,\mathbf{T}_2^{'}\mathbf{V}_2\,\mathbf{T}_{2-3}\ldots\mathbf{T}_i^{'}\mathbf{V}_i \tag{8.4}$$

Transform $\mathbf{A}_i^{''}$ can be expressed in the same form as Equation (4.1) such that:

$$\mathbf{A}_i^{''} = \begin{bmatrix} \mathbf{R}_{Ai}^{''} & \mathbf{p}_{Ai}^{''} \\ \mathbf{0}^T & 1 \end{bmatrix}, \tag{8.5}$$

where $\mathbf{R}_{Ai}^{''}$ is a 3×3 rotational matrix indicating the orientation of last frame of $i^{th}$ component relative to global frame of the assembly and $\mathbf{p}_{A2}^{''}$ is a 3×1 displacement vector indicating the position of last frame of $i^{th}$component relative to the global frame.

Here, the assembly variations are expressed as a position error in the location of the coordinate frame attached to top feature of the $i^{th}$ assembly component from its nominal position. These errors are described as the translation error between the actual assembly and the nominal assembly. The calculated translation error can be used to quantify the influence of component manufacturing variation on the assembly, where the translational error vector ($dp_i^{X''}, dp_i^{Y''}, dp_i^{Z''}$) for the assembly of $i$ components is given by:

$$\begin{bmatrix} dp_i^{X'''} \\ dp_i^{Y'''} \\ dp_i^{Z'''} \end{bmatrix} = \mathbf{p}'''_{Ai} - \mathbf{p}_{Ai}. \tag{8.6}$$

Now, if a part is not placed in its nominal mating position due to variations in assembly process, there is an error of mis-position and mis-orientation for the part. This variation is described by a transform $\mathbf{W}_i$ describing mis-position and mis-orientation for the part due to variability in the assembly process. Therefore, the transform representing the assembly of two components (Equation(8.3)) after considering assembly process error can be written as:

$$\mathbf{A}_2''' = \mathbf{W}_1\mathbf{T}_1'\mathbf{V}_1\,\mathbf{T}_{1-2}\mathbf{W}_2\mathbf{T}_2'\mathbf{V}_2 = \begin{bmatrix} \mathbf{R}'''_{A2} & \mathbf{p}'''_{A2} \\ \mathbf{0}^T & 1 \end{bmatrix} \tag{8.7}$$

If there are '$i$' components in the assembly, the transform representing the relationship between the last feature of the '$i^{th}$' assembly component relative to base feature of the first component in the assembly after considering assembly process error and measurement noise can be written as:

$$\mathbf{A}_i''' = \mathbf{W}_1\mathbf{T}_1'\mathbf{V}_1\,\mathbf{T}_{1-2}\mathbf{W}_2\mathbf{T}_2'\mathbf{V}_2\,\mathbf{T}_{2-3}\ldots\mathbf{W}_i\mathbf{T}_i'\mathbf{V}_i = \begin{bmatrix} \mathbf{R}'''_{Ai} & \mathbf{p}'''_{Ai} \\ \mathbf{0}^T & 1 \end{bmatrix} \tag{8.8}$$

In Equation (8.8), it is important to note that the process noise transform $\mathbf{W}_i$ is multiplied before transform $\mathbf{T}_i'$, and measurement noise transform $\mathbf{V}_i$ is multiplied after transform $\mathbf{T}_i'$. This is due to the fact that variations due to assembly process occur before the transform $\mathbf{T}_i'$ is accomplished (using the property of Equation (4.18)), and variations due to measurement system occur after the transform $\mathbf{T}_i'$ is accomplished.

Here, the assembly variations are expressed as a position error in the location of the coordinate frame attached to top feature of the $i^{th}$ assembly components from its nominal position. These errors are described as the translation error between the actual assembly and the nominal assembly. The calculated translation error can be used to quantify the influence of component manufacturing variation on the assembly, where the translational error vector ( $dp_i^{X'''}, dp_i^{Y'''}, dp_i^{Z'''}$ ) for the assembly of $i$ components is given by:

$$\begin{bmatrix} dp_i^{X'''} \\ dp_i^{Y'''} \\ dp_i^{Z'''} \end{bmatrix} = \mathbf{p}_{Ai}^{'''} - \mathbf{p}_{Ai} . \tag{8.9}$$

where, $\mathbf{p}_{Ai}^{'''}$ is a $3 \times 1$ displacement vector indicating the position of the top frame of the final component in the assembly relative to the global frame of the assembly after considering measurement and assembly process errors, and $\mathbf{p}_{Ai}$ is the $3 \times 1$ displacement vector indicating the corresponding nominal position of the top frame.

### 8.5.1 Results and Discussion

This section intends to investigate the impact of the assembly process error and variations due to measurement uncertainty on the overall assembly error using Monte Carlo simulations based on the exact model described in Chapter 4. In order to analyse the impact of assembly process noise and measurement noise, an assembly example of four axisymmetric components is considered. The dimensions of each assembly component are the same as given in Table 8-1. As discussed in Section 8.4.2, these dimensions represent the scaled versions of components forming part of an aero-engine assembly used in industry. The tolerances in each component are specified for size, and the axial and radial run-outs. Size tolerance is

taken as ±0.1 mm and the axial and radial run-out tolerances are taken as 0.05 mm.

For simulations, individual component tolerances are generated as independent normally distributed random variables. The generated tolerances are then converted to variations along degrees of freedom $(dX, dY, dZ, d\theta_x, d\theta_y, d\theta_z)$ for each assembly component using Equations (5.5) to (5.9). To measure the variation in the complete (or part) assembly, the Root-Mean-Square (RMS) variation for all components in the assembly is calculated, as described in Chapter 7 (using Equation 7.13) from both table axis and final-assembly axis. Assembly variations from table axis and final axis are calculated for the four straight-build optimisation methods and for the direct-build assembly for the comparison under conditions of different levels of measurement accuracy and process noise. In industries assembling rotating machines, the measurements usually are taken in the radial and axial directions to quantify the radial and axial run-out for rotationally symmetric components. Therefore measurement noise is assumed in both the radial and axial directions. Similarly the process noise is also assumed to incorporate variations in radial and axial directions. The measurement and process noise are taken for radial and axial errors and these values are assumed to be normally distributed random variables with in specified levels of the noise.

Initially, the assembly variability analysis is performed for measurement noise (without considering process noise) at four levels of measurement uncertainty (0.001 mm, 0.005 mm, 0.01 mm, and 0.05 mm) and the results are compared with assemblies without considering measurement noise. The results for the mean of RMS table axis error (Equation (7.13)) and similarly for final axis error are given in Figure 8-9. Also percentage increase in the mean of RMS assembly error (for table

axis and final axis) compared to assembly without considering measurement noise is given in Table 8-2.

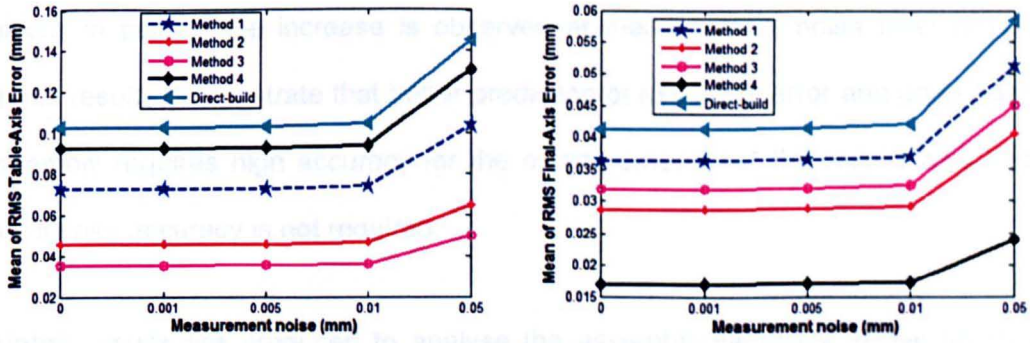


(a) (b)

**Figure 8-9: Comparison of five methods under various conditions of measurement noise based on 10,000 simulations, (a) Mean of RMS table axis error (b) Mean of RMS final axis error.**

| Measurement Noise (mm) | Table Axis Error (%) | | | | Final Axis Error (%) | | | |
|---|---|---|---|---|---|---|---|---|
| | **0.001** | **0.005** | **0.01** | **0.05** | **0.001** | **0.005** | **0.01** | **0.05** |
| Method-1 | 0.040 | 0.435 | 2.046 | 42.075 | 0.007 | 0.324 | 1.841 | 41.162 |
| Method-2 | 0.022 | 0.462 | 1.964 | 42.123 | 0.051 | 0.389 | 1.971 | 41.718 |
| Method-3 | 0.004 | 0.532 | 2.173 | 41.961 | 0.080 | 0.362 | 1.980 | 41.145 |
| Method-4 | 0.045 | 0.525 | 1.747 | 41.529 | 0.009 | 0.589 | 1.884 | 41.758 |
| Direct-build | 0.001 | 0.435 | 2.062 | 41.647 | 0.016 | 0.487 | 2.044 | 41.765 |

**Table 8-2: Percentage increase of assembly error with increase in measurement noise level.**

Figure 8-9 shows that the RMS assembly error increase with increase of measurement noise for all methods and the trend of the proposed optimisation methods compared to Figure 8-8 remain unchanged. The four optimisation methods produce smaller assembly variations compared to direct-build method, with Method 3 producing the smallest variations for table axis errors and Method 4 producing the smallest variations for final axis errors. Method 2 producing smaller variations than Methods 1, 4 and direct-build for table axis errors and smaller variations than Methods 1, 3 and direct-build for final axis errors. In Table 8-2, it can be observed that for measurement noise level of 0.001 and 0.005, the percentage increase of RMS assembly error compared to assembly without considering measurement

noise is very small for both table axis and final axis measures (less than 0.1% for table axis and less than 0.6% for final axis error). The percentage difference of RMS assembly error is increased with the increase of measurement noise level and the maximum percentage increase is observed at measurement noise level of 0.05. These results demonstrate that better prediction of assembly error and good quality assembly requires high accuracy for the measurement, but the results also show that infinite accuracy is not required.

Further results are produced to analyse the assembly variability at five levels of process noise (0.000 mm, 0.001 mm, 0.005 mm, 0.01 mm, and 0.05 mm) without considering measurement noise. The results for mean of RMS table axis error (for table axis and final axis) based on 10,000 repeated assemblies are given in Figure 8-10 and percentage increase in the mean of RMS assembly error compared to assembly without considering process noise is given in Table 8-3.

Figure 8-10 shows that the four optimisation methods produce assemblies with smaller variations compared to direct-build assembly for both table axis and final axis measures. Comparing the results of Figure 8-10 with Figure 8-9, it is observed that assemblies are produced with larger variations due to process noise compared to assemblies that are produced based on measurement noise of the same levels. For smaller levels of process noise (such as 0.001 mm, 0.005 mm and 0.01 mm), there is not much difference between the assembly results produced for process noise (see Figure 8-10) and those produced for measurement noise (see Figure 8-9). The results of Figure 8-10 are further confirmed by results provided in Table 8-3 for percentage increase in the mean of RMS assembly error for both table axis and final axis. Table 8-3 show that at each level of process noise, the assembly variations are larger compared to those obtained by measurement noise (see Table 8-2). For smaller levels of process noise (such as 0.001 mm, 0.005 mm and 0.01

mm), there is small increase in assembly error in Table 8-3 compared to Table 8-2. However, at process noise of 0.05 mm, there is significant increase in assembly variation measurement noise of same level. These results show that assembly variations are more dominated by process noise compared to measurement noise.

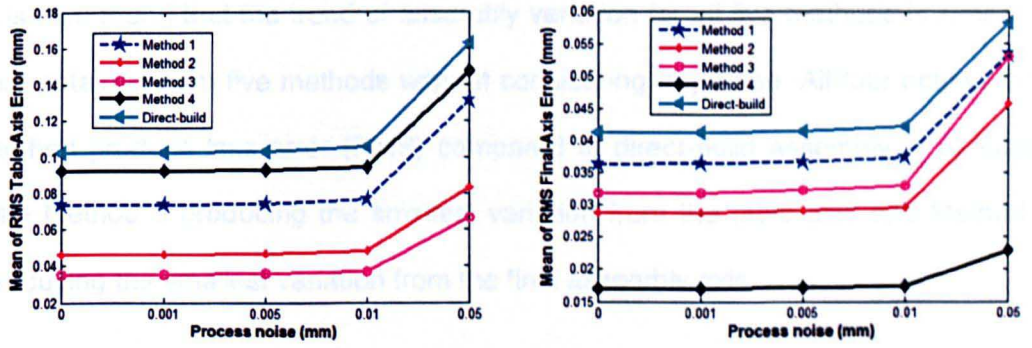


(a) (b)

**Figure 8-10: Comparison of five methods under various conditions of process noise based on 10,000 simulations, (a) Mean of RMS table axis error (b) Mean of RMS final axis error.**

| Measurement Noise (mm) | Table Axis Error (%) | | | | Final Axis Error (%) | | | |
|---|---|---|---|---|---|---|---|---|
| | **0.001** | **0.005** | **0.01** | **0.05** | **0.001** | **0.005** | **0.01** | **0.05** |
| Method-1 | 0.107 | 1.082 | 4.324 | 78.754 | 0.127 | 0.722 | 2.636 | 46.761 |
| Method-2 | 0.045 | 1.061 | 4.787 | 79.939 | 0.033 | 0.908 | 2.898 | 58.896 |
| Method-3 | 0.077 | 1.205 | 4.723 | 87.356 | 0.016 | 1.049 | 3.652 | 66.269 |
| Method-4 | 0.006 | 0.447 | 2.565 | 60.039 | 0.009 | 0.326 | 1.379 | 33.929 |
| Direct-build | 0.036 | 0.721 | 3.275 | 59.123 | 0.022 | 0.602 | 2.224 | 41.144 |

**Table 8-3: Percentage increase of assembly error with increase in process noise levels.**

Finally, results are produced to analyse the assembly variability at five levels of process noise (0.000 mm, 0.001 mm, 0.005 mm, 0.01 mm, and 0.05 mm) when measurement noise is considered as 0.001 mm (Figure 8-11), 0.005 mm (Figure 8-12), 0.01 mm (Figure 8-13), and 0.05 mm (Figure 8-14), respectively. Figures 8-11 to 8-14 show that there is no significant difference in the assembly variations due to the increase in measurement noise from 0.001 to 0.005. At the measurement noise of 0.01 mm, there is small increase in assembly variations (see Figure 8-13) compared to Figure 8-11 and Figure 8-12. At measurement noise value of 0.05 mm

there is relatively larger increase in the assembly variations (see Figure 8-14). In all cases for the five methods, it has been observed that the measurement noise contributes much less compared to process noise in the accumulation of assembly variation.

It is also found that the trend of assembly variation for all five methods is similar to that obtained from five methods without considering any noise. All four optimisation method produce less error (RMS) compared to direct-build assembly in all cases with Method 3 producing the smallest variation from the table axis and Method 4 producing the smallest variation from the final assembly axis.

All these results indicate that if special care is taken during the measurement of part variation for the assembly, it would provide a great improvement for the assembly. It can also be seen that as the measurement uncertainty increases, the assembly variation continues to increase with more significant rate.

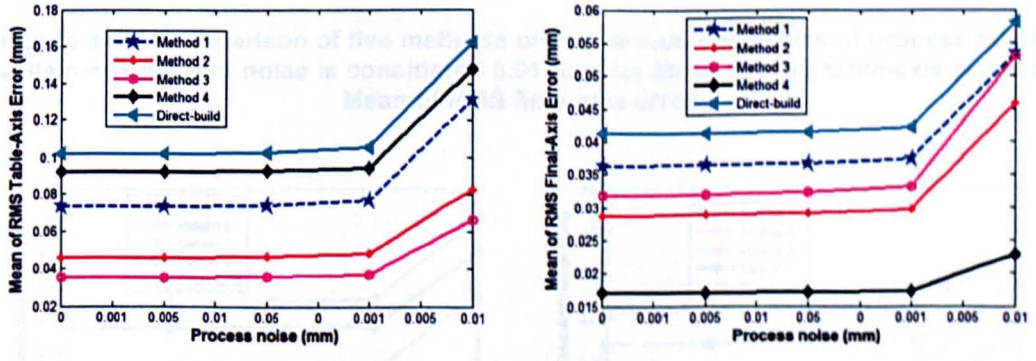


(a) (b)

**Figure 8-11: Comparison of five methods under various conditions of process noise while measurement noise is considered 0.001 mm, (a) Mean of RMS table-axis error (b) Mean of RMS final-axis error.**

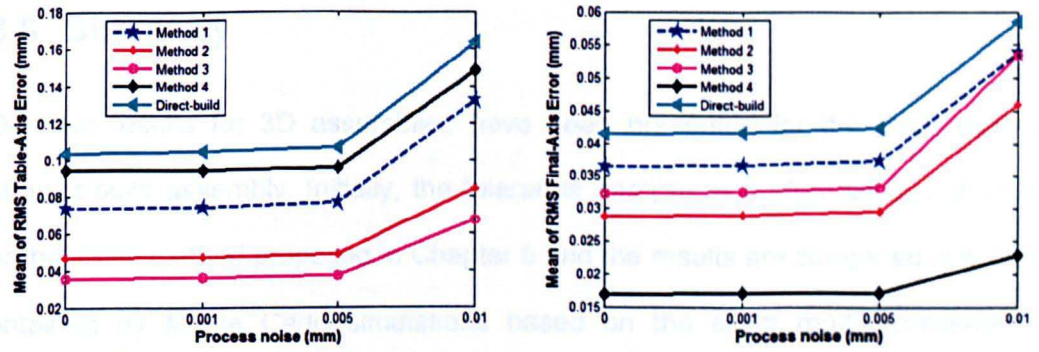


**Figure 8-12: Comparison of five methods under various conditions of process noise while measurement noise is considered 0.005 mm, (a) Mean of RMS table-axis error (b) Mean of RMS final-axis error.**

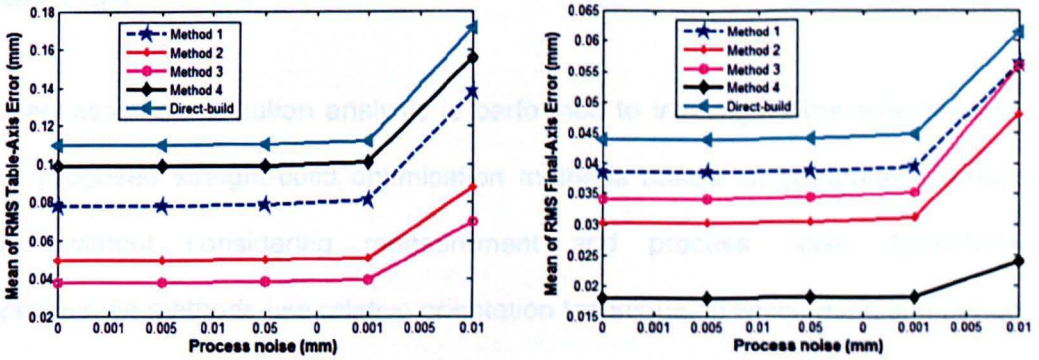


**Figure 8-13: Comparison of five methods under various conditions of process noise while measurement noise is considered 0.01 mm, (a) Mean of RMS table-axis error (b) Mean of RMS final-axis error.**

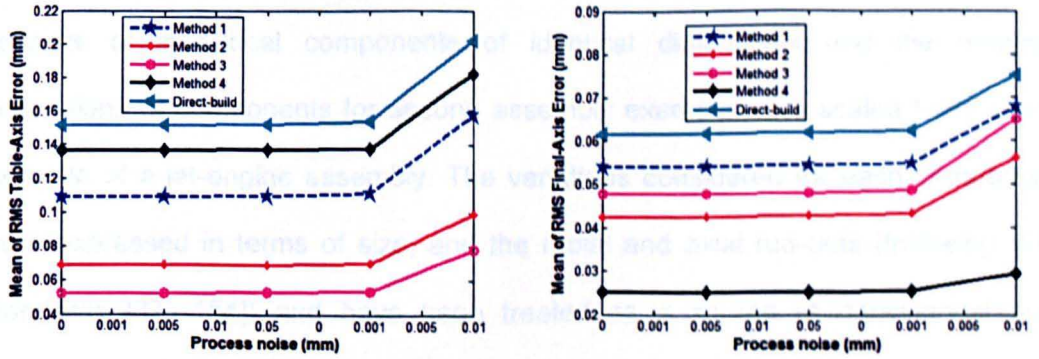


**Figure 8-14: Comparison of five methods under various conditions of process noise while measurement noise is considered 0.05 mm, (a) Mean of RMS table-axis error (b) Mean of RMS final-axis error.**

## 8.6 Summary

Detailed results for 3D assemblies have been presented for the case study of straight-build assembly. Initially, the tolerance analysis is performed based on the probabilistic method proposed in Chapter 6 and the results are compared with those obtained by Monte Carlo simulations based on the exact model presented in Chapter 4. The results show that the proposed probabilistic method is in excellent agreement with Monte Carlo simulations based on the exact method, and the probabilistic model is much more numerically efficient compared to Monte Carlo simulations.

Later, assembly variation analysis is performed to investigate the effectiveness of the proposed straight-build optimisation methods based on component variations and without considering measurement and process noise. Straight-build optimisation methods use relative orientation technique, in which each component is rotated (indexed) about its axis of symmetry to minimise assembly error and the optimum number of uniformly arranged indexing orientation was found to be 24. Based on 24 indexing orientations, analysis of the straight-build optimisation methods was performed using two assembly examples. The first assembly example consists of cylindrical components of identical dimensions and the nominal dimensions of components for second assembly example were scaled from a real example of a jet-engine assembly. The variations considered for each component were expressed in terms of size, and the radial and axial run-outs (following ISO standards [37, 154]) and have been treated as a source of translational and rotational error in the mating features for each component in the assembly. The results presented indicate that all proposed optimisation methods produce significantly improved eccentricities compared to direct-build method (without optimisation). It was found that Method 3 always yields the smallest possible

eccentricities from table axis, and Method 4 produces the smallest eccentricities from final axis. However, Method 2 produces assemblies with smaller variations than Methods 1 and 4 (but slightly larger than Method 3) for table axis measures and smaller variations than Methods 1 and 3 (but larger than method 4) for final-assembly axis measures. Methods 1 is not as effective as Method 2, 3 and 4 for reducing variations, but it produces good improvements compared to direct build, and helps in better understanding of the straight-build optimisation technique.

The assembly has also been analysed for different levels of measurement accuracy and process noise. It was found from the results that the prediction of overall assembly variation can be improved by increasing the measuring accuracy. Although, the measurement errors influence prediction accuracy of assembly variation, the overall effect of measurement error on assembly variation is quite small if the value of measurement noise is 0.01 mm or less for the assembly examples studied. Whatever value of measurement noise was considered an identical trend for the performance of optimisation methods was found when compared to assembly without considering measurement noise. It has been observed that the measurement noise contributes much less compared to process noise in the accumulation of assembly variation.

# Chapter 9 CONCLUSIONS & RECOMMENDATIONS FOR FUTURE WORK

## 9.1 Summary of the Thesis

In order to manufacture products with high quality, it is necessary to improve the assembly quality. Due to variability in manufacturing processes parts are not produced with precise dimensions. Therefore, the assembly process plays a major role in improving product quality by ensuring that the parts are assembled in a way to compensate for variation between the parts. This requires a robust and accurate assembly model to calculate assembly variation propagation and part models to represent part dimensions and geometric variations, in a form compatible with assembly variation propagation models. The goals of this thesis have been (a) to develop methods that use consistent mathematical approach, that enable the design engineer to quantify major contributing factors in the assembly variation and that produce accurate results, (b) to incorporate non-ideal geometry of parts, and (c)

to identify new methodologies to control variation propagations in assemblies of high-speed rotating machines, such as an aero-engine assembly.

Models have been presented to represent non-ideal geometries of manufactured components. In order to model geometric variations in manufactured components, Cartesian frames are attached to mating features on every part and variational constraints are defined to represent part variations into six degrees of freedom of error. A methodology has been presented to approximate the location of actual mating feature from inspection data obtained for axi-symmetric components.

Two approaches to model assemblies and assembly processes have been developed. Both approaches are based on connective assembly models [20]. The connective assembly is mathematically inconsistent because it uses linearised approach to model individual component but for modelling an assembly, connective model does not linearise the chain of matrix transform representing each assembly component. To overcome this discrepancy, the proposed models use consistent approach (either linear or fully non-linear) for modelling individual component or the assembly. The presented models are: i) Exact Model, based on fully non-linear matrix transforms; and ii) Linear Model, based on first order perturbation analysis of transformation matrices. The Exact Method is presented to obtain the exact solution, whereas the Linear Method is developed to enable a design engineer to characterise major contributing factors in assembly variation propagation, which otherwise cannot be identified in the exact method. The linear model has been extended to perform probabilistic analysis for assembly variability. The fully non-linear (exact) model has been extended to accommodate for assembly process and in-process measurement errors, for calculation of error build-up.

In order to implement the developed models, results are calculated for two case studies. The two assembly Case Studies are representative examples of two sub-assemblies of an aero-engine. The first case study represents the assembly of an engine rotor of a jet engine (named as straight-build assembly), whereas the second case study represents the assembly of an engine casing (named as circular-build assembly). In order to improve the quality of build after assembling components in each case study, optimisation methods are proposed to minimise error propagation. Four optimisation methods are proposed for the case study of straight-build assembly, and one optimisation method is proposed to minimise error propagation in the circular-build assembly. It was shown that for straight-build assemblies, the optimisation methods produce significantly improved assembly quality compared to assembly without optimisation. Also, the optimisation method for the circular-build assembly produces significantly improved assembly quality compared to assembly without optimisation.

## 9.2 Research Contribution

This section summarises the major contributions made by this thesis and highlights main findings and limitations.

### 9.2.1 Modelling Variations in axi-symmetric and uniformly-segmented circular Components

A methodology for modelling component variation was presented to represent non-ideal geometry of manufactured components in a form compatible with assembly variation propagation models. The assembly variation propagation models presented in this thesis are based on homogeneous transformations that require representation of manufactured components in terms of variations along a degree of

freedom (VDOF). In past no work has been carried out that model axi-symmetric and uniformly segmented circular components in terms of VDOF using variational constraints. The idea of modelling variations in manufactured components (in this thesis) was to represent the combined effect of size and geometric variation in terms of VDOF between the mating features of the axi-symmetric components and the uniformly segmented circular components. Equations for variational constraints have been developed to model the combined effect of size and run-out tolerances in the location of assembly features in axi-symmetric components. Also, equations for variational constraints have been developed to model the combined effect of size and flatness tolerances in the location of assembly features in uniformly segmented circular components. Variational constraints in both cases are defined based on design tolerances specified by aero-engine manufacturers and respecting the definitions given in ISO standards. A methodology to represent component variation has also been provided, based on inspection data. The aim of modelling inspection data is to facilitate assembly analysis for real assemblies on shop floor.

### 9.2.2 Modelling Assembly Variation Propagation

Variation propagation modelling is a method of calculating the accumulation of tolerances in a mechanical assembly during individual assembly stages. Variation propagation models are used for tolerance analysis and for the purpose of evaluating assembly design. In past various linear and non-linear models have been developed, but none of these are very accurate and capable to quantify major contributing factors in the assembly variation. Two models for calculating assembly variation propagation are proposed in this thesis. A fully non-linear model is proposed to obtain exact results for the assembly variations. Due to non-linear nature of the model it is not possible to characterise major contributing factors in assembly variation propagation. Therefore, a linear assembly model based on first

order perturbation analysis of homogeneous matrix transforms is also developed to precisely approximate assembly variation propagation and to enable the design engineer to quantify major contributing factors in the assembly variation. The non-linear model is termed as exact model in this thesis because it is capable of calculating exact location error accumulated during assembly. The exact model can be used as the performance benchmark in order to verify the accuracy of the simplified (linear) models. Another advantage of the exact model is that it can also accommodate for assembly process and in-process measurement errors, for calculation of error build-up in an assembly. On the hand, the main advantage of the linear model is that, for the linear model, it is possible to derive analytical expressions for the probability density function (pdf) to perform statistical tolerance analysis for predicting assembly variations, which otherwise is not possible in case of the exact model. Therefore statistical tolerance analysis based on exact model can only be performed using Monte Carlo Simulation (MCS) method. This highlights the competency of the linear model over the exact model, because the statistical tolerance analysis performed by analytical expressions of the pdf is much more efficient than the analysis based on the Monte Carlo simulation method that requires a very large number of repeated simulations.

In the light of existing state of art for the assembly modelling, both the linear and the non-linear model proposed in this thesis are novel in their nature. The proposed exact model is the only model of its kind that is the most accurate, capable to incorporate assembly process errors, in-process measurement errors, and any other parameter such as assembly optimisation in the calculation of variation propagation during the assembly. On the other hand the linear model is more simplified providing very precise approximation of the assembly error build-up, enabling the design engineer to quantify major contributing factors in the assembly

variation, easier to derive analytical expressions for the uni-variate probability density function (pdf) to perform statistical tolerance analysis more efficiently.

### 9.2.3 Probabilistic Tolerance Analysis for Assembly Variability

In order to perform tolerance analysis, a probabilistic model has been developed based on a linearised assembly model. Tolerance analysis based on a non-linear model is also performed in this thesis. The non-linear analysis is conducted using the Monte Carlo simulation (MCS) method. The main drawback of Monte Carlo simulations method is that it is necessary to generate a large number of samples to achieve accurate predictions, which may require intensive computation and the solution can become extremely time consuming. There is a substantial difference in capabilities between the MCS and the linearised method. The latter is well suited for design iteration due to its speed, because in linear method, uni-variate probability density functions (pdfs) are derived to calculate assembly variability more accurately. In past various probabilistic models have been developed [34, 35, 74, 88, 89] that do not provide precise/more accurate approximation, computationally in-efficient due to the complex form of pdf function, and are incapable of providing the approximation of assembly error in a particular degree of freedom of variation. On the other hand, MCS is advantageous over linearised probabilistic method because this method can be used for tolerance analysis based on fully non-linear method and tolerance analysis for assemblies considering assembly error minimisation and other factors such as assembly process and measurement errors. The probabilistic model proposed in this thesis is only developed to accommodate for manufacturing variations of each assembly component, however, it can be extended to incorporate assembly process errors, in-process measurement errors, and assembly error minimisation in the calculation of variation propagation during the assembly. The tolerance analysis using MCS based on fully non-linear method, when performed

considering the error minimisation, it is extremely time consuming and in efficient due to involvement of large number of iterative calculations. Thus it is highly recommended to extend the proposed probabilistic model to incorporate assembly error minimisation and other factors such as assembly process and in-process measurement errors.

### 9.2.4 Assembly Optimisation

In order to improve the assembly quality, optimisation methods are developed to minimise error propagation. Four methods are proposed for the case study of straight-build assembly, and one method is proposed to minimise error propagation in the case study of circular-build assembly.

The proposed optimisation methods for straight-build assemblies use a relative orientation technique to minimise error propagation during assembly. It was shown that for any rotationally-symmetric-component assembly, the assembly results can be changed by rotating the component about the axis of symmetry. Each method finds an optimum indexing orientation based on a given objective function for that method to minimise error propagation. In past no work has been reported that minimise eccentricity error build-up during the assembly of rotating parts of high speed rotating machines to maintain the assembly of rotor as straight as possible. The most important aspect of the proposed straight-build assembly optimisation methods is that these methods are cost effective and require no special tooling during the error minimisation process.

The results of the four optimisation methods are calculated and compared with those obtained by direct-build assembly (assembly without optimisation) to check the effectiveness of each method. It was found that the four optimisation methods produce assemblies with smaller variation compared to assembly without

optimisation. Method 3 always yields the smallest possible eccentricities from the table axis, and Method 4 produces the smallest eccentricities from final axis. Method 2 always produces small eccentricities (with respect to the table axis) compared to Methods 1 and 4, and slightly larger eccentricities compared to Method 3. For final-axis measures, Method 2 produces small eccentricities compared to Methods 1 and 3 and slightly larger eccentricities compared to Method 4. Method 2 is also computationally more efficient than Methods 3 and 4 and more suitable for practical implementation.

Method 1 is not as effective as Methods 2, 3 and 4 for reducing assembly variations, but it produces good improvements compared to direct-build (assembly without optimisation). Method 1 helps achieving better understanding for the concepts of the relative orientation technique.

A method to minimise assembly variation in circular build assemblies is also presented in this thesis. Method of minimising radial error in a circular-build assembly (casing assembly) has been studied for the first time in this thesis. The proposed optimisation method is aimed to find best mating sequence of the assembly components to produce assembly with minimum radial error and to maintain the build precisely circular after assembly. It was observed that the proposed optimisation method produces significantly improved assembly quality compared to assembly without optimisation.

## 9.3 Recommendations for Future Work

Based on the research conducted in this thesis, recommendations for future work are suggested as follows:

### 9.3.1 Modelling Geometric Variations in Manufactured Components

In order to get more realistic results for assembly variation, extensive work is required to evaluate the geometric variations at the mating surface(s) of the production parts and to know the contact points between two mating components.

### 9.3.2 Straight-Build Assemblies

In order to meet strict vibration requirements and performance of high-speed rotating machines, it is suggested to incorporate the mass balancing information of axisymmetric components in the variation propagation analysis and to find optimum assembly configuration based on the combined effect of part manufacturing variations and variations due to mass imbalance. Imbalance occurs if the principal axis of inertia of the rotor is not coincident with its geometric axis [194].

### 9.3.3 Probabilistic Modelling

Extend proposed probabilistic model (1) to analyse straight-build assemblies after taking into account for relative orientation technique (2) to analyse circular-build assembly after taking into account for best mating sequence to minimise assembly variations.

# REFERENCES

[1] Thimm, G., Britton, G. A., and Cheong, F. S. (2001). "Controlling Tolerence Stacks for Efficient Manufacturing", The International Journal of Advanced Manufacturing Technology, Vol. 18(1), p. 44-48.

[2] Zhang, W., Wang, C., and Yu, J., (2009), "A Design for Assembly System for Aero Engine", IEEE Computer Society, International Conference on Computer and Automation Engineering, Bangkok, Thailand, p. 328-331.

[3] Zha, X. F., Du, H. J., and Qiu, J. H. (2001). "Knowledge-Based Approach and System for Assembly Oriented Design, Part I: the Approach", Engineering Applications of Artifcial Intelligence, Vol. 14, p. 61-75.

[4] Thornton, A. C. (1999). "A Mathematical Framework for the Key Characteristic Process", Research in Engineering Design, Vol. 11, p. 145–157.

[5] Ertan, B., (1996), "Analysis of Key Characteristic Methods and Enablers Used in Variation Risk Management", MSc Thesis, Massachusetts Institute of Technology, Cambridge, Massachusetts, USA.

[6] Ai, Y., and Zhang, F., (2008), "Application of Principal Component Analysis in Relational Research Between Aeroengine Assembly Parameters and Its Vibration", Fourth International Conference on Natural Computation Washington, DC, USA Vol. 4, p. 95-99

[7] Webb, P., Jayaweera, N., Ye, C., and Johnson, C., (2008), "Robotic Assembly of Aero-Engine Components", Aerospace Manufacturing and Automated Fastening Conference & Exhibition, North Charleston, SC, USA.

[8] Shah, J. J. (1991). "Conceptual Development of Form Features and Feature Modelers", Research in Engineering Design, Vol. 2(2), p. 93-108.

[9] Gui, J. K., and Mäntylä, M. (1994). "Functional Understanding of Assembly Modelling", Computer-Aided Design, Vol. 26(6), p. 435-451.

[10] Mäntylä, M. (1990). "A Modeling System for Top-Down Design of Assembled Products", IBM Journal of Research and Development, Vol. 34(5), p. 636-659.

[11] Chan, C. K., and Tan, S. T. (2003). "Generating Assembly Features onto Split Solid Models", Computer-Aided Design, Vol. 35(14), p. 1315-1336.

[12] Holland, W. V., and Bronsvoort, W. F. (2000). "Assembly Features in Modeling and Planning", Robotics and Computer-Integrated Manufacturing, Vol. 16(4), p. 277-294.

[13] Mäntylä, M., Nau, D., and Shah, J. (1996). "Challenges in Feature-Based Manufacturing Research", Communications of the ACM, Vol. 39(2), p. 77-85.

[14] DeFazio, T. L., Edsall, A. C., Gustavson, R. E., Hernandez, J. A., Hutchins, P. M., Leung, H. W., Luby, S. C., Metzinger, R. W., Nevins, J. L., Tung, K. K., and Whitney, D. E., (1990), "A Prototype for Feature-based Design for Assembly", ASME Design Automation Conference, Chicago., p. 369-392.

[15] Whitney, D. E., Mantripragada, R., Adams, J. D., and Rhee, S. J. (1999). "Designing Assemblies", Research in Engineering Design, Vol. 11, p. 229–253.

[16] Boothroyd, G., and Alting, L. (1992). "Design for Assembly and Disassembly", CIRP Annals - Manufacturing Technology, Vol. 41(2), p. 625-636.

[17] Boothroyd, G. (1994). "Product Design for Manufacture and Assembly", Computer-Aided Design, Vol. 26(7), p. 505-520.

[18] Redford, A. H., and Chal, J., (1994), *Design for Assembly : Principles and Practice*, McGraw-Hill, London.

[19] Adams, J. D., and Whitney, D. E. (2001). "Application of Screw Theory to Constraint Analysis of Mechanical Assemblies Joined by Features", ASME Journal of Mechanical Design, Vol. 123, p. 26-32.

[20] Whitney, D. E., (2004), *Mechanical Assemblies: Their Design, Manufacture, and Role in Product Development*, Oxford Series Advanced Manufacturing, Oxford University Press, Oxford.

[21] Mantripragada, R., Cunningham, T. W., and Whitney, D. E., (1997), "Assembly Oriented Design : A New Approach to Designing Assemblies", Proceedings of the Fifth IFIP TC5/WG5.2 International Workshop on Geometric Modeling in Computer-Aided Design, USA, p. 308-324.

[22] Mantripragada, R., and Whitney, D. E. (1998). "The Datum Flow Chain: a Systematic Approach to Assembly Design and Modeling", Research in Engineering Design, Vol. 10, p. 150-165.

[23] Singh, J., (2003), "Key Characterictic Coupling and Resolving Key Characterictic Conflict", MSc Thesis, Massachusetts Institute of Technology, Cambridge, Massachusetts, USA.

[24] Ding, Y., Ceglarek, D., and Shi, J. (2002). "Design Evaluation of Multi-Station Assembly Processes by Using State Space Approach", ASME Journal of Mechanical Design, Vol. 124, p. 408-418.

[25] Mathieu, L., and Marguet, B. (2001). "Integrated Design Method to Improve Producibility based on Product Key Characteristics and Assembly Sequences", CIRP Annals - Manufacturing Technology, Vol. 50(1), p. 85-88.

[26] Ceglarek, D., Huang, W., Zhou, S., Ding, Y., Kumar, R., and Zhou, Y. (2004). "Time-Based Competition in Multistage Manufacturing: Stream-of-Variation Analysis (SOVA) Methodology—Review", International Journal of Flexible Manufacturing Systems, Vol. 16, p. 11-44.

[27] Mantripragada, R., and Whitney, D. E., (1998), "Modeling and Controlling Variation Propagation in Mechanical Assemblies Using State Transition Models", IEEE International Conference on Robotics & Automation, Leuven, Belgium, p. 219-226.

[28] Whitney, D. E. (2006). "The Role of Key Characteristics in the Design of Mechanical Assemblies", Assembly Automation, Vol. 26(4), p. 315–322.

[29] Lee, D. J., and Thornton, A., (1996), "The Identification and Use of Key Characteristics in the Product Development Process", Proceedings of The 1996

ASME Design Engineering Technical Conferences and Computers in Engineering Conference, Irvine, California.

[30] Maropoulos, P. G., Zhang, D., Rolt, S., Chapman, P., and Rogers, B. C. (2006). "Integration of Measurement Planning with Aggregate Product Modelling for Spacecraft Design and Assembly", Proceedings of the Institution of Mechanical Engineers: Part B, Journal of Engineering Manufacture, Vol. 220, p. 1687-1695.

[31] Maropoulos, P. G., Zhang, D., Chapman, P., Bramall, D. G., and Rogers, B. C. (2007). "Key Digital Enterprise Technology Methods for Large Volume Metrology and Assembly Integration", International Journal of Production Research, Vol. 45, p. 1539-1559.

[32] Popplestone, R. J., (1987), "The Edinburgh Designer System as a Framework for Robotics", Proc. IEEE Int. Conf. Robotics & Automation, p. 1972-1977.

[33] Nevins, J. L., and Whitney, D. E., (1989), *Concurrent Design of Products and Processes: A Strategy for the Next Generation in Manufacturing*, McGraw-Hill, New York.

[34] Chase, K. W., Gao, J., and Magleby, S. P. (1995). "General 2-D Tolerance Analysis of Mechanical Assemblies with Small Kinematic Adjustments", Journal of Design and Manufacture, Vol. 5, p. 263-274.

[35] Gao, J., Chase, K. W., and Magleby, S. P. (1998). "Generalized 3D Tolerance Analysis of Mechanical Assemblies with Small Kinematic Adjustments", IIE Transactions, Vol. 30, p. 367-377.

[36] ASME, (1994), ANSI Standard Y14.5M, American National Standards Institute: Dimensioning and Tolerancing for Engineering Drawings, New York.

[37] BSI, (2005), European Standard BS EN ISO 1101:2005, Geometric Product Specifications (GPS)-Geometrical Tolerance: Tolerances of Form, Orientation, Location and Run-out, London, UK.

[38] Juster, N. P. (1992). "Modelling and Representation of Dimensions and Tolerances: A Survey", Computer-Aided Design, Vol. 24(1), p. 3-17.

[39] Wu, Y., Shah, J. J., and Davidson, J. K. (2003). "Computer Modelling of Geometric Variations in Mechanical Parts and Assemblies", AMSE Journal of Computing and Information Science in Engineering, Vol. 3(1), p. 54-63.

[40] Hu, J., and Peng, Y. (2007). "Tolerance Modelling and Robust Design for Concurrent Engineering", Proceedings of the Institution of Mechanical Engineers, Part C: Journal of Mechanical Engineering Science, Vol. 221(4), p. 455-465.

[41] Hu, J., and Xiong, G. (2005). "Dimensional and Geometric Tolerance Design Based on Constraints", International Journal of Advanced Manufacturing Technology, Vol. 26(9), p. 1099-1108.

[42] Koura, M. M., Elewa, I. M., Gadh, R., Prabhu, B. S., and Mohamed, K. A., (2002), "Feature-Based Geometric Dimension and Tolerance Modelling System", Third Assiut University International Conference on Mechanical Engineering Advanced Technology for Industrial Production, Egypt.

[43] Sutherland, I. E., 1963, "Sketchpad: A Man-Machine Graphical Communication System", Technical Report No. MIT Lincoln Laboratory Technical Report No. 296, Lexington.

[44] Requicha, A. G. (1980). "Representations for Rigid Solids: Theory, Methods, and Systems", ACM Comput. Surv., Vol. 12(4), p. 437-464.

[45] Requicha, A. A. G., and Voelcker, H. B. (1985). "Boolean Operations in Solid Modeling: Boundary Evaluation and Merging Algorithms", Proceedings of the IEEE, Vol. 73(1), p. 30-44.

[46] Pasupathy, T. M. K., Morse, E. P., and Wilhelm, R. G. (2003). "A Survey of Mathematical Methods for the Construction of Geometric Tolerance Zones", Journal of Computing and Information Science in Engineering, Vol. 3(1), p. 64-75.

[47] Requicha, A. A. G., and Chan, S. C. (1986). "Representation of Geometric Features, Tolerances and Attributes in Solid Modelers Based on Constructive Geometry", IEEE Journal of Robotics and Automation, Vol. RA-2(3), p. 156–166.

[48] Park, S., and Lee, K., (1997), "Mathematical Foundation for Representing Propagation of Geometric Tolerances", ACM, Proceedings of the fourth ACM symposium on Solid modeling and applications, Atlanta, Georgia, United States, p. 240-247.

[49] Varadhan, G., and Manocha, D. (2006). "Accurate Minkowski Sum Approximation of Polyhedral Models", Graphical Models, Vol. 68(4), p. 343-355.

[50] Etesami, F. (1988). "Tolerance Verification through Manufactured Part Modeling ", Journal of Manufacturing Systems, Vol. 7(3), p. 223-232.

[51] Ramaswami, H., Kanagaraj, S., and Anand, S. (2007). "An Inspection Advisor for Form Error in Cylindrical Features", International Journal of Advance Manufacturing Technology, Vol. 40, p. 128-143.

[52] Ramaswami, H., Turek, S., Rajmohan, S., and Anand, S. (2011). "A Comprehensive Methodology for Runout Tolerance Evaluation using Discrete Data", International Journal of Advanced Manufacturing Technology, Vol. 56, p. 663–676.

[53] Jayaraman, R., and Srinivasan, R. (1989). "Geometric tolerancing: 1. Virtual boundary requirements", IBM Journal of Research and Development, Vol. 33(2), p. 90-104.

[54] Srinivasan, V., and Jayaraman, R. (1989). "Geometric Tolerancing: 2. Conditional Tolerances", IBM Journal of Research and Development, Vol. 33(2), p. 105-124.

[55] Hillyard, R. C., and Braid, I. C. (1978). "Analysis of Dimensions and Tolerances in Computer-Aided Mechanical Design", Computer-Aided Design, Vol. 10(3), p. 161-166.

[56] Hillyard, R. C., and Braid, I. C. (1978). "Characterizing Non-Ideal Shapes in Terms of Dimensions and Tolerances", SIGGRAPH Comput. Graph., Vol. 12(3), p. 234-238.

[57] Lin, V. C., Gossard, D. C., and Light, R. A. (1981). "Variational Geometry in Computer-Aided Design", Computer Graphics, Vol. 15(3), p. 171-177.

[58] Turner, J. U., (1987), "Tolerances in Computer-Aided Geometric Design", PhD Thesis, Rensselaer Polytechnic Institute, Troy, New York, USA.

[59] Turner, J. U., Srikanth, S., and Gupta, S. (1992). "Constraint Representation and Reduction in Assembly Modelling and Analysis", IEEE Trans. on Robotics and Automation, Vol. 8(6), p. 741-750.

[60] Turner, J. U., and Wozny, M. J., (1990), "The M-Space Theory of Tolerances", Proceedings of ASME 16th Design Automation Conference, Chicago, IL, USA, Vol. 1, p. 217–225.

[61] Inui, M., and Kimura, F., (1991), "Algebraic Reasoning of Position Uncertainties of Parts in an Assembly", ACM, Proceedings of the first ACM symposium on Solid modeling foundations and CAD/CAM applications, Austin, Texas, United States, p. 419-428.

[62] Inui, M., Otto, H., and Kimura, F., (1993), "Algebraic Interpretation of Geometric Tolerances for Evaluating Geometric Uncertainties in Solid Modeling", ACM, Proceedings on the second ACM symposium on Solid modeling and applications, Montreal, Quebec, Canada, p. 377-386.

[63] Mullins, S. H., and Anderson, D. C., (1995), "Algebraic Representation of Geometric and Size Tolerances", 21st ASME Design Automation Conference, Vol. 82, p. 309-316.

[64] Roy, U., and Li, B. (1998). "Representation and Interpretation of Geometric Tolerances for Polyhedral Objects- I. Form Tolerances", Computer-Aided Design, Vol. 30(2), p. 151-161.

[65] Roy, U., and Li, B. (1999). "Representation and Interpretation of Geometric Tolerances for Polyhedral Objects. II. Size, Orientation and Position Tolerances", Computer-Aided Design, Vol. 31, p. 273-285.

[66] Fleming, A. (1988). "Geometric Relationships Between Toleranced Features", Artificial Intelligence, Vol. 37(1-3), p. 403-412.

[67] Fortini, E., (1967), *Dimensioning for Interchangeable Manufacture*, Industrial Press Inc., New York.

[68] Bjorke, O., (1978), *Computer-Aided Tolerancing*, Tapir Publishers, Norway.

[69] Wirtz, A., (1993), "Vectorial Tolerancing A Basic Element for Quality Control", Proceedings of 3rd CIRP Seminars on "Computer Aided Tolerancing", Ecole Normale Superieure of Cachan, Cedex, France, p. 115-128.

[70] Chase, K. W., and Greenwood, W. H. (1988). "Design Issues in Mechanical Tolerance Analysis", Manufacturing Review ASME, Vol. 1(1), p. 50-59.

[71] Chase, K. W., and Parkinson, A. R. (1991). "A Survey of Research in the Application of Tolerance Analysis to the Design of Mechanical Assemblies", Research in Engineering Design, Vol. 3, p. 23-37.

[72] Chase, K. W., Gao, J., Magleby, S. P., and Sorensen, C. D. (1996). "Including Geometric Feature Variations in Tolerance Analysis of Mechanical Assemblies", IIE Transactions, Vol. 28(10), p. 795-807.

[73] Chase, K. W., Magleby, S. P., and Glancy, C. G., (1997), "A Comprehensive System for Computer-Aided Tolerance Analysis of 2-D and 3-D Mechanical Assemblies", Proceedings of the 5th International Seminar on Computer-Aided Tolerancing, Toronto, Canada.

[74] Whitney, D. E., Gilbert, O. L., and Jastrzebski, M. (1994). "Representation of Geometric Variations using Matrix Transforms for Statistical Tolerance Analysis in Assemblies", Research in Engineering Design, Vol. 6, p. 191-210.

[75] Roy, U., Liu, C. R., and Woo, T. C. (1991). "Review of dimensioning and tolerancing: representation and processing", Computer-Aided Design, Vol. 23(7), p. 466-483.

[76] Bernstein, N. X., (1989), "Representation and Analysis of Dimension and Tolerance Information in Solid Modeling", MSc Thesis, University of the Negev, Beer Shava, Israel.

[77] Denavit, J., and Hartenberg, R. S. (1955). "A Kinematic Notation for Lower Pair Mechanisms Based on Matrices", Journal of Applied Mechanics, Vol. 22, p. 215-221.

[78] Jastrzebski, M. J., (1991), "Software for Analysis of 3-D Statistical Tolerance Propagation in Assemblies using Closed-Form Matrix Transform", MSc Thesis, Massachusetts Institute of Technology, Cambridge, Massachusetts, USA.

[79] Clement, A., Desrochers, A., and Rivière, A., (1991), "Theory and Practice of 3D Tolerancing for Assembly", Proceedings of the 2nd CIRP Seminars on Computer Aided Tolerancing.

[80] Desrochers, A., and Rivière, A. (1997). "A Matrix Approach to the Representation of Tolerance Zones and Clearances", The International Journal of Advanced Manufacturing Technology, Vol. 13(9), p. 630-636.

[81] Shah, J. J., Anderson, D., Kim, Y. S., and Joshi, S. (2001). "A Discourse on Geometric Feature Recognition From CAD Models", Journal of Computing and Information Science in Engineering, Vol. 1(1), p. 41-51.

[82] Mujezinovic, A., Davidson, J. K., and Shah, J. J. (2004). "A New Mathematical Model for Geometric Tolerances as Applied to Polygonal Faces", ASME Journal of Machine Design, Vol. 126(3), p. 504-518.

[83] Liu, Y. S., Gao, S. M., and Cao, Y. L. (2009). "An Efficient Approach to Interpreting Rigorous Tolerance Semantics for Complicated Tolerance Specification", IEEE Transactions on Automation Science and Engineering, Vol. 6(4), p. 670-684.

[84] Cao, Y., Zhang, H., Mao, J., Xu, X., and Yang, J. (2010). "Study on Tolerance Modeling of Complex Surface", International Journal of Advance Manufacturing Technology, Vol. 53(9-12), p. 1183-1188.

[85] Veitschegger, W. K., and Wu, C. H. (1986). "Robot Accuracy Analysis Based on Kinematics", IEEE Journal of Robotics and Automation, Vol. 2(3), p. 171-179.

[86] Paul, R. P., (1981), *Robot Manipulators: Mathematics, Programming, and Control*, The MIT Press, USA.

[87] Gilbert, O. L., (1992), "Representation of Geometric Variations using Matrix Transforms for Statistical Tolerance Analysis in Assemblies", MSc Thesis, Massachusetts Institute of Technology, Cambridge, Massachusetts, USA.

[88] Mantripragada, R., (1998), "Assembly Oriented Design: Concepts, Algorithms and Computational Tools", PhD Thesis, Massachusetts Institute of Technology, Cambridge, Massachusetts, USA.

[89] Mantripragada, R., and Whitney, D. E. (1999). "Modeling and Controlling Variation Propagation in Mechanical Assemblies using State Transition Model", IEEE Transactions on Robotics and Automation, Vol. 15(1), p. 124-140.

[90] Zha, X. F., Du, H. J., and Qiu, J. H. (2001). "Knowledge-Based Approach and System for Assembly-Oriented Design, Part II: the System Implementation", Engineering Applications of Artificial Intelligence, Vol. 14, p. 239-254.

[91] Zhou, S., Huang, Q., and Shi, J. (2003). "State Space Modeling of Dimensional Variation Propagation in Multistage Machining Process using Differential Motion Vector", IEEE Transactions on Robotics and Automation, Vol. 19, p. 296-309.

[92] Liu, S. C., and Hu, S. J. (1997). "Variation Simulation for Deformable Sheet Metal Assemblies using Finite Element Methods", ASME Journal of Manufacturing Science and Engineering, Vol. 119, p. 368–374.

[93] Ding, Y., Ceglarek, D., and Shi, J., (2000), "Modeling and Diagnosis of Multistage Manufacturing Processes: Part I – State Space Model", JAPAN / USA

Symposium on Flexible Automation, Ann Arbor, Michigan, USA, Vol. 2000JUSFA-13146.

[94] Ding, Y., Shi, J., and Ceglarek, D. (2002). "Diagnosability Analysis of Multi-station Manufacturing Processes", Journal of Dynamic Systems, Measurement, and Control, Vol. 124, p. 1-13.

[95] Hu, M., Lin, Z., Lai, X., and Ni, J. (2001). "Simulation and Analysis of Assembly Processes Considering Compliant, Non-ideal Parts and Tooling Variations", International Journal of Machine Tools & Manufacture, Vol. 41, p. 2233-2243.

[96] Camelio, J., Hu, S. J., and Ceglarek, D. (2003). "Modelling Variation Propagation of Multi-Station Assembly Systems with Compliant Parts", Transactions of the ASME Journal of Mechanical Design, Vol. 125(4), p. 673-681.

[97] Camelio, J., and Hu, S. J. (2004). "Multiple Fault Diagnosis for Sheet Metal Fixtures Using Designated Component Analysis", ASME Journal of Manufacturing Science and Engineering, Vol. 126, p. 91-97.

[98] Camelio, J. A., Hu, S. J., and Ceglarek, D. (2004). "Impact of Fixture Design on Sheet Metal Assembly Variation", Journal of Manufacturing Systems, Vol. 23(3), p. 182-193.

[99] Camelio, J. A., Hu, S. J., and Marin, S. P. (2004). "Compliant Assembly Variation Analysis Using Component Geometric Covariance", ASME Journal of Manufacturing Science and Engineering, Vol. 126, p. 355-360.

[100] Kong, Z., Kumar, R., Gogineni, S., Zhou, Y., and Ceglarek, D. (2006). "Mode-Based Tolerance Analysis in Multi-Station Assembly using Stream of Variation Model", Transactions of North American Manufacturing Research Institution of SME, Vol. 34, p. 469-476.

[101] Lee, B., Shalaby, M. M., Collins, R. J., Crisan, V., Walls, S. A., Robinson, D. M., and Saitou, K., (2007), "Variation Analysis of Three Dimensional Non-Rigid Assemblies", IEEE International Symposium on Assembly and Manufacturing, Ann Arbor, Michigan, USA, p. 13-18.

[102] Huang, W., and Kong, Z. (2008). "Simulation and Integration of Geometric and Rigid Body Kinematics Errors for Assembly Variation Analysis", Journal of Manufacturing Systems, Vol. 27, p. 36-44.

[103] Merkley, K. G., (1998), "Tolerance Analysis of Compliant Assemblies", PhD Thesis, Brigham Young University, Provo, Utah, USA.

[104] Jamieson, A., (1982), *Introduction to Quality Control*, Reston Publishing, Virginia, USA.

[105] Trucks, H. E., (1987), *Designing for Economical Production*, Society of Manufacturing Engineers, Dearborn, Michigan.

[106] Hong, Y. S., and Chang, T. C. (2002). "A Comprehensive Review of Tolerancing Research", International Journal of Production Research, Vol. 40(11), p. 2425-2459.

[107] Haugland, L., (1987), "Combining Manufacturing Process Selection and Optimum Tolerance Allocation in Design Automation", MSc Thesis, Brigham Young University, Provo, Utah, USA.

[108] Loosli, B., (1987), "Manufacturing Tolerance Cost Minimization Using Discrete Optimization for Alternate Process Selection", MSc Thesis, Brigham Young University, Provo, Utah, USA.

[109] Chase, K. W., Greenwood, W. H., Loosli, B., and Hauglund , L. (1990). "Least Cost Tolerance Allocation for Mechanical Assemblies with Automated Process Selection", Manufacturing Review, Vol. 3(1), p. 49–59.

[110] Singh, P. K., Jain, P. K., and Jain, S. C. (2009). "Important Issues in Tolerance Design of Mechanical Assemblies. Part 2: Tolerance Synthesis", Proceedings of the Institution of Mechanical Engineers: Part B, Journal of Engineering Manufacture, Vol. 223, p. 1249-1287.

[111] Ostrovsky-Berman, Y., and Joskowicz, L., (2004), "Tolerance Envelopes of Planar Mechanical Parts", Eurographics Association, Aire-la-Ville, Switzerland,

Switzerland Proceedings of the Ninth ACM Symposium on Solid Modeling and Applications, p. 135-143.

[112] Ramani, B., Cheraghi, S. H., and Twomey, J. M. (1998). "CAD-Based Integrated Tolerancing System", International Journal of Production Research, Vol. 36(10), p. 2891-2910.

[113] Singh, P. K., Jain, P. K., and Jain, S. C. (2009). "Important Issues in Tolerance Design of Mechanical Assemblies. Part 1: Tolerance Analysis", Proceedings of the Institution of Mechanical Engineers: Part B, Journal of Engineering Manufacture, Vol. 223, p. 1225-1247.

[114] Greenwood, W. H., and Chase, K. W. (1988). "Worst Case Tolerance Analysis with Nonlinear Problems", Journal of Engineering for Industry, Vol. 110, p. 232–235.

[115] Greenwood, W. H., and Chase, K. W. (1987). "A New Tolerance Analysis Method for Designers and Manufacturers", Journal of Engineering for Industry, Vol. 109, p. 112-116.

[116] Trabelsi, A., and Delchambre, A. (2000). "Assessment on Tolerance Representation and Tolerance Analysis in Assemblies", SAGE Journals Online, Concurrent Engineering, Vol. 8(4), p. 244-262.

[117] Mansoor, E. M. (1963). "The Application of Probability to Tolerances used in Engineering Designs", Proceedings of the Institution of Mechanical Engineers, Vol. 178, p. 29-51.

[118] Greenwood, W. H., and Chase, K. W. (1990). "Root Sum Squares Tolerance Analysis with Nonlinear Problems", Journal of Engineering for Industry, Vol. 112, p. 232–235.

[119] Sitko, A. G. (1991). "Applying Variation Simulation Analysis to 2-D Problems.", SAE Technical Paper (Society of Automotive Engineers), Vol. SAE 910210.

[120] Gao, J., Chase, K. W., and Magleby, S. P., (1996), "A New Monte Carlo Simulation Method for Tolerance Analysis of Kinematically Constrained

Assemblies", Mechanical Engineering Department, Brigham Young University, Provo.

[121] Ceglarek, D., and Shi, J. (1995). "Dimensional Variation Reduction for Automotive Body Assembly", ASME Manufacturing Review, Vol. 8(2).

[122] Kong, Z., Ceglarek, D., and Huang, W. (2008). "Multiple Fault Diagnosis Method in Multistation Assembly Processes Using Orthogonal Diagonalization Analysis", ASME Journal of Manufacturing Science and Engineering, Vol. 130 / 011014-1.

[123] Rong, Q., Ceglarek, D., and Shi, J. (2000). "Dimensional Fault Diagnosis for Compliant Beam Structure Assemblies", Journal of Manufacturing Science and Engineering, Vol. 122(4), p. 773-780.

[124] Hu, S. J., and Camelio, J. A. (2006). "Modeling and Control of Compliant Assembly Systems", CIRP Annals - Manufacturing Technology, Vol. 55(1), p. 19-22.

[125] Dantan, J. Y., Mathieu, L., and Anwer, N. (2003). "Integrated Tolerancing Process for Conceptual Design", CIRP Annals - Manufacturing Technology, Vol. 52(1), p. 135-138.

[126] Forouraghi, B. (2002). "Worst-Case Tolerance Design and Quality Assurance via Genetic Algorithms", Journal of Optimization Theory and Applications, Vol. 13(2), p. 251-268.

[127] Zhang, C., and Wang, H. P. (1993). "Optimal Process Sequence Selection and Manufacturing Tolerance Allocation", Journal of Design and Manufacturing, Vol. 3, p. 135-146.

[128] Mansoor, E. N. (1961). "Selective Assembly - Its Analysis and Applications.", International Journal of Production Research, Vol. 1(1), p. 13-24.

[129] Pugh, G. A. (1992). "Selective Assembly with Components of Dissimilar Variance", Computers and Industrial Engineering, Vol. 23, p. 487-491.

[130] Mease, D., Nair, V. N., and Sudjianto, A. (2004). "Selective Assembly in Manufacturing: Statistical Issues and Optimal Binning Strategies", Technometrics, Vol. 46(2), p. 165-175.

[131] Matsuura, S., and Shinozaki, N. (2011). "Optimal Process Design in Selective Assembly when Components with Smaller Variance are Manufactured at Three Shifted Means", International Journal of Production Research, Vol. 49(3), p. 869-882.

[132] Turner, J. U. (1990). "Relative Positioning of Parts in Assemblies using Mathematical Programming", Computer-Aided Design, Vol. 22(7), p. 394-400.

[133] Li, B., and Roy, U. (2001). "Relative Positioning of Toleranced Polyhedral Parts in an Assembly", IIE Transactions, Vol. 33, p. 323-336.

[134] Jayaweera, N., Webb, P., and Johnson, C. (2010). "Measurement Assisted Robotic Assembly of Fabricated Aero-Engine Components", Assembly Automation, Vol. 30(1), p. 56–65.

[135] Cogorno, G., (2006), *Geometric Dimensioning and Tolerancing for Mechanical Design*, McGraw-Hill Professional Publishing, Blacklick, OH, USA.

[136] De Fazio, T. L., Edsall, A. C., Gustavson, R. E., Hernandez, J. A., Hutchins, P. M., Leung, H. W., Luby, S. C., Metzinger, R. W., Nevins, J. L., Tung, K. K., and Whitney, D. E., 1990, "A prototype of feature-based design for assembly", Technical Report No. The Charles Stark Draper Laboratory, Inc., Cambridge, Massachusetts.

[137] Astrom, P., (2004), "Simulation of Manufacturing Processes in Product Development", PhD Thesis, Lulea University of Technology, Lulea, Sweden.

[138] Roy, R., Hinduja, S., and Teti, R. (2008). "Recent Advances in Engineering Design Optimisation: Challenges and Future Trends", CIRP Annals - Manufacturing Technology, Vol. 57(2), p. 697-715.

[139] Mears, M. L., (2006), "Geometry Estimation and Adaptive Actuation for Centering Preprocessing and Precision Measurement", PhD Thesis, Georgia Institute of Technology, Atlanta, USA.

[140] Klocke, F., Veselovac, D., Auerbach, T., and Seidner, R. (2008). "Intelligent Assembly for Aero Engine Components", Proceedings of ICIRA, Vol. 2, p. 927–935.

[141] Henzold, G., (2006), *Geometrical Dimensioning and Tolerancing for Design, Manufacturing and Inspection*, Elsevier, Oxford, UK.

[142] Chase, K. W., (2004), *Basic Tools for Tolerance Analysis of Mechanical Assemblies.*, In: Geng H (ed) Manufacturing Engineering Handbook, Chapter 7. McGraw-Hill,

[143] Villeneuve, F., and Mathieu, L., (2010), *Geometric Tolerancing of Products*, John Wiley & Sons Inc,

[144] Rajmohan, S., (2008), "Runout Evaluation Methods for Cylindrical, Taperd and Flat Surfaces", MSc Thesis, University of Cincinnati, Ohio, USA.

[145] Cai, M., Yang, J.-x., and Wu, Z.-t. (2004). "Mathematical Model of Cylindrical Form Tolerance", Journal of Zhejiang University SCIENCE, Vol. 5(7), p. 890-895.

[146] Murthy, T. S. R. (1986). "A Comparison of Different Algorithms for Circularity Evaluation", Precision Engineering, Vol. 8(1), p. 19-23.

[147] Murthy, T. S. R., and Abdin, S. Z. (1980). "Minimum Zone Evaluation of Surfaces", International Journal of Machine Tools and Research, Vol. 20, p. 123-136.

[148] Turek, S., Ramaswami, H., Rajmohan, S., and Anand, S. (2008). "Runout Evaluation of Cylindrical Features using Discrete Surface Profile Data", Transactions of NAMRI/SME, Vol. 36, p. 129–136.

[149] Drake, P. J., (1999), *Dimensioning and Tolerancing Handbook*, McGraw-Hill, New York.

[150] Ngoi, B. K. A., Lim, B. H., and Ang, P. S. (2000). "Nexus Method for Stack Analysis of Geometric Dimensioning and Tolerancing (GDT) Problems", International Journal of Production Research, Vol. 38(1), p. 21-37.

[151] Murthy, T. S. R. (1982). "A Comparison of Different Algorithms for Cylindricity Evaluation", International Journal of Machine Tools and Research, Vol. 22(4), p. 283-292.

[152] Murthy, T. S. R., and Rao, S. Y. (1981). "A Simple Approach for Evaluation of Cylindrical Surfaces", CIRP Annals - Manufacturing Technology, Vol. 30(1), p. 441-444.

[153] Damodarasamy, S., and Anand, S. (1999). "Evaluation of Minimum Zone for Flatness by Normal Plane Method and Simplex Search", IIE Transactions, Vol. 31, p. 617-626.

[154] BSI, (2007), DD CEN ISO/TS 17450-1:2007, Geometric Product Specifications (GPS)-General Concepts; Part 1: Model for Geometrical Specification and Varification, Brussels

[155] Ballu, A., Bourdet, P., and Mathieu, L. (1991). "The Processing of Measured Points in Coordinates Metrology in Agreement with the Definition of Standardized Specifications", CIRP Annals - Manufacturing Technology, Vol. 40(1), p. 491-494.

[156] Dabling, J. G., (2001), "Incorporating Geometric Feature Variation with Kinematic Tolerance Analysis of 3d Assemblies", MSc Thesis, Brigham Young University, Provo, Utah, USA.

[157] Colosimo, B. M., Moroni, G., and Petrò, S. (2010). "A Tolerance Interval Based Criterion for Optimizing Discrete Point Sampling Strategies", Precision Engineering, Vol. 34(4), p. 745-754.

[158] Samuel, G. L., and Shunmugam, M. S. (2002). "Evaluation of Sphericity Error from Form Data using Computational Geometric Techniques", International Journal of Machine Tools & Manufacture, Vol. 42, p. 405-416.

[159] Samuel, G. L., and Shunmugam, M. S. (2003). "Evaluation of Circularity and Sphericity from Coordinate Measurement Data", Journal of Materials Processing Technology, Vol. 139, p. 90-95.

[160] Tsukada, T., Kanada, T., and Okuda, K. (1984). "An Evaluation of Roundness from Minimum Zone Center by Means of an Optimization Technique", Bulletin of the Japan Society of Precision Engineering Vol. 18(4), p. 317-322

[161] Carr, K., and Ferreira, P. (1995). "Verification of Form Tolerances Part. II: Cylindricity and Straightness of a Median Line", Precision Engineering, Vol. 17, p. 144-156.

[162] Yau, H.-T., and Menq, C.-H. (1996). "A Unified Least-Squares Approach to the Evaluation of Geometric Errors using Discrete Measurement Data", International Journal of Machine Tools and Manufacture, Vol. 36(11), p. 1269-1290.

[163] Xianqing, L., Chunyang, Z., Yujun, X., and Jishun, L. (2010). "Roundness Error Evaluation Algorithm Based on Polar Coordinate Transform", Measurement, Vol. 44(2), p. 345-350

[164] Chen, M.-C., and Fan, S.-K. S. (2002). "Tolerance Evaluation of Minimum Zone Straightness using Non-linear Programming Techniques: A Spreadsheet Approach", Computers & Industrial Engineering, Vol. 43(3), p. 437-453.

[165] Cheraghi, S. H., Lim, H. S., and Motavalli, S. (1996). "Straightness and Flatness Tolerance Evaluation: An Optimization Approach", Precision Engineering, Vol. 18(1), p. 30-37.

[166] Samuel, G. L., and Shunmugam, M. S. (1999). "Evaluation of Straightness and Flatness Error using Computational Geometric Techniques", Computer-Aided Design, Vol. 31, p. 829-843.

[167] Venkaiah, N., and Shunmugam, M. S. (2007). "Evaluation of Form Data using Computational Geometric Techniques—Part I: Circularity Error", International Journal of Machine Tools & Manufacture, Vol. 47, p. 1229-1236.

[168] Samuel, G. L., and Shunmugam, M. S. (2000). "Evaluation of Circularity from Coordinate and Form Data using Computational Geometric Techniques", Journal of the International Societies for Precision Engineering and Nanotechnology, Vol. 24, p. 251-263.

[169] Yau, H.-T. (1997). "Evaluation and Uncertainty Analysis of Vectorial Tolerances", Precision Engineering, Vol. 20(2), p. 123-137.

[170] Carr, K., and Ferreira, P. (1995). "Verification of Form Tolerances Part I: Basic Issues, Flatness, and Straightness ", Precision Engineering, Vol. 17, p. 131-143.

[171] Yau, H.-T. (1997). "Generalization and Evaluation of Vectorial Tolerances", International Journal of Production Research, Vol. 35(6), p. 1763-1783.

[172] Spotts, M. F., (1983), *Dimensioning and Tolerancing for Quantity Production*, Prentice-Hall, Inc, Englewood Cliffs, New Jersey.

[173] Lin, C.-Y., Huang, W.-H., Jeng, M.-C., and Doong, J.-L. (1997). "Study of an Assembly Tolerance Allocation Model Based on Monte Carlo Simulation", Journal of Materials Processing Technology, Vol. 70, p. 9-16.

[174] Fischer, B. R., (2004), *Mechanical Tolerance Stakeup and Analysis*, Marcel Dekker, New York.

[175] Cho, N., and Tu, J. F. (2002). "Quantitative Circularity Tolerance Analysis and Design for 2D Precision Assemblies", International Journal of Machine Tools & Manufacture, Vol. 42, p. 1391-1401.

[176] Behara, R. S., Fontenot, G. F., and Gresham, A. (1995). "Customer Satisfaction Measurement and Analysis using Six Sigma", International Journal of Quality & Reliability Management, Vol. 3, p. 9-18.

[177] Stewart, M. L., (2004), "Variation Simulation of Fixtured Assembly Processes for Compliant Structures using Piecewise-Linear Analysis", MSc Thesis, Brigham Young University, Provo, Utah, USA.

[178] DeDoncker, D., and Spencer, A. (1987). "Assembly Tolerance Analysis with Simulation and Optimization Techniques", SAE Transactions, Vol. 96(1), p. 1062–1067.

[179] Glancy, C. G., and Chase, K. W., (1999), "A Second-Order Method for Assembly Tolerance Analysis", Proceedings of the 1999 ASME Design Engineering Technical Conferences, Las Vegas, p. 1-8.

[180] Glancy, C. G., (1994), "A Second-Order Method for Assembly Tolerance Analysis", MSc Thesis, Bringham Young University, Provo, Utah, USA.

[181] Huang, W., Phoomboplab, T., and Ceglarek, D. (2009). "Process Capability Surrogate Model-Based Tolerance Synthesis for Multi-Station Manufacturing Systems", IIE Transactions, Vol. 41, p. 309–322.

[182] Nigam, S. D., and Turner, J. U. (1995). "Review of Statistical Approaches to Tolerance Analysis", Computer-Aided Design, Vol. 27(1), p. 6-15.

[183] Desrochers, A., Ghie, W., and Laperriere, L. (2003). "Application of a Unified Jacobian—Torsor Model for Tolerance Analysis", Journal of Computing and Information Science in Engineering, Vol. 3(1), p. 2-14.

[184] Pitman, J., (1993), *Probability*, Springer-Verlag, New York.

[185] DeGroot, M. H., and Schervish, M. J., (2012), *Probability and Statistics*, Pearsons, Boston.

[186] Simon, M. K., (2006), *Probability Distributions Involving Gaussian Random Variables: A Handbook for Engineers, Scientists and Mathematicians*, Springer Science, New York, USA.

[187] Pitman, E. J. G. (1939). "A Note on Normal Correlation", Biometrika, Vol. 31(1/2), p. 9-12.

[188] Fisher, R. A. (1915). "Frequency Distribution of the Values of the Correlation Coefficient in Samples from an Indefinitely Large Population", Biometrika, Vol. 10(4), p. 507-521.

[189] Chew, V., and Boyce, R. (1962). "Distribution of Radial Error in the Bivariate Elliptical Normal Distribution", Technometrics, Vol. 4(1), p. 138-140.

[190] Rencher, A. C., (2002), *Methods of Multivariate Analysis*, John Wiley & Sons, Inc., New York.

[191] Bowman, F., (1958), *Introduction to Bessel Functions*, Dover Publications, Inc., New York.

[192] Maropoulos, P., and Ceglarek, D. (2010). "Design Varification and Validation in Product Lifesysle", CIRP Annals - Manufacturing Technology, Vol. 59, p. 740-759.

[193] Maropoulos, P. G., Vichare, P., Martin, O., Muelaner, J., Summers, M. D., and Kayani, A. (2011). "Early design verification of complex assembly variability using a Hybrid - Model Based and Physical Testing - Methodology", CIRP Annals - Manufacturing Technology, Vol. 60(1), p. 207-210.

[194] Zhou, S., and Shi, J. (2001). "Active Balancing and Vibration Control of Rotating Machinery: A Survey", The Shock and Vibration Digest, Vol. 33(4), p. 361-371.

# Appendix: Evaluating Run-out Measurement Data

Industries assembling high-value rotating machines, measure the component to check for run-out in axial and radial direction (as shown in Figure 3-2). The radial run-out is measured to identify center of geometry offset from center of rotation, and axial run-out is obtained to identify the irregularities of surface profile of the mating surface. In order to measure axial and radial run-out, each component is places on rotating table of the measurement system and the measurements are taken during the complete revolution of the rotary table.

The measurement data obtained from run-out measurement instruments is obtained in polar form. For axial and radial run-out, the run-out values are measured in microns and the rotation of rotating table of measuring instrument are described in degrees or radians. Mathematically, the axial and radial run-out can be expressed in polar coordinates as follows:

$$R(\varphi) = R_n + r_{run-out}(\varphi) \quad \text{(A.1)}$$

$$Z(\varphi) = H + a_{run-out}(\varphi) \quad \text{(A.2)}$$

where $R(\varphi)$ is the radius of a point on the measured surface at table orientation $\varphi$, $R_n$ is the nominal radius, $r_{run-out}(\varphi)$ is the measured run-out in the radial direction and $Z(\varphi)$ is the height of a point on the measured surface at table orientation $\varphi$, $H$ is the nominal height, and $a_{run-out}(\varphi)$ is the measured run-out in the axial direction.

The radial run-out data is examined to find the location error of the actual mating feature in the direction perpendicular to a datum axis, whereas, the axial run-out data

is analysed to evaluate the relative orientation error of actual feature with reference to the nominal feature and the location error in direction along the datum axis.

### *Evaluation of Radial Run-Out*

The circular representation of radial run-out is shown in Figure A-1(a). It can be observed from Figure A-1(a), that large deviations in radial run-out from the ideal form can cause an unwanted shift in the rotational centre of the part.

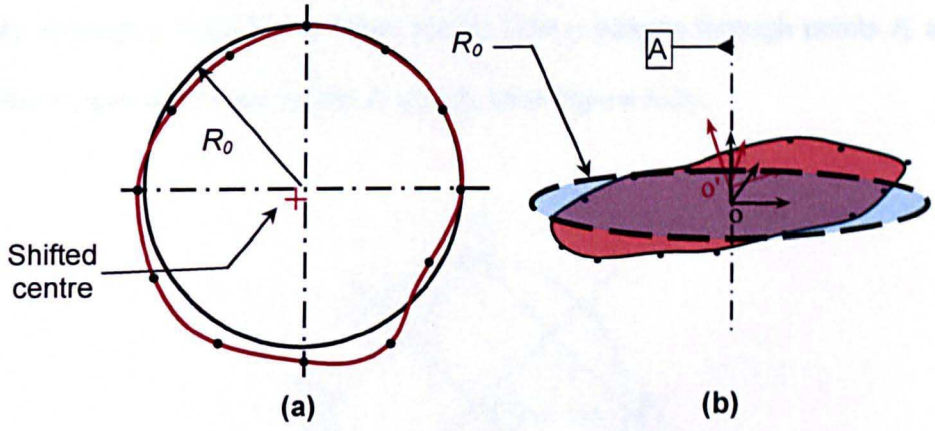


**Figure A-1: A typical example of axial and radial run-out measurement**

Let $n$ points are measured for radial run-out on a given mating feature. Each of measured point gives the reading of distance along the radial direction at given angle about the axis of rotation. Equation (A.1) describes each run-out measurement in polar coordinates. In order to best fit a circle to the given set of points, we first convert the polar form in to Cartesian form. Therefore $x$, $y$ coordinate with reference to table axis centre can be calculated as:

$$x_i(\theta_i) = (R_0 + R^i_{run-out}(\theta_i)) \cdot \cos(\theta_i) \quad (where\ i = 1,2,3,...n) \tag{A.3}$$

$$y_i(\theta_i) = (R_0 + R^i_{run-out}(\theta_i)) \cdot \sin(\theta_i) \quad (where\ i = 1,2,3,...n) \tag{A.4}$$

where $R_0$ is the nominal radius across the feature, $R^i_{run-out}$ is the radial run-out, and $\theta_i$ angle of rotation at which the radial run out is measured.

First step towards the best fit algorithm is to find an initial guess for the centre and radius of circle. Initial guess can be computed by averaging all the circles that can be built using all triplets of non-aligned points.

For any given triplet of non-aligned points, there is a single circle passing through all three points. Let $P_i(x_i, y_i)$, $P_j(x_j, y_j)$ and $P_k(x_k, y_k)$ be three points. Two lines can be formed through 2 pairs of the three points. Line $a$ passes through points $P_i$ and $P_j$, and line $b$ passes through points $P_j$ and $P_k$ (see Figure A-2).

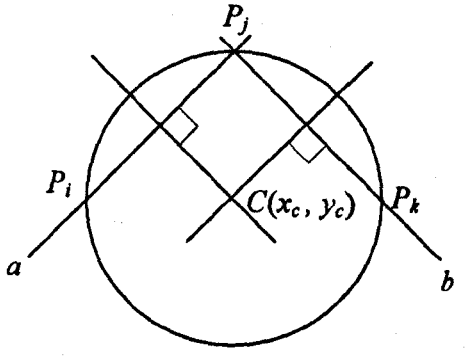


**Figure A-2: Three point circle**

The equation of these two lines can be written as:

$$y_a = m_a(x - x_i) + y_i \tag{A.5}$$

$$y_b = m_b(x - x_j) + y_j \tag{A.6}$$

where $m$ is the slope of the lines given by

$$m_a = \frac{(y_j - y_i)}{(x_j - x_i)} \quad and \quad m_b = \frac{(y_k - y_j)}{(x_k - x_j)} \tag{A.7}$$

Thus, centre of the circle is the intersection of the two lines perpendicular to and passing through the midpoints of the lines $a$ and $b$. Thus equations of the lines perpendicular to lines $a$ and $b$ and passing through their midpoints are:

$$y_c = -\frac{1}{m_a}\left\{x_c - \frac{(x_i + x_j)}{2}\right\} + \frac{(y_i + y_j)}{2} \tag{A.8}$$

$$y_c = -\frac{1}{m_b}\left\{x_c - \frac{(x_j + x_k)}{2}\right\} + \frac{(y_j + y_k)}{2} \tag{A.9}$$

Intersection of the two perpendicular bisectors can be calculated by solving Equation (A.8) and Equation (A.9) for $x_c$

$$x_c = \frac{m_a m_b (y_i - y_k) + m_b (x_i + x_j) - m_a (x_j + x_k)}{2(m_b - m_a)} \tag{A.10}$$

Substituting the value of $x_c$ in Equation (A.8) or (A.9) will give the value of $y_c$. Therefore, the radius of the three point circle can be calculated as:

$$r = \sqrt{(x_i - x_c)^2 + (y_i - y_c)^2} \tag{A.11}$$

The initial guess of the fitting circle can be built by averaging the coordinates and radii of the circles obtained from all triplets of non-aligned points. Total number of triplet combinations $nC_3$ for the set of $n$ measurement points is given by:

$$nC_3 = \frac{n!}{(n-3)! \cdot 3!} \tag{A.12}$$

Once an initial guess for the circle centre is known, best fit circle can be found using a least squares estimator based on the Euclidean distance between the points and the circle. The least square (LS) method for best fit circle can be mathematically expressed as:

$$LS\_circle = \min \sum_{i=1}^{n} \left( \sqrt{(x_i - a)^2 + (y_i - b)^2} - R \right)^2 \quad \text{(A.13)}$$

where $(a, b)$ represent the optimum location of the best fit circle. If the best fit is applied to base feature, then the $(a, b)$ represents $(dX_1, dY_1)$, and if best fit is applied for top feature measurements, $(a, b)$ represents $(dX_2, dY_2)$.

### *Evaluation of Axial Run-Out*

The best fit plane algorithm assumes that the circular element at which the axial run-out is measured has nominal radius $(R_0)$ with its centre at (0,0,0), and this circular element lies on the plane $XOY$ as shown in Figure A-1(b).

The step by step method of calculating translational and angular errors from axial run-out data for a given feature is described as follows:

1. Calculating the $n$ points in three-dimensional space as:

$$x_i(\theta_i) = R_0 \cdot \cos(\theta_i) \quad (where\ i = 1,2,3,...n) \quad \text{(A.14)}$$

$$y_i(\theta_i) = R_0 \cdot \sin(\theta_i) \quad (where\ i = 1,2,3,...n) \quad \text{(A.15)}$$

$$z_i(\theta_i) = H_0 + H^i_{run-out}(\theta_i) \quad (where\ i = 1,2,3,...n) \quad \text{(A.16)}$$

To find an initial guess for the best fit plane equation constants. Initial guess can be computed by averaging all the planes that can be built using all triplets of non-aligned points. The constant $A, B, C$ and $D$ for a plane containing points $P_i(x_i, y_i)$, $P_j(x_j, y_j)$ and $P_k(x_k, y_k)$ can be calculated as:

$$A = (y_i - y_k)(z_j - z_k) - (y_j - y_k)(z_i - z_k) \quad \text{(A.17)}$$

$$B = (x_j - x_k)(z_i - z_k) - (x_i - x_k)(z_j - z_k) \quad \text{(A.18)}$$

$$C = (x_i - x_k)(y_j - y_k) - (x_j - x_k)(y_i - y_k) \quad \text{(A.19)}$$

$$D = -Ax_k - By_k - Cz_k \quad \text{(A.20)}$$

Using a plane to fit the $n$ measurements to minimise the sum of squared distances from the measurement to the plane, provided Equation of the best fit plane is of following form:

$$Ax + By + Cz + D = 0 \quad \text{(A.21)}$$

If the distance of each point to the plane is given by:

$$\delta_i = \frac{|A \cdot x_i + B \cdot y_i + C \cdot z_i + D|}{\sqrt{A^2 + B^2 + C^2}} \quad (where\ i = 1,2,3,...n) \quad \text{(A.22)}$$

Then the best fit plane can be calculated as:

$$f(A,B,C,D) = \min\left[\sum_{i=1}^{n} (\delta_i)^2\right] \quad (where\ i = 1,2,3,...n) \quad \text{(A.23)}$$

Calculating unit normal vectors of the best fit plane through origin (0,0,0). If the unit normal vector of nominal plane is $(a, b, c) = (0,0,1)$ as the nominal plane is $z = 0$.Thus unit normal vector of the best fit plane $(a_1, b_1, c_1)$ can be calculated as:

$$(a_1, b_1, c_1) = \left( \frac{A}{\sqrt{A^2 + B^2 + C^2}}, \frac{B}{\sqrt{A^2 + B^2 + C^2}}, \frac{C}{\sqrt{A^2 + B^2 + C^2}} \right) \quad \text{(A.24)}$$

Calculating the angular errors about any axes from rotating the normal vectors. Thus angular errors $d\theta_x$ and $d\theta_y$ about the $x$, and $y$-axis can be calculated by:

$$\left.\begin{aligned} b &= b_1 \cos(d\theta_x) - c_1 \sin(d\theta_x) \\ c &= b_1 \sin(d\theta_x) + c_1 \cos(d\theta_x) \\ a &= a_1 \end{aligned}\right\} \quad \text{(A.25)}$$

$$\left.\begin{aligned} c &= c_1 \cos(d\theta_y) - a_1 \sin(d\theta_y) \\ a &= c_1 \sin(d\theta_y) + a_1 \cos(d\theta_y) \\ b &= b_1 \end{aligned}\right\} \quad \text{(A.26)}$$

As the component is assumed as rigid and it does not twist about its central axis, the angular error $d\theta_z$. If the angular errors $d\theta_{x1}$ and $d\theta_{y1}$ and translation error $dZ_1$ represents the deviation of the base of axi-symmetric component (as shown in Figure 5-15), and $d\theta_{x2}$, $d\theta_{y2}$ and $dZ_2$ are the variations at the top mating feature of the axi-symmetric component, therefore, the net translation and rotation error in the component obtained by axial run-out inspection data can be written as:

$$(d\theta_x, d\theta_y, dZ) = (d\theta_{x2} - d\theta_{x1}, d\theta_{y2} - d\theta_{y1}, dZ_2 - dZ_1) \quad \text{(A.27)}$$